Delft University of Technology

DESIGN SYNTHESIS EXERCISE AE3200

Secondary Rotor Vertical Axis Wind Turbine Final Report

Version 1

Group 21

July 2, 2019



Tutors:

Dr.ir. C.J. Simao Ferreira Prof.dr. S.J. Watson

Coaches:

Viswanath Dhanisetty Mariana Leandro Cruz

Group members:

Carlos Dos Santos Pereira Malveiro
Lukas Karolis Bajarūnas
Thomas Broertjes
Maarten van Nistelrooij
Cihangir Ozbek
Angela Hekker
Tetsuya Watanabe
Giel Kerkhofs
Anna Grozeva
Lidia Rzeplinska

Contents

Li	of Figures	V
Li	of Symbols	vi
E	ecutive Overview	1
1	Introduction	7
2	Requirements	ę
	2.1 Stakeholder Requirements	
	2.2 Technical Requirements	
	2.3 Killer Requirements	
	Driving Requirements	1e
3	Conceptual and preliminary design phases	14
	3.1 Conceptual designs	
	3.2 Preliminary designs	14
4	General layout and sizing	17
	4.1 General turbine layout	
	4.2 Sizing	
	4.3 Sensitivity analysis	20
5	Aerodynamic design	21
	5.1 Momentum theory	21
	5.2 Blade Element Theory	22
	5.3 Thrust and power coefficients	23
	5.4 Prandtl tip and root losses	24
	5.5 Prandtl-Glauert correction for lift coefficient	
	Blade Element Momentum theory	
	5.7 Design procedure and code	
	5.8 Airfoil selection	
	6.9 Results & Discussion	
	5.10 Sensitivity analysis	
	5.11 Verification and validation	
	5.12 Limitations	
	5.13 Recommendations	
	5.14 Turbine noise	
	5.14.1 Theory	_
	5.14.2 Simulation	
	5.14.4 Verification and Validation	
	5.14.5 Limitations and Recommendations	
6	Supervisory control and safety system 3.1 General	39 39
	6.1.1 Definitions	
	6.1.2 Assumptions	
	6.1.3 Operating conditions	
	3.2 Guidelines	
	3.3 Components	
	6.3.1 Sensors	
	6.3.2 Actuators	
	6.3.3 Other components	
	6.4 Communication flow diagram	
	6.5 Control system architecture and data handling	

		6.5.1 Generator torque control	
		6.5.2 Pitch control	. 47
		6.5.3 Braking system	. 48
		6.5.4 Parking and holding	. 48
	6.6	Nominal conditions: the supervisory control system	. 49
		6.6.1 Normal operation	. 49
		6.6.2 Malfunctions under nominal conditions	. 50
	6.7	Non-nominal conditions: the safety system	. 51
		6.7.1 Safety system activation criteria	
		6.7.2 Safety system functioning	
	6.8	Failure response overview	
	6.9	Functional Analysis	
		Limitations and recommendations	
	0.10		. 01
7	Con	ntrol optimisation strategy	57
	7.1	General	. 57
	7.2	Before rated	. 59
	7.3	After rated	
	7.4	Limiting values	
	7.5	Sensitivity analysis	
	7.6	Verification and validation	
	7.7	Limitations and recommendations	
8	Pow	ver and electronics	66
	8.1	Drivetrain	
		8.1.1 Direct drive vs gearbox	. 66
		8.1.2 Mass and cost	
		8.1.3 Sizing	. 67
		8.1.4 Summary table	. 68
	8.2	Electrical block diagram	. 68
	8.3	Sensitivity analysis	. 69
	8.4	Limitations and recommendations	. 69
9		uctural Analysis	70
	9.1	Structural analysis of the secondary rotor blades	
		9.1.1 Blade design	
		9.1.2 Requirements for the secondary blade design	
		9.1.3 Loads acting on the secondary rotor blade	
		9.1.4 Fatigue considerations	
		9.1.5 Co-Blade software	
		9.1.6 Results for the secondary rotor design	
	9.2	Structural design of the primary blade	
		9.2.1 Choice of chord length	
		9.2.2 Loading analysis	
		9.2.3 Metal wing box	
		9.2.4 Composite wing box	
		9.2.5 Comparison of designs	
	9.3	Connection points	
	9.4	Structural analysis of the tower	
		9.4.1 Vibrations and natural frequency	
		9.4.2 Failure criteria - von Mises	
		9.4.3 Failure criteria - Cylindrical buckling	. 88
	9.5	Structural analysis of the horizontal strut	. 88
	9.6	Mass breakdown	. 89
	9.7	Sensitivity analysis	. 90
	9.8	Verification and validation	. 90
10		duction plan	93
		Wind turbine components	
	10.2	Manufacturing	
		10.2.1 Blades	. 93

		10.2.2 Tower	 94
		10.2.3 Generator	 94
		10.2.4 Rotor hub	 94
	10.3	Offshore turbine installation	 94
		rations and logistics	97
	11.1	Commissioning	 97
	11.2	Maintenance strategy	 98
	11.3	Turbine health monitoring	
		11.3.1 Supervisory Control and Data Acquisition	 99
		11.3.2 Conditions monitoring systems	 99
		11.3.3 Structural health monitoring	 99
	11.4	Planning	 100
	11.5	Decommissioning Phase	 101
12		AS characteristics	102
	12.1	Reliability	 102
		12.1.1 Conventional turbine reliability	
		12.1.2 SRVAWT reliability	 102
		12.1.3 Results and comparison	
	12.2	Availability	
		Maintainability	
	12.0	12.3.1 Service and inspections	
		12.3.2 Repair	
		12.3.3 Overhaul and modernization	
	10.4		
	12.4	Safety	
		12.4.1 Personnel safety	
		12.4.2 Turbine safety	 107
19	Tool	nical right management	108
19		nical risk management	
		Risk identification and assessment	
	13.2	Risk mitigation	 110
11	Sugt	ainable development strategy	112
14		Design, production and installation phase	
		Operational phase	
		Decommissioning phase	
		Key sustainability goals	
	14.5	Turbine Noise	
		14.5.1 Sources of Noise	
		14.5.2 Effects of noise	
		14.5.3 Recommendations	 115
4 P	a		110
		analysis	116
		Cost breakdown structure	
		Return on investment and operational profit	
		Sensitivity analysis	
		Verification and validation	
	15.5	Limitations and recommendations	 121
	3.6		100
16		ket analysis	122
	16.1	The current wind energy market	
		16.1.1 The global market	
		16.1.2 The European offshore market	
		Developments	
		Competitive designs	
	16.4	The SRVAWT on the market	
		16.4.1 SWOT analysis	 124
		16.4.2 Qualitative market performance prediction	
		16.4.3 Quantitative market performance prediction	

17	Technical Resource Budgeting 17.1 Turbine mass	126 . 126 . 126
18	Sensitivity analysis	128
19	Compliance matrix	130
20	Conclusion	131
2 1	Limitations and recommendations 21.1 Limitations 21.2 Recommendations	
22	Future planning	133
Bi	bliography	140

List of Figures

3.1	Proposed concepts	5
4.1	General layout of the wind turbine	7
4.2	Top view of vertical axis primary rotor	0
5.1	Axial and tangential velocity through an actuator disc model [11]	
5.2	Flow and forces on a blade element [11]	
5.3	Aerodynamic design procedure flow diagram including Python calculations $\dots \dots 2$	
5.4	Secondary rotor planform design	
5.5	Power coefficient, thrust coefficient and induction factors for different operational cases 3	
5.6	Angle of attack distribution over the secondary rotor blade for different operational cases \dots 3	
5.7	Data obtained from QBlade to validate the developed Python code	
5.8	Overview of steps taken during noise prediction	
5.9	Z-weighted total far-field pressure for an observer located 0m from the tower	7
5.10	Z-weighted root-mean-squared far-field pressure for an observer located 100m from the tower.	
	Each colour represents a single harmonic	7
5.11	A-weighted root-mean-squared far-field pressure for an observer located 100m from the tower.	_
	Each colour represents a single harmonic	8
6.1	Diagrams showing the different operation regions related to rotational speed and power $[21]$ 4	
6.2	Communication flow diagram	
6.3	Overview of the control system architecture	5
6.4	Hardware and software layout of the control system	
6.5	Torque control data handling scheme	
6.6	Pitch control data handling diagram	
6.7	Different regions in the power curve [31]	9
6.8	An overview of the data handling during normal operation, with a division between primary and secondary rotor	0
6.9	Start-up procedure of the wind turbine during nominal operating conditions	0
	Shutdown procedure of the wind turbine during nominal operating conditions	
	Emergency shutdown procedure in case of failure of the supervisory control system 5	1
6.12	Data flow from faults and failures to the control system and the braking system. Template used from [21]	2
7.1	Control strategy	7
7.3	Power curve primary and secondary rotors	
7.2	Control strategy before rated conditions	
7.4	Power output of secondary rotors over primary rotor rotation	
7.5	Control strategy after rated conditions	
7.6	Change of Induction factor secondary rotor over velocity range	
7.7	Induction factor variation secondary rotor at $17.5m/s$	
7.8	Rotational velocity of primary rotor	
8.1	Energy conversion in a wind turbine [35]	6
8.2	Electrical block diagram wind farm configuration	
9.1	Graph showing stiffness to weight ratios for different materials, the CFRP and GFRP are highlighted 7	1
9.2	The structure of a wind turbine blade [44]	
9.3	Loads the structure will experience during wind turbine operation	3
9.4	Free body diagrams of the loads acting on the cross section of the secondary rotor blade (in the x-y axis frame) and along the length of the blade (in the x-z axis frame)	
9.5	Applied Loads	
9.6	Resultant forces and moments on the secondary rotor blade structure	
9.7	Thickness variation	
9.8	Effective Young's modulus	
9.9	Effective shear modulus of the secondary rotor blade	
	· · · · · · · · · · · · · · · · · · ·	

9.10	Maximum normal stress experienced by the secondary rotor structure and the corresponding
	penalty factor
9.11	Maximum shear stress experienced by the secondary rotor structure and the corresponding
	penalty factor
	Displacements of the secondary rotor blade along its centroidal axes
	Primary blade free body diagram Y-Z coordinate
9.14	Primary blade free body diagram X-Y coordinate
9.15	Maximum stress (S) versus the logarithm of the number of cycles to fatigue failure (N) for seven
	metal alloys [53]
9.16	Different buckling coefficient
9.17	The T-bolt (left) and the insert connection concepts for the secondary rotor blade attachment to
	the rotor hub
9.18	Attachment concepts
	Tower free body diagram
	Free body diagram strut
	Maximum stress on the secondary blade structure model made with QBlade
10.1	Blade manufacturing flowchart
	Tower manufacturing flowchart
	Installation plan
	Installation plan
11.1	Maintenance logistics plan
11.2	Flow diagram showing the different steps within the decommissioning phase
12.1	Subsystem contributions to the annual failure rate, for both conventional turbines and the SRVAWT104
12.2	Subsystems contributions to the annual repair time, for both conventional turbines and the
	SRVAWT
	Cost breakdown
15.2	Operational Profit vs Time
	Future Project Design & Development Logic Flow Diagram part 1
22.2	Future Project Design & Development Logic Flow Diagram part 2

C_{T_n} Thrust coefficient of primary rotor List of Symbols Thrust coefficient of the downwind secondary $C_{T_{s_{up}}}$ Thrust coefficient of the upwind secondary ro-Latin Thrust coefficient of secondary rotor δA_D $C_{T_{\circ}}$ Annular ring area Thrust coefficient δF_{T_s} Thrust force exerted by a secondary rotor blade C_T DRotor diameter m δQ Torque exerted by a secondary rotor blade ele-Generator diameter D_q mDiameter secondary rotor D_{sr} m δr Radial width of a blade element EYoung's Modulus PaMaximum lift over drag ratio of an airfoil Young's modulus in longitudinal direction Pa E_{11} Maximum thickness over chord ratio of an air- E_{12} Young's modulus in transverse direction Pa $\Psi_V(k_X)$ Volume wise source transform E_{eff} effective Young's modulus PaPoisson ratio F_B Braking force N v_{12} kN/m^2 Secondary rotor tangential induction factor a'_{s} Force density m^2 F_{nor} A_b Turbine blade area Normal force on a blade element N m^2 Area of primary rotor Power factor A_p Rotor area A_r Root loss factor A_s Area of secondary rotor F_{T_s} Secondary rotor thrust force N a_s Secondary rotor axial induction factor Tangential force on a blade element N m^2 Actuator disc area A_D Tip loss factor f_{tip} a_l width of a laminate Shear modulus Pa G_{12} Tower cross-sectional area effective shear modulus PabScaling factor for thrust coefficient HTower height m b_l length of a laminate mhHub height mStringer pitch m^4 b_s mΤ Second moment of area C_i Constant specified by the number i Imaginary number Secondary rotor blade chord length c_s m k_x Wave number C_d Airfoil drag coefficient K_c Compression buckling coefficients C_{l_0} Airfoil lift coefficient for M=0 K_{opt} Optimal mode gain $C_{l_{des}}$ Design lift coefficient Shear buckling coefficients K_s C_l Airfoil lift coefficient l_g Generator length m C_m Airfoil moment coefficient Overall A-weighted sound intensity level dB(A) L_{pA} C_{P_n} Power coefficient of primary rotor l_s Vertical axis secondary rotor blade length Power coefficient of the downwind secondary Overall A-weighted sound power level dB(A) L_{WA} rotor MMach number $C_{P_{s_{np}}}$ Power coefficient of the upwind secondary rotor mStructure mass kg M_{∞} Mach number incoming flow C_{P_s} Power coefficient of secondary rotor m_{blade} Blade mass Chord-to-diameter ratio kg c_{sD} Secondary rotor centrifugal force C_{SR} N M_{qen} Generator mass kg

m_{harm}	The m^th harmonic of the natural freque	ency –	t_b	Thickness-to-chord ratio	_
M_{max}	Maximum achieved Mach number	_	T_g	Generator torque	Nm
M_{rel}	Relative section mach number	_	t_t	time	sec
M_{SR}	Secondary rotor torque	Nm	T_B	Braking torque	Nm
M_{tip}	Mach number acting on SR rip	_	t_l	thickness of a laminate	m
m_{tower}	Tower mass	kg	T_p	Torque generated by primary rotor	Nm
MOM	max Maximum aerodynamic moment	Nm	$T_{s_{down}}$	Braking torque generated by the downwin	
n	Number of investment years	_		ondary rotor	Nm
N_b	Number of blades secondary rotor	_	$T_{s_{up}}$	Braking torque generated by the upwind ondary rotor	$\frac{1}{Nm}$
N_{b_p}	Number of blades primary rotor	_	T_{SR}	Secondary rotor thrust force	N
p	Sound pressure	Pa	T_s	Braking torque generated by secondary	rotor
P_D^+	Pressure in front of actuator disc	Pa			Nm
P_D^-	Pressure behind actuator disc	Pa	V_{∞}	Free stream velocity	m/s
P_g	Generator power	W	V_{cut-ir}	¹ Cut in wind speed	m/s
$P_{\rm inf}$	Free stream pressure of actuator disc mo	del Pa	V_{cut-o}	ut Cut out wind speed	m/s
P_{gen}	Power output capacity of generator	MW	V_D	Wind velocity at actuator disc	m/s
P_{loadm}	harm Fourier transform for loading effects	s –	V_F	fibre volume fraction	Pa
P_{mB}	Fourier transform of the pressure	_	V_{rel}	Relative wind velocity at blade element	m/s
P_{mV}	Fourier transform for thickness effects	_	V_r	Rated velocity	m/s
P_p	Power extracted by the primary rotor	W	$V_{s_{\omega}}$	Upstream velocity secondary rotor due to mary rotor rotation	o pri- m/s
	T 0			· ·	
p_{ref}	Reference pressure $2 \cdot 1$	$0^{-5}Pa$	$V_{s_{down}}$	Wind velocity seen by the downwind second	ndary
p_{ref} P_r	Reference pressure $2 \cdot 1$ Turbine rated power	$0^{-5}Pa$ W	$V_{s_{down}}$	Wind velocity seen by the downwind secon rotor	m/s
		W	$V_{s_{down}}$ $V_{s_{up}}$		m/s
P_r	Turbine rated power Power extracted by the downwind second	W ondary W y rotor	$V_{s_{up}}$	rotor Wind velocity seen by the upwind second	m/s and ary m/s
P_r $P_{s_{down}}$ $P_{s_{up}}$	Turbine rated power Power extracted by the downwind secondar rotor Power extracted by the upwind secondar	W ondary W y rotor W	$V_{s_{up}}$	rotor Wind velocity seen by the upwind second rotor	m/s and ary m/s
P_r $P_{s_{down}}$	Turbine rated power Power extracted by the downwind second rotor	W ondary W y rotor	$V_{s_{up}}$ V_{s}	rotor Wind velocity seen by the upwind secondary rotor Total upstream velocity of secondary rotor	m/s mdary m/s r m/s
P_r $P_{s_{down}}$ $P_{s_{up}}$	Turbine rated power Power extracted by the downwind secondar rotor Power extracted by the upwind secondar	W ondary W y rotor W W	$V_{s_{up}}$ V_{s} $V_{t_{p}}$	rotor Wind velocity seen by the upwind secondary rotor Total upstream velocity of secondary rotor Tip speed primary rotor	m/s and ary m/s or m/s m/s
P_r $P_{s_{down}}$ $P_{s_{up}}$ P_{sys}	Turbine rated power Power extracted by the downwind secondar Total power of the system	W ondary W y rotor W W	$V_{s_{up}}$ V_{s} $V_{t_{p}}$ $V_{t_{s}}$	rotor Wind velocity seen by the upwind secondary rotor Total upstream velocity of secondary rotor Tip speed primary rotor Tip speed secondary rotor	m/s and ary m/s ar m/s m/s m/s
P_r $P_{s_{down}}$ $P_{s_{up}}$ P_{sys} P_s	Turbine rated power Power extracted by the downwind secondar Power extracted by the upwind secondar Total power of the system Power extracted by the secondary rotor	W ondary W y rotor W W W	$V_{s_{up}}$ V_{s} $V_{t_{p}}$ $V_{t_{s}}$ V_{t}	rotor Wind velocity seen by the upwind secondary rotor Total upstream velocity of secondary rotor Tip speed primary rotor Tip speed secondary rotor Tip speed	m/s ndary m/s r m/s m/s m/s m/s m/s m/s
P_r $P_{s_{down}}$ $P_{s_{up}}$ P_{sys} P_s r_0	Turbine rated power Power extracted by the downwind secondar Power extracted by the upwind secondar Total power of the system Power extracted by the secondary rotor Distance tower base to observer	W ondary W y rotor W W W m	$V_{s_{up}}$ V_{s} $V_{t_{p}}$ $V_{t_{s}}$ V_{t} V_{wind}	rotor Wind velocity seen by the upwind secondary rotor Total upstream velocity of secondary rotor Tip speed primary rotor Tip speed secondary rotor Tip speed V_{∞} perpendicular to SR	m/s ndary m/s r m/s m/s m/s m/s m/s m/s
P_r $P_{s_{down}}$ $P_{s_{up}}$ P_{sys} P_s r_0 r_i	Turbine rated power Power extracted by the downwind secondar Power extracted by the upwind secondar Total power of the system Power extracted by the secondary rotor Distance tower base to observer Inner radius	W ondary W y rotor W W W m m	$V_{s_{up}}$ V_s V_{t_p} V_t V_t V_{wind} V_W	rotor Wind velocity seen by the upwind secondary rotor Total upstream velocity of secondary rotor Tip speed primary rotor Tip speed secondary rotor Tip speed Component of V_{∞} perpendicular to SR Far wake wind velocity of the actuator disc	m/s ndary m/s r m/s m/s m/s m/s m/s m/s c m/s
P_r $P_{s_{down}}$ $P_{s_{up}}$ P_{sys} P_s r_0 r_i	Turbine rated power Power extracted by the downwind secondar Power extracted by the upwind secondar Total power of the system Power extracted by the secondary rotor Distance tower base to observer Inner radius Outer radius	W ondary W y rotor W W W m m	$V_{s_{up}}$ V_s V_{t_p} V_t V_t V_{wind} V_W v_l	rotor Wind velocity seen by the upwind secondary rotor Total upstream velocity of secondary rotor Tip speed primary rotor Tip speed secondary rotor Tip speed Component of V_{∞} perpendicular to SR Far wake wind velocity of the actuator discontant of a laminate	m/s adary m/s x m/s
P_r $P_{s_{down}}$ $P_{s_{up}}$ P_{sys} P_s r_0 r_i r_o r_{gearbo}	Turbine rated power Power extracted by the downwind secretor Power extracted by the upwind secondar Total power of the system Power extracted by the secondary rotor Distance tower base to observer Inner radius Outer radius Gearbox ratio	W ondary W y rotor W W m m -	$V_{s_{up}}$ V_{s} V_{t_p} V_{t_s} V_{t} V_{wind} V_{W} w_l W_{SR}	wind velocity seen by the upwind secondary rotor Total upstream velocity of secondary rotor Tip speed primary rotor Tip speed secondary rotor Tip speed Component of V_{∞} perpendicular to SR Far wake wind velocity of the actuator discondary rotor weight	m/s adary m/s x m/s
P_r $P_{s_{down}}$ $P_{s_{up}}$ P_{sys} P_s r_0 r_i r_o r_{gearbo} r_{obs}	Turbine rated power Power extracted by the downwind secretor Power extracted by the upwind secondar Total power of the system Power extracted by the secondary rotor Distance tower base to observer Inner radius Outer radius Gearbox ratio Distance rotor hub to observer	W ondary W y rotor W W m m m	$V_{s_{up}}$ V_{s} V_{t_p} V_{t_s} V_{t} V_{wind} V_{W} w_l W_{SR} z	rotor Wind velocity seen by the upwind secondary rotor Total upstream velocity of secondary rotor Tip speed primary rotor Tip speed secondary rotor Tip speed Component of V_{∞} perpendicular to SR Far wake wind velocity of the actuator disc transverse displacement of a laminate Secondary rotor weight Radius ratio secondary rotor Imaginary number	m/s ndary m/s r m/s m/s m/s m/s m/s m/s m/s m/s n/s m/s -
P_r $P_{s_{down}}$ $P_{s_{up}}$ P_{sys} P_s r_0 r_o r_{obs} r_p	Turbine rated power Power extracted by the downwind secondar Power extracted by the upwind secondar Total power of the system Power extracted by the secondary rotor Distance tower base to observer Inner radius Outer radius Gearbox ratio Distance rotor hub to observer Radius of the primary rotor	W ondary W y rotor W W m m m m	$V_{s_{up}}$ V_{s} V_{t_p} V_{t_s} V_{t} V_{wind} V_{W} W_{SR} z	rotor Wind velocity seen by the upwind secondary rotor Total upstream velocity of secondary rotor Tip speed primary rotor Tip speed secondary rotor Tip speed Component of V_{∞} perpendicular to SR Far wake wind velocity of the actuator disc transverse displacement of a laminate Secondary rotor weight Radius ratio secondary rotor Imaginary number	m/s ndary m/s r m/s m/s m/s m/s m/s m/s m/s m/s n/s m/s -
P_r $P_{s_{down}}$ $P_{s_{up}}$ P_{sys} P_s r_0 r_i r_{obs} r_p R_s	Turbine rated power Power extracted by the downwind secretor Power extracted by the upwind secondar Total power of the system Power extracted by the secondary rotor Distance tower base to observer Inner radius Outer radius Gearbox ratio Distance rotor hub to observer Radius of the primary rotor Secondary rotor radius	W ondary W y rotor W W m m m - m m - m	$V_{s_{up}}$ V_s V_{t_p} V_{t_s} V_t V_{wind} V_W w_l W_{SR} z i	rotor Wind velocity seen by the upwind secondary rotor Total upstream velocity of secondary rotor Tip speed primary rotor Tip speed secondary rotor Tip speed Component of V_{∞} perpendicular to SR Far wake wind velocity of the actuator disc transverse displacement of a laminate Secondary rotor weight Radius ratio secondary rotor Imaginary number k	m/s andary m/s m/s
P_r $P_{s_{down}}$ $P_{s_{up}}$ P_{sys} P_s r_0 r_i r_{obs} r_p R_s Re	Turbine rated power Power extracted by the downwind secretor Power extracted by the upwind secondar Total power of the system Power extracted by the secondary rotor Distance tower base to observer Inner radius Outer radius Gearbox ratio Distance rotor hub to observer Radius of the primary rotor Secondary rotor radius Reynolds number	W ondary W y rotor W W m m m - m m - m	V_{sup} V_s V_{t_p} V_{t_s} V_t V_{wind} V_W w_l W_{SR} z i $Gree$	rotor Wind velocity seen by the upwind secondary rotor Total upstream velocity of secondary rotor Tip speed primary rotor Tip speed secondary rotor Tip speed Component of V_{∞} perpendicular to SR Far wake wind velocity of the actuator disc transverse displacement of a laminate Secondary rotor weight Radius ratio secondary rotor Imaginary number k Angle of attack	m/s adary m/s r m/s m/s m/s m/s m/s m/s m/s m/s
P_r $P_{s_{down}}$ $P_{s_{up}}$ P_{sys} P_s r_0 r_i r_o r_{obs} r_p R_s Re s_{11C}	Turbine rated power Power extracted by the downwind secondar Power extracted by the upwind secondar Total power of the system Power extracted by the secondary rotor Distance tower base to observer Inner radius Outer radius Gearbox ratio Distance rotor hub to observer Radius of the primary rotor Secondary rotor radius Reynolds number ultimate longitudinal compressive streng	W ondary W y rotor W W m m m - m m m m P gth Pa	V_{sup} V_{sup} V_{tp} V_{ts} V_{twind} V_{W} W_{SR} z i $Gree$ α β	rotor Wind velocity seen by the upwind secondary rotor Total upstream velocity of secondary rotor Tip speed primary rotor Tip speed secondary rotor Tip speed Component of V_{∞} perpendicular to SR Far wake wind velocity of the actuator disc transverse displacement of a laminate Secondary rotor weight Radius ratio secondary rotor Imaginary number k Angle of attack Geometric angle of twist	m/s adary m/s r m/s m/s m/s m/s m/s m/s m/s m/s
P_r $P_{s_{down}}$ $P_{s_{up}}$ P_{sys} P_s r_0 r_i r_o r_{gearbo} r_{obs} r_p R_s Re s_{11C} s_{11T}	Turbine rated power Power extracted by the downwind secondar Power extracted by the upwind secondar Total power of the system Power extracted by the secondary rotor Distance tower base to observer Inner radius Outer radius Gearbox ratio Distance rotor hub to observer Radius of the primary rotor Secondary rotor radius Reynolds number ultimate longitudinal compressive streng ultimate longitudinal tensile strength	W ondary W y rotor W W m m m - m m m Pa	V_{sup} V_{sup} V_{tp} V_{ts} V_{twind} V_{W} W_{SR} z i $Gree$ α β	rotor Wind velocity seen by the upwind secondary rotor Total upstream velocity of secondary rotor Tip speed primary rotor Tip speed secondary rotor Tip speed Component of V_{∞} perpendicular to SR Far wake wind velocity of the actuator disc transverse displacement of a laminate Secondary rotor weight Radius ratio secondary rotor Imaginary number k Angle of attack Geometric angle of twist Efficiency	m/s adary m/s r m/s m/s m/s m/s m/s m/s m/s m/s

γ_2	Blade pitch angle signal from second sensor rad	FCR Fixed charge rate $1/yr$
γ_d	Desired blade pitch angle signal input to con-	FFD Functional Flow Diagram
	trol loop rad	GDPE Labor cost escalator
γ_{in}	Blade pitch angle signal input to control loop rad	GRFP Glass fiber reinforced polymer
λ	Annual turbine failure rate $failures/yr$	HASR Horizontal Axis Secondary Rotor
λ_p	Tip speed ratio of primary rotor –	HAWT Horizontal Axis Wind Turbine
λ_s	Tip speed ratio of secondary rotor –	HVAC High voltage alternating current $-$
λ_a	Tip speed ratio	HVDC High voltage direct current $-$
μ_f	Friction coefficient –	ICC Initial capital cost \$
μ_r	Non-dimensional radial position –	IRENA International Renewable Energy Agency
μ_{root}	Non-dimensional radial position of rotor	LLC Land lease cost $$/yr$
	blade's root –	LRC Levelised replacement/overhaul cost $$/yr$
ω_g	Generator rotational velocity rad/s	MIMO Multi-Input Multi-Output
ω_1	Angular velocity signal from first sensor rad/s	MTBF Mean time between failures hours
ω_2	Angular velocity signal from second sensor rad/s	MTTF Mean time to failure hours
Ω_{gen}	Rotational speed of generator rpm	MTTR Mean time to repair hours
ω_{in}	Angular velocity signal input to control loop	MVDC Medium voltage direct current $-$
111	rad/s	NREL National Renewable Energy Laboratory
Ω_p	Angular velocity of the primary rotor pm	O&M Levelised $O&M$ cost $$/yr$
ω_p	Angular velocity of the primary rotor rad/s	OP Operational Profit \$
Ω_s	Angular velocity of the secondary rotor pm	PdM Predictive maintenance –
ω_s	Angular velocity of the secondary rotor $\ rad/s$	PI Proportional-Integral
Φ	Inflow angle rad	PID Proportional-Integral-Derivative
ho	Air density kgm^{-3}	POE Price Of Energy $$/MWh$
σ_{cl}	Critical load Pa	PPA Power Purchasing Agreements
θ	Angle of rotation of primary rotor rad	PR Primary Rotor
θ_{obs}	Radiation angle observer rad	PvM Preventive maintenance –
Acre	onyms	RAMS Reliability, availability, maintainability,
AC	Alternating current –	safety –
AEP_n	kWh/yr Net annual energy production kWh/yr	RCC Reliability-centred maintenance –
AOE	Annual operation expenses $\$/yr$	RM Reactive maintenance –
BCE	Blade material cost escalator	ROI Return on investment %
BEM	Blade Element Momentum	rpm Rotations per minute
BLC	Bottom Lease Cost $\$/yr$	RTM Resin Transfer Moulding
BPF	Blade pass frequency	SPL Sound Pressure Level $dB(A)$
CFD	Computational fluid dynamics –	SR Secondary Rotor
CLT	Classical Lamination Theory	SRVAWT Secondary Rotor Vertical Axis Wind Tur-
COE	Cost of Energy $\$/MWh$	bine
CRFI	Carbon fiber reinforced polymer	VASR Vertical Axis Secondary Rotor
DC	Direct current –	VAWT Vertical Axis Wind Turbine
FBS	Functional Breakdown Structure	VSE Variable Speed Electronics

List of Changes

Overview of changes made to the report.

Version 1.1

- The cost analysis has been revisited. It has a new (lower) Fixed Charge Rate which lowers the cost of energy. The wholesale cost has also been changed which lowers the return of investment.
- General spelling, grammar and consistency errors have been corrected
- The pie charts in the reliability and availability sections (section 12.1 and section 12.2) have been replaced by bar charts showing the annual failure rates and repair times, respectively
- \bullet Operations and logistics section within executive overview has been re-formulated
- Attachment section in the structures section has been changed
- Correction of mass breakdown
- Alteration of the key sustainability goals

Executive overview

Wind turbines have been growing in size and capacity rapidly the past years. A shift is also happening from onshore wind turbines to offshore applications. Going offshore means that there are higher wind speeds and turbines can be bigger. A limit to this increase in size however is the drivetrain, as it becomes very large and heavy for increasing capacities.

The aim of this project is to reduce the drive train weight of a 10MW offshore wind turbine and by doing so, reduce the overall weight of the turbine. This shall be done using a large vertical axis primary rotor that will support secondary rotors attached to generators. Due to the rotation of this primary rotor, the secondary rotors will see larger wind speeds, increasing the rotational velocity of these rotors. This increase in rotational velocity reduces the torque and drivetrain mass. In this project, it has to be ensured that this decrease in mass does not increase the cost or decrease the reliability of the system, as it still has to be competitive on the wind energy market.

Conceptual and preliminary design phases

The project was started by performing a conceptual brainstorm session. Here, many ideas were put forward and nine concepts were proposed. Of these nine, only three made it to the preliminary design phase, at the end of which a trade off was held. In this trade off, the three designs were scored on cost of energy, mass, RAMS and risk. It was found that two primary rotor blades, both with a 5-bladed horizontal axis secondary rotor attached to it at the end of their lower blades, is best. This design was taken forward into a more detailed design phase, which is the scope of this report.

Layout and sizing

As one final design is chosen to move forward with, a more detailed analysis is done on the chosen design. This starts with an initial sizing. An equation is derived to estimate the size of the primary rotor and it is seen that the induction factor of the secondary rotor will be a key parameter, since it represents the efficiency loss between primary and secondary rotor. Based on the chosen induction factor, both a primary and secondary rotor are sized and the required generator capacity can be determined. The results of this chapter are shown in Table 1. With these initial sizes, an aerodynamic analysis can be performed.

Table 1: Summary table initial sizing

Parameter	Value
a_s	0.05
$A_p [m^2]$	33,108
$r_p [m]$	90.98
A_s $[m^2]$	469
r_s $[m]$	12.22
$P_{gen}[MW]$	7.5

Aerodynamic Design

The aerodynamic design of the secondary rotors only requires the power and thrust coefficients, and most importantly, the axial induction factor, that needs to be designed for, as found by the sizing of the system. Using a BEM model in Python, including Prandtl tip and root losses, many different designs are analysed on their performance. First off, two different airfoils are chosen. The LS-0417 MOD airfoil is used for the part of the blades ranging from the root up until 70% of the blade length. The rest of the blade contains the NASA SC-0410 airfoil because of its performance at transonic flow conditions. Next, it is found that the hub needs a radius of 20% of the rotor radius. The planform of the blades are represented by a linear chord distribution and a quadratic twist distribution. The chord varies linearly from 2.95m at the root to 0.75m at the tip. The twist varies quadratically from 37.8 degrees at the root to 5 degrees at the tip. This design is able to reach an axial induction factor of 0.05 at a tip speed ratio of 2.2 and non pitched blades. In addition, it is able to achieve an

axial induction of 0.25 at a tip speed ratio of 3.8 and non pitched blades.

Once the aerodynamic shape and loading of the secondary rotor are determined, a noise analysis is performed to determine the sound pressure levels the entire system would produce. The sound pressure levels are determined over one full rotation of the primary rotor. In case of the observer standing at the foot of the tower, the sound pressure level experienced will be approximately 62.2dB(A). When the observer is located at a distance of 100 meters away from the tower, it is estimated one will experience a sound pressure level of 79.2dB(A). Since for the latter the pressure is averaged out over one rotation of the turbine, actual experienced values will fluctuate significantly due to this rotation. With the aerodynamics analysis done, the control system can be defined. After that, the aerodynamic characteristics will be used to simulate the control system.

Supervisory control and safety system

To ensure automatic and safe operation a control concept is developed. This consists of a supervisory control concept and a safety concept. Both concepts are enforced by an arrangement of sensors and actuators. The safety system is activated by certain failures such as the primary rotor pitch system failing. The safety system is also triggered such that rotor overspeed and runaway can be prevented. Two systems are used to decelerate the rotor. The first way is to pitch the primary blades to feather. The second is by increasing the thrust in the secondary rotors, which will create a torque that will counter the torque of the primary rotor. This method in reverse is used to jump start the wind turbine. Data handling, communication flow and architecture diagrams are used to give a clear overview of how the control system and its parts work, but also functional block diagrams are made to show what the start and (emergency) stop procedures of the turbine look like. To make it complete, a table was made showing a set of failures and faults, together with a list of the components that they affect, what the cause can be, how it can be detected, the effect that it will have on the turbine and what measures have to be taken. A functional analysis including a functional flow diagram and breakdown structure help by determining the control concepts and designing the control systems. With the interactions between the control systems known, a control optimization strategy can be defined.

Control optimization strategy

The control optimization strategy is a method to estimate the required tip velocities, rotational velocities, torques and other performance characteristics for the primary and secondary rotors. This is done by using a python program that has the aerodynamic characteristics, dimensions of the rotors and range of wind velocities as input. The limit input and output values come as a result from the control strategy simulation and are shown in Table 2. These are the limiting values that can be obtained and for which must be designed.

Table 2: Summary of the limiting input and output design values at a wind velocity of 25 m/s

Innut nanamatan	Limiting
Input parameter	value
$a_{s_{max}}$	0.20
$Cp_{s_{max}} (a_s = 0.05)$	0.13
$\lambda_{s_{opt}} \ (a_s = 0.05)$	2.10
$Cp_{p_{max}}$	0.39
$\lambda_{p_{ont}}$	4.65

Output parameter	Limiting value
$V_{tip_p}[\frac{m}{s}]$	85.5
Mach secondary	0.75
$\Omega_p[rpm]$	6.35
$\Omega_s[rpm]$	200
Generator torque [kNm]	770

Power and electronics

Once a torque is obtained from the performance analysis based on the control strategy, a generator can be sized. First, the mass is obtained based on the assumption that the mass relates to torque linearly by $25\frac{kg}{kNm}$. With the mass, the cost of the generator is estimated based on material mass fractions and specific costs. Finally, the generator is sized using initial sizing formulas. The results of this analysis are shown in Table 3. Here, the cost of power electronics is also included as well as the fact that there are two generators in this wind turbine. Finally, an electrical block diagram is constructed that shows the flow of energy from power extraction from the wind offshore to power supply to the grid onshore. The generator mass obtained from these calculations will be used in the structural analysis, in combination with all other loads, such as those found from the aerodynamics analysis. The generator cost can be used for the cost analysis later on.

Table 3: Summary table drivetrain

Generator torque [kNm]	770
Generator length [m]	1.2
Generator diameter [m]	4.0
Mass of single generator [ton]	19.25
Cost of single generator [k€]	189.4
Total power electronics cost [k€]	600
Total drivetrain cost [k€]	987.8

Structures

In order to start a structural analysis of the wind turbine, parameters such as the size of the wind turbine, blade characteristics and the dynamics of the wind turbine are required, which are obtained from the previous chapters. These values are used to calculate the loading on the main wind turbine components such as the secondary rotor, the primary rotor, the strut and the tower. Based on the loading cases, the structure of the each component is made and optimised. In order to design a complex structure of the secondary rotor, the program called Co-Blade was used. With the help of Co-blade, the structure of secondary rotor was designed and optimized. The metal wingbox structure was designed for the primary rotor at the beginning, however, it was later changed to the glass fiber composite wingbox due to the metal wingbox calculated to be too heavy. As for the strut, the steel wingbox structure was implemented to account for the high bending moment. The tower is made with steel tubular structure as this structure is commonly used for the wind turbine tower. Table 4 shows material and mass of each component where mass of the secondary rotor includes 10 secondary rotor blades and mass of the primary rotor includes 2 upper blades and 2 lower blades.

Table 4: Summary table structure

Component	Material	Mass [ton]
Secondary rotor	Glass fiber, epoxy, foam	21.7
Primary rotor	Glass fiber, epoxy	314
Tower and strut	Steel	500

Production plan

As of this point, the design is finished and a plan can be made on how the turbine should be built. The production plan contains a description of the manufacturing, assembly and installation phases of the secondary rotor vertical axis wind turbine. The manufacturing methods of the key components are presented. The glass fiber reinforced polymer (GFRP) wind turbine blades are produced by the Vacuum Assisted Resin Transfer Moulding (VARTM) method since this method is most suited to large composite structures. The steel towers are manufactured by the process of rolling and the composite nacelle structure is produced by filament winding. The manufactured parts are then transported to an assembly site onshore, close to the waterfront such that the loading of the components on the installation vessels is more cost and time efficient. The components are assembled as much as possible to reduce installation time, and therefore cost, offshore. The installation process of the SRVAWT is then presented in order to show how the wind turbine is going to be installed and put into operation.

Operations

After producing, manufacturing and installing a wind turbine, one more phase is required before the turbine can be operated, namely commissioning. During commissioning, the whole systems is tested within its operational environment. This includes the safety and braking systems and the supervisory control system, as well as data registration systems. After being commissioned, the turbine operates and is susceptible to degradation or damage. Therefore, a combination of preventive and predictive maintenance strategies is proposed. This includes monitoring the turbine's health from the start, by use of the Supervisory Control and Data Acquisition (SCADA) system, the Condition Monitoring system and the Structural Health Monitoring (SHM) system. In addition to the predictive maintenance strategy development, preventive maintenance activities were planned on a half yearly basis, comprising to 50 hours of preventive routine maintenance annually. The last logistical

problem encountered in the turbine's life is decommissioning. The turbine should be taken away from its location and investigated for reusable items. During the operational life time of the turbine, however, some more aspects are to be considered. These include reliability, availability and safety issues.

RAMS

Reliability and availability estimates are made using numbers from a 2015 Strathclyde study, on which modifications are made to account for the difference in turbine configuration of the SRVAWT compared to conventional turbines. An annual failure rate of about 13.4 is expected, which is significantly higher than that of conventional turbines (8.27 failures/year) and can be largely attributed to the increase in number of pitch systems. A total annual repair time of 131.8 hours is expected, again slightly higher than that of conventional turbines (111.9 hours), resulting in slightly lower availability. To improve availability, a failure-tolerant mode of operation is proposed, in which the turbine continues operation after the failure of a secondary rotor pitch system. An outline of maintenance activities is provided, including service and inspections, repairs and overhaul and modernization activities. Safety is elaborated on, including the safety of personnel during activities on the turbine, as well as the safety of the turbine itself. Turbine safety is described using a list of safety critical functions, as well as a description of how redundancy has been applied in the SRVAWT design.

Risk

To properly manage the risks of the turbine, several steps have to be taken. The first step is to identify the technical risks that the current design has. These events are then assessed based on the likelihood of occurrence and the severity of the risk. A risk register is made with the identified and assessed risk events, but also a risk map is made to identify the risks that could be threat to the turbine. For certain risk events a mitigation plans is developed to reduce the risk of these events. All of these risk events can be found in a risk register, together with there possible cause, the consequence that they will have and their scores on likelihood of occurrence and severity. Since the risk register is a thing that changes continuously, most of the risks were already assessed in previous stages. However, a few risks can be added and removed as a result of this design stage. Most notably, the risk of gearbox failure is no longer applicable due to the choice for a direct-drive configuration. Based on the high rotational velocities of the secondary rotors, the risk of excessive erosion is added. Fatigue of the pitch bearings is also added, due to the intensive use of pitching to follow the power curve.

Sustainability

Wind energy is already a crucial part of the global energy supply and its importance is steadily increasing. As the world population and the demand for green energy are both increasing there is a demand for more efficient and thus larger wind turbines. For a good sustainability approach, it is therefore necessary to minimise the environmental impact during the entire lifetime of the system while still providing a low cost of energy. During the design, production and installation phase there are some sustainability aspects that must be considered with respect to the environment: material choice, required production energy, required energy for the onshore and offshore assembly, transportation, installation at sea and the trenching cables under the seabed. During the operational phase, the following sustainability aspects must be considered: noise effects, vibration effects, harmful materials and coatings, fish surrounding the wind farm, transition of sediment, life cycle and maintenance. During the decommissioning phase, the following aspects must be considered: re-powering of the wind turbines, detachment of the wind turbines, transportation and recycling.

Cost

Now that the whole turbine has been developed and assessed, it is time to determine its most important characteristic, namely the price for which it generates electrical power. Cost analysis of the wind turbine is done using design parameters obtained from sizing, power and structures. A cost breakdown structure was made by calculating non recurring cost and recurring cost. Cost of energy is calculated to have a range of 47.8 to 58.5[€/MWh] based on the cost breakdown, which is below the range of conventional offshore wind turbine [1]. Based on the cost breakdown structure and substation cost, operational profit is calculated over 25 years operational period. Payback period is calculated to be 11 years from the operational profit. Furthermore, return on investment is calculated according to operational profit which is determined to be 67.8%. Finally, an annual return on investment of 2.09% is calculated from the operational profit.

Market analysis

An updated market analysis is performed, this time using the actual cost of energy of the SRVAWT. It is found that the cost of energy is within the range of conventional turbines $(60 - 80 \\in / MWh)$. It is thus not especially cheaper or more expensive than currently operating turbines, which is why more emphasis is placed on the future: a lot of competitiveness is expected from jumping in on market trends and developments. Most notably, a benefit of the SRVAWT is that is expected to be relatively simple to upscale by adding more primary rotors, whereas upscaling introduces significant additional loading within conventional turbines. Based on the installation of 200 to 500 SRVAWTs, a 5% market share is taken as a goal within the European offshore wind energy market by the year 2040.

Technical Resource Budgeting

With the design in place and the cost of the current design determined, a look can be taken at how the mass and cost of the turbine evolved over the several different design maturities. An overview is given in Table 5. Initially budgets for the total turbine mass an cost of energy had been set, which were 1300 tonnes and 60-80 euros per MWh respectively. Over the different design phases values for mass and COE have been determined and compared to the budget to make sure their values would not get unbounded. In the end it was found that both the turbine mass and the COE were within their set bounds.

	Total mass	COE [€/MWh]
Budget	1300 tonnes	60-80
Preliminary design	2487 tonnes	90.25
Refined preliminary design	914 tonnes	47.8 to 58.5

Table 5: Overview of budgets for different design maturities

Sensitivity analysis

The current design is not a final, detailed design that will be built. More design iterations and more sophisticated analyses are needed. At this point, a maximum offset of 10% is used. To check this, a sensitivity analysis is performed on the system as a whole. By changing the values of secondary rotor tip speed ratio and the secondary rotor's maximum power coefficient by 10% and analysing the resulting new design on mass and cost characteristics, a range of new limiting values is established. From this analysis it is concluded that the design will perform within acceptable ranges if design parameters change by a maximum of 10%.

Conclusion

The aim of the project was to reduce drive train mass, this has definitely been accomplished as a drive train mass reduction of 84% was achieved compared to a conventional wind turbine of the same power output. The design can achieve this power output with a primary rotor radius of 91m and a secondary rotor radius of 12.2m. The cost of energy was calculated to have a range of 47.8 to $58.5 \le /MWh$ and stays below the competitive boundaries with this range. Even though there is no gearbox or yaw system in this design, the reliability could not be improved. This is caused by the many pitch systems that are involved in the control of this wind turbine. As the secondary rotor rotates at high speeds, causing Mach numbers up to 0.75 at the blade tips, the noise levels have to be assessed. These noise levels were calculated to be 79.2dB at a distance of 100m.

Limitations and recommendations

During the project, some limitations were encountered. During most of the BSc courses, the focus has been on designing aircraft. This means that a lot of literature study and additional research had to be done along the way as this design is also a very new concept. This additional research gave rise to an additional problem, the time limitations. Due to time constraints, not all analyses have been done and there is still room for improvement. Recommendations that can be made for future activities are first of all upscaling of the system. Secondly, the operation and maintenance cost can be looked into in more detail to reduce the cost of energy. This design might be well suited for a floating offshore structure. This is something that can also be investigated further.

Chapter 1: Introduction

Renewable forms of energy have been used for a long time. Starting simple with solar energy that powers entire ecosystems for the production of food and using biomass like wood for heating. Wind energy has been used in the past as a primary means of propulsion for sail ships and to power windmills. The first type of windmill was used by the Persians in the 9th century. This was a drag based vertical axis windmill that was used to grind corn. The first lift based windmills date back to the 12th century. The windmills usually had four blades attached to a post or tower. The entire system could then be rotated to face the wind. An example of this is the Dutch four arm wind mill [2]. This type of wind mill converted energy of the wind into mechanical energy that could be used by industries. In the early decades of the 20th century, a change in the power system occurred. Electrification was happening rapidly and the coal industry proved to be the cheapest for power production [3]. Renewable energy sources were not really considered anymore and the technology improvements in this sector could not keep up with the fossil fuels. This effect was reinforced by the increased use of oil as fuel in the transportation sector and the use of natural gas. The improvements in nuclear technology also meant that renewable energy sources became redundant. Denmark however kept investing in wind turbine technology. In the early years of the 20th century there were already hundreds of horizontal axis wind turbines installed to generate electricity. These were the first wind turbines as we know them today, however they only had a rotor diameter of 23m with power outputs up to 25kW [4]. Around the same time, the French engineer Darrieus also patented a vertical axis wind turbine. This type of wind turbine is also lift based like a conventional horizontal axis wind turbine. The difference is that it rotates around a vertical axis. The main advantage of such a turbine is that it is omnidirectional, meaning that there is no need to rotate it to face the wind. Furthermore, the turbine is more symmetric than a horizontal axis wind turbine, improving the stability [5].

By the end of the 20th century, people became more aware of the environment and emissions due to burning fossil fuels were questioned. This boosted the research in renewable energy and technological improvements were made in the field of wind energy. In the past decades, wind turbines have increased significantly in size and efficiency. While in 1990 the installed capacity of wind turbines in the world was close to 0GW, in 2009 this was already 160GW [6]. At the time of writing this report, the total installed wind power capacity has reached almost 600GW. The size of wind turbines has increased significantly over the past years as well. Where wind turbines had a rotor diameter of 25m in 1989, they currently have a rotor diameter of 162m. Over this period of time, the capacity of wind turbines also increased from 0.5MW to 10MW. Currently, a 12MW wind turbine is being built with a rotor diameter of 220m. A trend that is seen in the past years in the field of wind energy, is the fact that offshore wind energy is becoming increasingly popular. The reason for this is the reduction in cost of offshore wind energy, there have already been some zero-subsidy bids for offshore wind farms [7]. Before that, the wind energy sector relied on subsidies in order to attract investors. A downside of the increasing size of wind turbines is the increase in mass, especially the drivetrain mass of the turbine.

The aim of this project is to reduce this drivetrain mass and by doing so, reduce the total mass of the turbine. The challenge is reducing this mass while still being competitive on the wind energy market, this competitiveness can be analysed through the cost and RAMS characteristics of the system. In this project, a 10MW wind turbine will be designed for offshore purposes. The solution for the reduction in drivetrain weight is inspired by a concept drafted by the University of Strathclyde [8]. The main idea behind the concept is a vertical axis rotor that will convert energy from the wind in a rotational motion. However, this rotational motion will not be immediately converted into electrical power by a generator like in conventional turbines. Secondary rotors equipped with a generator are attached to the blades of the larger vertical axis rotor instead, these serve as a means to brake the primary rotor by producing thrust. Due to the displacement from the axis of rotation of the primary rotor, these secondary rotors will see larger wind speeds and thus rotate at higher rotational velocities than conventional turbines. These higher rotational velocities allow the torque on the rotating shaft to be lower, reducing drivetrain size and mass. In this report, a wind turbine will be designed and extensively analysed based on this concept and design challenges will be discussed and tackled. Due to the large rotational velocities of the secondary rotors, compressible flow phenomena have to be considered. Furthermore, the interaction between primary and secondary rotors in the control of this system has to be looked into.

The report is structured in the following manner. First, chapter 2 will give an overview of the requirements that the design should comply with. These requirements will drive the design. The chapter will cover technical

¹https://www.turbinegenerator.org/evolution-wind-turbines/ cited 20-06-2019

²https://wwindea.org/information-2/information/ cited 20-06-2019

³https://lynceans.org/tag/wind-turbine/ cited 20-06-2019

 $^{^{4} \}texttt{https://www.ge.com/renewableenergy/wind-energy/offshore-wind/haliade-x-offshore-turbine\ cited\ 20-06-2019}$

requirements as well as stakeholder requirements. Once the requirements are known, a brief overview of previous work is given in chapter 3. It will cover the conceptual design phase where multiple design options are shown. A trade-off is then performed in order to end up with one final design that enters the final design phase. This final design is more extensively described in chapter 4. The general layout of the system will be shown here, together with an initial sizing of both the primary and secondary rotors. After this initial sizing, a more detailed analysis of the design can be started as part of the preliminary design refinement phase.

This detailed design will begin with an aerodynamic analysis in chapter 5. It will output the required aerodynamic characteristics for other design departments. A general overview of the control system is given in chapter 6. It describes the sensors and actuators in the turbine, the nominal control operations and safety system. In chapter 7, this control strategy will then be translated into performance parameters using the previously calculated aerodynamic parameters as input. With these performance parameters, the drivetrain can be sized in chapter 8. An overview of the electrical components in a potential wind farm layout is also given in this chapter. The overall system is now sized, the aerodynamic parameters are known and the drivetrain mass is calculated. This means that all inputs are present in order to do a structural analysis. This analysis is done in chapter 9 for all the subsystems. The structural analysis will be performed starting from the outside and moving toward the center. This means that the secondary rotors will be analysed first. After that, the primary rotor and the horizontal strut are designed. Finally, the tower is considered and a total structural mass is calculated. After the structural analysis, a production plan is made in chapter 10. Here, manufacturing processes are considered based on the material choices made in the structural analysis. The assembly of the components and the offshore installation of the wind turbine will be discussed in this chapter as well. The report then continues with the operational phase in chapter 11, describing commissioning procedures, maintenance activities and the decommissioning phase. Now, the system is designed and the maintenance plan is drafted. These will flow into a RAMS analysis in chapter 12. After that, chapter 13 gives an overview of the technical risks involved in the design. Considering the previously described installation, decommissioning, maintenance and manufacturing activities together with the noise estimations from the aerodynamic analysis, a sustainability strategy is given in chapter 14. After all these analyses, a conclusion can almost be drawn regarding the design. The final element that is required for this is a cost estimation, which is done in chapter 15. In this chapter, a cost breakdown of the system is made. Using this, a cost of energy and payback period can be estimated.

The complete system is now analysed, so a market analysis is done in chapter 16. The focus of this chapter will be the current wind energy market and the place that the designed wind turbine will have in the wind energy market. A resource budgeting management is then described in chapter 17, this is required in order to know the margins of the budgets and the accuracy of the calculated design values. This accuracy is then used in the sensitivity analysis in chapter 18, where possible changes in input values are considered and the consequences of these changes for the design are described. This chapter covers the sensitivity analysis of the complete system. The sensitivity for each subsystem has already been done and is described in the analysis of each subsystem throughout the report. In chapter 19 a compliance matrix is shown where the user requirements are considered that were discussed in the beginning of the report. It can then be seen which requirements are met by the design. The requirements that were not met during the design process can influence the further recommendations for later design stages. After the compliance matrix, a conclusion can be drawn about the design in chapter 20. Limitations and recommendations will be given after the conclusion in chapter 21. A future planning will then be given in chapter 22. As a final note, it is important that all models and calculations are verified and validated. This is done separately for each subsystem and described in the corresponding chapter.

Chapter 2: Requirements

This chapter considers the requirements that have to be met by the design. It is important to take these requirements into account during the entire design phase. An overview of the stakeholders and their requirements is given in section 2.1. The technical requirements can be found in section 2.2. Out of these requirements, the killer requirements are identified in section 2.3 while the driving requirements are stated in section 2.4. This is done to make a clear distinction between requirements based on their importance.

2.1 Stakeholder Requirements

Stakeholder requirements include non-technical requirements flowing from the constraints of the product's mission with respect to its surroundings and operational situation. First the stakeholders must be identified, after which the requirements they set on the product design can be identified. For this wind energy project, the following stakeholders are identified:

- Client
- Government
- Environmental Considerations
- Manufacturers
- Offshore Contractors
- Media
- Fishing Industry
- Investors
- Energy Distributors

The identified requirements are listed in the following subsections per stakeholder.

Client

```
SRVAWT-CLI-01: Shall have a reduction in total cost from conventional wind turbines SRVAWT-CLI-01.1: Shall have a reduction in manufacturing costs SRVAWT-CLI-01.2: Shall have a reduction material costs SRVAWT-CLI-02: Shall have a reduction in overall structure weight compared to conventional wind turbines SRVAWT-CLI-03: Reliability shall be equivalent to conventional wind turbine SRVAWT-CLI-04: Shall have no increased risk from conventional wind turbine SRVAWT-CLI-05: Shall be more appealing in the market than competing designs
```

Government

```
SRVAWT-GOV-01: Shall follow codes and regulations
SRVAWT-GOV-01.1: Shall follow safety codes related to transport, on-site operations, installation
SRVAWT-GOV-01.2: Shall comply with noise regulations for its location
SRVAWT-GOV-01.2.1: Shall have acceptable noise levels during operation
SRVAWT-GOV-01.2.2: Shall have acceptable noise levels during installation of wind turbine
SRVAWT-GOV-02: Shall not interfere with existing naval activity
SRVAWT-GOV-02.1: Shipping lanes shall be avoided
SRVAWT-GOV-02.2: Military activity shall not be interfered with
SRVAWT-GOV-03: Shall not infringe on existing patents
```

Environmental Considerations

```
SRVAWT-ENV-01: Operational life shall have minimal impact on local wildlife
SRVAWT-ENV-01.1: Habitat and activity of fish shall be minimally disturbed
SRVAWT-ENV-01.2: Habitat and activity of birds shall be minimally disturbed
SRVAWT-ENV-02: Failure of system shall not result in harm to environment
SRVAWT-ENV-03: Maintenance of the system shall have low impact on environment
SRVAWT-ENV-04: Manufacture of the wind turbine shall be done with consideration to the environment
SRVAWT-ENV-04.1: Sustainable materials shall be utilized where possible
SRVAWT-ENV-04.2: Sustainable production methods shall be considered
SRVAWT-ENV-05: The parts shall be properly disposed of, when broken or turbine decommissioned
```

Manufacturers

```
SRVAWT-MNF-01: The system shall be possible to manufacture without requiring a giant leap in current knowledge
SRVAWT-MNF-02: The time constraint for manufacture shall be possible to meet for the manufacturer
SRVAWT-MNF-03: Materials used in manufacturing shall be safe
SRVAWT-MNF-04: Production methods required shall be safe
```

Offshore Contractors

```
SRVAWT-OSC-01: The system shall be safe to transport to its location SRVAWT-OSC-02: The sub-components shall be transportable with available resources SRVAWT-OSC-03: The method of installation shall be feasible SRVAWT-OSC-04: Installation shall be possible through the assembly of the sub-components SRVAWT-OSC-05: Location of the wind turbine shall be reachable from land
```

Media

SRVAWT-MED-01: The project shall have a good public image to prevent public or government interference

Fishing Industry

```
SRVAWT-FIS-01: There shall be no impact on the health of the fish in the surrounding area SRVAWT-FIS-02: The system shall not interfere with local fishing activity
```

Investors

```
SRVAWT-INV-01: The risks of the project shall be clearly communicated to the investors SRVAWT-INV-02: The project shall make a profit in its lifetime SRVAWT-INV-02.1: The break-even point shall be acceptable SRVAWT-INV-03: Association with the project shall not cause negative public relations impact
```

Energy Distributors

```
SRVAWT-NRG-01: Shall be at a location easily reachable by the electrical grid on-shore SRVAWT-NRG-02: Power output shall be compatible with the grid SRVAWT-NRG-03: Shall have a predictable range of operational power output
```

2.2 Technical Requirements

Technical requirements flow from physical constraints that a product faces. Some of these are specified by a client, in this case in [1], but most have to be established by the design team themselves. The technical requirements that have been identified are grouped in four branches, some of which were subdivided as well:

- Performance
- Safety and reliability
- Sustainability
- Engineering specifications of subsystems

Performance

Power Curve

```
SRVAWT-PRF-CUR-01: Cut-in speed shall be 3 ms<sup>-1</sup> SRVAWT-PRF-CUR-02: Furling speed shall be 25 ms<sup>-1</sup>
```

SRVAWT-PRF-CUR-03: Shall convert 10MW of power at rated speed

Power production mode

```
SRVAWT-PRF-PPM-01: Primary rotor shall not convert energy directly to electricity SRVAWT-PRF-PPM-01.1: The primary rotor shall not be connected to a generator SRVAWT-PRF-PPM-02: There shall be secondary rotors attached to the main rotor SRVAWT-PRF-PPM-03: Below rated speed, the secondary rotor torque shall counteract the primary rotor torque SRVAWT-PRF-PPM-04: Above rated speed, the control mechanism shall limit the RPM to the optimal value of [VAL]
```

Safety and Reliability

Operational Modes

```
SRVAWT-SAR-OPM-01: Safe mode shall be engaged above furling speed of 25 ms<sup>-1</sup>
SRVAWT-SAR-OPM-02: Safe mode shall not hinder future operation of wind turbine
SRVAWT-SAR-OPM-03: Safe mode shall be able to engage without external power
SRVAWT-SAR-OPM-04: Idle mode shall be activated when grid does not require energy
SRVAWT-SAR-OPM-05: Idle mode shall have an RPM within a range of acceptable values
SRVAWT-SAR-OPM-06: If wind speed is insufficient, secondary rotors shall activate for primary rotor to reach an acceptable RPM
SRVAWT-SAR-OPM-07: The wind turbine shall be able to switch between the modes at will
SRVAWT-SAR-OPM-08: Wind gust factors shall be considered when deciding whether to enter safe mode
```

Risk and Reliability

```
SRVAWT-SAR-RSK-01: Each individual rotor shall not have an increased risk of blades detaching, compared to conventional wind turbines - DRIVER SRVAWT-SAR-RSK-02: The system of generators shall not have a decreased reliability due to increased complexity
```

SRVAWT-SAR-RSK-03: The structure with the added weight of the secondary rotors, shall not have an increased risk of failure

SRVAWT-SAR-RSK-04: The electrical system shall not decreased in reliability due to the increased connections between subsystems

SRVAWT-SAR-RSK-05: The electrical system shall be protected from external weather conditions SRVAWT-SAR-RSK-06: Design for maintenance possibility shall not decrease reliability of the system SRVAWT-SAR-RSK-07: The increased breaking capability compared to conventional wind turbines shall not result in a decreased reliability

Sustainability

Maintainability

```
SRVAWT-SUS-MNT-01: Parts shall be primarily designed to be repairable SRVAWT-SUS-MNT-02: It shall be clear when maintenance is needed SRVAWT-SUS-MNT-03: If not repairable, it shall be replaceable SRVAWT-SUS-MNT-04: Internal systems shall be easily accessible
```

Engineering specifications of subsystems

Electrical systems

```
SRVAWT-ENG-GRD-01: There shall be a connection to the electrical grid SRVAWT-ENG-GRD-02: There shall not be more than [VAL]% energy losses in the conversion process SRVAWT-ENG-GRD-03: The energy output shall be in a format compatible with the grid SRVAWT-ENG-GRD-04: There shall not be more than [VAL]% energy losses in transportation to the grid
```

Measurement system

```
SRVAWT-ENG-MSY-01: Shall be able to measure the local air pressure
SRVAWT-ENG-MSY-02: Shall be able to measure the local air density
SRVAWT-ENG-MSY-03: Shall be able to measure the local air temperature
SRVAWT-ENG-MSY-04: Shall be able to measure the wind speed
SRVAWT-ENG-MSY-05: Shall be able to measure the wind direction
SRVAWT-ENG-MSY-06: Shall have knowledge of the current RPM of the primary and secondary turbines
SRVAWT-ENG-MSY-07: Shall have knowledge of the current pitch of the blades of the primary and secondary turbines
SRVAWT-ENG-MSY-08: Shall be able to measure the temperature of its internal components
SRVAWT-ENG-MSY-09: Measurement system shall be redundant
```

Decision-making main computer

```
SRVAWT-ENG-COM-01: The main computer shall always have a power supply SRVAWT-ENG-COM-02: The main computer shall have a safe mode, which shall use minimal power SRVAWT-ENG-COM-03: Shall be connected to every subsystem in the wind turbine SRVAWT-ENG-COM-04: The safe mode of the computer must have redundancy
```

Pitch systems

SRVAWT-ENG-PIT-01: The pitch system shall be able to pitch the primary and secondary rotor blades between 0 and 25 degrees with respect to the nominal orientation

Drivetrain systems

```
SRVAWT-ENG-GEN-01: The generators shall have a rated power output of [VAL] MW SRVAWT-ENG-GEN-02: The generators shall have a rated angular velocity of [VAL] rpm
```

More detailed requirements for the control systems of the wind turbine will be presented in chapter 6.

2.3 Killer Requirements

Killer requirements drive a design to unacceptable extents if not complied with. These are therefore considered of utmost importance. The following four killer requirements have been identified:

```
SRVAWT-GOV-01: Shall follow codes and regulations
```

SRVAWT-MNF-01: The system shall be possible to manufacture without requiring a giant leap in current browledge.

knowledge

SRVAWT-CLI-01: Shall have a reduction in cost from conventional wind turbines

SRVAWT-PRF-CUR-03: Shall convert 10MW of power at rated speed

2.4 Driving Requirements

Requirements that have a major influence on the design of the system or its subsystems are driving requirements. These requirements are considered most important after the killer requirements. They are often directly linked to the project's objective.

```
SRVAWT-PRF-CUR-01: Cut-in speed shall be 3~\mathrm{ms}^{-1}
```

SRVAWT-PRF-CUR-02: Furling speed shall be 25 ms⁻¹

SRVAWT-PRF-PPM-02: There shall be secondary rotors attached to the main rotor SRVAWT-SAR-OPM-02: Safe mode shall not hinder future operation of wind turbine

SRVAWT-SAR-RSK-01: Each individual rotor shall not have an increased risk of blades detaching, compared

to conventional wind turbines

Chapter 3: Conceptual and preliminary design phases

Some previous work has already been done on the subject, as presented in [9]. A brief overview is given in this chapter. The conceptual design phase, where different options for the secondary rotors were explored, is discussed in section 3.1. Three of these concepts were chosen to enter the preliminary design phase. In the preliminary design phase described in section 3.2, a trade-off was made and one design was chosen to enter the final design phase. This is the design that will be treated in the remainder of this report.

3.1 Conceptual designs

The concept of placing secondary rotors on a vertical axis wind turbine might seem like a well defined concept. However, while constructing a Design Option Tree, which is presented in [10], and brainstorming about all the possibilities, it became apparent that a lot of conceptual design choices were still to be made. The choices that were to be made included, among others, to decide on vertical or horizontal axis secondary rotors, number of secondary rotors, number of blades per secondary rotor and secondary rotor position on the vertical axis wind turbine. From these options a total of nine concepts were proposed, these are presented in Figure 3.1.

An elaboration on these concepts can be found in [9]. Having established these concepts, they needed to be analysed. Soon it became apparent that six of the nine concepts were either infeasible, not fitting the project purpose or too hard to design accurately for the current team. Therefore, only the first three concepts were held onto (Figure 3.1a, Figure 3.1b and Figure 3.1c). These concepts were taken into the preliminary design phase.

3.2 Preliminary designs

In the preliminary design phase, the three concepts were designed in more detail to be able to perform a decisive trade off to find the best design to continue with. The results of this sizing are shortly presented in Table 3.1. For design 2 the results are presented for the inner and outer secondary rotor separately where applicable, the first result corresponding to the inner rotor. An elaboration on this sizing can be found in [9] and is presented again in chapter 4 for the final design choice which is found at the end of this chapter.

Design	A_s $[m^2]$	P_{gen}	M_{max}	Ω [rpm]	a_s	r_p [m]	l_s [m]	Inset [m]
1 - One 5-bladed HASR	666.4	7.5	0.69	130-153	0.05	105.0	-	-
2 - Two 5-bladed HASR	362.5; 185.6	3.86	0.69	122-151; 246-289	0.1	107.8	-	-
3 - One 3-bladed VASR	666.4	7.5	0.96	177-215	0.05	105.0	30.0	15.0

Table 3.1: Sizing results

Based on the sizing results, a preliminary structural analysis was performed on each of the designs. Free body diagrams, shear force diagrams, bending moment diagrams and Campbell plots for resonance analysis were created per design. Based on these, material choices were considered and masses of components were estimated. The results from this mass estimation can be found in Table 3.2, whereas a detailed elucidation for the preliminary structural analysis is presented in [9].

Table 3.2: Mass comparison of preliminary designs

Preliminary design	Tower [t]	Primary rotor [t]	Secondary rotor [t]	Generator [t]	Total [t]
1	760	425	2.2(x2)	59-64(x2)	1312.4
2	760	468	1.4(x2)	53-58(x2)	1341.8
3	760	425	8.1(x2)	50-55(x2)	1306.2





(a) Concept 1:

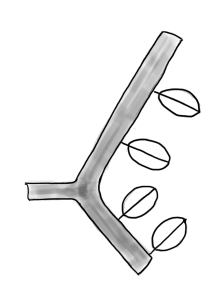
(b) Concept 2: Two 5-One bladed HASRs per lower 5-bladed HASR at the primary rotor blade, one tip of the lower primary at 80% of the primary bottom blades rotor blade length, the concept 3: One 3-set of contra-rotating 5-bladed VASR per lower primary rotor blade primary rotor blade primary rotor blade primary rotor blade other at 100%

(c) Concept 3: One 3-

(d) Concept 4: One







(e) Concept 5: One 5-bladed HASR placed (f) Concept 6: Four 3on an outward strut bladed HASRs per lower per lower primary rotor primary rotor blade blade

(g) Concept 7: One large 3-bladed VASR sweeping around the lower primary rotor blade per lower primary mary rotor blade was per primary rotor blade rotor bladee

(h) Concept 8: Four 2-



(i) Concept 9: One movable 5-bladed HASR per lower primary rotor blade

Figure 3.1: Proposed concepts

In addition to a structural analysis of each preliminary design, also control mechanisms and sustainability aspects were investigated per design. A preliminary estimation of the cost of energy was performed as well, which is presented in Table 3.3 [9].

Table 3.3: Cost of energy of preliminary designs

Preliminary design	Initial capital cost [€]	O&M [€]	COE [€/MWh]
1	27,684,900	1,374,000	87.30
2	28,990,500	1,438,800	91.48
3	27,841,900	1,381,700	88.02

Lastly, also reliability, availability, maintainability and safety (RAMS) and risk were assessed per preliminary design.

Having established all the foregoing characteristics of the different designs, sufficient information was available to perform a trade off and make a final decision on the preliminary design to continue with. It was decided to

base the trade off on four criteria, namely RAMS characteristics, cost of energy, mass and risk. Initially also sustainability was considered in the trade off, but the scoring of the designs on this criterion turned out to be indistinct and was therefore taken out. In addition to the criteria themselves, the trade off included weights assigned to the criteria to indicate their relative importance. The results of this trade off were clear and design 1, the single horizontal axis secondary rotor per lower primary rotor blade (Figure 3.1a), turned out the best. Also a sensitivity analysis on the trade off process did not alter the final decision. A trade off summary matrix is presented in Table 3.4, where yellow represents a bad score, blue represents a medium score and green represents a good score.

Table 3.4: Summary table describing each concept in terms of trade-off criteria

Criterion Concept	Risk (4)	RAMS (3)	Cost of Energy (3)	Mass (2)
1 - One HASR	blue - redundancy to failure of one secondary rotor	green - highest reliability, less components, better maintainability	green - lower capital cost, less components, less transport needed, lower installation costs	green - smaller primary rotor
2 - Two HASRs	green - more redundancy due to additional rotors, smaller generator capacity so more options to choose from, inner rotors experience less compressibility effects	yellow - more difficult maintainability due to inner rotor, more components that can fail	blue - higher capital cost, higher production costs, installation costs, maintenance	blue -larger primary rotor
3 - One VASR	yellow - less data for VAWT so TRL is lower, higher Mach number of secondary rotor blades	blue - rotor less accessible due to longer blades	green - Similar to first concept in terms of cost	green - smaller primary rotor

Chapter 4: General layout and sizing

In this chapter, the design that was chosen in chapter 3 is described in more detail. The general layout of the system can be found in section 4.1. An initial sizing of the system will be done in section 4.2, this sizing will form the basis of the further subsystem design. Finally, a sensitivity analysis will be performed in order to get an understanding of how a change in certain variables influences the size of the system in section 4.3.

4.1 General turbine layout

The layout of the wind turbine is shown in Figure 4.1. It shows the primary rotor which is a vertical axis wind turbine. It has two top blades and two bottom blades, where the top and bottom blade are connected to a strut on each side. The rotor is supported by a tower, which is connected to the seabed through a monopile foundation as it will be placed offshore. A horizontal axis secondary rotor is connected to the tip of each bottom primary blade. Each secondary rotor has five blades and is connected to a generator through a rotating shaft. It is the rotation of the secondary rotors that will output power, since the primary rotor does not have a generator connected to it. A more detailed layout of every subsystem will be discussed in the following chapters.



Figure 4.1: General layout of the wind turbine

The working principle of this wind turbine is different from conventional turbines. The primary rotor converts energy from the incoming airflow into a rotational motion around its shaft. Due to the combination of displacement of the secondary rotors from the primary shaft and the rotational motion, the secondary rotor will see a higher incoming airflow. The energy in this airflow is converted into a rotational motion around the secondary rotor shaft. This shaft is connected to a generator, that converts the mechanical energy into electrical energy. This electrical energy is the output. However, the main purpose of the secondary rotor is not to generate power. Its main purpose is to brake the primary rotor. Once the primary rotor has reached a certain rotational velocity, the secondary rotor has to make sure it does not accelerate by counteracting the torque of the primary rotor. This is done by producing thrust with the secondary rotor. A side effect of producing this thrust is power extraction. Based on this working principle, an initial sizing of the system will be performed in section 4.2.

4.2 Sizing

In order to start the design of the subsystems, some general parameters have to be known. An initial sizing of both the primary and secondary rotors is done in this section. This sizing is done based on the working principle described previously. This means that the starting point will be that the torque produced by the

secondary rotors has to be equal to the torque of the primary rotor around the primary rotor shaft, as shown in Equation 4.1.

$$T_p = T_s \tag{4.1}$$

The torque of the primary rotor can be calculated based on the relation between torque, power and rotational velocity given by Equation 4.2. The torque of the secondary rotor around the shaft of the primary rotor is caused by the thrust it produces and the distance from the primary rotor shaft as shown in Equation 4.3. Here, it is assumed that there is one secondary rotor per primary bottom blade and that the secondary rotor is placed at the tip of this blade. Substituting Equation 4.2 and Equation 4.3 into Equation 4.1 gives Equation 4.4.

$$T_p = \frac{P_p}{\omega_p} \tag{4.2}$$

$$T_s = N_{b_p} F_{T_s} r_p \tag{4.3}$$

$$\frac{P_p}{\omega_p} = N_{b_p} F_{T_s} r_p \tag{4.4}$$

In Equation 4.4, the power of the primary rotor can be substituted using the power equation shown in Equation 4.5. The thrust force of the secondary rotor can be substituted using Equation 4.6. Performing these substitutions results in Equation 4.7.

$$P_p = \frac{1}{2} C_{P_p} \rho A_p V_\infty^3 \tag{4.5}$$

$$F_{T_s} = \frac{1}{2} C_{T_s} \rho A_s V_{t_p}^2 \tag{4.6}$$

$$\frac{\frac{1}{2}C_{P_p}\rho A_p V_{\infty}^3}{\omega_p} = N_{b_p} \frac{1}{2}C_{T_s}\rho A_s V_{t_p}^2 r_p \tag{4.7}$$

Here, the power equation for the secondary rotor from Equation 4.8 can be rewritten to find an expression for the area of the secondary rotor resulting in Equation 4.9. Substituting this expression in Equation 4.7 gives Equation 4.10.

$$P_s = \frac{1}{2} C_{P_s} \rho A_s V_{t_p}^3 \tag{4.8}$$

$$A_s = \frac{P_s}{\frac{1}{2}C_{P_s}\rho V_{t_n}^3} \tag{4.9}$$

$$\frac{\frac{1}{2}C_{P_p}\rho A_p V_{\infty}^3}{\omega_p} = N_{b_p} \frac{1}{2}C_{T_s}\rho \frac{P_s}{\frac{1}{2}C_{P_s}\rho V_{t_p}^3} V_{t_p}^2 r_p \tag{4.10}$$

It is then considered that the tip speed of the primary rotor is a function of its rotational velocity and the distance between the blade tip and the rotor shaft, defined as the radius of the primary rotor. This relation is depicted in Equation 4.11. Substituting this into Equation 4.10 gives the expression shown in Equation 4.12. This can be simplified by cancelling out the equal terms as shown in Equation 4.13.

$$V_{t_p} = \omega_p r_p \tag{4.11}$$

$$\frac{\frac{1}{2}C_{P_p}\rho A_p V_{\infty}^3}{\omega_p} = N_{b_p} \frac{1}{2}C_{T_s} \rho \frac{P_s}{\frac{1}{2}C_{P_s}\rho(\omega_p r_p)^3} (\omega_p r_p)^2 r_p$$
(4.12)

$$\frac{1}{2}C_{P_p}\rho A_p V_{\infty}^3 = \frac{N_{b_p}C_{T_s}P_s}{C_{P_s}} \tag{4.13}$$

In Equation 4.14 it is considered that the number of blades multiplied by the power of a secondary rotor is equal to the total power of the system. Furthermore, Equation 4.15 describes the relation between power coefficient and thrust coefficient through the induction factor. Using Equation 4.14 and Equation 4.15 in Equation 4.13, gives a final expression as shown in Equation 4.16. This expression can then be rewritten to Equation 4.17.

$$N_{b_p}P_s = P_{sys} (4.14)$$

$$\frac{C_{P_s}}{C_T} = 1 - a_s \tag{4.15}$$

$$\frac{1}{2}C_{P_p}\rho A_p V_{\infty}^3 = \frac{P_{sys}}{1 - a_s} \tag{4.16}$$

$$P_{sys} = \frac{1}{2} C_{P_p} \rho A_p V_{\infty}^3 (1 - a_s)$$
(4.17)

Equation 4.17 shows that by adding secondary rotors to a primary rotor, a loss factor is introduced to the power equation. This efficiency loss is proportional to the induction factor of the secondary rotor. This means that in order to keep the system efficiency as high as possible, the induction factor of the secondary rotor should be as low as possible. There are limitatios to this induction factor however, especially considering that a conventional wind turbine operates at an induction factor of $a = \frac{1}{3}$ as this optimises the design. For this design however, an induction factor for the secondary rotor of $a_s = 0.05$ is chosen. During the design, this value could be reiterated if it proves to be unfeasible.

The primary rotor is sized for rated conditions, Equation 4.17 is rewritten to Equation 4.18. Here, the air density is equal to $\rho = 1.225 \ [kg/m^3]$ and the optimal power coefficient of the primary rotor is assumed to be $C_{p_p,opt} = 0.39 \ [8]$. The rated power is $P_r = 10 \ [\text{MW}]$ and the rated velocity is chosen to be $V_r = 11 \ [\frac{m}{s}]$. If this velocity is chosen too low, the torque of the generators will become larger. If it is chosen too high, the mach numbers at the tips of the secondary rotor blades will become too large and the wind turbine capacity factor will decrease.

$$P_r = \frac{1}{2} C_{P_{p,opt}} \rho A_p V_r^3 (1 - a_s)$$
(4.18)

Using the values mentioned above, a value of $A_p = 33,108m^2$ is found for the area of the primary rotor. Assuming that the primary rotor area is a square with side length of $2r_p$ as shown in Equation 4.19, a radius of $r_p = 90.98m$ is found.

$$A_p = (2r_p)^2 (4.19)$$

The size of the secondary rotor can also be calculated. This is done using Equation 4.20. The rated power of a secondary rotor is $P_{r_s} = 5MW$. The rated velocity is calculated using Equation 4.21 where $\lambda_{p_{opt}} = 4.65$ [8]. The optimal power coefficient of the secondary rotor is $C_{p_s,opt} = 0.13$

$$P_{r_s} = \frac{1}{2} C_{P_{s,opt}} \rho A_s V_{r_s}^3 \tag{4.20}$$

$$V_{r_s} = \lambda_{p_{out}} V_r \tag{4.21}$$

This gives a secondary rotor area of $A_s = 469 \ [m^2]$ and a secondary rotor radius of $r_s = 12.22m$.

A problem arises when the system is analysed further. Figure 4.2 shows a top view of the primary rotor, where the tips of the bottom blades are shown to be at $\theta = \frac{\pi}{2} rad$ and $\theta = \frac{3\pi}{2} rad$. The secondary rotors are attached to these blade tips. They see an incoming airflow velocity caused by the rotational motion of the primary rotor. However, depending on the location over the rotation, these secondary rotors also see part of the general wind

 V_{∞} . This means that the wind velocity that the secondary rotors see varies over the rotation of the primary rotor.

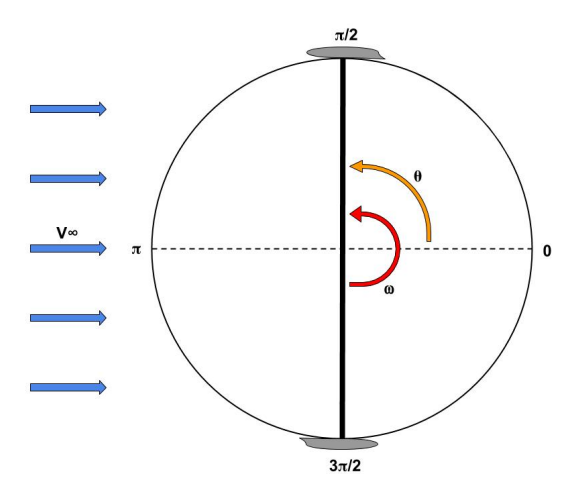


Figure 4.2: Top view of vertical axis primary rotor

When the secondary rotor is moving downwind between $\theta=\pi$ and $\theta=0$, it will see a lower velocity, meaning it will generate less power. When it is moving upwind between $\theta=0$ and $\theta=\pi$, it will see a larger velocity and generate more power. Initially this is not a problem, since the power increase upwind is larger than the decrease in power downwind. However, this does become a problem when the upwind rotor reaches its maximum generator capacity. If the velocity increases further from that moment, the power of the downwind rotor will keep reducing while the power of the upwind rotor cannot increase any further. This means that the total power output will decrease.

The solution for this problem that is used in this design is the implementation of larger generators. Instead of using two 5MW generators to output 10MW of power, the generators are scaled up to 7.5MW each to generate a total power output of 10MW at rated conditions due to the effect described above. Table 4.1 gives an overview of the most important values of the initial sizing.

Table 4.1: Summary table initial sizing

Parameter	Value
$A_p[m^2]$	33,108
$r_p[m]$	90.98
$A_s[m^2]$	469
$r_s[m]$	12.22
$P_{gen}[MW]$	7.5

4.3 Sensitivity analysis

The most important variables that can change are the power coefficient of the primary rotor and the power coefficient of the secondary rotor. Furthermore, the chosen induction factor and rated velocity will have an impact on the size of the system as well. The effect of these changes are shown in Table 4.2, where the first column shows the parameter that is changed. The second column shows the new value of the parameter and the other columns shown the effect of that change on the size of the primary and secondary rotor. Both the new values and change with respect to the initially calculated values in percentage are given.

Table 4.2: Sensitivity analysis sizing

Parameter	New value	New A_p [m^2]	New r_p [m]	New A_s [m^2]	New r_s [m]
C_{P_p}	0.351 (-10%)	36,786 (+11%)	95.9 (+5.4%)	_	-
C_{P_s}	0.117 (-10%)	-	-	521 (+11%)	$12.9 \; (+5.4\%)$
a_s	$0.33\ (+666\%)$	47,178 (+42%)	108.6 (+19.4%)	-	-
V_r	9.9 (-10%)	$45,\!415\ (+37\%)$	106.6 (+17.2%)	644 (+37%)	14.3 (+17.1%)

Chapter 5: Aerodynamic design

The aerodynamic design of the secondary rotor comprises choosing the airfoil, twist distribution and chord distribution such that the required thrust and power are generated. This is done in an iterative manner with the control department of which the results will be shown in the subsequent chapters. The aerodynamic analysis is shown first in the report as it requires the least amount of inputs from other subsystems.

First, an overview of the theory is shown. Starting with the momentum theory in section 5.1 and moving on to blade element theory in section 5.2. Both of these are then combined in order to estimate thrust and power coefficients in section 5.3. Tip and root losses are discussed in section 5.4 and corrections for the lift coefficient are described in section 5.5. A final piece of theory is shown in section 5.6, which concerns the blade element momentum theory. After that, the secondary rotor can be designed aerodynamically. The design procedure and the code that was used for this will be described in section 5.7. After that, an airfoil selection is done in section 5.8. The final design is then given in section 5.9. The sensitivity analysis together with the verification and validation procedures for the aerodynamic analysis are covered in section 5.10 and section 5.11, respectively. The limitations are shown in section 5.12 and based on this, recommendations are made in section 5.13. Finally, the noise of the wind turbine is assessed in section 5.14. This noise will serve as input for the sustainability assessment of the design later in the report.

The theory described in this chapter has been taken from [11] and adjusted to the secondary rotor concept. The equations and figures were also taken from this reference and modified with the parameters for this project. The results of this chapter are important for both the control calculations and the structural analysis.

5.1 Momentum theory

Extracting power from the wind is done by slowing down air passing through the secondary rotors. The degree to which the air is slowed down at the rotor itself, is represented by the induction factor, a_s , as in Equation 5.1.

$$V_D = V_s(1 - a_s) \tag{5.1}$$

By slowing down the air, the momentum of the air is decreased. Momentum theory says this is only possible if an external force acts upon the air. The simplest model to represent this is an actuator disc model. An actuator disc model is only valid theoretically and it simply represents a rotor with infinitely many blades. In practise this is not possible, because the air would not be able to pass through the rotor. This actuator disc represents the secondary rotor and slows the air by establishing a pressure difference across the rotor, see Figure 5.1a. By doing so, the air across the rotor expands, as the mass flow rate has to stay constant. From the momentum and pressure difference, it is found that the velocity in the far wake of the rotor has been reduced by twice the induction factor.

The force exerted by rotor on the air, the thrust force, is found from Equation 5.2. This force is directly linked to the power extracted from the air according to Equation 5.3.

$$F_{T_s} = 2\rho A_D V_s^2 a_s (1 - a_s) \tag{5.2}$$

$$P_s = F_{T_s} V_D = 2\rho A_D V_s^3 a_s (1 - a_s)^2$$
(5.3)

The above only considers the axial flow across the actuator disc. In reality the rotor rotates and induces a tangential velocity component to the flow as well. This component acts in the direction opposite to the rotor's rotation and is proportional to the angular velocity and the radial position within the rotor. In addition this tangential velocity component is determined by the tangential induction factor and it equals $a'_s\omega_s\mu_r R_s \frac{m}{s}$ in the middle of the rotor. Just after the rotor it equals twice this value. Unlike for the axial velocity, the tangential velocity increases due to the force of the rotor. This effect causes the flow behind the rotor, the wake, to be rotating. This is visualised in Figure 5.1b.

The tangential velocity component varies across the blade radius. Therefore the rotor is divided into annular rings, defined by their radial position and radial width. The reaction to accelerating the air tangentially, is

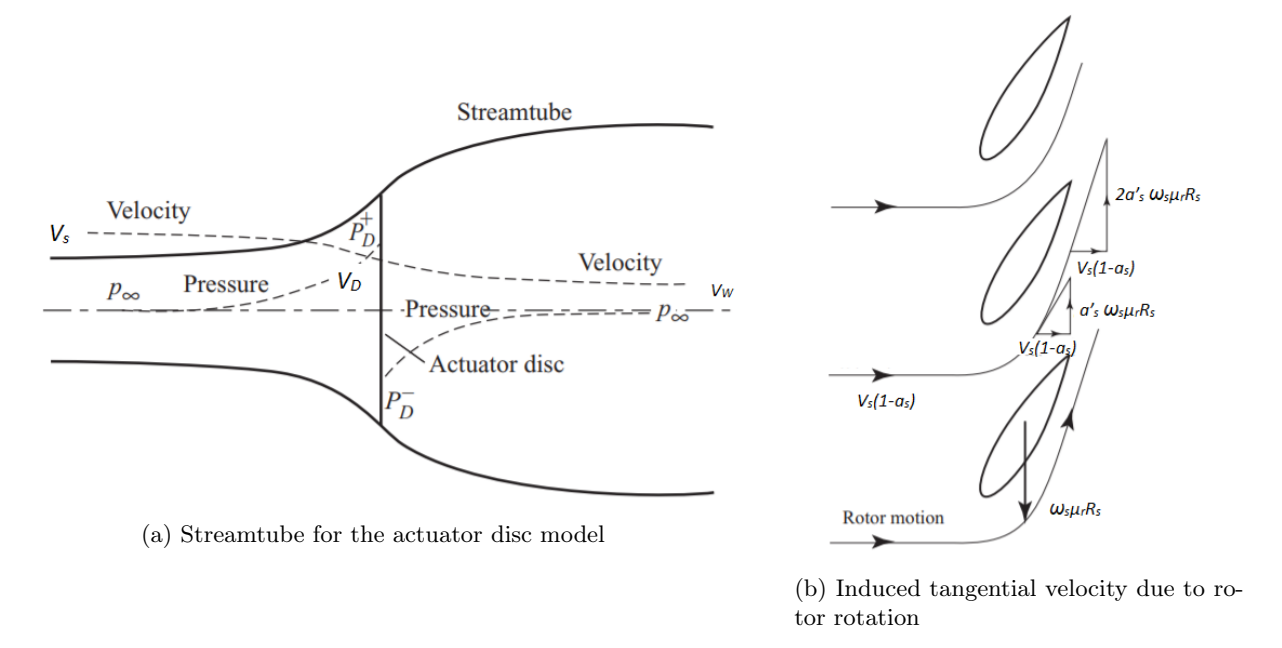


Figure 5.1: Axial and tangential velocity through an actuator disc model [11]

to exert a force on the annular ring which causes the rotor to rotate. This torque provides the power to the generator in conventional turbines and should be equal, according to actuator disc theory, to the power from Equation 5.3 for each annular ring, as provided in Equation 5.4. It follows that the axial and tangential induction factor are related.

$$P_s = 2\rho \delta A_D V_s^3 a_s (1 - a_s)^2 = \rho \delta A_D V_s (1 - a_s) 2\omega_s^2 a_s' (\mu_r R_s)^2$$
(5.4)

The thrust for such an annular ring follows from Equation 5.2, by replacing A_D by δA_D , which equals $2\pi\mu_r R_s \delta r$ $[m^2]$. This last quantity can also be implemented in Equation 5.4.

From the momentum theory, an important design conclusion can be drawn. As the primary rotor rotates, the blades induce tip vortices. These tip vortices are directed around the blade, from high to low pressure, from below to above the blade. The secondary rotors can be used to cancel out these vortices (partly). This can be done by making sure the secondary rotors rotate in the same direction as the tip vortices induced by the primary rotor blades. As such, the secondary rotor induces rotational velocities in the opposite direction of the vortices, cancelling them out. Seen from above, The primary rotor rotates counter-clockwise, as in Figure 4.2. Therefore, the secondary rotors have to rotate clockwise for someone looking from the upwind side of the secondary rotors.

5.2 Blade Element Theory

Momentum theory can be used to determine the thrust force and power extracted by a rotor, given a certain free stream wind velocity, rotor area, induction factors, angular velocity and air density. However, as the actuator disc model is not a physically possible representation of a rotor, another model is needed. Moreover, to design a limited number of blades, Blade Element Theory is considered.

Blade Element Theory considers the forces on a part of a rotor blade, called a blade element. The blade element is defined by its airfoil, radial position, radial width, chord length, geometric twist angle and pitch angle. Other important assumptions of this theory are:

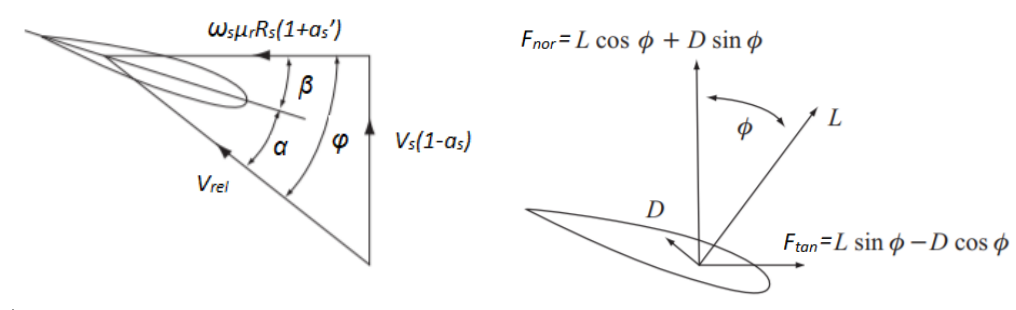
- Forces on a blade element can be calculated from two dimensional airfoil data
- There is no radial velocity component across the blade

The relative wind velocity on a blade element consists of a normal and tangential component, due to the general wind seen by the secondary rotor and due to the secondary rotor's rotation, respectively, including the corresponding induction factors. The relative wind velocity follows from Equation 5.5.

$$V_{rel} = \sqrt{V_s (1 - a_s)^2 + (\omega_s \mu_r R_s (1 + a_s'))^2}$$
(5.5)

The direction of this relative wind velocity determines the angle with respect to the rotor's plane of rotation, called the inflow angle. This follows from Equation 5.6. In addition, the inflow angle, Φ , is the sum of the geometric twist of a blade, β , which is a function of radial position, and the angle of attack, α . If the blade is pitched as well, this also adds to the inflow angle. A schematic representation of the flow is available in Figure 5.2a for a non-pitched blade.

$$\sin \Phi = \frac{V_s(1 - a_s)}{V_{rel}} \tag{5.6}$$



- (a) Incoming flow with the corresponding angles for a non-pitched blade
- (b) Forces on a blade element

Figure 5.2: Flow and forces on a blade element [11]

The force on such a blade element due to this wind, can be decomposed in lift and drag forces, normal and tangential to the relative wind velocity, respectively. However, the resultant force can also be divided in forces normal and tangential to the rotor's plane of rotation, F_{nor} and F_{tan} , respectively, which can be found from the lift and drag forces. This normal force contributes to the total thrust force produced by the secondary rotor. The tangential force contributes to the torque driving the rotor's rotation and thus the extracted power. These forces are depicted in Figure 5.2b. The values of thrust and torque produced by one blade element are found from Equation 5.7 and Equation 5.8, respectively.

$$\delta F_{T_s} = \frac{1}{2} \rho V_{rel}^2 c_s (C_l \cos \Phi + C_d \sin \Phi) \delta r \tag{5.7}$$

$$\delta Q = \frac{1}{2} \rho V_{rel}^2 c_s \mu_r R_s (C_l \sin \Phi - C_d \cos \Phi) \delta r$$
 (5.8)

Finally, the power extracted by the entire rotor is found by summing the torque of all blade elements multiplied by the number of blades and the angular velocity of the rotor, see Equation 5.9.

$$P_s = \sum_{\mu=0}^{\mu=1} \delta Q B \omega_s \tag{5.9}$$

5.3 Thrust and power coefficients

A combination of Momentum Theory and Blade Element Theory can be used to design a rotor given certain specifications. The most important parameters one wants to know are the thrust force exerted and power extracted by the rotor. However, these vary significantly for different scenarios in which the rotor operates. For example, free stream wind velocity, pitch angle and tip speed ratio can have a major influence on the thrust exerted and power extracted by the rotor. In order to compare different operation cases, non-dimensional coefficients are used. The secondary rotor thrust coefficient, C_{T_s} , and the secondary rotor power coefficient, C_{P_s} , are defined by Equation 5.10 and Equation 5.11, respectively. It should be noted that these coefficients are not entirely independent of free stream wind velocity, as the thrust force and power are calculated using V_{rel} and V_s is used for non-dimensionalising.

$$C_{T_s} = \frac{F_{T_s}}{\frac{1}{2}\rho V_s^2 A_D} \tag{5.10}$$

$$C_{P_s} = \frac{P_s}{\frac{1}{2}\rho V_s^2 A_D} \tag{5.11}$$

5.4 Prandtl tip and root losses

As mentioned, some aerodynamic losses can be implemented in the BEM model. It was chosen to include tip and root losses according to Prandtl's approximation as suggested by [11]. By this approximation, the tip loss factor is found by Equation 5.12, whereas the root loss factor is found by Equation 5.13.

$$f_{tip}(\mu_r) = \frac{2}{\pi} \cos^{-1} \left(e^{-\frac{N_b}{2} \frac{1 - \mu_r}{\mu_r} \sqrt{1 + \frac{(\lambda_s \mu_r)^2}{(1 - a_s)^2}}} \right)$$
 (5.12)

$$f_{root}(\mu_r) = \frac{2}{\pi} \cos^{-1} \left(e^{-\frac{N_b}{2} \frac{\mu_r - \mu_{root}}{\mu_r} \sqrt{1 + \frac{(\lambda_s \mu_r)^2}{(1 - a_s)^2}}} \right)$$
 (5.13)

The combined effect of the tip and root losses are found by multiplying the tip and root loss factor per blade element. The effect of these aerodynamic losses, is that the axial and tangential induction factors change according to Equation 5.14 and Equation 5.15, respectively.

$$a_s = \frac{a_s}{f_{tip}f_{root}} \tag{5.14}$$

$$a_s' = \frac{a_s'}{f_{tiv} f_{root}} \tag{5.15}$$

5.5 Prandtl-Glauert correction for lift coefficient

Since the secondary rotor rotates at quite high angular velocities, the Reynolds and Mach numbers that are achieved are significant. This has an influence on accuracy of the airfoil data that is used. Fortunately, the programme QBlade, that was used to obtain the airfoil data, implements the Prandtl-Glauert correction to the lift coefficient according to Equation 5.16. Similarly, this correction is applied to the drag coefficient.

$$C_l = \frac{C_{l_0}}{\sqrt{|1 - M^2|}} \tag{5.16}$$

5.6 Blade Element Momentum theory

A major difference between Momentum Theory and Blade Element Theory is that Momentum Theory does not account for aerodynamic losses. However, in Blade Element Theory one has the opportunity to implement models for aerodynamic losses, such as tip and root losses. However, this does not mean that Momentum Theory becomes superfluous. Momentum Theory is still greatly appreciated to find induction factors that characterise a rotor for a certain operational case. For this reason, a Blade Element Momentum (BEM) model is developed for the rotor's aerodynamic design. This model assumes that the thrust force exerted and the power extracted according to Momentum Theory equals the thrust force exerted and power extracted according to Blade Element Theory, respectively. This can done for all annular rings, but to do this correctly, the equations from Blade Element Theory have to be multiplied by the number of blades comprising the rotor, N_b . Equating Equation 5.2 and Equation 5.7 for an annular ring gives Equation 5.17. Equating the power from both theories implies the same as equating the torque exerted on the rotor, as the angular velocity is the same. Therefore, equating the torque from Blade Element Theory, Equation 5.8, and the power divided by angular velocity from Momentum theory, Equation 5.4, for an annular ring results in Equation 5.18. Thus, this model assumes that

the normal force on a blade element is solely responsible for the change in axial momentum and the torque is solely responsible for the change in angular momentum.

$$\delta F_{T_s} = 2\rho \delta A_D V_s^2 a_s (1 - a_s) = \frac{1}{2} \rho V_{rel}^2 N_b c_s (C_l \cos \Phi + C_d \sin \Phi) \delta r$$

$$(5.17)$$

$$\delta Q = \rho \delta A_D V_s (1 - a_s) 2\omega_s a_s' (\mu_r R_s)^2 = \frac{1}{2} \rho V_{rel}^2 N_b c_s \mu_r R_s (C_l \sin \Phi - C_d \cos \Phi) \delta r$$

$$(5.18)$$

5.7 Design procedure and code

The BEM model was used to determine all geometrical aspects of the secondary rotors. These include the chord distribution and twist distribution for a given rotor size.

A python code was obtained to perform the aerodynamic analysis. This code was obtained from [12] and includes a BEM model for a horizontal axis rotor.

Before using this code and diving into designing the rotor, a consistent procedure was developed for the design process. This design procedure is visualised in the flow diagram in Figure 5.3. This flow diagram contains decisions to be made by the aerodynamics department as well as calculations performed by the Python code. A short elucidation of the flow diagram will be given next.

The procedure starts off by establishing initial rotor characteristics, such as general wind speed, rotor radius, blade design and airfoil choice. The aerodynamic polars of these airfoils are obtained and initialised in the Python code. Ranges for tip speed ratios and pitch angles are established to determine the cases for which rotor performance is to be analysed. The purple box in Figure 5.3 then defines the start for analysing performance for different combinations of tip speed ratio and pitch angle.

Per combination an iterative procedure is initialised with induction factors equal to zero. Per blade element the aerodynamic normal and tangential loads are computed from general wind speed, induction factors, tip speed ratio, local chord length, local twist angle, blade pitch angle and airfoil polar according to Blade Element Theory. In the process inflow angle, angle of attack, local wind speed, lift, drag and aerodynamic moment are computed. The normal and tangential loads per blade element are then multiplied by the number of blades to find the loads per annular ring, which is used to find the thrust coefficient per annular ring. Also the axial and tangential induction factors can be found by linking the loads to Momentum Theory. Next, aerodynamic tip and root loss factors are computed and implemented on the induction factors per annular ring. These new induction factors are compared to the induction factors that started the iteration. If close enough, the code continues, if not, another iteration is done starting with the new induction factors until the new values are close enough to the values at the start of an iteration. When this is achieved, the total power and thrust are computed by summing those of all annular rings. From these values the overall rotor power coefficient and thrust coefficient are found. This ends the performance analyse of the design for a specific combination of tip speed ratio and pitch angle. In the same way, all combinations are analysed.

When all combinations are analysed, the results are plotted to easily assess the outcomes. This is done by plotting C_{P_s} - λ_s , C_{T_s} - λ_s and a_s - λ_s curves for various pitch angles. Also lift coefficient, angle of attack and drag coefficient distributions along the blade are plotted for a selection of cases, i.e. combinations of tip speed ratio and pitch angle. These curves are analysed with the control departments, which has restrictions on power coefficients, thrust coefficients and induction factors for the secondary rotor. If the tested design is deemed unsatisfactory, a new design (mainly chord and twist distributions, possibly airfoil choice) is established and the entire performance analysis is done over. When the results are deemed satisfactory, the secondary rotor blade design is confirmed.

The above described procedure requires interference by the designer on a small timescale by having to assess the design and establishing new ones. As it was found that the code takes a significant amount of time to do all iterations for a single design, it was decided to loop to entire performance analysis for different designs, i.e. different chord and twist distribution combinations, at night. The produced results were plotted per design and the next day the designer was able to assess multiple designs in a short amount of time.

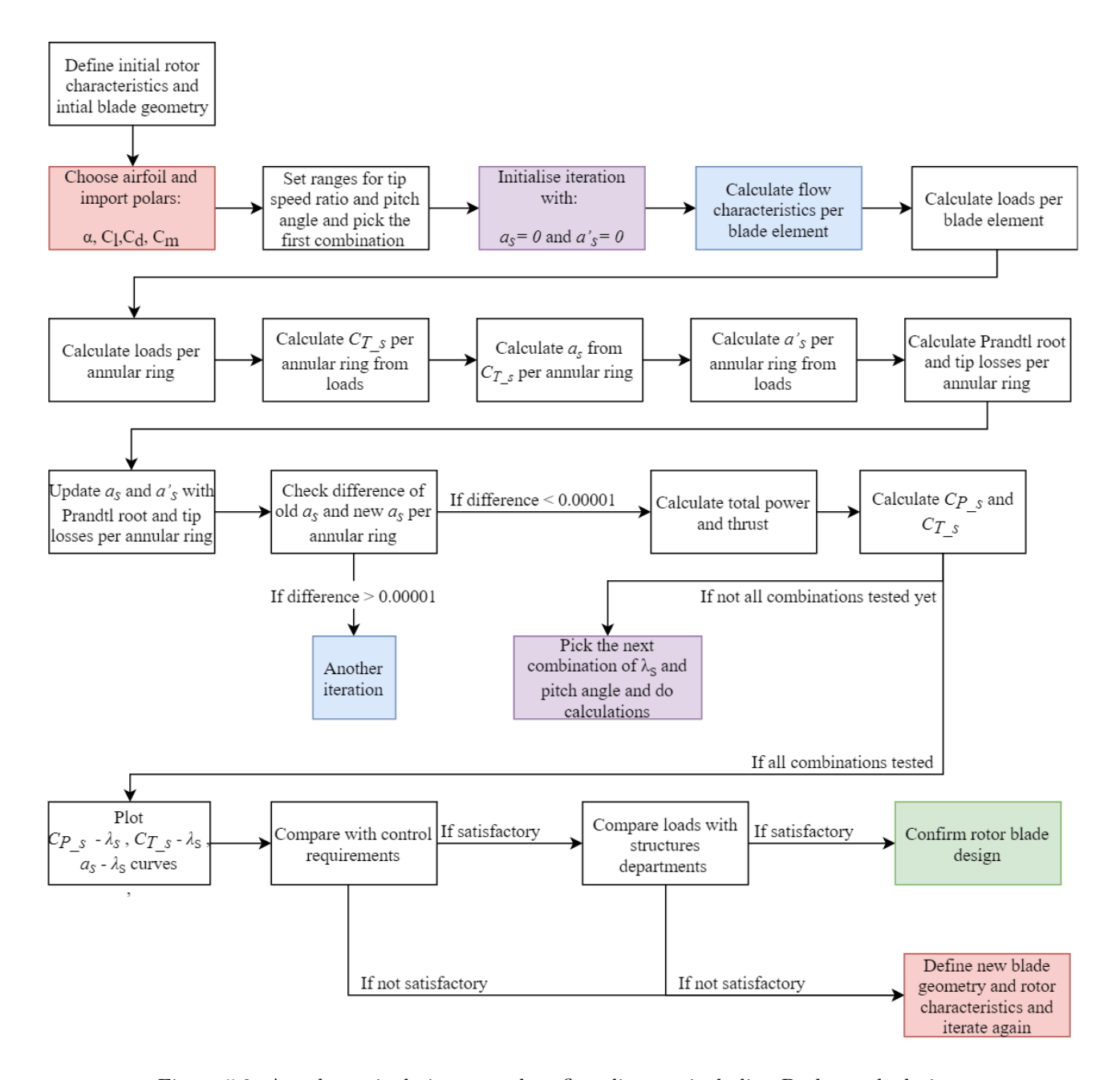


Figure 5.3: Aerodynamic design procedure flow diagram including Python calculations

5.8 Airfoil selection

Before the rotor planform can be designed, the airfoil distribution along the blade length is to be confirmed. Without airfoils, no lift and drag polars are available and the loads on the blade elements can not be determined. Therefore, an airfoil selection is performed first.

For this selection, several requirements were established for the airfoil to comply with. These requirements were obtained from literature, from discussions with experts in the field of rotor design and from limits set by the control department and include the following:

- The airfoil shall be designed to have low sensitivity to leading edge roughness [13] This reduces performance losses over time
- The tip of the blade shall perform well at transonic Mach numbers

 The high rotational speed makes the tip experience high Mach numbers, to reduce drag losses well performing airfoils are needed here
- The airfoil shall have a high maximum lift over drag ratio To reduce drag losses

 The airfoil shall have a wide range of lift coefficients between the design lift coefficient and maximum lift coefficient

Since a wide range of induction factors are needed, a wide range of lift coefficients is needed

To comply with these requirements, first a short literature study on airfoil data was performed. From this, a few airfoils were selected to be studied further and to do a trade off on afterwards. It was found that the family of NASA/Langley LS-04XX MOD airfoils, were specifically designed for low sensitivity to leading edge roughness [13]. Initially, the LS-0417 MOD airfoil ¹ was selected for the trade off. The family of DU airfoils, designed by Delft University of Technology [14], were also designed for low sensitivity to leading edge roughness. However, the most important consideration was airfoil thickness for structural advantages. The DU96 W180 [14] airfoil was selected for its intermediate design lift coefficient, corresponding to a high lift over drag ratio. Also the NREL S815 ² was selected for the trade off. Its selection was based on being primarily designed for variable pitch and speed horizontal axis wind turbines having a diameter of 20 to 40 meters [11]. Also the Riso airfoils developed in Denmark were studied and considered, however none of these were selected for the trade off because they have high design lift coefficients. Also NASA supercritical airfoils were studied [15]. Initially the NASA SC-0403 airfoil ³ was chosen, because of its low thickness, to limit the flow velocity increase on the airfoil, and its low design lift coefficient.

Table 5.1: Airfoils selected for trade off and corresponding data

Airfoil	$\begin{bmatrix} \frac{t}{c} \\ max \\ [\%] \end{bmatrix}$	$C_{l_{des}}$ [-]	$C_{l_{max}}$ [-]	$\begin{bmatrix} \frac{L}{D} max \\ [-] \end{bmatrix}$	Re [10 ⁶]	Leading edge roughness sensitivity	Design objective
LS-0417 MOD	17.0	1.3	2.0	135	3	Low	Low sensitivity to leading edge roughness
DU96 W180	18.0	1.	1.26	145	3	Low	Low sensitivity to leading edge roughness and structural advantages
NREL S815	26.2	1.0	1.6	122	3	Medium	Variable speed pitch control HAWT with 20-40 m diameter
NASA SC-0403	3.0	0.2	0.85	45	1	Medium	Performance at transonic free stream Mach numbers

After having selected these airfoils, a small airfoil trade off was performed. This trade off was based on the data that was found for the selected airfoils, which is summarised in Table 5.1. The trade off has four criteria, namely those described by the airfoil requirements. All criteria were found to be equally important in the trade off because all of them can crush the design if not sufficiently designed for. The scoring of each airfoil to those requirements is summarised in Table 5.2. Here, green represents a good score, blue represents a medium score and yellow represents a bad score.

Table 5.2: Airfoil selection trade off matrix

Airfoil	Leading edge roughness sensitivity	Performance at transonic Mach numbers	$\frac{L}{D}$	C_l rang
LS-0417 MOD	green	yellow	green	green
DU96 W180	green	yellow	green	blue
NREL S815	yellow	yellow	blue	green
NASA SC-0403	yellow	green	blue	green

Before coming to the final airfoil decision, a short reasoning for the scores is given. First off is the LS-0417 MOD airfoil. As it is specifically designed for low sensitivity to leading edge roughness, it scores good. Due to its camber and thickness and because it is not a supercritical airfoil, this airfoil is found to perform bad at transonic Mach numbers. The maximum lift over drag ratio has a very reasonable value, as such it scores good on this criterion. The design lift coefficient is found to be sufficiently low with a high maximum lift coefficient,

¹http://airfoiltools.com/airfoil/details?airfoil=ls417mod-il

²http://airfoiltools.com/airfoil/details?airfoil=s815-nr

 $^{^3 \}verb|http://airfoiltools.com/airfoil/details?airfoil=sc20403-il$

making it score good on the last criterion as well. The DU 96-W-180 airfoil scores the same as the LS-0417 MOD airfoil for the same reasons, except for the lift coefficient range criterion. This range is significantly lower and the maximum lift coefficient is very low, therefore it only scores medium on this criterion. The NREL S815 airfoil scores also similar to the LS-0417 MOD airfoil, for similar reasons. However, it scores significantly worse on leading edge roughness sensitivity, because this aspect was not considered in its design. Also its maximum lift over drag ratio was found to be significantly lower, so it only scores medium there. The same goes for the NASA SC-0403 airfoil for which the maximum lift over drag ratio is very low and which was also not specifically designed for leading edge roughness sensitivity. However, this airfoil was designed specifically to perform well at transonic Mach numbers, therefore it scores good at that criterion. For this airfoil, the lift coefficient range is rather large and therefore it scores good at the last criterion.

In conclusion, the LS-0417 MOD airfoil scores best according to the trade off. The decisive aspect is its larger lift coefficient range. Although its design lift coefficient is significantly larger than for the DU96 W180 airfoil, which was desired to be low, it is found better, because this can be dealt with in the planform design by choosing smaller chord lengths. However, it was noted that this airfoil does not perform well enough for the transonic Mach number that will occur at the tip of the blade. Therefore, it was decided to implement the NASA SC-0403 airfoil for the blade part ranging from 70% of the radius to the tip. The low design lift coefficient of this airfoil seems disturbing, however this can be compensated by the lift produced by the inner part of the blade having the LS-0417 MOD airfoil. This also shows that the higher lift coefficients of the LS-0417 MOD airfoil actually make it a better option than the DU96 W180 airfoil.

Later in the design process, it was realised that structure wise the NASA SC-0403 airfoil would give rise to problems regarding structure thickness. As a result, it was decided to change the airfoil once more. Structurally motivated, a maximum airfoil thickness over chord ratio of about 10% is needed. First the NASA SC-0410 ⁴ was studied, from the same family of airfoils. It was found that this airfoil has satisfactory aerodynamic characteristics and it was therefore chosen to be implemented. The results of the airfoil selection and some airfoil characteristics are given in Table 5.3.

The lift, drag and moment polars used for these airfoils were obtained through QBlade⁵. Here, a correction was made for finite Mach numbers. These were established for the outermost cases along the blade, so at 70% and 100%. The velocities were initially taken as the highest ones achieved as found by [9]. After a more detailed analysis by the control department, these values changed and were implemented accordingly. These include Mach numbers of 0.525 and 0.75, respectively. Also corrections are added for Reynolds numbers. The Reynolds numbers were found to be 18 and 12 million.

Airfoil	$\begin{bmatrix} \frac{t}{c} \\ \% \end{bmatrix}$	$C_{l_{des}}$ [-]	$\begin{bmatrix} C_{l_{max}} \\ [-] \end{bmatrix}$	$\frac{L}{D}_{max}$	Re $[10^6]$	Position on blade
LS-0417 MOD	17.0	1.3	2.0	135	3	Root - $0.7R_s$
NASA SC-0410	10.0	0.85	1.45	75	1	$0.7R_s$ - Tip

Table 5.3: Airfoil selection results and some data

5.9 Results & Discussion

The objective of the aerodynamic design is to be able to achieve axial induction factors ranging from below 0.05 to almost 0.20, which is based on the required thrust delivered by the secondary rotors throughout one primary rotor rotation. An elaboration is provided in chapter 7. Adhering to the procedure described in section 5.7 a suitable planform design was developed. The structural considerations and issues concerning production taken into account in the design choices will be elaborated upon as well.

Possible twist distributions include constant, linear decreasing, linear increasing, quadratic decreasing and quadratic increasing distributions. It was immediately determined that the twist distribution needs to be decreasing along the blade length, as the rotational component of wind velocity gets larger and therefore the local general wind velocity more aligned with the rotational plane.

Concerning the chord, similar distributions would be possible. However, concerning production and structural complications, here it was established as well that the chord lengths should decrease towards the tip.

⁴http://airfoiltools.com/airfoil/details?airfoil=sc20410-il

⁵http://www.q-blade.org/#welcome, retrieved 07-06-2019

Concerning production, linear variations would be better than quadratic variations for both chord and twist distributions. However, it was expected that as the chord decreases (linearly), it may be necessary, considering the aerodynamic performance, to vary twist quadratic, or vice versa if twist were to decrease linearly. From conventional turbines it was found that it is usual to decrease the chord linearly and pick a suitable twist distribution accordingly.

Having chosen a linear decreasing chord distribution and either a linear or quadratic varying twist distribution, the coefficients C_1 to C_5 were to be determined, see Equation 5.19. First, a large range of coefficients were analysed. Based on corresponding results these ranges were adjusted and decreased until a narrow range was acquired.

$$c_s = C_1 \mu_r + C_2, \quad \beta = C_3 \mu_r^2 + C_4 \mu_r + C_5$$
 (5.19)

It is to be mentioned that the analysis of these combinations of twist distributions is somewhat subject to intuitive decisions. The reason for this is that it sometimes occurred that quite distinct distributions would give similar results. It was then chosen based on thoughts concerning production and structural strength what the best option would be. When a final design was confirmed, it was, together with its performance prediction, provided to the structures and control department, so that structural integrity and system performance could be evaluated. Initially it was found sometimes that this was not sufficient and that the aerodynamic design had to be adjusted.

In the very end, it was found that the combination of a linear decreasing chord length, with $C_1 = -2.75$ and $C_2 = 3.5$, and a quadratic decreasing twist distribution, with $C_3 = 20$, $C_4 = -65$ and $C_5 = 50$, was best. The planform design is presented in Figure 5.4.

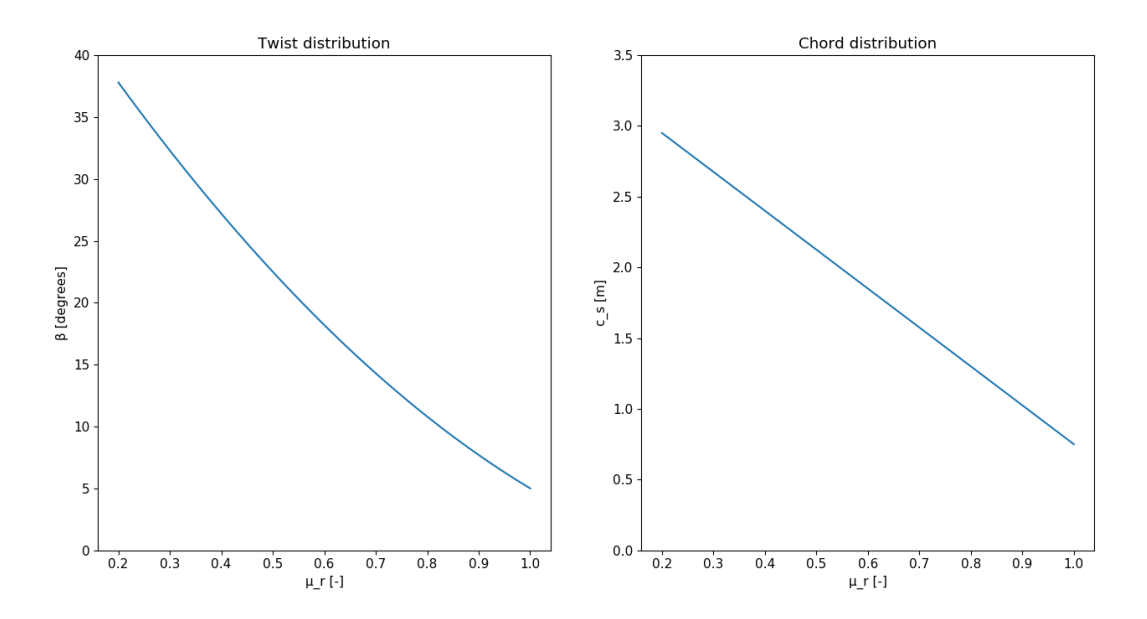


Figure 5.4: Secondary rotor planform design

The data given to the control department include power coefficients, thrust coefficients and inductions factors for different combinations of tip speed ratios and pitch angles. These are provided in Figure 5.5.

It should be noted that, to minimise the tip speed ratio for low induction factors, higher pitch angles are required than in conventional turbines. Here, pitch angles up to 25-30 degrees seem to be needed. This seems strange considering the operational angle of attack range of the used airfoils. In addition, two peaks in the curves are visible, especially for these larger pitch angles. At first, the validity of these results was questioned. To investigate the validity, plots were made of the angle of attack distribution along the blade for different scenarios. Moreover, the angle of attack distributions were checked for a pitch angle of zero degrees with tip speed ratios of 2.5 and 4.5, as well as a pitch angle of 20 degrees with tip speed ratios of 1.0 and 1.75. These operational conditions were selected as they apply to the different peak regions for two distinct pitch angles. The resulting angle of attack distributions are presented in Figure 5.6. Here, the blue and orange line are to be compared (0 degree pitch) and the green and red curve are to be compared (20 degrees pitch). Before analysing the results, it must be noted, that the inner 70% of the blade stalls at an angle of attack of 12.5 degrees, whereas

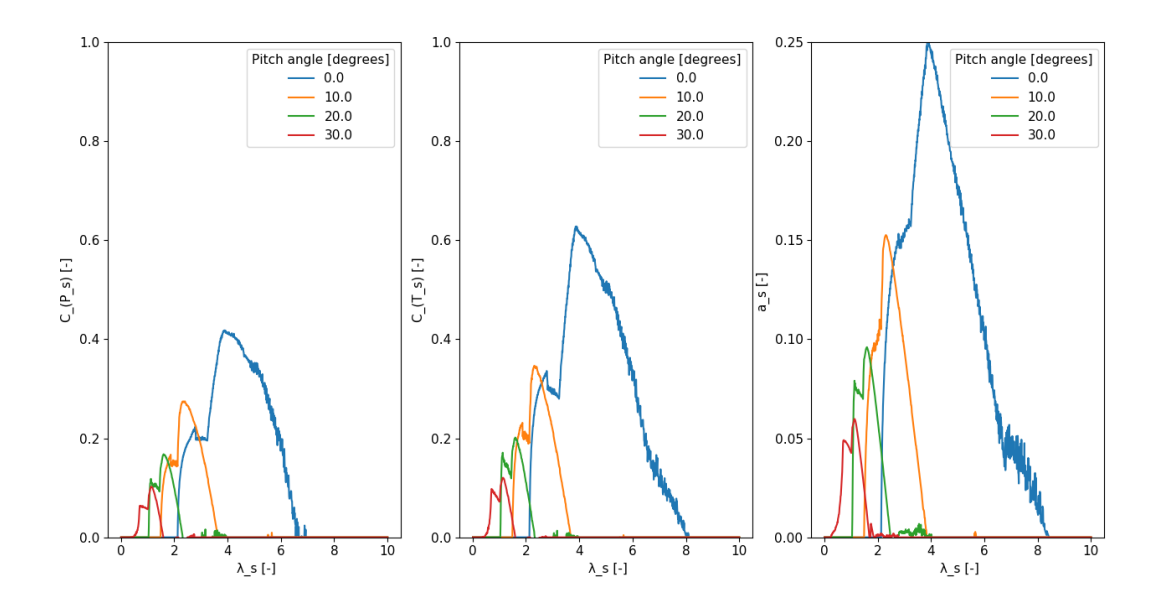


Figure 5.5: Power coefficient, thrust coefficient and induction factors for different operational cases

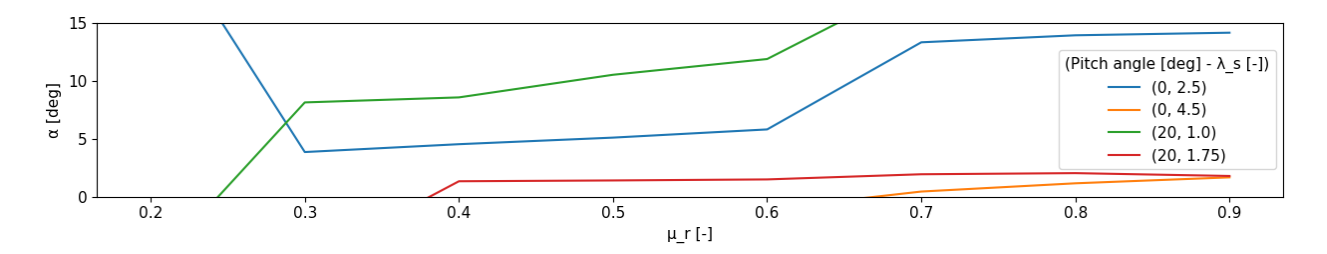


Figure 5.6: Angle of attack distribution over the secondary rotor blade for different operational cases

the outer 30% stalls at 4.0 degrees. In the angle of attack distributions, significant differences are observed for the different cases. For both pitch angles, the outer part of the blades stalls for the lower tip speed ratio. The inner part, however, operates within the linear part of the lift curve. For the higher tip speed ratio, it is found that the outer part of the blades does operate within the linear part of its lift curve whereas the inner part operates at very low angle of attack, considering its angle of attack at stall. These differences in angle of attack distributions, and thus load distributions, may be the cause of having two peaks in the curves of Figure 5.5. It may also be the reason why such high pitch angles seem to be needed. Because both parts of the blade seem to be operating in their operational angle of attack range for different pitch angles, a wider range of pitch angles is required to be able to use both airfoils to their full potential. In conclusion, this means that the design is not optimal. At this point, the twist distribution was chosen continuous throughout the blade length. Better performance may be achieved by imposing a different twist distribution for the outer 30% of the blade, with the supercritical airfoil. This is expected to undo the need of pitch angles up to 30 degrees. This is something to be investigated in the future and which was not within the time constraints of the current project.

Analysing the performance curves further, another aspect is found which causes questioning of the validity of the results. From the momentum theory, as described in section 5.1, it can be derived that the ratio of C_{P_s} over C_{T_s} should equal $1-a_s$. This equality follows from an actuator disc model and does not represent reality as it is precisely. However, it is found to be a good initial estimation for an engineer [11]. Analysing these quantities for several cases within the performance curves, significant discrepancies were found. For example, at a zero degree pitch angle and a tip speed ratio of 2.2, $\frac{C_{P_s}}{C_{T_s}}$ equals 0.63 and $1-a_s$ equals 0.94, which is more than 30% difference. For a 30 degree pitch angle and a tip speed ratio of 0.7 $\frac{C_{P_s}}{C_{T_s}}$ equals 0.53 and $1-a_s$ equals 0.97, which is roughly a 45% difference. For a 0 degree pitch angle and a tip speed ratio of 4.3, $\frac{C_{P_s}}{C_{T_s}}$ equals 0.68 and $1-a_s$ equals 0.78, a difference of almost 15%. These are just some examples of many operational conditions which show this significant difference. At this point it is unclear whether these results are plausible and accurate enough to be accepted. Performing verification and validation on these results should therefore be done in order to draw a conclusion. More detail on this can be found in section 5.11.

The data given to the structures department included the planform design, the tangential and normal forces along the blade length, and the aerodynamic moment along the blade for the critical loading cases. However, it was decided that it would be beyond the scope of the current project phase and take too much time to determine all critical loading cases exactly from all possible combinations of tip speed ratio and pitch angles, because the force distributions are very complex, partly due to the airfoil transition along the blade. Therefore, to be able to assess the loading, it was decided to take the maximum loads per blade element for all operational cases and superimpose them. Moreover, the normal (thrust), tangential (causing the torque) and aerodynamic moment loads per blade element for every operational condition were assessed, and the maximum for all three loads per blade element were taken and superimposed on the blade. The results are presented in Figure 9.3 of chapter 9. It must be noted that this is a gross over estimation of the loading cases that the structure will experience. Therefore, it is most certain that the structure is determined heavier than needed. Emphasis is put once again on the fact that this was chosen considering time constraints and must be looked at in the future in more detail to optimise the structure.

5.10 Sensitivity analysis

A sensitivity analysis is performed on the aerodynamic design to establish a confirmation on the accuracy of the outcomes. Moreover, the inputs are varied and a check is done on the influence that has on the outcomes. For this design stage, an accuracy of 10% is desired. Moreover, a change of 10% in the inputs is tested. If the outcomes are found to be too different, a new preliminary design iteration is needed.

The parameters that are input for the aerodynamic analysis are the geometrical aspects of the rotor. It may be said that these are actually the outcomes of the aerodynamic analysis, as they are chosen to achieve certain power and thrust coefficients and induction factors. However, for the sensitivity analysis it makes sense to test changes in performance due to changing geometrical aspects. This may be necessary due to structural considerations. One could argue as well, that different power and thrust coefficients and induction factors may be needed by the control department. However, it is decided that it is not necessary to perform a sensitivity analysis on this, as the control department can change the strategy based on aerodynamic results. In addition, if the maximum power and thrust coefficients and induction factors set by the control department are achieved, the design can still be used for other values if needed, by changing the tip speed ratio. This would only make the rotor not operate at optimal tip speed ratios, but it would make the design comply with the requirements of all departments.

The geometrical aspects that are changed include the chord and twist distribution, the location of airfoil transition, the blade's root location (hub radius) and the rotor radius. A summary of the results of this sensitivity analysis are provided in Table 5.4. As can be seen, the power and thrust coefficients, and the tip speed ratios do not change much, except when the twist is changed. This makes sense, as increasing the twist is the same as pitching the blades, which from the original results gives significantly different outputs. What causes more concerns are the changes in maximum loads. The maximum difference is just above 20% for increasing the chord lengths, which is a very significant increase. It is concluded, though, that these numbers do make sense. As the chord length increase, the two-dimensional loads lift and drag increase with the same proportion. This is directly translated to the aerodynamic moment by another multiplication with the chord length. An increase in chord of 10% thus causes a 21% increase $(1.1 \cdot 1.1 = 1.21)$ in aerodynamic moment, which is very similar to the results from the sensitivity analysis. Concerning changing the rotor radius, the loads are also affected significantly. Analysing the loading distributions, the maximum tangential forces occur near the root. As the rotor radius increases, the root radius also increases, as it stays at 20% with the same chord length. As such the relative wind velocity at the root increases and the forces scale with this velocity squared. The same effect is seen for decreasing the rotor radius, but here the forces decrease due to lower velocities at the root. In conclusion, changes in rotor radius may have a larger effect on the loads than initially expected. Therefore, the results of the sensitivity analysis are accepted.

Table 5.4: Results of aerodynamic sensitivity analysis

Parameter	New value	$C_{P_{s_{max}}}$ at 0 pitch	$C_{T_{s_{max}}}$ at 0 pitch	λ_s for $a_s = 0.05$ 0 pitch	λ_s for $a_s = 0.2$ 0 pitch	$F_{nor_{max}}$	$F_{tan_{max}}$	MOM_{max}
Original [,]	values	0.42	0.63	2.2	3.5	7080 N	7140 N	-6550 Nm
Increasing	values							
R_s	13.88m	0%	-3.2%	0%	2.9%	17.2%	16.2%	9.8%
$c_s(root-tip)$	3.25-0.83m	0%	3.2%	0%	-2.9%	3.0%	-5.0%	21.1%
$\beta(root-tip)$	$41.6 - 5.5^{o}$	-7.1%	-11.1%	-9.1%	2.9%	-6.1%	-18.2%	-17.3%
Airfoil transition	9.72m	0%	0%	-4.5%	0%	0%	0%	0%
R_{hub}	2.78m	0%	-1.6%	0%	0%	0%	5.5%	0%
Decreasing	yalues							
R_s	11.47m	2.4%	3.2%	0%	-2.9%	-15.0%	-18.1%	-9.2%
$c_s(root-tip)$	2.68-0.68m	0%	-3.2%	0%	2.9%	-3.1%	-3.9%	-17.6%
$\beta(root-tip)$	$34.36 - 4.55^{o}$	4.8%	11.1%	4.5%	0%	5.9%	6.9%	1.5%
Airfoil transition	8.03m	0%	-1.6%	0%	0%	0%	0%	-15.7%
R_{hub}	2.29m	0.4%	0%	0%	0%	0%	-12.7%	0%

5.11 Verification and validation

In addition to a sensitivity analysis, verification and validation are needed to draw conclusions on the validity of the obtained results, as already mentioned in section 5.9. This was partly done already when the code was developed. During coding small tests were performed to check whether bugs were developed within the code. When this was the case, the bug was solved before continuing. These tests included mostly cases from which results were already known, for example from literature. If the code gave a significantly different output, it was revisited. These tests were performed on all performance and geometrical calculations, as well as the airfoil polars inclusion.

Afterwards, validation was performed on the results that the code gave as a whole. This was done by using the QBlade program, which also provided the airfoil polars. This program actually uses XFoil to extract airfoil polars and includes a BEM model to analyse a wind turbine's performance. In addition it also gives the possibility to implement tip and root losses according to Prandtl's estimations. The C_{P_s} , $C_{T_s} - \lambda_s - pitch$ curves were compared, see Figure 5.7.

Here, C_{P_s} , $C_{T_s} - \lambda_s$ curves are shown for the same pitch angles as in Figure 5.5. The aspects provided in Table 5.5 are identified to validate the results. As can be seen, some quantities are completely similar, whereas others show some discrepancies. Mostly the tip speed ratios at which C_{P_s} and C_{T_s} are zero for low pitch angles are an underestimation, whereas for high pitch angles they occur to be an overestimation. In contrast, the optimal tip speed ratios get more accurate for higher pitch angles. The maximum power and thrust coefficients show similar discrepancies for the entire pitch angle range, but they are acceptable. Because the wind turbine will mostly be controlled to operate at these optimal conditions, it is most important that these conditions are modelled well, which thus is the case. A possible reason for the discrepancies is the blade element distribution. The Python Code includes a constant spacing of blade elements, whereas the QBlade program implements a sinusoidal spacing [16]. The latter means that more blade elements are located near the root and tip of the blades, as it is expected that larger differences in induction factors occur there because of the Prandtl tip and root losses. It is suggested to also implement this sinusoidal spacing of blade elements in the Python code in the next design phase.

In conclusion, the results are deemed valid for the current state of the design. The big difference between the ratio of C_{P_s} over C_{T_s} and $1-a_s$, as described in section 5.9, are also observed in the validation data obtained through QBlade. Therefore, this is assumed to be correct and no longer an issue. As the project furthers to the detailed design phase, a more detailed study on the discrepancies between the obtained results and the validation data obtained through QBlade is to be done, first of all by implementing the sinusoidal blade element spacing in the Python code.

Table 5.5: Result comparison of the model in Python and the model in QBlade

Quantity	Own	QBlade
$C_{P_{s_{max}}}$ at 0 pitch	0.42	0.44
$C_{T_{s_{max}}}$ at 0 pitch	0.63	0.66
$\lambda_{s_{opt}}$ at 0 pitch	4	3.5
$C_{P_{s_{max}}}$ at 10 pitch	0.27	0.31
$C_{T_{s_{max}}}$ at 10 pitch	0.35	0.38
$\begin{array}{c} \lambda_{s_{opt}} \\ \text{at 10 pitch} \end{array}$	2.3	2.5

Quantity	Own	QBlade
$C_{P_{s_{max}}}$ at 20 pitch	0.17	0.19
$C_{T_{s_{max}}}$ at 20 pitch	0.20	0.24
$\lambda_{s_{opt}}$ at 20 pitch	1.6	1.5
$C_{P_{s_{max}}}$ at 30 pitch	0.10	0.13
$C_{T_{s_{max}}}$ at 30 pitch	0.12	0.16
$\lambda_{s_{opt}}$ at 30 pitch	1.1	1.1

Quantity	Own	QBlade
λ_s for $C_{P_s} = 0$ and 0 pitch	6.6	5.8
λ_s for $C_{P_s} = 0$ and 10 pitch	3.6	3.7
λ_s for $C_{P_s} = 0$ and 20 pitch	2.3	2.4
λ_s for $C_{P_s} = 0$ and 30 pitch	1.6	1.6
λ_s for $C_{T_s} = 0$ and 0 pitch	8	7.0
λ_s for $C_{T_s} = 0$ and 10 pitch	3.6	4.0
λ_s for $C_{T_s} = 0$ and 20 pitch	2.3	2.5
$\lambda_s \text{ for } C_{T_s} = 0$ and 30 pitch	1.6	2.1

5.12 Limitations

Now, the aerodynamic planform design is confirmed with the corresponding performance. However, it must be noted that the implemented models have some limitations. Some of which have already been mentioned, but for clarity all of them will be discussed here.

First off, the code does not allow for identification of the critical loading cases. Moreover, it identifies the maximum loads occurring at each blade element over the whole range of operational cases and superimposes them on the blade as one case. This way, the critical loading is over estimated, as this loading case will never be experienced.

Secondly, the QBlade program used to extract the airfoil polars does only provide lift and drag curves for an angle of attack range up to 360 degrees. The moment coefficients are only available for the linear part of the lift curve. If a blade element operates outside this range, the moment coefficient is manually set to 0. In reality this is never the case and therefore the maximum moment loads may be an underestimation.

The airfoil transition is placed at 70% of the blade radius. For now, this is modelled as a discontinuity, which in practise will not be the case. This transition is also expected to impose aerodynamic losses on the design, which have not been modelled yet.

The Reynolds and Mach numbers vary over the rotor blade. This is not modelled as airfoil data is taken for Reynolds and Mach numbers at the outer locations of the blade. In addition to that, the rotor experiences different Reynolds and Mach numbers at different operational conditions. This is also not taken into account in the airfoil polars and therefore inaccuracies may arise.

5.13 Recommendations

The limitations described above need to be accounted for in a later stage in the design process. Some actions are proposed to overcome some of the limitations.

First off, it is suggested to investigate the critical loading cases more accurately. By assessing the force distributions for every operational case, one can conclude on what loading cases are critical and must be assessed by the structures department.

It is advised to search for more accurate data on the aerodynamic moment coefficients outside the linear part of the lift polar. This may be done using the program XFoil. This will give more accurate results on the loading cases that will be experienced by the rotor.

Thirdly, it is recommended to implement a smooth transition between the blade parts with different airfoils. In addition, the aerodynamic losses regarding this transition must be investigated, implemented in the model and optimised for the rotor's performance. This might include analysing different chord and twist distributions

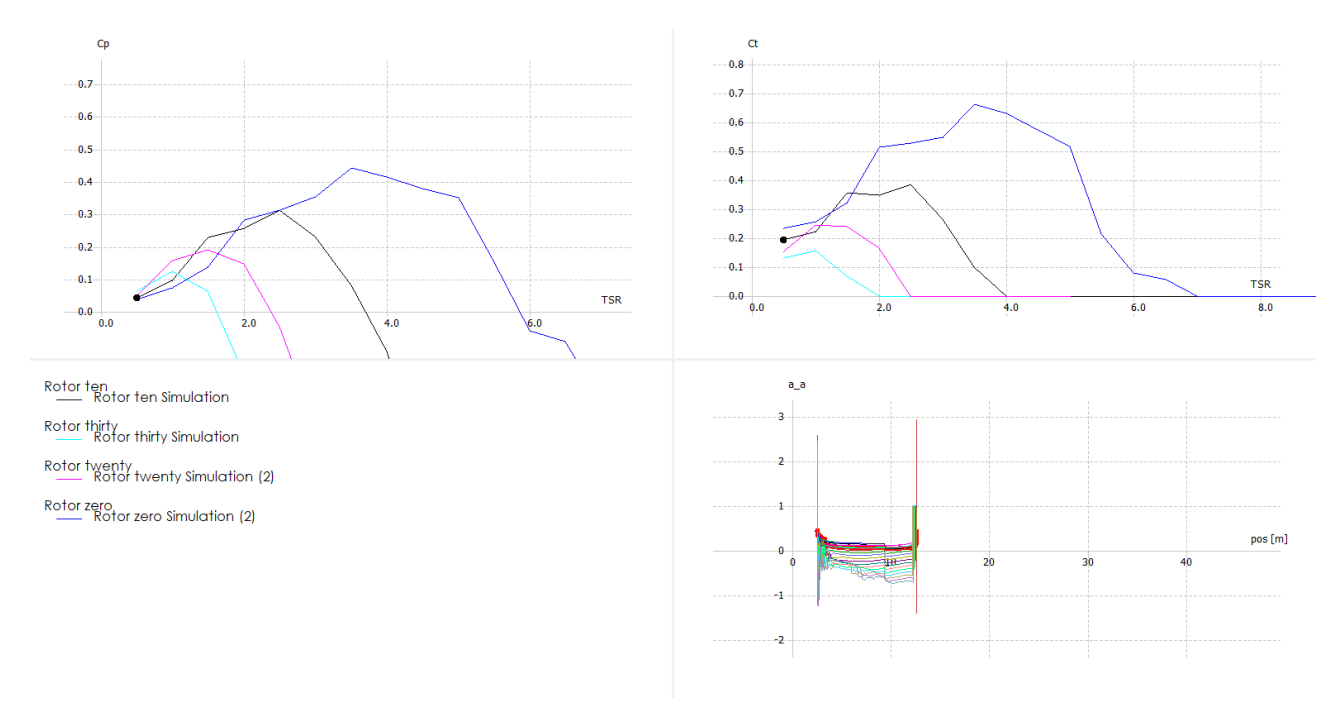


Figure 5.7: Data obtained from QBlade to validate the developed Python code

for the outer part of the blade. This optimisation may cancel out the two peaks the performance curves, as mentioned in section 5.9, by causing more even load distributions. However, this may not be the only way to achieve cancelling out having two peaks.

Considering high lift devices, such as flaps, is also recommended. The current design has been designed for both high and low induction factors, which may cause a sub optimal design. Using high lift devices for one of the cases, may allow for a more optimal design for other cases. This may also help in cancelling out the two peaks in the performance curves. However, even though high lift devices may increase rotor performance, they must be traded off with the structural implications they impose.

Analysing the Reynolds and Mach numbers variation along the blade and for each operational condition, is recommended. Implementing these results within the airfoil data will give more accurate results for the rotor simulation.

As already mentioned in section 5.12, more accurate results may be achieved by using sinusoidal spacing of blade elements. Thus, implementing smaller blade elements near the root and tip of the blade is recommended.

Currently only the secondary rotor is designed and the dimensions of the primary rotor are obtained by scaling the system as presented by the University of Strathclyde [8]. To be sure the design is feasible also a study should be done on the primary rotor. For this an actuator cylinder model could be employed, as initially introduced by Helge Aagaard Madsen [17]. Initially it was the plan to perform such an actuator cylinder analysis, and determine for example the primary rotor chord distribution and other design parameters. Due to unforeseen circumstances and time constraints however, the team in the end has not been able to perform the analysis and therefore it is recommended to perform such an analysis in the future.

5.14 Turbine noise

Once the aerodynamic design of the turbine is known, it is important to get an idea how much noise the design produces. Two types of noise exist, aerodynamic noise and mechanical noise. In this section a look will be taken at the aerodynamic noise of the turbine.

5.14.1 Theory

The method used to perform the prediction of the noise levels is taken from a publication by NASA on the aeroacoustics of flight vehicles [18]. Since the secondary rotors can be compared to propellers of an aircraft, a method is used which is for noise coming from propellers and propfans.

To perform the analysis, use will be made of the frequency domain first, after which it will later be transformed back to the time domain to get an indication of the noise levels the operating, and thus rotating, turbine produces when standing at a certain distance from the tower of the turbine. First several assumptions will be made:

- It is assumed that the noise of the primary rotor is negligible compared to the secondary rotors, hence only the secondary rotors will be analysed during the analysis. Due to the slow rotating nature of the primary rotor, the sound pressure levels (SPL) produced by this movement will be small compared to the secondary rotors. Since SPL is measured in the logarithmic decibel scale, the contribution of the primary rotor will add very little to the overall SPL compared to driving contribution coming from the secondary rotors. As a result of this assumption the SPL estimated will be lower than what it actually will be.
- It is assumed both thickness of the rotor and aerodynamic loading act on the advanced helix, hence on the surface swept by a rotating radial line translating through space with ω_s and $V_{S_{\omega}}$. Blade loading, thrust and torque per blade element, are known prior to the analysis from blade element momentum theory, section 5.6, and thickness distribution from the detailed design. These are transferred to the advanced helix to take their effects into account.
- It is assumed the noise coming from the rotors is radiated equally in all directions. This causes the predicted noise to differ from what it would be in real life, hence the noise determined at a certain location from the turbine could either be higher or lower than what is obtained. The current analysis only gives a general idea on noise levels. The effects of pressure waves getting reflected by the ground, and therefore interfering with each other is also neglected.
- It is assumed the chordwise thickness distribution can be approximated to be parabolic to make the analysis easier. When comparing this to the actual thickness distribution of the chosen airfoils it was determined this simplification was allowed for the current accuracy of the analysis. Also a uniform chord-wise lift distribution is assumed.
- The effects of Doppler shifts are neglected to simplify the analysis, hence it is assumed no frequency shift occurs. The effect of this on the analysis it that the frequencies as experienced by the observer are constant instead of raised when the rotor comes towards the observer and lowered when it moves away. Also the effects of wind are neglected, which would influence the frequency as experienced by the observer.

With these assumptions in place the sound pressure levels of the turbine can be assessed. The far field pressure can be found from Equation 5.20, where $2P_{m_{harm}B}$ represents the Fourier transform of the pressure at the mth harmonic of the blade passing frequency. The value for $P_{m_{harm}B}$ summarizes the effects of blade volume $P_{m_{harm}V}$ and the blade loading $(P_{load})_{m_{harm}}$, hence $P_{m_{harm}B} = P_{m_{harm}V} + (P_{load})_{m_{harm}}$.

$$p(t_t) = 2Re \left[\sum_{m_{harm}=1}^{\infty} P_{m_{harm}B} \exp\left(-im_{harm}N_b\omega_s t\right) \right]$$
 (5.20)

The noise harmonics related to blade volume are given by Equation 5.21. In this equation $J_{m_{harm}B}()$ is a Bessel function. Ψ_V , given by Equation 5.23, is the source transform of the chord-wise thickness distribution and k_x is the wave number given by Equation 5.22. The value for relative mach number is given by the relation $M_{rel}^2 = M_{\infty}^2 + z^2 M_{tip}^2$. The distance and angle to the observer, r_{obs} and θ_{obs} , are determined using trigonometric relations. The magnitude for $P_{m_{harm}V}$ is determined by integrating the thickness distribution over the blade. Its value has to be determined for each of the harmonics of the system.

$$P_{Vm_{harm}} = -\frac{\rho a_0^2 N_b \sin\left(\theta_{obs}\right) \exp\left(i m_{harm} N_b \left(\frac{\omega_s r_{obs}}{a_0} - \frac{\pi}{2}\right)\right)}{8\pi (h/D_{sr}) (1 - M_\infty \cos\theta_{obs})} \int_{z_{hub}}^1 M_{rel}^2 J_{mB} \left(\frac{m N_b z M_{tip} \sin\theta_{obs}}{1 - M_\infty \cos\theta_{obs}}\right) k_x^2 t_b \Psi_V(k_x) dz$$

$$(5.21)$$

$$k_x = \frac{2m_{harm}N_bc_{sD}M_{tip}}{M_{rel}(1 - M_\infty\cos\theta_{obs})}$$
(5.22)

$$\Psi_V(k_x) = \begin{cases} \frac{2}{3} & (k_x = 0) \\ \frac{8}{k_x^2} \left[\frac{2}{k_x} \sin\left(\frac{k_x}{2}\right) - \cos\left(\frac{k_x}{2}\right) \right] & (k_x \neq 0) \end{cases}$$
 (5.23)

Noise harmonics related to section-wise blade loading, $(P_{load})_{m_{harm}}$, are given by Equation 5.24. Here Ψ_L , given by Equation 5.25, is the source transform of the chord-wise lift distribution when uniform lift over the chord is assumed, $J_{m_{harm}B}$ is the same Bessel function as in Equation 5.21 and $\frac{dT}{dz}$ and $\frac{dQ}{dz}$ are the magnitudes of thrust and torque acting on the specific blade section. For both Equation 5.21 and Equation 5.24 the integrals are

taken over the normalized radius of the blade, z, which spans from the start of the blade at the hub, up until the tip.

$$(P_{load})_{m_{harm}} = \frac{im_{harm} N_b M_{tip} \sin \theta_{obs}}{4\pi h R_s (1 - M_\infty \cos \theta_{obs})} \int_{z_{hub}}^1 \left[\frac{\cos \theta_{obs}}{1 - M_\infty \cos \theta_{obs}} \frac{dT}{dz} - \frac{1}{z^2 M_{tip} R_s} \frac{dQ}{dz} \right] \Psi_L J_{m_{harm} B} dz \quad (5.24)$$

$$\Psi_L = \begin{cases} 1 & (k_x = 0) \\ \frac{2}{k_x} \sin\left(\frac{k_x}{2}\right) & (k_x \neq 0) \end{cases}$$
 (5.25)

With the noise harmonics known, and the far field pressure calculated a filter must be applied to the results. The noise levels must be adjusted to the human ear since this is not equally sensitive to all frequencies [19]. By applying this correction lower frequencies are de-emphasized in the same manner as the human ear does and the SPL experienced will be lower.

5.14.2 Simulation

With the key equations and assumptions being defined in the previous section, subsection 5.14.1, a program is written using Python. The purpose of the program is to simulate the rotation of the secondary rotors along their fixed circular path and to determine the far-field pressure they produce at each location along the circle they travel. A brief description of how the program works will be given in this section. Also a simple overview of the program is given in Figure 5.8.

First, dimensions with regard to the primary and secondary rotor must be specified, together with the atmospheric properties, rotational speeds of both primary and secondary rotor and thrust and torque. Next some parameters must be defined specific to the simulation, these are rotational speeds of both secondary and primary rotor, mach numbers experienced by the SR, number of harmonics to be analyzed, number of rotations to simulate and the time step for the simulation.

Once all parameters are defined the actual analysis can be performed. For each time step, first the relative angle, θ_{obs} , and distance towards the observer r_{obs} are determined by simple trigonometric relations. With these values in place the Fourier transforms of the pressure, $P_{m_{harm}V}$ and $(P_{load})_{m_{harm}}$, are determined for each harmonic. The integral from Equation 5.21 and Equation 5.24 are solved by employing a loop over them, analyzing each radial section. Also for each harmonic the A-weighted correction factors are determined.

With the Fourier coefficients known, far-field pressures can be computed using Equation 5.20. To obtain the total Z-weighted far-field pressure the pressures for each harmonic are summed. To obtain the A-weighted far-field pressure, the A-weighted correction is applied to each specific harmonic. To obtain the total A-weighted far-field pressure, all corrected pressures are summed.

To obtain the total sound pressure level in dB(A) as observed by the observer, located at a certain distance from the turbine tower, the root-mean-squared value is taken from the far-field pressure for one entire primary rotor rotation. The total SPL is then computed using Equation 5.26. Next to this the program also outputs a plot of the total far-field pressure and the contribution of the different harmonics before and after the A-weighted correction.

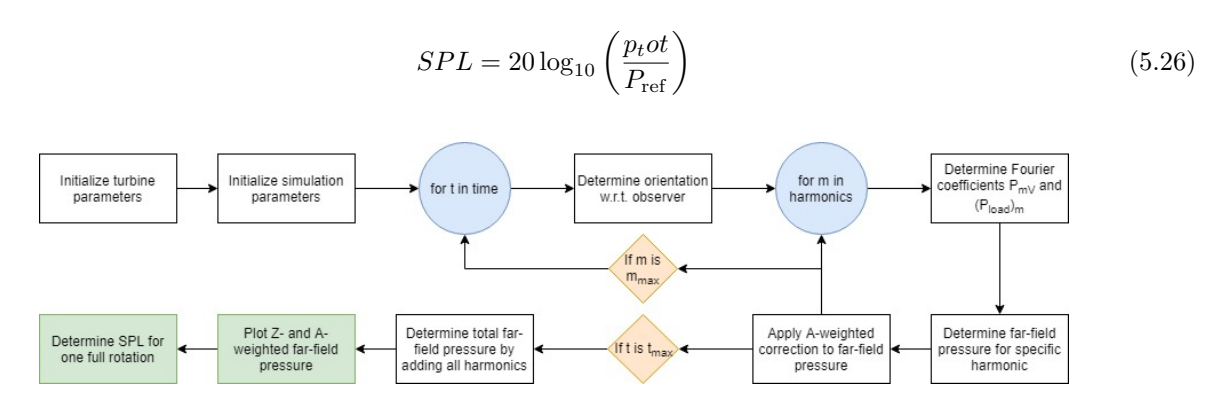


Figure 5.8: Overview of steps taken during noise prediction

5.14.3 Results

The results obtained from the program described in subsection 5.14.2 for the prediction of noise will be discussed in this chapter. Noise levels will be analyzed at two different locations. Location one being next to the tower, hence the rotors being located at the same distance for the entire simulation and location two being 100 meters away from the tower.

When located at the center of the primary rotor, the overall A-weighted SPL is equal to 62.2dB(A) when taken over one entire primary rotor rotation. The far-field sound pressure as experienced by the observer is more or less constant over the rotation as can be seen in Figure 5.9, hence the noise level experienced will also be more or less constant.

When located at 100 meters distance from the turbine, the overall A-weighted SPL is equal to 79.2dB(A) when

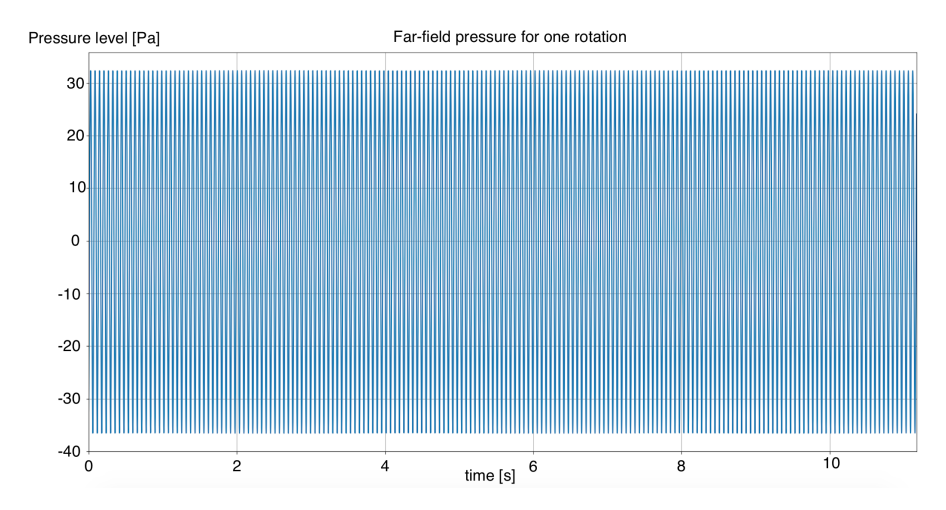


Figure 5.9: Z-weighted total far-field pressure for an observer located 0m from the tower

taken over one entire primary rotor rotation. For this case both Z-weighted and A-weighted root-mean-squared far-field pressures are shown in Figure 5.10 and Figure 5.11, respectively. In the figures each colour represents their own harmonic. The corresponding colours in the graphs for both Z- and A-weighting represent the same harmonic. When comparing the Z- and A-weighted figures, it can be seen that for Z-weighted pressure the low harmonics are driving for the pressure levels (blue with highest amplitude), however when the A-weighting is applied, their magnitude is damped drastically and the higher frequency harmonics start to play a more important role when it comes to experienced SPL. The fluctuations in the far-field pressure over the time span gives an indication that the SPL as experienced by the observer fluctuates heavily over the turbine rotation.

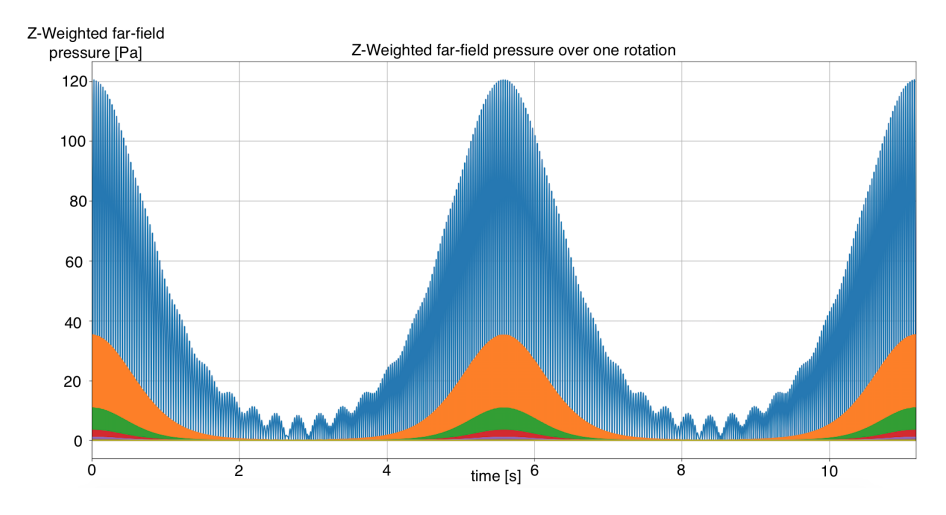


Figure 5.10: Z-weighted root-mean-squared far-field pressure for an observer located 100m from the tower. Each colour represents a single harmonic

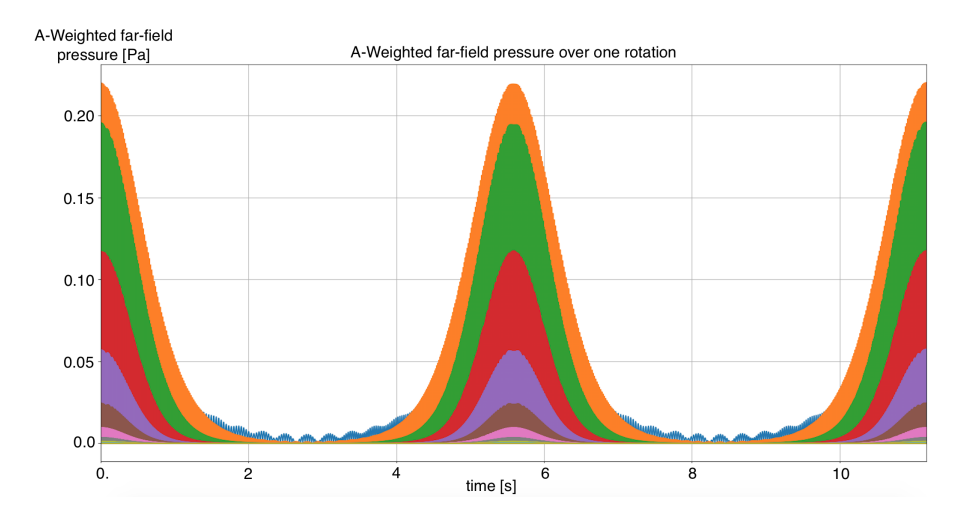


Figure 5.11: A-weighted root-mean-squared far-field pressure for an observer located 100m from the tower. Each colour represents a single harmonic

5.14.4 Verification and Validation

The results as obtained by the code, together with the code itself, must be verified and validated before one can take the estimated noise levels as close to reality. During programming of the analysis the several blocks of code were checked on any errors by the means of unit tests, hence giving an input from which the output is known and checking if the output corresponds to the expected output. In case of disagreement between obtained and expected results the code was revisited and the bug was fixed. Once it was found no bugs were present in the code two limiting cases were tested, namely analyzing the noise for the case where the turbine is not rotating and for the case where the observer was placed extremely far away from the turbine. As expected the first limiting case gave as output that no noise was present and the second limiting case indeed gave negligible decibel levels. Once the code passed these two limiting tests it was said to be verified.

Validation of the code has not been performed at this point in time. The reason for this is the fact that no validation data could be found. There are however some ideas on how validation could be performed. The most simple way to validate the code is to implement the blade geometry and blade element loading for an existing turbine from which SPLs it produces are known. If the prediction of the code is similar to the actual measured turbine noise levels, it can be assumed the code is validated. Another way to validate the code is to perform a noise analysis by employing CFD-software. If the sound pressure levels of the CFD model are equivalent to the values obtained from the written code, the code also is validated.

5.14.5 Limitations and Recommendations

Each model has its limitations. Most of the limitations of this model were already discussed in the list of assumptions given in subsection 5.14.1. One of the main limitations which was not discussed there is that the travelling of sound between atmosphere layers it is not taken into account in this analysis. This could influence the determined noise levels dramatically, causing high SPLs to reach much further than what is expected from this analysis.

The point just discussed leads us immediately to one of the main recommendations, which is that the effect of the previously described effect must be analyzed. Another recommendation would be that the shape of the rotor could be optimized for noise, hence trying different designs and picking the one that produces the least amount of noise.

Chapter 6: Supervisory control and safety system

This chapters serves as a smooth transitions between chapter 5 and chapter 7. In the previous chapter, aerodynamic values were calculated. These values will be used in the next chapter to simulate the control system and output the performance of the wind turbine. However, interactions between control systems have to be defined first, which will be done in this chapter. This will help to gain a better understanding of how the control of this wind turbine works, which can be used to optimise the control strategy in the next chapter.

In section 6.1, a general overview of control systems in a wind turbine is given. Due to the fact that regulations play a very large role in the supervisory control and safety system design, the procedures and guidelines described in this chapter are largely based on the wind turbine certification guidelines from DNV GL [20] [21], together with those from the International Electrotechnical Commission (IEC) [22]. The guidelines for the control system are listed in section 6.2. In section 6.3, the components required to control the wind turbine are listed as well.

After that, a top down approach is used to describe the wind turbine control interactions. In section 6.4, the communications flow diagram is shown. This gives an idea on which systems are involved for communications between turbines and an onshore supervisory system. In section 6.5, the systems within the turbine are isolated and discussed. It shows the architecture of the control system within the turbine and also contains an overview of the data handling. After that, the supervisory control system is discussed in more detail in section 6.6 after which also the safety system is discussed in section 6.7. A final overview of the system is shown in section 6.8 after which a functional analysis is done in section 6.9, this flows into the conclusion of the chapter that can be found in section 6.10. Here Using the interactions of the control systems described in this chapter, a control strategy can be chosen and programmed to simulate this system. This will be described in the next chapter.

6.1 General

The main purpose of the control system is to ensure safe and automatic operation of the wind turbine, to be achieved continuously and in an optimized way. 'Optimized' can be related to maximizing energy capture, preventing the turbine from excessive dynamic mechanical loads and ensuring that the quality of the power output conforms the standards of the grid [23]. The overall depth of this report only allows for an optimization on the control system with respect to controlling the system to convert wind energy to electric power. The strategy that will be used for this can be found in the next chapter. This chapter will focus on giving a clear overview of the control system including sensors and actuators and discussing concepts and procedures that can be used for the overall control system. The design of the safety system that ensures safety in case of emergency is also key for a successful control system.

6.1.1 Definitions

First of all, it is important to clearly define the terms used throughout this chapter which may be ambiguous or somewhat open to interpretation. Listed below are those terms, with a concise definition.

- Supervisory control concept The supervisory control concept is a procedure aimed at operating the wind turbine efficiently, safely and lightly stressed [21].
- Safety concept The safety concept describes how to keep the turbine safe at the event of a serious failure, a loss of grid power or during potentially dangerous environmental conditions [21].
- Supervisory control system The supervisory control system is there to enforce the supervisory control concept, in other words is it responsible for the controlling, monitoring and regulating the wind turbine in accordance with the control concept [21]
- Safety system In some documents also called the protection system. This is a fail-safe and highly reliable system which acts independently from the supervisory control system and serves to enforce the safety concept. When activated, it takes over from the supervisory control system and safely brings the turbine to a halt.
- **Nominal condition** The normal operating conditions where the turbine is managed by the supervisory control system.

- Non-nominal condition: Conditions that are deviant from the normal operating range of the wind turbine. Non-nominal conditions are those conditions which trigger the safety system.
- Nominal shutdown Normal shutdown procedure where for instance the risk of overspeed is low and thus allow for a more controlled shutdown
- Emergency shutdown When the safety system is activated, it will perform an emergency shutdown. Generally this involves, among other things, pitching of the blades at the maximum achievable pitch rate, imposing high loads on the turbine [21]
- Fault As defined by the IEC: "an unplanned occurrence or defect in an item which may result in one or more failures of the item itself or of other associated equipment" ¹
- Failure As defined by the IEC: "termination of the ability of an item to perform a required function" ².
- Braking system System that is capable of slowing the system down to a stop. The braking system does not necessarily have to operate on mechanical principles, but can also operate on electrical or aerodynamic principles, or a combination of these principles [22].

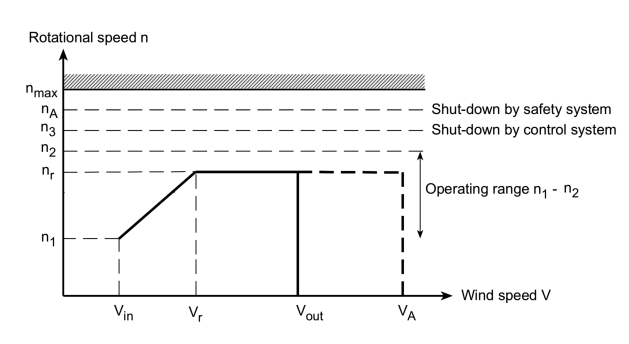
6.1.2 Assumptions

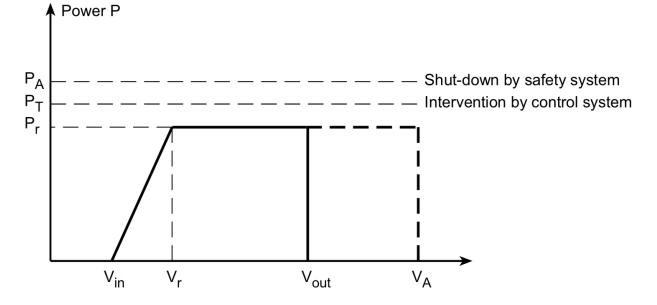
During the design of the supervisory control and safety systems, some assumptions have been made. Firstly, it is assumed that it is highly unlikely that multiple failures occur simultaneously. The turbine is therefore designed to be brought to a halt when a single failure occurs.

In addition, it is assumed it is unlikely that the extreme wind condition which the turbine is to be designed for, the wind speed at the site which has a 50-year return period, coincides with a turbine failure. For this reason, the turbine is to be designed for the 50-year extreme gust under no-fault conditions, and a 1-year return gust under fault conditions [11].

6.1.3 Operating conditions

To ensure the correct level of reliability and safety, environmental and electrical parameters shall be taken into account. The conditions that the turbine operates in can be divided in nominal conditions and non-nominal conditions. During nominal conditions the control concept is enforced by the supervisory control system. Correspondingly, during non-nominal conditions the safety concept is enforced by the safety system.





(a) Sketch of the rotational speed ranges

(b) Sketch of a power curve showing the triggering values for the control and safety system

Figure 6.1: Diagrams showing the different operation regions related to rotational speed and power [21]

In Figure 6.1, the different operating regions can be identified. Nominal conditions are when the rotational speed is above n_1 , the minimum operating speed and below n_3 , the rotational speed at which shutdown of the wind turbine should be initiated by the supervisory control system. The rotational speed which is reached at rated wind speed V_r , is denoted by n_r . When n_3 is reached, the control system is supposed to shut the turbine down. A non-nominal condition is when rotational activation speed n_A is reached, at this rotational speed the safety system should kick in and bring the wind turbine to an immediate shutdown [21]. Maximum overspeed n_{max} is the rotational velocity which the turbine shall never reach, not even briefly.

 $^{^2} http://std.iec.ch/terms/terms.nsf/9bc7f244dab1a789c12570590045fac8/ad2f6aba27e6c2e6c125750e003a78b0? OpenDocument$

When looking at Figure 6.1b, a similar division between nominal and non-nominal conditions can be made. Conditions below P_T , the power level at which the supervisory control system must initiate a power reduction, are considered to be nominal conditions [21]. When activation power P_A is reached, the wind turbine has to be shutdown by the safety system [21].

The wind speeds which can be identified in both diagrams Figure 6.1 are V_{in} , which is the cut-in wind speed, V_r the wind speed at which rated power is reached and V_{out} , which is the wind speed where the control system should initiate a nominal shut-down. Non-nominal conditions occur when a wind speed of V_A is reached, here the safety system must perform an emergency shutdown immediately. A summary of what is considered to be nominal or non-nominal is given in Table 6.1.

Table 6.1: A summary of what is considered as a nominal or non-nominal condition

Nominal conditions	Non-nominal conditions
$V < V_A$	$V \ge V_A$
$n < n_3$	$n_A \le n \le n_{max}$
$P < P_T$	$P \ge P_A$

At this point in the design phase it is not possible to give values to the parameters in Figure 6.1 and Table 6.1. A detailed analysis on the structural design and other subsystems is required for this.

6.2 Guidelines

The guidelines which are specifically applicable on the control and safety system are listed below. All the guidelines can be divided into the following categories: general (GEN), safety (SAFE), control (CONT), monitoring (MONT), pitch system (PITCH) and finally the braking system (BRAKE).

- GEN-1 Wind turbine operation and safety shall be governed by a control and safety system [22]
- **GEN-2** Manual or automatic intervention shall not compromise the safety functions of the safety system [22]
- GEN-3 Settings of the control and safety system shall be protected against unauthorized interference [22]
- **SAFE-1** The safety system shall be operational or in activated mode (triggered) in all modes of the wind turbine, e.g. power production, parked, grid loss or maintenance [21]
- **SAFE-2** Any function of the safety system shall have a higher priority than the function of the control system [21]
- **SAFE-3** The safety system shall have access to at least two mutually independent braking systems, independently of any function of the control system [21]
- SAFE-4 The safety system shall have access to equipment for grid disconnection of the generator, independently of any function of the control system [21]
- SAFE-5 The limiting values triggering the safety system shall be defined [21]
- SAFE-6 The safety system shall carry out its task without delay [20]
- SAFE-7 The safety system shall be able to decelerate the rotor with the aid of two braking systems [20]
- SAFE-8 At least one emergency stop button shall be provided at the foot of the tower and one in each nacelle of the secondary rotors as a possibility for manual intervention [21]
- **SAFE-9** The emergency stop buttons shall be available and functional at all times. Triggering the emergency stop function must override all other functions and operations in all modes of the wind turbine [21]
- CONT-1 The control system shall have access to at least two mutually independent braking systems [21].
- MONT-1 The rotational speed shall be measured at least twice by systems mutually independent from each other [20]
- MONT-2 The power shall be measured at least twice by systems mutually independent from each other [20]

- MONT-3 The wind speed shall be measured continuously at hub height with at least one measurement system [20]
- MONT-4 The rotational speed signal shall be supplied at least twice to the control system and at least once to the safety system [20]
- MONT-5 The control system shall continuously monitor the plausibility of the wind speed signal by comparison with a second wind speed signal measured independently, or by comparison with other measurements related to the wind speed. [20]
- MONT-6 At least one power signal shall be monitored by the control system [20]
- MONT-7 Independent of the power signal measured in MONT-6, another power signal shall be monitored by another device outside of the control system
- MONT-8 At least one of the rotational speed measurement systems shall measure the speed of a component of the wind turbine that runs at rotor speed [20]
- MONT-9 The control system shall continually monitor the plausibility of at least two of the measured speed signals with regard to each other [20]
- MONT-10 If the monitoring detects an error in the two signals described in MONT-9 and less then two rotational speed signals are available, the wind turbine shall be shut down immediately [20]
- MONT-11 If the monitoring system described in MONT-5 detects an error, the wind turbine shall be shut down immediately [20]
- MONT-12 The control system shall shut down the wind turbine immediately if the rotational speed exceeds the upper operating limit n_3 [20]
- MONT-13 If the control system detects exceedance of the activation power P_A the wind turbine shall be shut down immediately and the safety system shall be activated. [20]
- MONT-14 The safety system shall overrule the control system if the rotational speed exceeds n_A [20]
- MONT-15 The trigger value for the safety system (n_A) shall be adjusted such that the maximum speed n_{max} may never be exceeded [20]
- MONT-16 The wind speeds sensor(s) shall never have ice on them [20]
- PITCH-1 The pitch angle of each blade shall be monitored [20]
- PITCH-2 The plausibility of the monitored pitch angle described in PITCH-1 shall be supervised [20]
- PITCH-3 To achieve guideline PITCH-2 each blade shall have a second blade pitch angle that is measured independently [20]
- PITCH-4 If the monitoring task described in PITCH-1, PITCH-2 and PITCH-3 cannot be carried out continuously, then automatic tests shall be performed at least weekly [20]
- PITCH-5 The wind turbine shall be shutdown immediately if the monitoring or tests, described in PITCH-4, reveals an abnormal result [20]
- PITCH-6 If the deviation between the measured pitch angles of the different rotor blades exceeds the limiting value, the wind turbine shall be shut down by the control system [20]
- BRAKE-1 The braking system shall be designed that they remain operable at grid loss [20]
- BRAKE-2 If power supply from accumulators (e.g. from the hydraulic unit from batteries) is necessary for the functioning of braking systems, it shall be automatically monitored that a sufficient amount of energy is made available in the accumulators [20]
- BRAKE-3 If the automatic monitoring described in BRAKE-2 of the energy storage cannot be carried out continuously, then automatic tests shall be performed at least weekly to show that a sufficient amount of energy is available [20]
- BRAKE-4 The wind turbine shall be shut down immediately if the automatic monitoring or test yields an abnormal result or the automatic test cannot be carried out [20]

6.3 Components

This section describes all components which together make up the supervisory control and safety system. The components are split into three categories: sensors, which perform and communicate measurements; actuators, which perform certain actions upon being given a command; and all other components which are not sensors or actuators, such as the main control computer, back-up power supply, electrical infrastructure, etc. These components can then be put together to define certain subsystems, which are later used by the supervisory control system and the safety system.

6.3.1 Sensors

Correct sensors are required to maintain the wind turbine stability and enhance performance under continuously changing wind conditions [24]. To ensure safety and optimal control there will be two independent sensors for making those measurements which are considered critical, as also prescribed by guidelines MONT-1, MONT-2, MONT-4 and PITCH-3. The supervisory control system always compares the outputs of these two sensors, and if the variance between the two values is too big the wind turbine will be shutdown, corresponding to guidelines MONT-10 and PITCH-6. For other measurements, one sensor is sufficient, such as the ones described in MONT-3 and MONT-6. A summary of the sensors used on the SRVAWT is given in Table 6.2.

Category	Type	Quantity	Location
Power	Voltage meter	2	At the generators
Power	Current meter	2	At the generators
Power	Frequency meter	2	At the generators
Power	RPM meter	6	At the generators and vertical axis main shaft
Pitch	Blade pitch angle sensor	24	Two sensors on each blade
Structures	Load sensor	13	At the root of each blade and at tower
Structures	Vibration sensor	13	On each blade and at tower
Structures	Accelerometer	13	On each blade and at tower
General	Wind vane	1	On top of tower
General	Anemometer	1	On top of tower
General	Temperature sensor	10	At the generator
General	Icing sensor	13	At the tip of each blade and on top of tower
General	Noise sensor	3	In tower and the nacelles
General	Multi-sensor smoke detector	3	In tower and the nacelles

Table 6.2: Overview of the different sensors used in the wind turbine

6.3.2 Actuators

A list of the actuators used in the design can be found in Table 6.3. Again these actuators are part of different subsystems that are used by the supervisory control and safety systems.

Category	Type	Quantity	Location
Pitch	Electrical pitch motor	12	At the root
1 10011	Electrical pitch motor	12	of each blade
Control	Mechanical parking brake	3	On each shaft
General	Fine water spray system	3	In each nacelle and tower
Power	Generator	2	In each nacelle
Control	Parking lock	3	At each shaft

Table 6.3: Overview of the different actuators used in the wind turbine

6.3.3 Other components

The supervisory control and safety system consists of more components than just sensors and actuators. Other hardware, such as the back-up power supply, electrical infrastructure including fail safe relays and fuses, and the main control computer also play a crucial role in the successful operation of the supervisory control and safety system. In addition, a lot of software is involved in ensuring the correct response to given inputs.

The supervisory control computer is a central on-board computer which oversees the operation of the supervisory control system and, in turn, the operation and performance of the entire turbine. In addition, the electrical infrastructure is very important for connecting the components and making communication between them possible.

The back-up power supply, supporting the safety system, is vital especially in case a loss of grid power occurs in the turbine. Multiple options exist, of which the conventionally most common is the use of batteries. However, due to their electrochemical nature, they are prone to deterioration, especially in harsh and highly fluctuating environmental conditions, such as those found offshore. This results in failure after, on average, two to four years and subsequent maintenance costs and revenue losses [25]. A more recently emerged concept which is gaining popularity, is the use of ultracapacitors for back-up energy storage. Their main advantages compared to leadacid batteries are their longer lifetime (hundreds of thousands of cycles - or about 12 years of operational lifetime - versus hundreds of cycles [25]), less required maintenance, lower weight, and higher reliability, efficiency and operability even in very hot and cold climates [26]. This leads to reduced maintenance costs and operational risks, combined with improved safety conditions due to the fewer replacements and maintenance activities which are needed, while the upfront costs are similar to those for lead-acid batteries. Additionally, ultracapacitors charge faster and can deliver quick bursts of power within short timeframes, which is especially useful when the blades need to be pitched as quickly as possible in the case of an emergency. The reduction in cost of energy, size and mass which comes with the use of ultracapacitors, combined with their suitability for offshore conditions, leads to the choice to use this system for energy storage on this turbine. The back-up power supply should be monitored to make sure there is enough energy for at least one emergency stop, also corresponding to guideline BRAKE-2.

Finally, there must be emergency stop buttons, at least at the foot of the tower and in each secondary rotor nacelle, which must trigger the activation of the safety system when pressed and which must be available and functional at all time. This corresponds to guidelines **SAFE-8** and **SAFE-9**.

6.4 Communication flow diagram

In order to give a general overview of the control system a communication flow diagram, Figure 6.2 is constructed. It is important that the wind turbine can be continuously monitored in order to plan maintenance trips or collect accurate data on power production.

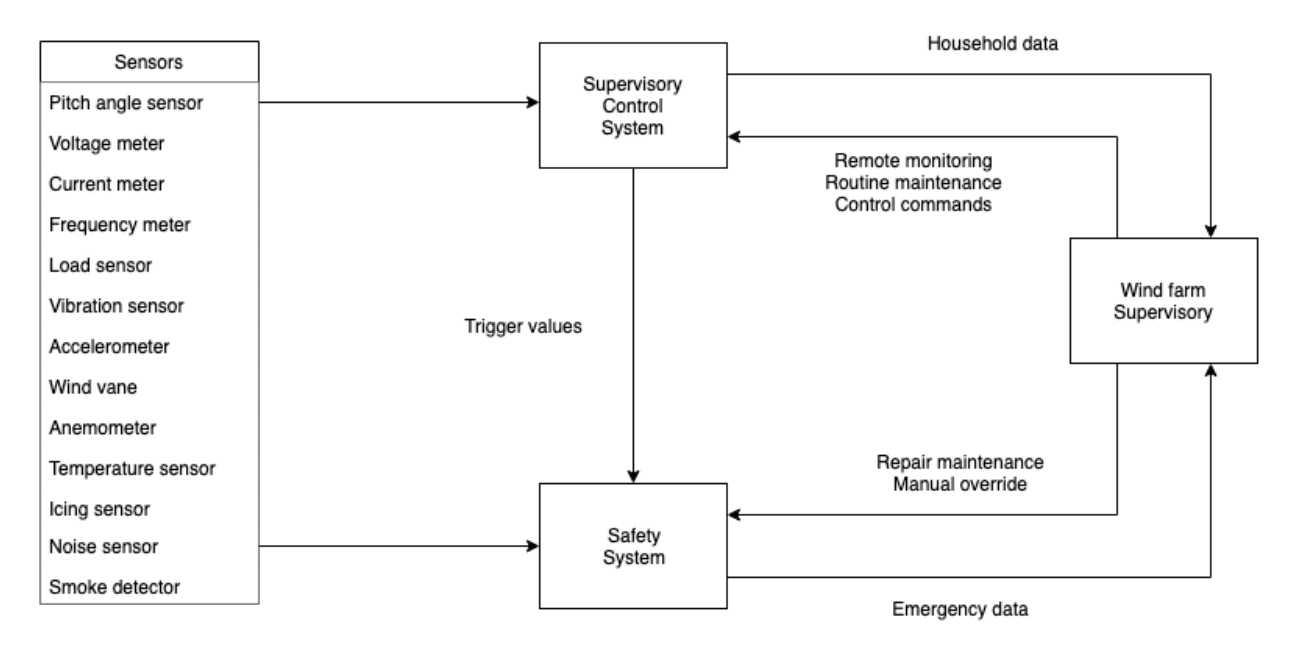


Figure 6.2: Communication flow diagram

First, data is collected by the sensors in the wind turbine. These sensors are connected to both the supervisory control system of the turbine and the safety system in order to have redundancy in case the supervisory control system fails. If the supervisory control system does not fail, it provides data to the safety system. The supervisory control system of the turbine sends household data to the wind farm supervisory system. This household data is used to monitor the operations and conditions of the turbine remotely. Routine maintenance can be planned accordingly. Commands can be sent to the turbine as well, for example a nominal shutdown can be enforced to stop the turbine during maintenance activities or if a reset of the turbine is needed [21].

The safety system can send data to the wind farm supervisory system as well. This concerns emergency stops and serious failures. Usually repair maintenance and a manual override of the system are required to restart the wind turbine after an emergency shutdown.

6.5 Control system architecture and data handling

The control system of this wind turbine is more complicated than for conventional wind turbines, since there are more rotors and components to take into account. However, the general idea remains the same. In order to control the turbine, both pitch and torque control are used. Figure 6.3 shows an overview of how the system is controlled. The primary rotor is controlled using pitch and torque control, which is done for most conventional turbines as well. The pitch control is done by pitching the primary rotor blades. The difference here is that usually, torque control is done by the generator, which the primary rotor does not have. However, it does have two secondary rotors attached to the blade tips. Those secondary rotors can be used for torque control by controlling the thrust that they provide. In order to control the thrust of the secondary rotor, they have to be controlled separately as well. The control of the secondary rotor is again done by using pitch and torque control. Pitch control is again done by pitching the blades of the secondary rotor. Torque control can be done by using the generator. In the following subsections, each form of control will be explained in more detail.

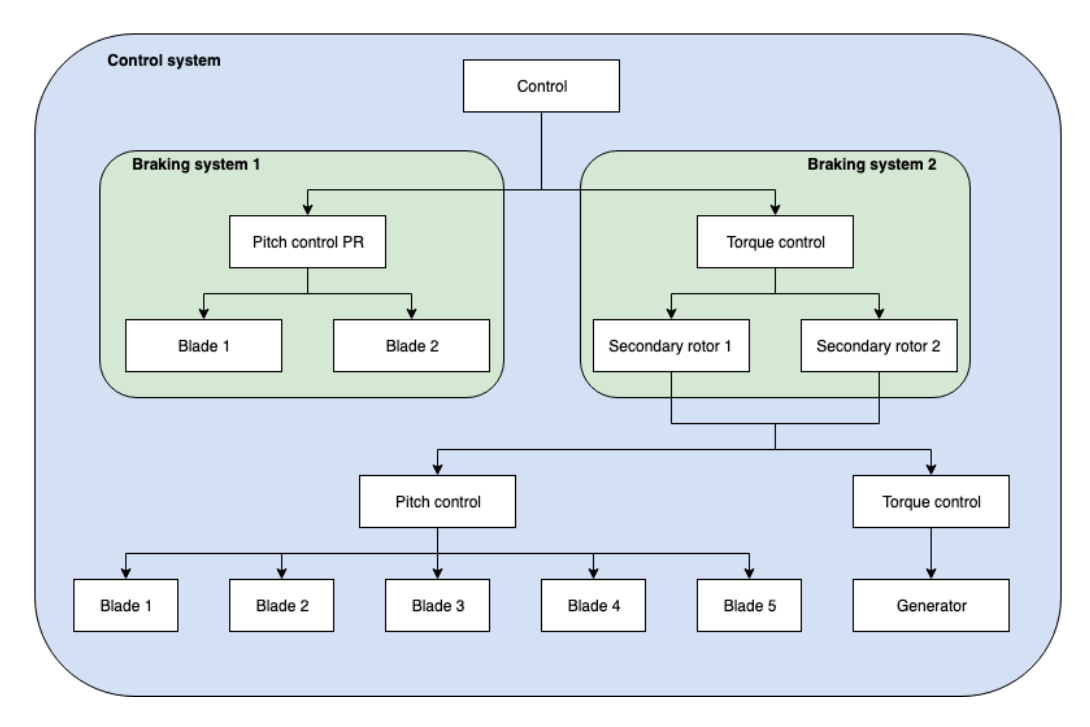


Figure 6.3: Overview of the control system architecture

The control system described in the figure above can be translated to hardware and software required to implement the control strategy in practise, this is shown in Figure 6.4. On the left it shows all the sensors that are required in order to assure safe operation of the system. These sensors provide data to both the supervisory control system system and the safety system in the middle of the diagram. These systems will be responsible for the data handling in the wind turbine. After data handling, these systems control the actuators in order to make changes to the system when required. These actuators are shown in the right. In the middle, the power supply is shown. Power is provided to all systems of the wind turbine. The mechanical brake and rotor lock are powered by hydraulics. All other components use electricity, which is usually provided by the grid. When

there is a disturbance in the grid, there is a backup power supply in the form of an ultracapacitor. This will provide enough power to the safety system and other components to shut down the turbine.

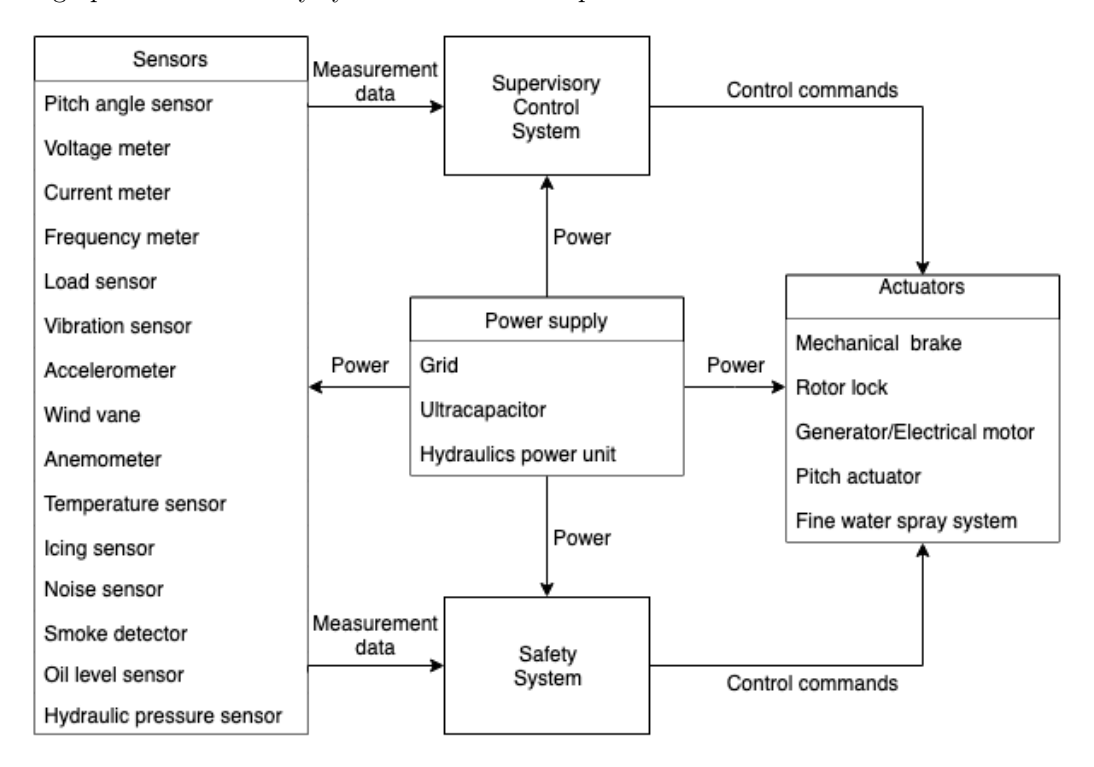


Figure 6.4: Hardware and software layout of the control system

6.5.1 Generator torque control

Torque control is a means of control which is accomplished by the turbine generator, and used in variable speed turbines. Essentially, it functions by finding the amount of torque that is necessary for an optimal rotor speed and which the generator should then command from the rotor [27]. This control method can be used to optimize energy extraction in partial load, but also to limit power conversion in full load.

Within this turbine, torque control is applied by both secondary rotor generators. Due to the fact that it is a direct-drive turbine, the rotor speed ω_{in} is the same as the generator speed. This can be straightforwardly and accurately measured by the RPM meter mentioned previously. The desired torque T is then obtained from using the mode gain K, that can be seen in Equation 6.1 [28]. The mode gain is calculated according to Equation 6.2 [28].

$$T = K\omega_{in}^2 \tag{6.1}$$

$$K = \frac{0.5\rho\eta_{gearbox}A_rR^2}{r_{gearbox}^3} \cdot \left(\frac{c_p}{\lambda_a^3}\right)$$
 (6.2)

In which for this turbine, the gearbox efficiency $\eta_{gearbox}$ and the gearbox ratio $r_{gearbox}$ both are equal to 1 due to the absence of a gearbox.

During the energy conversion process, the primary rotor determines how much electrical power can be produced. Before rated wind speed the goal is to capture the maximum energy possible, this happens at one specific c_p value, together with its matching value for λ_a . So, it can be concluded that for the primary rotor before rated, $\left(\frac{c_p}{\lambda_a^3}\right)$ is constant and thus the optimal mode gain K_{opt} is constant. Because there is no generator connected to the shaft of the main vertical axis rotor, its rotational speed and hence its torque is controlled by the secondary rotors. When looking at Figure 6.5, ω_1 is the first signal that gives an rpm measurement, ω_2 is the second. The obtained values are compared to each other. If there are no anomalies the rpm signal, ω_{in} , goes into the closed feedback loop together with K_{opt} .

When controlling the primary rotor, the box "Process" indicates the secondary rotors, since they must change the torque of the primary rotor. The torque of the secondary rotors is controlled by the generator. Since

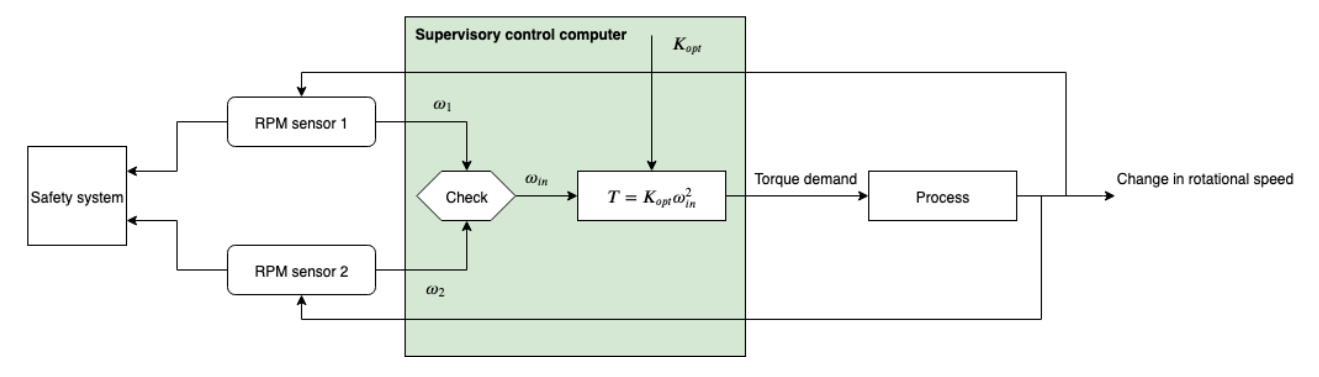


Figure 6.5: Torque control data handling scheme

the main goal of the secondary rotors is not to maximize energy extraction, and therefore do not operate at maximum c_p , there is no fixed value for $\left(\frac{c_p}{\lambda^3}\right)$ for which one can aim. At what instant in time which c_p -value should be obtained is discussed in more detail in the upcoming chapter, chapter 7. The control option discussed here is just an example of proportional control, there is only one gain. Other control options are for instance, the use of a Proportional-Integral (PI) or a Proportional-Integral-Derivative (PID) control system.

6.5.2 Pitch control

Pitch control will be used on the primary and on the secondary rotor blades to control their inflow angle. How this influences the power and thrust is discussed in chapter 5. This is done not only to ensure that the turbine follows the power curve in an efficient way, but it also serves as a means of aerodynamic braking. It has already been decided previously to use active pitch control in [9], however, multiple options still exist within this type of system.

Despite the fact that pitch control typically only accounts for about 3% of the capital costs of the turbine, several studies on turbine reliability [29],[30] have identified it as the component which contributes the most to turbine failure rate and downtime. This is mainly due to the harsh conditions experienced in the rotor hub, such as extreme temperatures, humidity and vibrations. For this reason, and considering the fact that this turbine will have a lot more pitch systems than conventional turbines (and they will probably be used more intensively), pitch system selection is important within wind turbine design.

One of the choices to make is whether to use collective or individual pitch control, i.e. whether all blades will be pitched at once, or each separately. The main benefit of collective pitch control is the fact that, within conventional turbines, only one pitch system is required to pitch all blades. This has a positive effect on overall failure rate. However, in case the pitch system does fail, the turbine cannot be operated since it no longer has two independent braking systems. In addition, a collective pitch control system poses very large loads on the turbine.

Individual pitch control provides a more precise pitch control of all blades. It also significantly reduces the loads exerted on the turbine, which has a positive effect on the maintenance requirements, and the turbine lifetime. In addition, individual pitch control is inherently redundant, meaning that after the failure of one pitch system, the turbine can still be aerodynamically braked using the other pitch system(s) [28]. For this reason, individual pitch is chosen for now on all rotor blades.

Another choice which must be made is the decision between the use electric or hydraulic pitch. Hydraulic pitch is the most common pitch system found in wind turbines, however electric pitch systems are becoming increasingly more popular. One benefit of an electric pitching system is that it does not require oil under high pressure, and therefore does not introduce the risk of leaking hydraulic fluid. This is obviously good not only for environmental and sustainability reasons, but also for the public image of the project. Additionally, electric systems require less power due to the fact that they do not need a pump running at all times. This is why electric pitch systems will be used on the SRVAWT.

Electric pitch systems require a slip ring [11], through which power supply, and control signals for the pitch systems are transferred. The slip ring is connected to a central control unit, which has clamps for power distribution, and control signals for the three individual blade drive units. These components will thus also be introduced within the SRVAWT.

Figure 6.6 shows a data handling diagram for a general pitch control system. It contains the hardware and software involved in blade pitching, and shows the data flow through the components. A pitch angle sensor

measures the pitch angle at a certain moment in time. This signal γ_{in} is the first input to the supervisory control computer, the second input is the desired pitch angle γ_d . Both of those signals are processed, and the computer will output a signal to the actuator that will pitch the blade. This data flow is then iterated until the desired pitch angle is achieved. For safety reasons, there are two pitch sensors that measure the blade pitch angle. Both γ_1 and γ_2 are checked with respect to each other in order to determine if they are correct. When the difference between the measurements is too large, the safety system is initiated.

Again the control diagram shown in Figure 6.6 is a simple representation of the pitch control system. There again exist more advanced controllers, but again, which type of controller is best for the current system will not be discussed in this report.

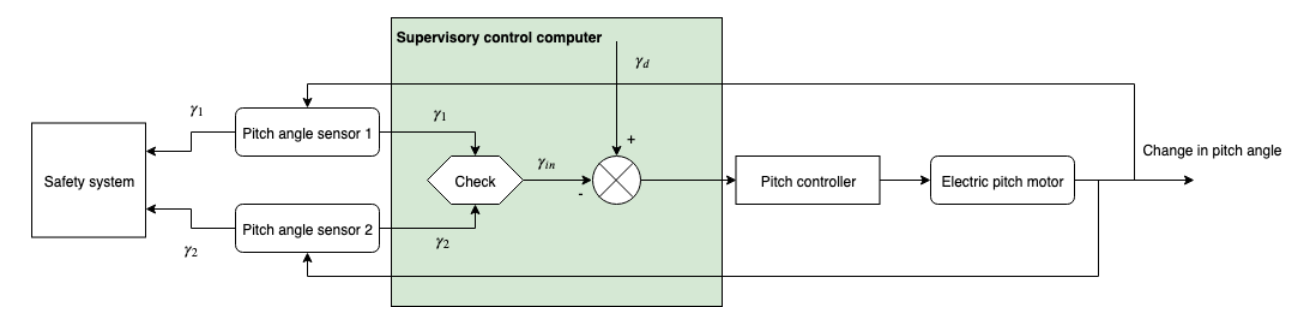


Figure 6.6: Pitch control data handling diagram

6.5.3 Braking system

A critical part of the supervisory control and safety system is the braking system, as this is required to ensure safe operations. The braking system is used to reduce the rotational speed of the rotors, and bringing it to a complete standstill when necessary. According to guidelines SAFE-3 and CONT-1, the whole braking system should be consisting of two individual, mutually independent braking systems. The whole turbine consists of one vertical axis rotor, and two horizontal axis rotors. Each one of the three rotors has a pitching system on every blade, but the main way to brake the rotor is by pitching the primary rotor blades to feather. This is the first braking system that contribute to fulfilling guidelines SAFE-3 and CONT-1. The second contribution to the overall braking system comes from the thrust produced by the secondary rotors. Both breaking systems are also depicted in Figure 6.3. The reason why a mechanical braking system is not chosen, is the high rotational speeds on the secondary rotor and high torque on the primary rotor. This has significant effects on the sizing of the mechanical brake, the wear it experiences during its lifetime and the temperature increase which occurs in the nacelle while the rotor is being mechanically braked. In this design case, the mechanical brake only needs to be able to bring the turbine to a standstill from a very small rotational velocity, meaning that the brake can be small and its main function is to park the turbine.

6.5.4 Parking and holding

Every now and then, the turbine will have to be brought to a complete standstill, such as during an emergency shutdown, when the wind speed exceeds cut-out speed (depending on the choice of the operator), and when maintenance is scheduled to take place.

As mentioned before, the mechanical brakes are only used to park each rotor from low rotational velocities, after the previously mentioned braking systems. Each rotor has its own parking brake, resulting in a total of three parking brakes. Once the parking brake has brought the rotor to a complete standstill, a rotor lock is applied to ensure no further rotation. The rotor lock is the primary means of holding and must be capable of holding the rotor still by itself, even in worst-case conditions. This is due to the fact that, although the parking brake is often used as a secondary means of holding the rotor, it must still be inspected regularly, removed from the rotor for a different reason. Even then, it must be possible to keep the rotor in place. Each rotor lock consists of a lock disk, and a lock bolt, which is driven into the disk when the system is activated. This turbine will have a rotor lock on each of the three rotors, as well as on each blade to ensure no pitching motion.

6.6 Nominal conditions: the supervisory control system

The supervisory control system oversees the efficient and automatic operation of the turbine under nominal operations, such that the turbine is able to follow its power curve. An example of an power curve is shown in Figure 6.7.

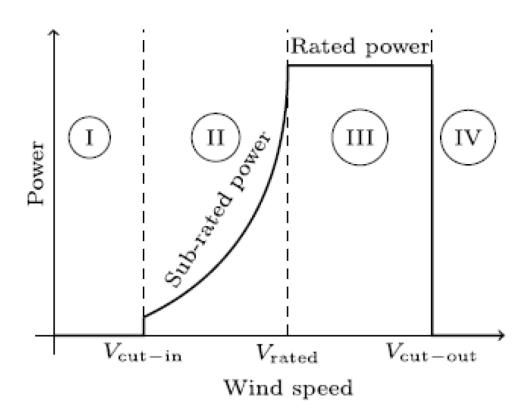


Figure 6.7: Different regions in the power curve [31]

Within the turbine power curve, four regions are distinguished. Region 1 is the region below cut-in speed, i.e. wind speeds below 3 m/s. Within this region, the turbine is in idle condition and not converting energy. Region 2 is between cut-in and rated velocity, i.e. between 3 m/s and 11 m/s. Region 3 is the region between rated wind speed and cut-out speed, i.e. between 10 m/s and 25 m/s. Region 4 is the region above cut-out speed, i.e. above 25 m/s. The turbine will be parked within this region to prevent damage.

The DNV GL guidelines stipulate that for certification, the control concept, and system must be described. This entails a description of the control system behavior during normal operation, as well as the behavior on detection of a malfunction. In addition, the starting and stopping sequence shall be described, and the structure of the control system shall be described or shown visually [21]. All aforementioned items are included in this section.

6.6.1 Normal operation

An overview of the nominal operation is given in figure Figure 6.8. The rectangular blocks in Figure 6.8 represent different states the turbine can be in. These states can then be further divided in transitional, or stationary states. During the system check, (transitional state), different inputs for the control system are determined such as the rotor positions, and different faults are cleared. When these operations are done and the wind speed has reached the cut-in speed of 3m/s, the turbine is ready for operation. This is the beginning of the start-up procedure. The start-up procedure ends when power production starts in Figure 6.8.

The start-up procedure is explained in more detail in Figure 6.9. During the start-up, the subsystems are powered up and initialized, such that they are ready for power production.

The power production phase is a stationary phase where current flows into the electrical grid [13]. The supervisory controller performs a number of tasks during power production including continuous monitoring of power and rotor speed, system fault detection, and determining set points for the controllers, such as γ_d and K_{opt} [13]. In high wind gusts, the turbine's rated power is allowed to be exceeded for short periods of time to limit the duty cycle of pitch actuators, and not having to continuously start-stop the system [13]. This is the P_T as explained in subsection 6.1.3. During normal operation, the power production phase can be interrupted, such as when the wind speed drops below cut-in speed, or when it exceeds cut-out speed. If the wind speed drops below cut-in speed the rotors will be allowed to freely spin in idle mode until cut-in speed is reached again [13]. In both cases the generators will be disconnected. Additionally, the power production phase can be interrupted as a result of the operator invoking a nominal shutdown, for example when scheduled maintenance or inspection is going to take place on the turbine.

For maintenance activities, the turbine is brought to a complete standstill. If cut-out speed is reached the system will be shut down in order to prevent damage to the turbine structure. The shutdown procedure is explained in more detail in Figure 6.10. An alternative option to a grid disconnection and a complete turbine

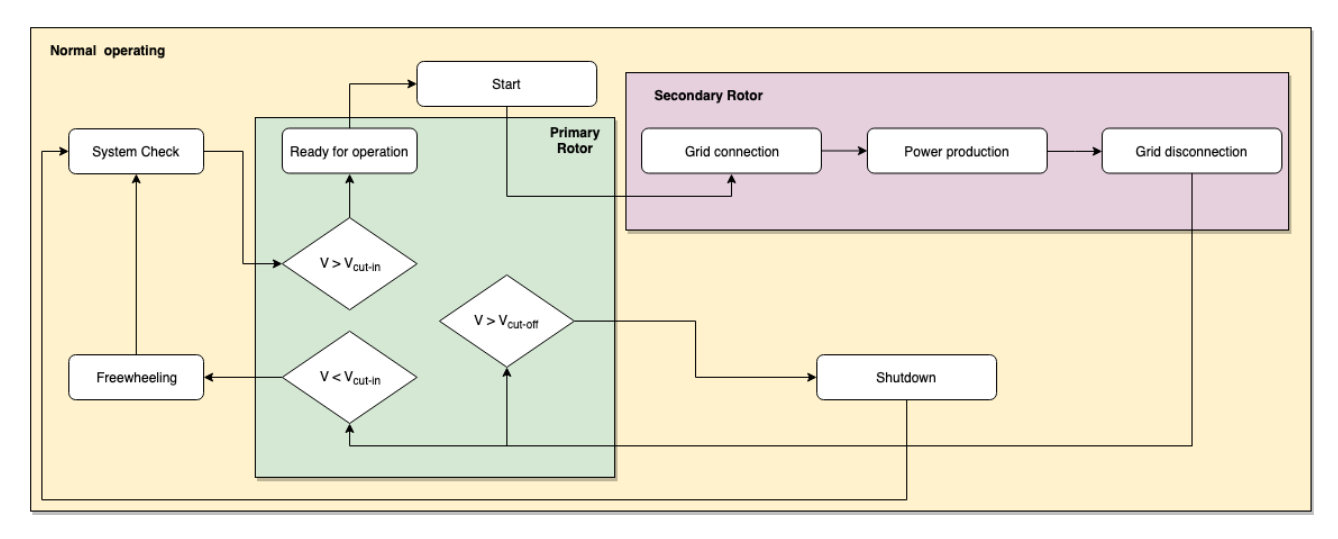


Figure 6.8: An overview of the data handling during normal operation, with a division between primary and secondary rotor.

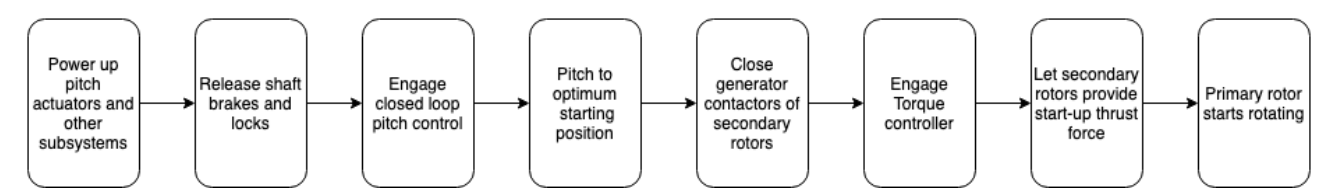


Figure 6.9: Start-up procedure of the wind turbine during nominal operating conditions

shutdown beyond cut-out speed, is to allow for a so-called soft cut-out. This approach allows to continue power production beyond cut-out, albeit at a lower capacity. It has been investigated in [32], where it was found that designing for a soft cut-out means that a 5% increase in extreme loading will have to be taken into account. Due to the fact that one of the top-level requirements of this project is a decrease in mass compared to conventional turbines, combined with the relatively rare occurrence of wind speeds beyond 25 m/s, it is decided that this turbine will follow sharp cut-out procedure. However, one option which could be considered in the future, is the choice to set the primary rotor still beyond cut-out speed but to leave the secondary rotors spinning. This means power can still be produced beyond rated power, and thus could be a form of a soft cut-out. This idea should however be investigated structurally to see if the current design could withstand the loads imposed in this scenario, which is recommended for future research.

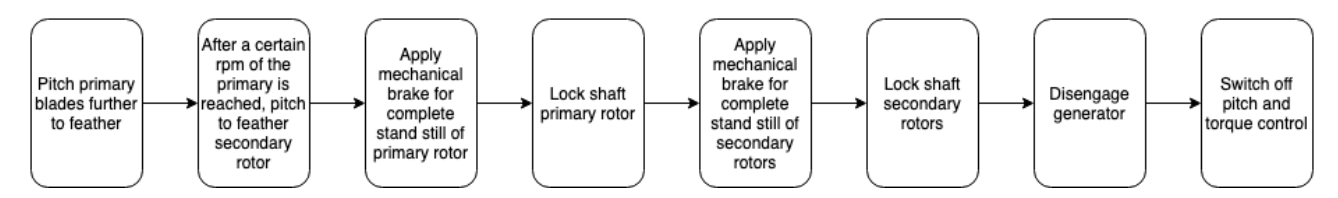


Figure 6.10: Shutdown procedure of the wind turbine during nominal operating conditions

6.6.2 Malfunctions under nominal conditions

Even under nominal conditions, small malfunctions may occur. These must always be detected, communicated, and responded to in a quick and efficient way. These malfunctions do not necessarily lead to unsafe situations that ask for an emergency shutdown. These malfunctions are listed below.

- 1. Exceeding rotational speed of n_3 , as discussed in subsection 6.1.3
- 2. Exceeding power P_T , as discussed in subsection 6.1.3
- 3. Braking system in bad condition due to wear and tear
- 4. Faults in machinery components
- 5. Abnormal frequencies and voltages in power system

6.7 Non-nominal conditions: the safety system

The safety system ensures that the turbine can come to a halt in a safe and quick manner, as soon as a condition which warrants an emergency shutdown, is detected. This shall be possible even under a loss of power, meaning the safety system must work fail-safe and independently from the nominal control system, as also prescribed in guideline **BRAKE-1**. Safety system activation is always superior to the supervisory control system functions. What this means is that the safety system should always override the control system, when activated, which follows from guideline **SAFE-2**. Similar to the control system, also a safety concept and system must be described in the design phase. This entails a description of the turbine behavior following the activation of the safety system, as well as a statement of the criteria for which the safety system is triggered. The structure of the safety system shall also be described or shown visually [21].

6.7.1 Safety system activation criteria

Listed below are all cases which trigger the activation of the safety system, complying with guideline **SAFE-5**. The list consists of failures which are deemed serious enough to require an immediate emergency shutdown, undesirable and potentially unsafe conditions, as well as the operator invoking an emergency shutdown.

- Failure of a primary rotor pitch control system
- Supervisory control system failure
- Grid loss
- Generator failure
- Fire
- Blade or rotor ejection
- Emergency button pressed
- A shock, for instance due to an earthquake

On top of these failures, there are also values regarding speeds and power which, when exceeded, activate the safety system. These are: V_A , n_A and P_A . What these parameters mean is explained in subsection 6.1.3. Again in this stage of the design it is not possible to determine exact numbers for these values.

6.7.2 Safety system functioning

In order to ensure a quick and safe stop after activation of the safety system, it shall be specified exactly how the safety system behaves upon activation.

The main function of the safety system is to quickly, and safely bring the turbine to a halt, even after a serious failure, using those systems which are still operational. Activation of the safety system is achieved through the supervisory control system. The first step in its functioning is to separate from the power grid, after which the back-up power supply is used to power the safety system functions. It has to be decided which sensors will be powered by the back-up power supply. For now it is decided to power all of them. A disadvantage of this is the fact that both mass and cost will increase. It might be not necessary to power all the components during non-nominal conditions, for instance only the pitch actuators. The sensors are then not available, and thus a closed control loop is not possible. An open-loop control system with values pre-computed beforehand can be used for maneuvering the turbine during an emergency shutdown [33].

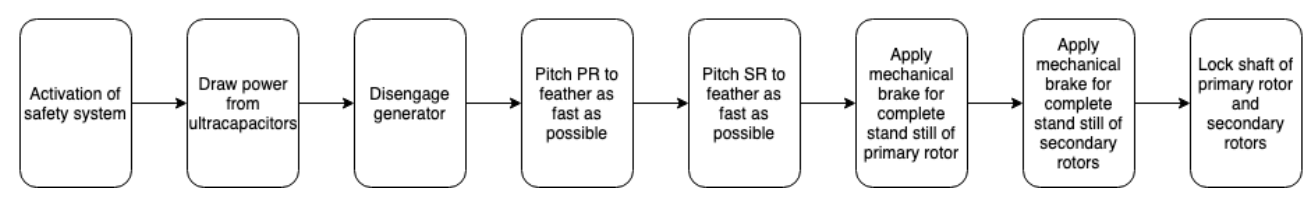


Figure 6.11: Emergency shutdown procedure in case of failure of the supervisory control system

In subsection 6.1.1 it was already explained that during an emergency shutdown the blades will be rapidly pitched to feather. A more complete procedure is shown in Figure 6.11. It should be noted that this particular

procedure does not always hold. Depending on the type of failure, parts of the procedure will be changed or moved further away, or closer towards the start of the procedure. The procedure shown in Figure 6.11 was shaped for the case when the supervisory control system fails. Later in the design phase, for all the activation criteria which trigger an emergency shutdown a separate procedure should be made. During the selection of the procedure the extra stress on the components and structure of the wind turbine should be considered. By doing a trade-off regarding reducing peak loads and the amount of overspeed allowed, an optimum can be found [33]. This can also be done for a normal shutdown procedure.

6.8 Failure response overview

The guidelines from DNV GL suggest that it should be made as clear as possible how different failures and faults are detected, which components the fault or failure effect, what the possible causes are, and what actions have to be taken. An overview of some of these faults and failures are given in Table 6.4. This is just a small fraction of the different faults and failures which could occur during the operation of the wind turbine. In later design stages a Failure Mode & Effect Analysis (FMEA) can be performed, followed by a risk assessment. This would show the most critical failures and faults that could occur, and the supervisory control and safety concepts can be described to account for these failures and faults. An overview on how certain operational data regarding faults and failures are handled by the supervisory control and safety system is shown in Figure 6.12.

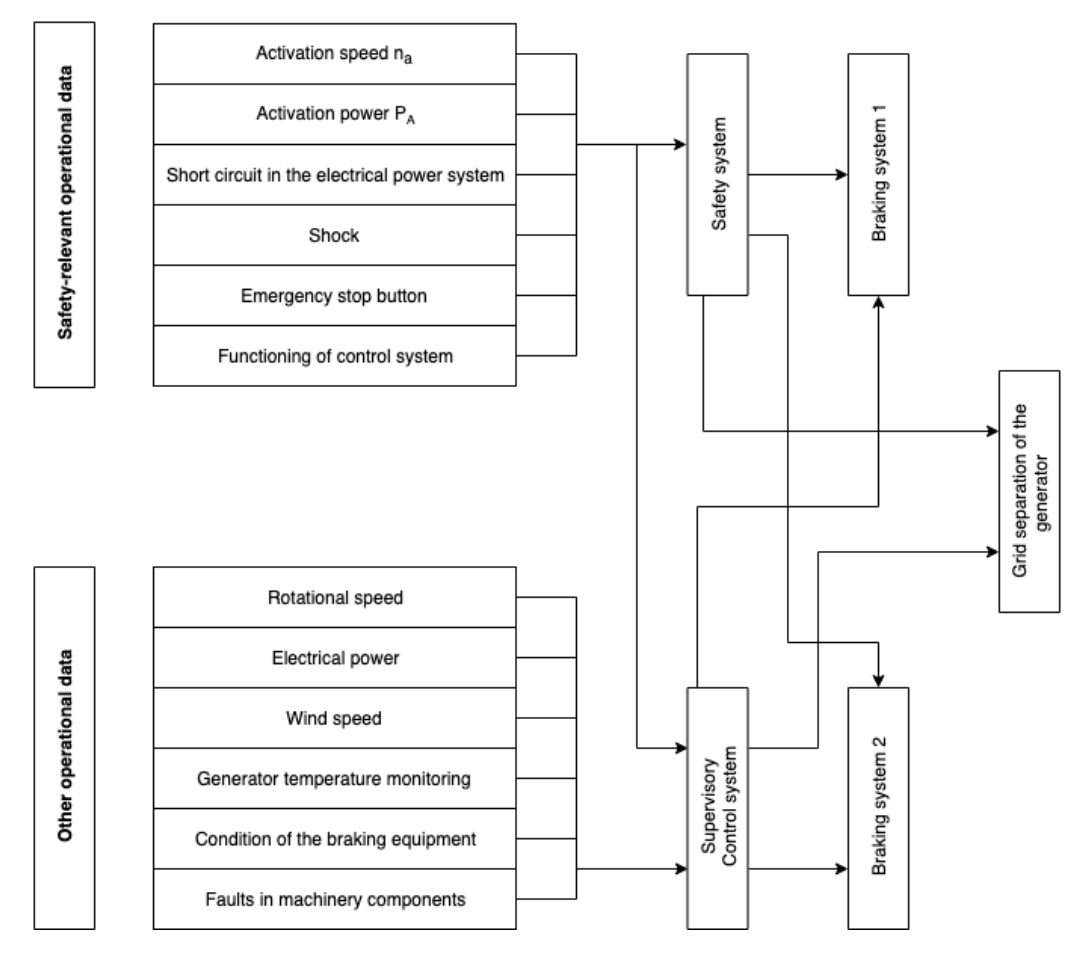


Figure 6.12: Data flow from faults and failures to the control system and the braking system. Template used from [21]

Table 6.4: Description of different faults and failures with the effect that they have, the possible cause and how they are detected

Description of the fault or failure	Affected components	Possible cause	Type of detection	Effects of the fault	Measures which have to be taken
Failure of PR pitch system	Pitch actuators, pitch sensors	Actuator jammed, power loss	Pitch sensor read out	Not able to ensure safe operation	Emergency shutdown
Fault of sensors	Sensors	Mechanical fault, operating at exceeding temperatures	Comparing read out of the sensor with other sensor	Possible wrong input for the actuators	Normal shutdown if possible
Failure of the generator	Generator, parts of the drivetrain	Overpower	Voltage, current, frequency meters readouts	Possible failure of the whole turbine	Emergency shutdown
Grid loss	All components in the wind turbine that require power	Cable failures	Fuses and other protective relays	No power to supervisory control system, possible overspeed	Emergency shutdown
Fire in the turbine	All components	Lightning, overheating of components	Smoke detectors	Possible destruction of the whole turbine	Fire suppression by the fine water spray system together with emergency shutdown
Rotor overspeed	Blade and rotor bearings	High wind speeds, loss of complete control	RPM meter read outs or possible over power detection	Overloaded generator, possible failure of bearings	Normal shutdown if possible, otherwise emergency shutdown
Over power	Generator	Overspeed of the rotor	Voltage, current, frequency meter read outs	Fire hazard	Emergency shutdown
Oil spill	Hydraulic system	Seal loosened	Oil spill sensors	Loss of hydraulic power to lock the rotor	Normal shutdown
Blade/Rotor ejection	Whole turbine	Failure of bearings	Deduct from load and vibrations sensors and accelerometers	Complete failure of the turbine	Emergency shutdown
Failure of the supervisory control system	The whole turbine	Grid-loss, situations not considered in design phase	Exceeding certain parameter values	Failure of the whole turbine	Emergency shutdown

6.9 Functional Analysis

The wind turbine has many subsystems that must be controlled, and many requirements which must be met along its life cycle. Therefore a functional analysis should be done to get a strong grasp on the operating systems of the turbine. This is particularly useful to find out what the best way of controlling the turbine is.

The Functional Flow Diagram (FFD) is a good way of showing which phases the turbine will go through in a chronological order, and which input and output each function has. The Functional Breakdown Structure (FBS) is a good way of showing all the specific functions the system and subsystems have to perform in order to meet the requirements as set in chapter 2.

In Figure 6.12 the FFD can be seen where, at the top left the top-level functions are located. These four blocks contain the complete life cycle of the wind turbine. Each of the blocks can be broken down into smaller and simpler functions (level 1). Those again can be broken down into even smaller functions (level 2), and even smaller (level 3). The top level functions are coloured white, the level 1 functions all have different colours and the level 2 functions have different shades of the level 1 colour to which they are connected to. The third level all have grey colours.

In the FFD, only the second top-level function (operate wind turbine) is split into smaller functions. The other three top-level functions are explained elsewhere in the report in more detail. The flow diagram of the installation of the wind turbine is shown in Figure 10.3 and Figure 10.4, the maintenance and decommissioning plan is explained in Figure 11.1 and Figure 11.2 respectively.

The FBS as portrayed in Figure 6.13 uses the functions form the FFD but shows them differently. The FBS shows all functions the wind turbine will perform, but not in a flow like manner as it also includes functions that do not flow. The FBS also has one more level of detail where possible compared to the FFD, so that it can be checked if the subsystem requirements are also being met. The top level functions are coloured blue, the first level is coloured green, the second level is coloured yellow, the third level is coloured grey and the fourth level is coloured white.

6.10 Limitations and recommendations

The whole wind turbine contains a number of sensors and actuators. Together with the supervisory control and safety computer they are part of a complete system which ensures safety and automatic operation. Since no elaborate analytical or simulation model is used, a sensitivity analysis, and verification & validation operations cannot be performed. During most of its operational lifetime the turbine has no human supervision, which means the turbine should be able to operate autonomously. This calls for a simple and robust design, however, the SRVAWT design and control mechanism is relatively complex compared to conventional wind turbines. Using individual pitch control allows for load control, and makes the system redundant. However, since the load variation during rotation, which causes fatigue, will not be analyzed in this report it can be argued a collective pitch system might be a better option for the secondary rotors. There might also be better start-up and (emergency) shutdown procedures that can reduce the stress on elements of the turbine. Again, the depth of the aerodynamic and structural analysis does not allow for a comparison of the possible procedures. In this chapter the feasibility of certain controllers are not discussed. From the next chapter it will be clear that the controller has a very active job. This is why it is recommended to investigate the different choices for the controller. PI or PID controllers were mentioned before, however the use of a MIMO (Multi-Input Multi-Output) controller has to be investigated as well.

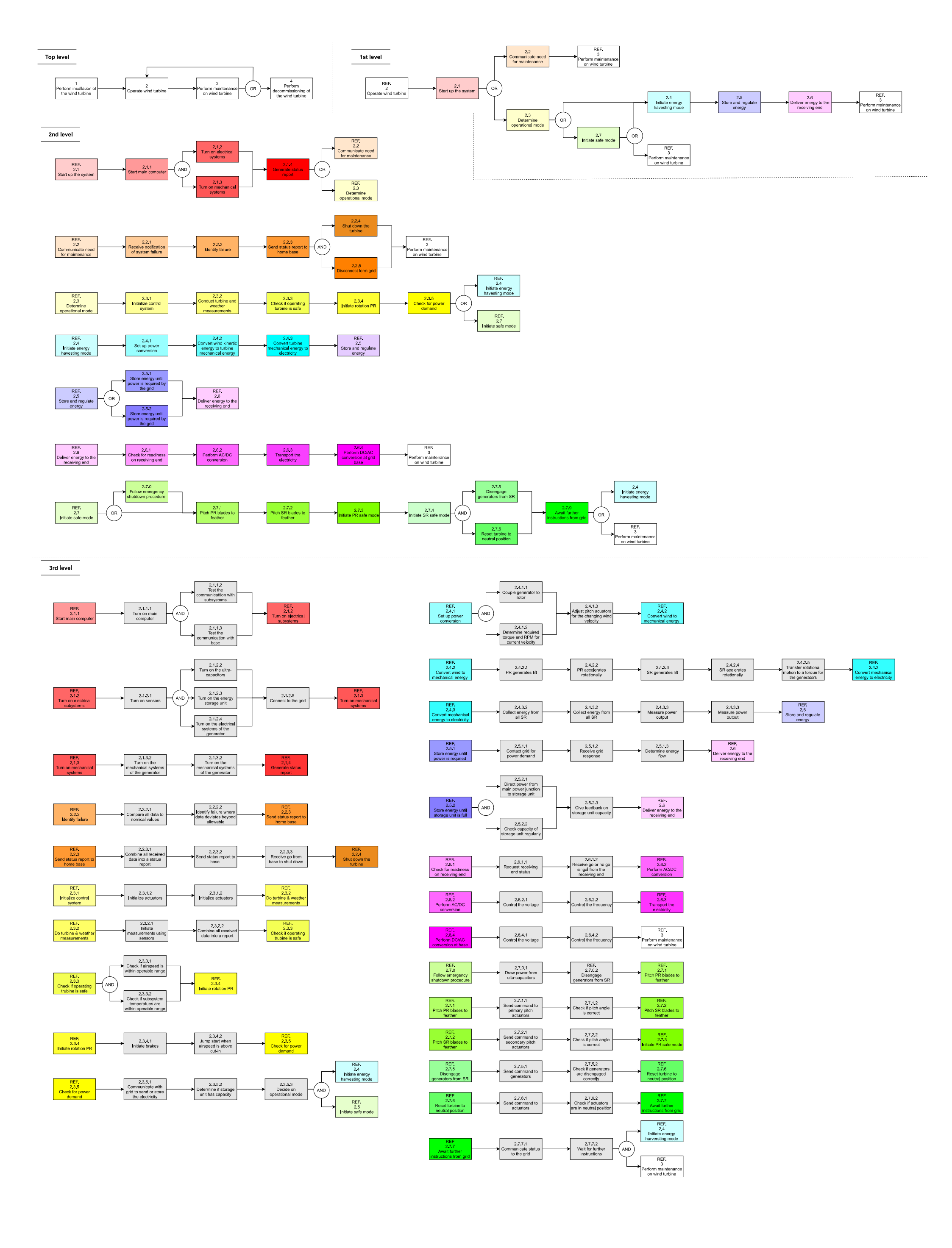


Figure 6.12: Functional Flow Diagram

2 Operate the wind turbine		2.4					
2.1 Start up the system 2.1.1 Start main computer	2	2.4 Initia 2.4.1	ite energy harve Set up po	sting mode <mark>wer convers</mark>	ion		
2.1.1.1 Turn on main computer			2.4.1.1		nerator to r		
2.1.1.2 Test the communication with subsystems 2.1.1.2.1 Send test signal to subsystems						mand to genera innection was s	
2.1.1.2.2 Receive go or no go signal response fi	rom subsystems		2.4.1.2				for current velocity
2.1.1.3 Test the communication with base							n measurement report
2.1.1.3.1 Send test signal to base 2.1.1.3.2 Receive go or no go signal response fi	rom hase		2.4.1.3				RPM are required ng wind velocity
2.1.2 Turn on electrical subsystems	Tom base		2.4.1.3			_	ng torque and RPM da
2.1.2.1 Turn on sensors						I to actuators	
S.1 - S.11 Turn on sensors 2.1.2.1.12 Receive go or no go from the sensors		2.4.2	Convert			tuators are in t <mark>Irbine mechani</mark>	he desired position
2.1.2.2 Turn on the ultra-capacitors		2.4.2	2.4.2.1	PR genera		i bille illecham	arenergy
M.1 - M.3 Monitor the ultra-capacitors						s over PR blade	
2.1.2.2.4 Receive go or no go from the ultra-ca 2.1.2.3 Turn on the energy storage unit	pacitors		2.4.2.2		Pressure d ates rotatio		erienced on the blade
M.1 - M.3 Monitor the energy storage unit			2.4.2.2			eriences force re	esultant
2.1.2.3.4 Receive go or no go from the energy	storage unit					ltant initiates m	novement of the PR
2.1.2.4 Turn on the electrical systems of the generator M.1 - M.3 Monitor the electrical systems of the	generator		2.4.2.3	SR general		lled through the	a air
2.1.2.4.4 Receive go or no from the generator	Beriefator					_	ver rotor blades
2.1.2.5 Connect to the grid							erienced on the blade
2.1.2.5.1 Request grid operational status 2.1.2.5.2 Receive go or no go to connect to grid	4		2.4.2.4		ates rotatio	nally eriences force re	esultant
2.1.3 Turn on mechanical systems	•				•		novement of the SR
2.1.3.1 Turn on actuators			2.4.2.5				torque on the genera
A.1 - A.7 Turn on actuators 2.1.3.1.8 Receive go or no go from the actuato	rs						xerts torque on shaft transfer mechanism
2.1.3.2 Turn on the mechanical systems of the generato						•	es torque to generato
2.1.3.2.1 Start monitoring the mechanical system	ems of the generator	2.4.3				gy to electricity	
2.1.3.2.2 Receive go or no from the generator 2.1.4 Generate status report			2.4.3.1			orque to electric exerted on gene	•
2.1.4.1 Combine all received data into a status report						_	rator rator windings change
2.1.4.2 Receive a final go or no go from the system					_	_	field create an AC volta
2.2 Communicate need for maintenance 2.2.1 Receive notification of system failure			2.4.3.2		Electricity ergy form a		
2.2.2 Identify failure			2.7.3.2				main power junction
2.2.2.1 Compare all data to nominal values							for redistribution
2.2.2.2 Identify failure where data deviates beyond allow 2.2.3 Send status report to home base	wable		2.4.3.3		ower outpu		each generator
2.2.3.1 Combine all received data into a status report						otal power outp	•
2.2.3.2 Send status report to base	2		e and regulate e				
2.2.3.3 Receive go from base to shut down 2.2.4 shut down the turbine		2.5.1	Store ene 2.5.1.1		wer is requi id for powe	red by the grid	
2.2.5 Disconnect from grid			2.5.1.2	J	id response		
3 Perform maintenance on wind turbine			2.5.1.3		power flow		
M Maintenance is explained in more detail in Opera 2.3 Determine operational mode	ations and logistics	2.5.2	Store ene 2.5.2.1				naximum threshold ion to storage unit
2.3 Determine operational mode			2.5.2.2			age unit regula	
2.3.1 Initialize control system			2.5.2.3	Give feedb	ack on stor	age unit capaci	
2.3.1.1 Initialize sensors S.1 - S.11 Initialize sensors	2	2.6 Delive 2.6.1	er energy to the	receiving e readiness o		end	
2.3.1.2 Initialize actuators		2.0.1	2.6.1.1		ceiving end		
A.1 - A.7 Initialize actuators			2.6.1.2	_		gnal from the re	eceiving end
2.3.2 Conduct turbine and weather measurements 2.3.2.1 Initiate measurements using sensors		2.6.2	2.6.2.1	C/DC conve Control vo			
S.1 - S.11 Initiate measurements using sensors			2.6.2.2	Control fre	_		
2.3.2.2 Combine all received data into a report		2.6.3	•	the electric	•		
2.3.3 Check if operating turbine is safe 2.3.3.1 Check if airspeed is within operable range		2.6.4	2.6.4.1	Control vo		d base	
2.3.3.1.1 Compare weather measurements wit	h limiting values		2.6.4.2	Control fre	_		
2.3.3.1.2 Receive go or no go from weather me			2.0.4.2				
	rable range		ite safe mode				
2.3.3.2 Check if subsystem temperatures are within ope A.1 - A.7 Check if acuator temperatures are wi		2.7 Initia 2.7.0	ite safe mode Follow en	nergency sho			
A.1 - A.7 Check if acuator temperatures are within ope A.2 - A.7 Check if acuator temperatures are within ope 2.3.3.2.8 Compare generator temperature data	thin operable range		ite safe mode	Draw pow		a-capacitors	
A.1 - A.7 Check if acuator temperatures are wi 2.3.3.2.8 Compare generator temperature data 2.3.3.2.9 Compare capacitor temperature data	thin operable range a with limiting values with limiting values		Follow en 2.7.0.1 2.7.0.2 Pitch PR b	Draw pow Disengage lades to fea	er from ultr generators <mark>ther</mark>	a-capacitors from SR	
A.1 - A.7 Check if acuator temperatures are wi 2.3.3.2.8 Compare generator temperature data	thin operable range a with limiting values with limiting values ata with limiting values	2.7.0	rte safe mode Follow en 2.7.0.1 2.7.0.2	Draw pow Disengage lades to fea Send com	er from ultr generators <mark>ther</mark>	a-capacitors from SR mary pitch actu	ators
A.1 - A.7 Check if acuator temperatures are wi 2.3.3.2.8 Compare generator temperature data 2.3.3.2.9 Compare capacitor temperature data 2.3.3.2.10 Compare storage unit temperature data	thin operable range a with limiting values with limiting values ata with limiting values	2.7.0	Follow en 2.7.0.1 2.7.0.2 Pitch PR & 2.7.1.1 2.7.1.2 Pitch SR & 2.7.1.2	Draw pow Disengage lades to fea Send com Check if pi lades to fea	er from ultr generators ther mand to pri tch angle is ther	a-capacitors from SR mary pitch actu correct	
A.1 - A.7 Check if acuator temperatures are wi 2.3.3.2.8 Compare generator temperature data 2.3.3.2.9 Compare capacitor temperature data 2.3.3.2.10 Compare storage unit temperature data 2.3.3.2.11 Receive go or no go from temperature 2.3.4 Initiate rotation PR 2.3.4.1 Initiate brakes	thin operable range a with limiting values with limiting values ata with limiting values	2.7.0	The safe mode 2.7.0.1 2.7.0.2 Pitch PR & 2.7.1.1 2.7.1.2 Pitch SR & 2.7.2.1	Draw pow Disengage lades to fea Send com Check if pi lades to fea Send com	er from ultr generators ther mand to pri tch angle is ther mand to sec	a-capacitors from SR mary pitch actu correct condary pitch ac	
A.1 - A.7 Check if acuator temperatures are wi 2.3.3.2.8 Compare generator temperature data 2.3.3.2.9 Compare capacitor temperature data 2.3.3.2.10 Compare storage unit temperature data 2.3.3.2.11 Receive go or no go from temperature 2.3.4 Initiate rotation PR	thin operable range a with limiting values with limiting values ata with limiting values	2.7.0	Telescope (1997) Telesc	Draw pow Disengage lades to fea Send com Check if pi lades to fea Send com	er from ultr generators ther mand to pri tch angle is ther	a-capacitors from SR mary pitch actu correct condary pitch ac	
A.1 - A.7 Check if acuator temperatures are wi 2.3.3.2.8 Compare generator temperature data 2.3.3.2.9 Compare capacitor temperature data 2.3.3.2.10 Compare storage unit temperature data 2.3.3.2.11 Receive go or no go from temperature data 2.3.4.1 Initiate brakes 2.3.4.1.1 Check if brakes are activated	thin operable range a with limiting values with limiting values ata with limiting values e sensors	2.7.02.7.12.7.22.7.3	Follow en 2.7.0.1 2.7.0.2 Pitch PR b 2.7.1.1 2.7.1.2 Pitch SR b 2.7.2.1 2.7.2.1 Initiate PF In.1 - In.2	Draw pow Disengage Dlades to feat Send com Check if pi Ilades to feat Send com Check if pi R safe mode Initiate PR	er from ultr generators ther mand to pri tch angle is ther mand to sec tch angle is	a-capacitors from SR mary pitch actu correct condary pitch ac	
A.1 - A.7 Check if acuator temperatures are wi 2.3.3.2.8 Compare generator temperature data 2.3.3.2.9 Compare capacitor temperature data 2.3.3.2.10 Compare storage unit temperature data 2.3.3.2.11 Receive go or no go from temperature data 2.3.4.1 Initiate brakes 2.3.4.1.1 Check if brakes are activated 2.3.4.1.2 Release brakes 2.3.4.1.3 Check if brakes are released correctly 2.3.4.2 Jump start when airspeed is above cut-in	thin operable range a with limiting values with limiting values ata with limiting values e sensors	2.7.0 2.7.1 2.7.2	Follow en 2.7.0.1 2.7.0.2 Pitch PR b 2.7.1.1 2.7.1.2 Pitch SR b 2.7.2.1 2.7.2.1 Initiate PF In.1 - In.2 Initiate SF	Draw pow Disengage plades to fea Send com Check if pi lades to fea Send com Check if pi & safe mode Initiate PR	er from ultr generators ther mand to pri tch angle is ther mand to sec tch angle is safe mode	a-capacitors from SR mary pitch actu correct condary pitch ac	
A.1 - A.7 Check if acuator temperatures are wi 2.3.3.2.8 Compare generator temperature data 2.3.3.2.9 Compare capacitor temperature data 2.3.3.2.10 Compare storage unit temperature data 2.3.3.2.11 Receive go or no go from temperature data 2.3.4.1 Initiate brakes 2.3.4.1.1 Check if brakes are activated 2.3.4.1.2 Release brakes 2.3.4.1.3 Check if brakes are released correctly	thin operable range a with limiting values with limiting values ata with limiting values e sensors	2.7.02.7.12.7.22.7.3	Follow en 2.7.0.1 2.7.0.2 Pitch PR b 2.7.1.1 2.7.1.2 Pitch SR b 2.7.2.1 2.7.2.1 Initiate PF In.1 - In.2 Initiate SF In.1 - In.2 Initiate SF In.1 - In.2	Draw pow Disengage Dlades to feat Send com Check if pi Ilades to feat Send com Check if pi R safe mode Initiate PR	er from ultr generators ther mand to pri tch angle is ther mand to sec tch angle is safe mode	a-capacitors from SR mary pitch actu correct condary pitch ac	
A.1 - A.7 Check if acuator temperatures are wi 2.3.3.2.8 Compare generator temperature data 2.3.3.2.10 Compare storage unit temperature data 2.3.3.2.11 Receive go or no go from temperature 2.3.4 Initiate rotation PR 2.3.4.1 Initiate brakes 2.3.4.1.1 Check if brakes are activated 2.3.4.1.2 Release brakes 2.3.4.1.3 Check if brakes are released correctly 2.3.4.2 Jump start when airspeed is above cut-in 2.3.4.2.1 Compare velocity measurements to c 2.3.4.2.2 Use generator to rotate the SRs 2.3.4.2.3 SRs produce thrust force to rotate PR	thin operable range a with limiting values with limiting values ata with limiting values e sensors ut-in speed	2.7.0 2.7.1 2.7.2 2.7.3	rite safe mode 2.7.0.1 2.7.0.2 Pitch PR b 2.7.1.1 2.7.1.2 Pitch SR b 2.7.2.1 2.7.2.1 Initiate PF In.1 - In.2 Initiate SF In.1 - In.2 Disengage 2.7.5.1	Draw pow Disengage plades to fea Send com Check if pi lades to fea Send com Check if pi & safe mode Initiate PR & safe mode Initiate SR & generators Send com	er from ultr generators ther mand to pri tch angle is ther mand to sec tch angle is safe mode safe mode from SR mand to ger	a-capacitors from SR mary pitch actu correct condary pitch ac correct	ctuators
A.1 - A.7 Check if acuator temperatures are wi 2.3.3.2.8 Compare generator temperature data 2.3.3.2.9 Compare capacitor temperature data 2.3.3.2.10 Compare storage unit temperature data 2.3.3.2.11 Receive go or no go from temperature 2.3.4 Initiate rotation PR 2.3.4.1 Initiate brakes 2.3.4.1.1 Check if brakes are activated 2.3.4.1.2 Release brakes 2.3.4.1.3 Check if brakes are released correctly 2.3.4.2 Jump start when airspeed is above cut-in 2.3.4.2.1 Compare velocity measurements to c 2.3.4.2.2 Use generator to rotate the SRs 2.3.4.2.3 SRs produce thrust force to rotate PR 2.3.5 Check for power demand	thin operable range a with limiting values with limiting values ata with limiting values e sensors	2.7.0 2.7.1 2.7.2 2.7.3 2.7.4	rte safe mode 2.7.0.1 2.7.0.2 Pitch PR b 2.7.1.1 2.7.1.2 Pitch SR b 2.7.2.1 2.7.2.1 Initiate PF In.1 - In.2 Initiate SF In.1 - In.2 Disengage 2.7.5.1 2.7.5.2	Draw pow Disengage Send com Check if pi Idades to fea Send com Check if pi R safe mode Initiate PR R safe mode Initiate SR E generators Send com Check if ge	er from ultr generators ther mand to pri tch angle is ther mand to sec tch angle is safe mode safe mode from SR mand to generators an	a-capacitors from SR mary pitch actu correct condary pitch ac correct	ctuators
A.1 - A.7 Check if acuator temperatures are wi 2.3.3.2.8 Compare generator temperature data 2.3.3.2.9 Compare capacitor temperature data 2.3.3.2.10 Compare storage unit temperature data 2.3.3.2.11 Receive go or no go from temperature 2.3.4 Initiate rotation PR 2.3.4.1 Initiate brakes 2.3.4.1.1 Check if brakes are activated 2.3.4.1.2 Release brakes 2.3.4.1.3 Check if brakes are released correctly 2.3.4.2 Jump start when airspeed is above cut-in 2.3.4.2.1 Compare velocity measurements to c 2.3.4.2.2 Use generator to rotate the SRs 2.3.4.2.3 SRs produce thrust force to rotate PR	thin operable range a with limiting values with limiting values ata with limiting values e sensors	2.7.0 2.7.1 2.7.2 2.7.3	rte safe mode 2.7.0.1 2.7.0.2 Pitch PR b 2.7.1.1 2.7.1.2 Pitch SR b 2.7.2.1 2.7.2.1 Initiate PF In.1 - In.2 Initiate SF In.1 - In.2 Disengage 2.7.5.1 2.7.5.2	Draw pow Disengage Send com Check if pi Idades to fea Send com Check if pi R safe mode Initiate PR R safe mode Initiate SR E generators Send com Check if ge	er from ultr generators ther mand to pri tch angle is ther mand to sec tch angle is safe mode safe mode from SR mand to generators an	ea-capacitors from SR mary pitch actu correct condary pitch ac correct	ctuators
A.1 - A.7 Check if acuator temperatures are wi 2.3.3.2.8 Compare generator temperature data 2.3.3.2.9 Compare capacitor temperature data 2.3.3.2.10 Compare storage unit temperature data 2.3.3.2.11 Receive go or no go from temperature 2.3.4 Initiate rotation PR 2.3.4.1 Initiate brakes 2.3.4.1.1 Check if brakes are activated 2.3.4.1.2 Release brakes 2.3.4.1.3 Check if brakes are released correctly 2.3.4.2 Jump start when airspeed is above cut-in 2.3.4.2.1 Compare velocity measurements to c 2.3.4.2.2 Use generator to rotate the SRs 2.3.4.2.3 SRs produce thrust force to rotate PR 2.3.5 Check for power demand 2.3.5.1 Communicate with grid if either direct power to 2.3.5.2 Determine if storage unit has capacity 2.3.5.2.1 Measure energy stored in storage unit	thin operable range a with limiting values with limiting values ata with limiting values e sensors ut-in speed grid or to storage is required	2.7.0 2.7.1 2.7.2 2.7.3 2.7.4 2.7.5	rite safe mode 2.7.0.1 2.7.0.2 Pitch PR b 2.7.1.1 2.7.1.2 Pitch SR b 2.7.2.1 2.7.2.1 Initiate PF In.1 - In.2 Initiate SF In.1 - In.2 Company C	Draw pow Disengage slades to fea Send com Check if pi lades to fea Send com Check if pi R safe mode Initiate PR R safe mode Initiate SR e generators Send com Check if ge Dine to neut Send com Check if ac	er from ultrigenerators ther mand to pritch angle is ther mand to sectch angle is safe mode from SR mand to generators arral position mand to actituators are	ra-capacitors from SR mary pitch actured to the correct condary pitch accorrect merators re disengaged country uators in neutral position	ctuators
A.1 - A.7 Check if acuator temperatures are wi 2.3.3.2.8 Compare generator temperature data 2.3.3.2.9 Compare capacitor temperature data 2.3.3.2.10 Compare storage unit temperature data 2.3.3.2.11 Receive go or no go from temperature data 2.3.4.1 Initiate brakes 2.3.4.1 Check if brakes are activated 2.3.4.1.2 Release brakes 2.3.4.1.3 Check if brakes are released correctly 2.3.4.2 Jump start when airspeed is above cut-in 2.3.4.2.1 Compare velocity measurements to c 2.3.4.2.2 Use generator to rotate the SRs 2.3.4.2.3 SRs produce thrust force to rotate PR 2.3.5 Check for power demand 2.3.5.1 Communicate with grid if either direct power to 2.3.5.2 Determine if storage unit has capacity 2.3.5.2.1 Measure energy levels to maximum to the compare velocity to maximum to the compare velocity acuation of the compared vel	thin operable range a with limiting values with limiting values ata with limiting values e sensors ut-in speed grid or to storage is required	2.7.0 2.7.1 2.7.2 2.7.3 2.7.4	rite safe mode 2.7.0.1 2.7.0.2 Pitch PR b 2.7.1.1 2.7.1.2 Pitch SR b 2.7.2.1 2.7.2.1 Initiate PF In.1 - In.2 Initiate SF In.1 - In.2 Company C	Draw pow Disengage Send com Check if pi Idades to fea Send com Check if pi R safe mode Initiate PR R safe mode Initiate SR E generators Send com Check if ge Dine to neut Send com Check if ac Check if ac Check if ac	er from ultrigenerators ther mand to pritch angle is ther mand to sectch angle is safe mode from SR mand to generators arral position mand to act tuators are ions from g	ea-capacitors from SR mary pitch actured correct condary pitch accorrect merators re disengaged contacts in neutral position	ctuators
A.1 - A.7 Check if acuator temperatures are wi 2.3.3.2.8 Compare generator temperature data 2.3.3.2.9 Compare capacitor temperature data 2.3.3.2.10 Compare storage unit temperature data 2.3.3.2.11 Receive go or no go from temperature data 2.3.4.1 Initiate brakes 2.3.4.1 Initiate brakes 2.3.4.1.1 Check if brakes are activated 2.3.4.1.2 Release brakes 2.3.4.1.3 Check if brakes are released correctly 2.3.4.2 Jump start when airspeed is above cut-in 2.3.4.2.1 Compare velocity measurements to c 2.3.4.2.2 Use generator to rotate the SRs 2.3.4.2.3 SRs produce thrust force to rotate PR 2.3.5 Check for power demand 2.3.5.1 Communicate with grid if either direct power to 2.3.5.2 Determine if storage unit has capacity 2.3.5.2.1 Measure energy stored in storage unit	thin operable range a with limiting values with limiting values ata with limiting values e sensors ut-in speed grid or to storage is required	2.7.0 2.7.1 2.7.2 2.7.3 2.7.4 2.7.5	rite safe mode 2.7.0.1 2.7.0.2 Pitch PR b 2.7.1.1 2.7.1.2 Pitch SR b 2.7.2.1 2.7.2.1 Initiate PF In.1 - In.2 Initiate SF In.1 - In.2 Company C	Draw pow Disengage Send com Check if pi Idades to fea Send com Check if pi R safe mode Initiate PR R safe mode Initiate SR E generators Send com Check if ge Dine to neut Send com Check if ac Check if ac Check if ac Check if ac Check if ac Check if ac	er from ultrigenerators ther mand to pritch angle is ther mand to sectch angle is safe mode from SR mand to generators arral position mand to actituators are	ea-capacitors from SR mary pitch actu correct condary pitch ac correct merators re disengaged co uators in neutral posit rid to the grid	ctuators
A.1 - A.7 Check if acuator temperatures are wi 2.3.3.2.8 Compare generator temperature data 2.3.3.2.9 Compare capacitor temperature data 2.3.3.2.10 Compare storage unit temperature data 2.3.3.2.11 Receive go or no go from temperature data 2.3.4.1 Initiate brakes 2.3.4.1 Initiate brakes 2.3.4.1.1 Check if brakes are activated 2.3.4.1.2 Release brakes 2.3.4.1.3 Check if brakes are released correctly 2.3.4.2 Jump start when airspeed is above cut-in 2.3.4.2.1 Compare velocity measurements to c 2.3.4.2.2 Use generator to rotate the SRs 2.3.4.2.3 SRs produce thrust force to rotate PR 2.3.5 Check for power demand 2.3.5.1 Communicate with grid if either direct power to 2.3.5.2 Determine if storage unit has capacity 2.3.5.2.1 Measure energy stored in storage unit 2.3.5.2.2 Compare energy levels to maximum to 2.3.5.2.3 Report available storage capacity 2.3.5.3 Decide on operational mode 2.4 Initiate energy harvesting mode	thin operable range a with limiting values with limiting values ata with limiting values e sensors ut-in speed grid or to storage is required	2.7.0 2.7.1 2.7.2 2.7.3 2.7.4 2.7.5	rite safe mode 2.7.0.1 2.7.0.2 Pitch PR b 2.7.1.1 2.7.1.2 Pitch SR b 2.7.2.1 2.7.2.1 Initiate PF In.1 - In.2 Initiate SF In.1 - In.2 2.7.5.1 2.7.5.2 Reset turl 2.7.6.1 2.7.6.2 Await furd 2.7.7.1	Draw pow Disengage Slades to fea Send com Check if pi Ilades to fea Send com Check if pi R safe mode Initiate PR R safe mode Initiate SR Send com Check if ge Dine to neut Send com Check if ac Cher instruct Communic Wait for fu	er from ultrigenerators ther mand to pritch angle is ther mand to sect tch angle is safe mode afrom SR mand to generators are rall position mand to act tuators are ions from grate status further instru	ra-capacitors from SR mary pitch actured correct condary pitch accorrect merators re disengaged contains in neutral position rid to the grid actions ergy harvesting	orrectly tion mode
A.1 - A.7 Check if acuator temperatures are wi 2.3.3.2.8 Compare generator temperature data 2.3.3.2.9 Compare capacitor temperature data 2.3.3.2.10 Compare storage unit temperature data 2.3.3.2.11 Receive go or no go from temperature data 2.3.4.1 Initiate brakes 2.3.4.1 Check if brakes are activated 2.3.4.1.2 Release brakes 2.3.4.1.3 Check if brakes are released correctly 2.3.4.2 Jump start when airspeed is above cut-in 2.3.4.2.1 Compare velocity measurements to c 2.3.4.2.2 Use generator to rotate the SRs 2.3.4.2.3 SRs produce thrust force to rotate PR 2.3.5 Check for power demand 2.3.5.1 Communicate with grid if either direct power to 2.3.5.2 Determine if storage unit has capacity 2.3.5.2.1 Measure energy stored in storage unit 2.3.5.2.2 Compare energy levels to maximum to 2.3.5.3 Decide on operational mode 2.4 Initiate energy harvesting mode Initiate safe mode	thin operable range a with limiting values with limiting values ata with limiting values e sensors ut-in speed grid or to storage is required it hreshold	2.7.0 2.7.1 2.7.2 2.7.3 2.7.4 2.7.5 2.7.6	rite safe mode 2.7.0.1 2.7.0.2 Pitch PR b 2.7.1.1 2.7.1.2 Pitch SR b 2.7.2.1 2.7.2.1 Initiate PF In.1 - In.2 Initiate SF In.1 - In.2 Company C	Draw pow Disengage Send com Check if pi Idades to fea Send com Check if pi R safe mode Initiate PR R safe mode Initiate SR E generators Send com Check if ge Dine to neut Send com Check if ac Check if ac	er from ultrigenerators ther mand to pritch angle is ther mand to sect tch angle is safe mode afrom SR mand to generators are rall position mand to act tuators are ions from grate status further instru	ea-capacitors from SR mary pitch actured correct condary pitch accorrect merators re disengaged contains in neutral positions to the grid actions	orrectly tion mode
A.1 - A.7 Check if acuator temperatures are wi 2.3.3.2.8 Compare generator temperature data 2.3.3.2.9 Compare capacitor temperature data 2.3.3.2.10 Compare storage unit temperature data 2.3.3.2.11 Receive go or no go from temperature data 2.3.4.1 Initiate brakes 2.3.4.1 Initiate brakes 2.3.4.1.1 Check if brakes are activated 2.3.4.1.2 Release brakes 2.3.4.1.3 Check if brakes are released correctly 2.3.4.2 Jump start when airspeed is above cut-in 2.3.4.2.1 Compare velocity measurements to c 2.3.4.2.2 Use generator to rotate the SRs 2.3.4.2.3 SRs produce thrust force to rotate PR 2.3.5 Check for power demand 2.3.5.1 Communicate with grid if either direct power to 2.3.5.2 Determine if storage unit has capacity 2.3.5.2.1 Measure energy stored in storage unit 2.3.5.2.2 Compare energy levels to maximum to 2.3.5.2.3 Report available storage capacity 2.3.5.3 Decide on operational mode 2.4 Initiate energy harvesting mode Initiate safe mode Sensors A Actuators	thin operable range a with limiting values with limiting values ata with limiting values e sensors ut-in speed grid or to storage is required it hreshold	2.7.0 2.7.1 2.7.2 2.7.3 2.7.4 2.7.5 2.7.6	rite safe mode 2.7.0.1 2.7.0.2 Pitch PR b 2.7.1.1 2.7.1.2 Pitch SR b 2.7.2.1 2.7.2.1 Initiate PF In.1 - In.2 Initiate SF In.1 - In.2 2.7.5.1 2.7.5.2 Reset turl 2.7.6.1 2.7.6.2 Await furd 2.7.7.1	Draw pow Disengage Send com Check if pi Idades to fea Send com Check if pi R safe mode Initiate PR R safe mode Initiate SR E generators Send com Check if ge Dine to neut Send com Check if ac Check i	er from ultrigenerators ther mand to pritch angle is ther mand to sect tch angle is safe mode afrom SR mand to generators are rall position mand to act tuators are ions from grate status further instru	ra-capacitors from SR mary pitch actured correct condary pitch accorrect merators re disengaged contains in neutral position rid to the grid actions ergy harvesting	orrectly tion mode
A.1 - A.7 Check if acuator temperatures are wi 2.3.3.2.8 Compare generator temperature data 2.3.3.2.9 Compare capacitor temperature data 2.3.3.2.10 Compare storage unit temperature data 2.3.3.2.11 Receive go or no go from temperature data 2.3.4.1 Initiate brakes 2.3.4.1 Initiate brakes 2.3.4.1.1 Check if brakes are activated 2.3.4.1.2 Release brakes 2.3.4.2 Jump start when airspeed is above cut-in 2.3.4.2.1 Compare velocity measurements to c 2.3.4.2.2 Use generator to rotate the SRs 2.3.4.2.3 SRs produce thrust force to rotate PR 2.3.5 Check for power demand 2.3.5.1 Communicate with grid if either direct power to 2.3.5.2 Determine if storage unit has capacity 2.3.5.2.1 Measure energy stored in storage unit 2.3.5.2.2 Compare energy levels to maximum to 2.3.5.2.3 Report available storage capacity 2.3.5.3 Decide on operational mode 2.4 Initiate energy harvesting mode 2.5 Initiate safe mode Sensors A Actuators S.1 Blade pitch sensor A.1 Pit S.2 RPM sensor A.2 Pa	thin operable range a with limiting values with limiting values ata with limiting values e sensors ut-in speed grid or to storage is required it hreshold	2.7.0 2.7.1 2.7.2 2.7.3 2.7.4 2.7.5 2.7.6 M Mon M.1 M.2	te safe mode Follow en 2.7.0.1 2.7.0.2 Pitch PR b 2.7.1.1 2.7.1.2 Pitch SR b 2.7.2.1 2.7.2.1 Initiate PF In.1 - In.2 Initiate SF In.1 - In.2 Company C	Draw pow Disengage Ilades to fea Send com Check if pi Ilades to fea Initiate PR Ilades mode Initiate SR Ilades mode Ilades mode Initiate SR Ilades mode I	er from ultrigenerators ther mand to pritch angle is ther mand to sect tch angle is safe mode afrom SR mand to generators are rall position mand to act tuators are ions from grate status further instruction.	ra-capacitors from SR mary pitch actured correct condary pitch accorrect merators re disengaged contains in neutral positivity rid to the grid functions ergy harvesting aintenance on the service of the service correct correct.	orrectly tion mode wind turbine
A.1 - A.7 Check if acuator temperatures are wi 2.3.3.2.8 Compare generator temperature data 2.3.3.2.9 Compare capacitor temperature data 2.3.3.2.10 Compare storage unit temperature data 2.3.3.2.11 Receive go or no go from temperature data 2.3.4.1 Initiate brakes 2.3.4.1 Initiate brakes 2.3.4.1.1 Check if brakes are activated 2.3.4.1.2 Release brakes 2.3.4.1.3 Check if brakes are released correctly 2.3.4.2 Jump start when airspeed is above cut-in 2.3.4.2.1 Compare velocity measurements to c 2.3.4.2.2 Use generator to rotate the SRs 2.3.4.2.3 SRs produce thrust force to rotate PR 2.3.5 Check for power demand 2.3.5.1 Communicate with grid if either direct power to 2.3.5.2 Determine if storage unit has capacity 2.3.5.2.1 Measure energy stored in storage unit 2.3.5.2.2 Compare energy levels to maximum to 2.3.5.2 Decide on operational mode 2.4 Initiate energy harvesting mode 2.5 Initiate safe mode Sensors A Actuators A.1 Pit S.2 RPM sensor A.2 Pa S.3 Temperature sensor A.3 Fin	thin operable range a with limiting values with limiting values ata with limiting values et a with limiting values et sensors ut-in speed grid or to storage is required it hreshold ch actuator rking brake ne water spray system	2.7.0 2.7.1 2.7.2 2.7.3 2.7.4 2.7.5 2.7.6 M Mon M.1	te safe mode Follow en 2.7.0.1 2.7.0.2 Pitch PR b 2.7.1.1 2.7.1.2 Pitch SR b 2.7.2.1 2.7.2.1 Initiate PF In.1 - In.2 Initiate SF In.1 - In.2 Company C	Draw pow Disengage Ilades to fea Send com Check if pi Ilades to fea Initiate PR Ilades mode Initiate SR Ilades mode Ilades mode Initiate SR Ilades mode I	er from ultrigenerators ther mand to pritch angle is ther mand to sect tch angle is safe mode afrom SR mand to generators are rall position mand to act tuators are ions from grate status further instruction.	ra-capacitors from SR mary pitch actured correct condary pitch accorrect merators re disengaged contains in neutral position rid to the grid actions ergy harvesting	orrectly tion mode wind turbine
A.1 - A.7 Check if acuator temperatures are wi 2.3.3.2.8 Compare generator temperature data 2.3.3.2.9 Compare capacitor temperature data 2.3.3.2.10 Compare storage unit temperature data 2.3.3.2.11 Receive go or no go from temperature data 2.3.4.1 Initiate brakes 2.3.4.1 Initiate brakes 2.3.4.1.1 Check if brakes are activated 2.3.4.1.2 Release brakes 2.3.4.2 Jump start when airspeed is above cut-in 2.3.4.2.1 Compare velocity measurements to c 2.3.4.2.2 Use generator to rotate the SRs 2.3.4.2.3 SRs produce thrust force to rotate PR 2.3.5 Check for power demand 2.3.5.1 Communicate with grid if either direct power to 2.3.5.2 Determine if storage unit has capacity 2.3.5.2.1 Measure energy stored in storage unit 2.3.5.2.2 Compare energy levels to maximum to 2.3.5.2.3 Report available storage capacity 2.3.5.3 Decide on operational mode 2.4 Initiate energy harvesting mode 2.5 Initiate safe mode Sensors A Actuators S.1 Blade pitch sensor A.2 Pa S.3 Temperature sensor A.3 Fin S.4 Vibration sensor A.4 Ro	thin operable range a with limiting values with limiting values ata with limiting values et a with limiting values at with limiting values et sensors ut-in speed grid or to storage is required it hreshold ch actuator rking brake ne water spray system tor locks	2.7.0 2.7.1 2.7.2 2.7.3 2.7.4 2.7.5 2.7.6 M Mon M.1 M.2 M.3	te safe mode Follow en 2.7.0.1 2.7.0.2 Pitch PR b 2.7.1.1 2.7.1.2 Pitch SR b 2.7.2.1 2.7.2.1 Initiate PF In.1 - In.2 Initiate SF In.1 - In.2 Company C	Draw pow Disengage Islades to fea Send com Check if pi Islades to fea Send com Check if pi Islades to fea Send com Check if pi Islades mode Initiate PR Islafe mode Initiate SR Islafe mode Initiate S	er from ultrigenerators ther mand to pritch angle is ther mand to sect tch angle is safe mode afrom SR mand to generators are rall position mand to act tuators are ions from grate status further instruction.	ra-capacitors from SR mary pitch actured correct condary pitch accorrect merators re disengaged contains in neutral positivity rid to the grid functions ergy harvesting aintenance on the service of the service correct correct.	orrectly tion mode wind turbine
A.1 - A.7 Check if acuator temperatures are wi 2.3.3.2.8 Compare generator temperature data 2.3.3.2.9 Compare capacitor temperature data 2.3.3.2.10 Compare storage unit temperature data 2.3.3.2.11 Receive go or no go from temperature data 2.3.4.1 Initiate brakes 2.3.4.1 Initiate brakes 2.3.4.1.1 Check if brakes are activated 2.3.4.1.2 Release brakes 2.3.4.2 Jump start when airspeed is above cut-in 2.3.4.2.1 Compare velocity measurements to c 2.3.4.2.2 Use generator to rotate the SRs 2.3.4.2.3 SRs produce thrust force to rotate PR 2.3.5 Check for power demand 2.3.5.1 Communicate with grid if either direct power to 2.3.5.2 Determine if storage unit has capacity 2.3.5.2.1 Measure energy stored in storage unit 2.3.5.2.2 Compare energy levels to maximum to 2.3.5.2.3 Report available storage capacity 2.3.5.3 Decide on operational mode 2.4 Initiate energy harvesting mode 2.5 Initiate safe mode Sensors A Actuators S.1 Blade pitch sensor A.2 Pa S.3 Temperature sensor A.3 Fir S.4 Vibration sensor A.4 Ro A.5 Po	thin operable range a with limiting values with limiting values ata with limiting values et a with limiting values at with limiting values et sensors ut-in speed grid or to storage is required it hreshold ch actuator rking brake ne water spray system tor locks	2.7.0 2.7.1 2.7.2 2.7.3 2.7.4 2.7.5 2.7.6 M Mon M.1 M.2 M.3	te safe mode Follow en 2.7.0.1 2.7.0.2 Pitch PR b 2.7.1.1 2.7.1.2 Pitch SR b 2.7.2.1 2.7.2.1 Initiate PR In.1 - In.2 Disengage 2.7.5.1 2.7.5.2 Reset turl 2.7.6.2 Await furl 2.7.7.2 itoring Monitor of Monitor of Check if volater models Monitor of Check if volater models Author of Check if volater models Author of Check if volater models Monitor of Check if volater models Author of Check if volater models Aut	Draw pow Disengage Islades to fea Send com Check if pi Islades to fea Send com Check if pi Islades to fea Send com Check if pi Islades mode Initiate PR Islafe mode Initiate SR Islafe mode Initiate S	er from ultrigenerators ther mand to pritch angle is ther mand to sect tch angle is safe mode afrom SR mand to generators are rall position mand to act the control of the	ra-capacitors from SR mary pitch actured correct condary pitch accorrect merators re disengaged contains in neutral positivity rid to the grid functions ergy harvesting aintenance on the service of the service correct correct.	orrectly tion mode wind turbine
A.1 - A.7 Check if acuator temperatures are wi 2.3.3.2.8 Compare generator temperature data 2.3.3.2.9 Compare capacitor temperature data 2.3.3.2.10 Compare storage unit temperature data 2.3.3.2.11 Receive go or no go from temperature data 2.3.4.1 Initiate brakes 2.3.4.1 Initiate brakes 2.3.4.1.1 Check if brakes are activated 2.3.4.1.2 Release brakes 2.3.4.2 Jump start when airspeed is above cut-in 2.3.4.2.1 Compare velocity measurements to c 2.3.4.2.2 Use generator to rotate the SRs 2.3.4.2.3 SRs produce thrust force to rotate PR 2.3.5 Check for power demand 2.3.5.1 Communicate with grid if either direct power to 2.3.5.2 Determine if storage unit has capacity 2.3.5.2.1 Measure energy stored in storage unit 2.3.5.2.2 Compare energy levels to maximum to 2.3.5.2.3 Report available storage capacity 2.3.5.3 Decide on operational mode 2.4 Initiate energy harvesting mode 2.5 Initiate safe mode Sensors A Actuators S.1 Blade pitch sensor A.1 Pit S.2 RPM sensor A.2 Pa S.3 Temperature sensor A.3 Fir S.4 Vibration sensor A.4 Ro S.5 Voltage sensor A.5 Po S.6 Current sensor A.6 Op S.7 Frequency sensor A.7 Hy	thin operable range a with limiting values with limiting values ata with limiting values ata with limiting values at sensors withing values at	2.7.0 2.7.1 2.7.2 2.7.3 2.7.4 2.7.5 2.7.6 2.7.7 M Mon M.1 M.2 M.3 In Initia	te safe mode Follow en 2.7.0.1 2.7.0.2 Pitch PR b 2.7.1.1 2.7.1.2 Pitch SR b 2.7.2.1 2.7.2.1 Initiate PF In.1 - In.2 Disengage 2.7.5.1 2.7.5.2 Reset turl 2.7.6.2 Await furl 2.7.7.2 itoring Monitor of Monitor of Check if v atterotor safe monitor of Check if v Activate b In.1.1	Draw pow Disengage Islades to fea Send com Check if pi Islades to fea Send com Check if pi Islades to fea Send com Check if pi Islades mode Initiate PR Islafe mode Initiate SR Islafe mode Initiate SR Islafe mode Initiate SR Islafe mode Initiate SR Islafe mode Initiate TR Islafe mode Initiate TR Islafe mod	er from ultrigenerators ther mand to pritch angle is ther mand to sect tch angle is safe mode afrom SR mand to generators are rall position mand to act the status of the instructions from generators are status of the instruction from mand to rotor	a-capacitors from SR mary pitch actuations correct condary pitch accorrect condary pitch accorrect correct accorrect merators de disengaged contains in neutral position in neutral position contains contains de disengaged contains contai	orrectly tion mode wind turbine aries
A.1 - A.7 Check if acuator temperatures are wi 2.3.3.2.8 Compare generator temperature data 2.3.3.2.9 Compare capacitor temperature data 2.3.3.2.10 Compare storage unit temperature data 2.3.3.2.11 Receive go or no go from temperature data 2.3.4.1 Initiate brakes 2.3.4.1 Initiate brakes 2.3.4.1.1 Check if brakes are activated 2.3.4.1.2 Release brakes 2.3.4.2 Jump start when airspeed is above cut-in 2.3.4.2.1 Compare velocity measurements to c 2.3.4.2.2 Use generator to rotate the SRs 2.3.4.2.3 SRs produce thrust force to rotate PR 2.3.5 Check for power demand 2.3.5.1 Communicate with grid if either direct power to 2.3.5.2 Determine if storage unit has capacity 2.3.5.2.1 Measure energy stored in storage unit 2.3.5.2.2 Compare energy levels to maximum to 2.3.5.2.3 Report available storage capacity 2.3.5.2.3 Report available storage capacity 2.3.5.3 Decide on operational mode 2.4 Initiate energy harvesting mode 2.4 Initiate energy harvesting mode 3.5 Initiate safe mode Sensors A Actuators S.1 Blade pitch sensor A.1 Pit S.2 RPM sensor A.2 Pa S.3 Temperature sensor A.3 Fir S.4 Vibration sensor A.4 Ro S.5 Voltage sensor A.5 Po S.6 Current sensor A.5 Po S.6 Current sensor A.6 Opperature sens	thin operable range a with limiting values with limiting values ata with limiting values ata with limiting values at sensors withing values at sensors with limiting values at sensor	2.7.0 2.7.1 2.7.2 2.7.3 2.7.4 2.7.5 2.7.6 2.7.7 M Mon M.1 M.2 M.3 In Initial	te safe mode Follow en 2.7.0.1 2.7.0.2 Pitch PR b 2.7.1.1 2.7.1.2 Pitch SR b 2.7.2.1 2.7.2.1 Initiate PF In.1 - In.2 Disengage 2.7.5.1 2.7.5.2 Reset turl 2.7.6.2 Await furl 2.7.7.2 itoring Monitor of Monitor of Check if v activate b In.1.1 In.1.2	Draw pow Disengage Islades to fea Send com Check if pi Islades to fea Send com Check if pi Islades to fea Send com Check if pi Islades mode Initiate PR Islafe mode Initiate SR Islafe mode Initiate SR Islafe mode Initiate SR Islafe mode Initiate SR Islafe mode Initiate TR Islafe mode Initiate TR Islafe mod	er from ultrigenerators ther mand to pritch angle is ther mand to see the angle is safe mode afrom SR mand to generators are rall position mand to act the angle is the angle is the angle is the angle is rall position mand to act the angle is the angle	a-capacitors from SR mary pitch actured correct condary pitch accorrect merators re disengaged contains in neutral positions to the grid for the gri	orrectly tion mode wind turbine aries
A.1 - A.7 Check if acuator temperatures are wi 2.3.3.2.8 Compare generator temperature data 2.3.3.2.9 Compare capacitor temperature data 2.3.3.2.10 Compare storage unit temperature data 2.3.3.2.11 Receive go or no go from temperature data 2.3.4.1 Initiate brakes 2.3.4.1.1 Check if brakes are activated 2.3.4.1.2 Release brakes 2.3.4.1.3 Check if brakes are released correctly 2.3.4.2.1 Loompare velocity measurements to c 2.3.4.2.1 Compare velocity measurements to c 2.3.4.2.2 Use generator to rotate the SRs 2.3.4.2.3 SRs produce thrust force to rotate PR 2.3.5.1 Communicate with grid if either direct power to 2.3.5.2 Determine if storage unit has capacity 2.3.5.2.1 Measure energy stored in storage unit 2.3.5.2.2 Compare energy levels to maximum to 2.3.5.2.3 Report available storage capacity 2.3.5.3 Decide on operational mode 2.4 Initiate energy harvesting mode 2.5 Initiate safe mode Sensors A A Actuators A.1 Pit S.2 RPM sensor A.2 Pa S.3 Temperature sensor A.3 Fir S.4 Vibration sensor A.4 Ro S.5 Voltage sensor A.5 Po S.6 Current sensor A.6 Op S.7 Frequency sensor A.7 Hy Shock sensor	thin operable range a with limiting values with limiting values ata with limiting values ata with limiting values at sensors withing values at sensors with limiting values at sensor	2.7.0 2.7.1 2.7.2 2.7.3 2.7.4 2.7.5 2.7.6 2.7.7 M Mon M.1 M.2 M.3 In Initia	te safe mode Follow en 2.7.0.1 2.7.0.2 Pitch PR b 2.7.1.1 2.7.1.2 Pitch SR b 2.7.2.1 2.7.2.1 Initiate PF In.1 - In.2 Disengage 2.7.5.1 2.7.5.2 Reset turl 2.7.6.2 Await furl 2.7.7.2 itoring Monitor of Monitor of Check if v activate b In.1.1 In.1.2	Draw pow Disengage Islades to fea Send com Check if pi Islades to fea Send com Check if pi Islades to fea Send com Check if pi Islades mode Initiate PR Islafe mode Initiate SR Islafe mode Initiate SR Islafe mode Initiate SR Islafe mode Initiate SR Islafe mode Initiate TR Islafe mode Initiate TR Islafe mod	er from ultrigenerators ther mand to pritch angle is ther mand to see the angle is safe mode afrom SR mand to generators are rall position mand to act the angle is the angle is the angle is the angle is rall position mand to act the angle is the angle	a-capacitors from SR mary pitch actuations correct condary pitch accorrect condary pitch accorrect correct accorrect merators de disengaged contained content positions content prid conte	orrectly tion mode wind turbine aries

Chapter 7: Control optimisation strategy

Using the aerodynamic characteristics calculated in chapter 5 and the interactions between the subsystems for control defined in chapter 6, the control strategy can be chosen and simulated using a python code. This will output values related to performance of the wind turbine which will be presented in this chapter. These performance characteristics are important for the remainder of the report.

The general control strategy, together with an overview of the equations used in this chapter is shown in section 7.1. The control strategy before rated conditions is covered in section 7.2, section 7.3 shows the results after rated conditions. An overview of the limiting values is shown in section 7.4. A sensitivity analysis is done in section 7.5 and verification and validation of the code is described in section 7.6. Finally, some limitations and recommendations are given in section 7.7.

7.1 General

Since the system consists of several rotors, the control strategy will be more complex than for conventional turbines. The control strategy is depicted in Figure 7.1. The starting point of all calculations is the fact that the secondary rotors have to provide a braking torque equal in magnitude to the torque of the primary rotor. The rest of this control strategy will be discussed in more detail in the next sections. The main idea behind it is that the upwind rotor will produce maximum thrust to extract maximum power until it reaches its generator capacity. After that, it is limited to that capacity and the downwind secondary rotor has to compensate the thrust in order to keep braking the primary rotor. At some point this will no longer be possible and the induction factor of the secondary rotors is increased in an attempt to increase their thrust. When even this is not sufficient anymore, the primary rotor is allowed to accelerate to reduce its torque. This should be sufficient to keep the torque of the primary rotor equal to the braking torque of the secondary rotors during the operational velocity range. If this is not the case, the emergency system will take over.

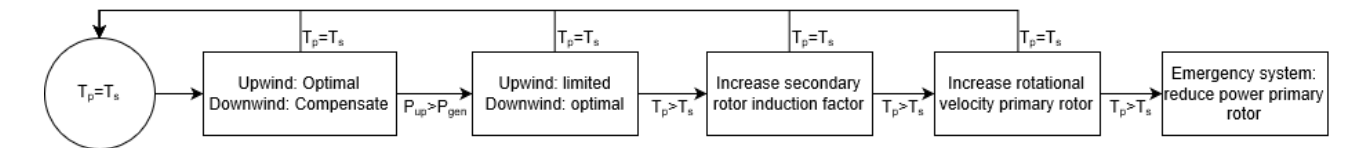


Figure 7.1: Control strategy

An overview of the equations used in this chapter is given in Table 7.1. Throughout the chapter use will be made of flow diagrams to describe the python code. In these flow diagrams, the identifiers of these equations will be used in order to show which equation is used in a certain step. This is done in an attempt to visualize and structure the information in a more coherent manner. Additional explanation of the flow diagrams is given in the following sections.

Table 7.1: Primary rotor control equations

Identification number	Equation	Units
Eq. 8.1	$V_{wind} = sin(\theta)V_{\infty}$	[m/s]
Eq. 8.2	$V_{s_{up}} = V_{t_p} + V_{wind}$	[m/s]
Eq. 8.3	$V_{s_{down}} = V_{t_p} - V_{wind}$	[m/s]
Eq. 8.4	$\omega_p = \frac{\lambda_p V_{\infty}}{r_p}$	[rad/s]
Eq. 8.5	$\lambda_p = \frac{\omega_p r_p}{V_{\infty}}$	[-]
Eq. 8.6	$V_{t_p} = \omega_p r_p$	[m/s]
Eq. 8.7	$P_p = \frac{1}{2}\rho V_{\infty}^3 C_{P_p} A_p$	[W]
Eq. 8.8	$P_{s_{up}} = \frac{1}{2} C_{P_{s_{up}}} \rho A_s V_{s_{up}}^3$	[W]
Eq. 8.9	$P_{s_{down}} = \frac{1}{2} C_{P_{s_{down}}} \rho A_s V_{s_{down}}^3$	[W]
Eq. 8.10	$C_{P_p} = \frac{2P_p}{\rho V_{\infty}^3 A_p}$	[-]
Eq. 8.11	$C_{P_{s_{up}}} = C_{T_{s_{up}}}(1 - a_s)$	[-]
Eq. 8.12	$C_{P_{s_{up}}} = \frac{2P_{s_{up}}}{\rho V_{\infty}^3 A_s}$	[-]
Eq. 8.13	$C_{P_{s_{down}}} = C_{T_{s_{down}}} (1 - a_s)$	[-]
Eq. 8.14	$C_{P_{s_{down}}} = \frac{2P_{s_{down}}}{\rho V_{\infty}^3 A_s}$	[-]
Eq. 8.15	$T_p = \frac{P_p}{\omega_p}$	[Nm]
Eq. 8.16	$T_p = T_{s_{down}} + T_{s_{up}}$	[Nm]
Eq. 8.17	$T_{s_{up}} = F_{T_{s_{up}}} r_p$	[Nm]
Eq. 8.18	$T_{s_{down}} = T_p - T_{s_{up}}$	[Nm]
Eq. 8.19	$F_{T_{s_{up}}} = \frac{T_{s_{up}}}{r_p}$	[N]
Eq. 8.20	$F_{T_{s_{up}}} = \frac{1}{2} C_{T_{s_{up}}} \rho A_s V_{s_{up}}^2$	[N]
Eq. 8.21	$F_{T_{s_{down}}} = \frac{T_{s_{down}}}{r_p}$	[N]
Eq. 8.22	$F_{T_{s_{down}}} = \frac{1}{2} C_{T_{s_{down}}} \rho A_s V_{s_{down}}^2$	[N]
Eq. 8.23	$C_{T_{sup}} = \frac{C_{P_{sup}}}{1 - a_s}$	[-]
Eq. 8.24	$F_{T_{s_{down}}} = \frac{1}{2} C_{T_{s_{down}}} \rho A_s V_{s_{down}}^2$ $C_{T_{s_{up}}} = \frac{C_{P_{s_{up}}}}{1 - a_s}$ $C_{T_{s_{up}}} = \frac{2F_{T_{s_{up}}}}{\rho A_s V_{s_{up}}^2}$	[-]
Eq. 8.25	$C_{T_{s_{down}}} = \frac{C_{P_{s_{down}}}}{1 - a_s}$	[-]
Eq. 8.26	$C_{T_{s_{down}}} = \frac{2F_{T_{s_{down}}}}{\rho A_s V_{s_{down}}^2}$ $a_s = 1 - \frac{C_{P_{s_{up}}}}{\rho A_s V_{s_{down}}}$	[-]
Eq. 8.27	$a_{s_{up}} = 1 - \frac{C_{P_{s_{up}}}}{C_{T_{-}}}$	[-]
Eq. 8.28	$a_{s_{up}} = 1 - \frac{C_{P_{s_{up}}}}{C_{T_{s_{up}}}}$ $a_{s_{down}} = 1 - \frac{C_{P_{s_{down}}}}{C_{T_{s_{down}}}}$	[-]

7.2 Before rated

The flow diagram for the control of the turbine before rated conditions is shown in Figure 7.2. The top part of the figure concerns the general calculation of values for the primary rotor for every velocity in the operational range. It shows that before rated velocity, the primary rotor operates at optimal conditions for power extraction, meaning it operates at maximum power coefficient corresponding to the optimal tip speed ratio. After rated conditions, the rotational velocity and power of the primary rotor are kept constant. After this first part, calculations for the secondary rotor can be performed for every velocity and every angle over the primary rotor rotation, as the wind speed that the secondary rotor sees will vary with the angle of rotation of the primary rotor

At first, the upwind going secondary rotor is controlled such that it produces thrust at maximum thrust coefficient as this maximizes the use of the additional wind. The downwind secondary rotor will then compensate the thrust that still has to be provided to counteract the primary rotor torque. At this point in time, the secondary rotors operate at an induction factor of $a_s = 0.05$. However, it can be seen in Figure 7.3 that the power produced by the secondary rotors is almost equal to the power of the primary rotor. This means that the efficiency loss introduced by the induction factor of the secondary rotor is almost completely compensated by the additional power that the secondary rotors extract from the general wind during the upwind phase.

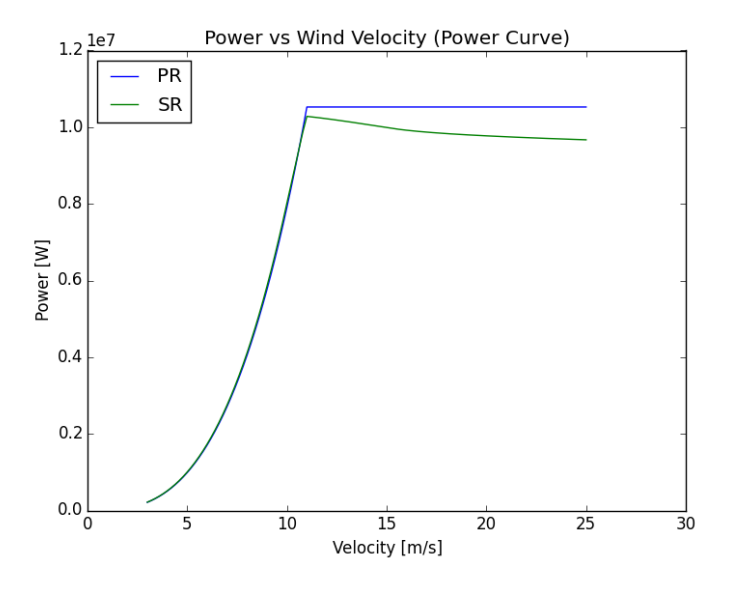
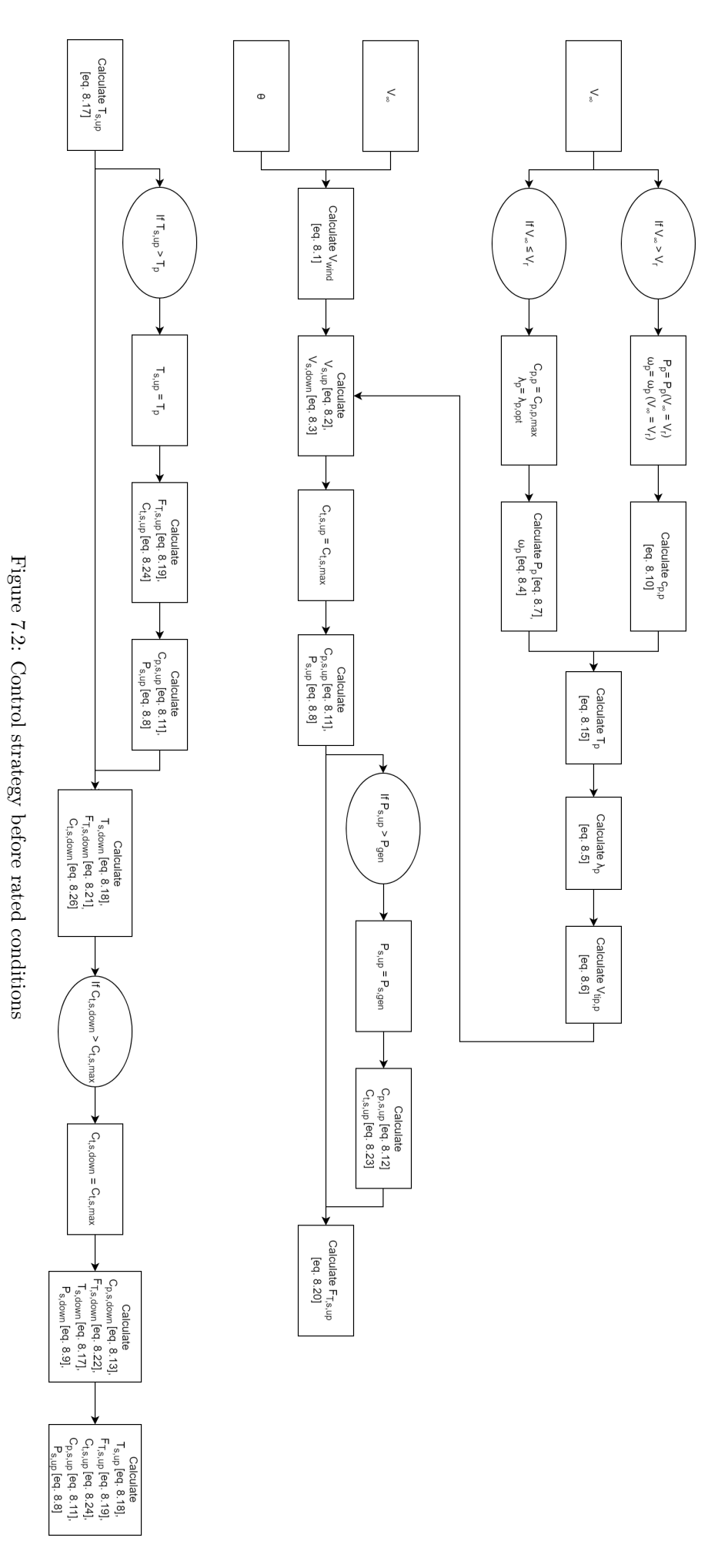


Figure 7.3: Power curve primary and secondary rotors

At some point, the power of the upwind secondary rotor will exceed the capacity of the generator. This means that the power of the upwind going secondary rotor will be limited to the generator capacity, and the downwind going secondary rotor will have to increase its thrust force until it reaches the maximum thrust coefficient. This can be seen in Figure 7.3 at a velocity of 10.5m/s. Here the slope of the secondary rotor power curve decreases slightly at that point. Figure 7.4 shows the power of the secondary rotors over a full rotation of the primary rotor at a velocity of 10.5m/s. It can be seen that the upwind rotor reaches its generator capacity of 7.5MW here. It must be noted these are theoretical values. In reality, the transition between upwind and downwind will occur smoothly, this means that the power production will not abruptly change from 4.8MW to 3.9MW when a transition from upwind to downwind is made.



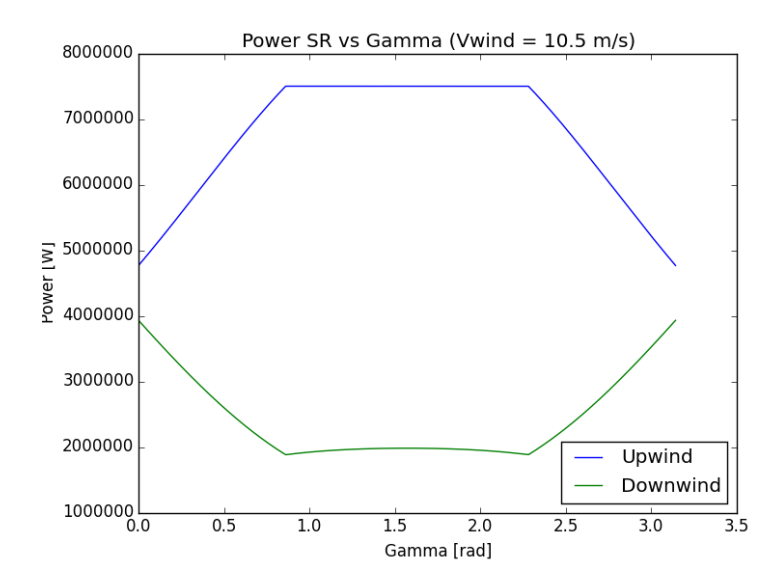


Figure 7.4: Power output of secondary rotors over primary rotor rotation

7.3 After rated

The flow diagram for control after rated conditions is shown in Figure 7.5. The downwind secondary rotor will have reached its maximum thrust, which means another method has to be used to counteract the primary rotor torque. This will be done by increasing the induction factor of the the secondary rotors. Increasing the induction factor will increase the thrust that the secondary rotor can provide. The power of the upwind rotor is set to its maximum power output, the induction factor is then increased in order to counteract the primary rotor torque. When the induction factor of the upwind secondary rotor reaches its maximum value of $a_s = 0.2$, the induction factor of the downwind secondary rotor is increased as well. Note that in the aerodynamic analysis, higher induction factors were found. However, these higher induction factors can only be reached at higher tip speed ratios, which makes the Mach numbers too large. This is why an upper limit of $a_s = 0.2$ was chosen to be within boundaries. Figure 7.6 shows the change in induction factor over the velocity range. It can be seen that the induction factor of the upwind secondary rotor increases from rated velocity onward. This increase in induction factor is enough to counteract the primary rotor torque until a velocity of 14m/s. After that, the induction factor of the downwind secondary rotor is increased as well.

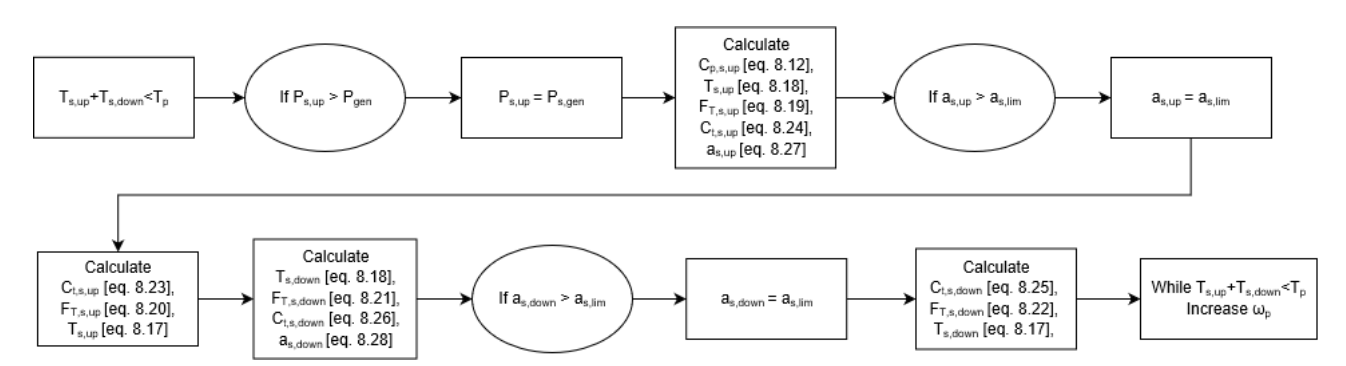


Figure 7.5: Control strategy after rated conditions

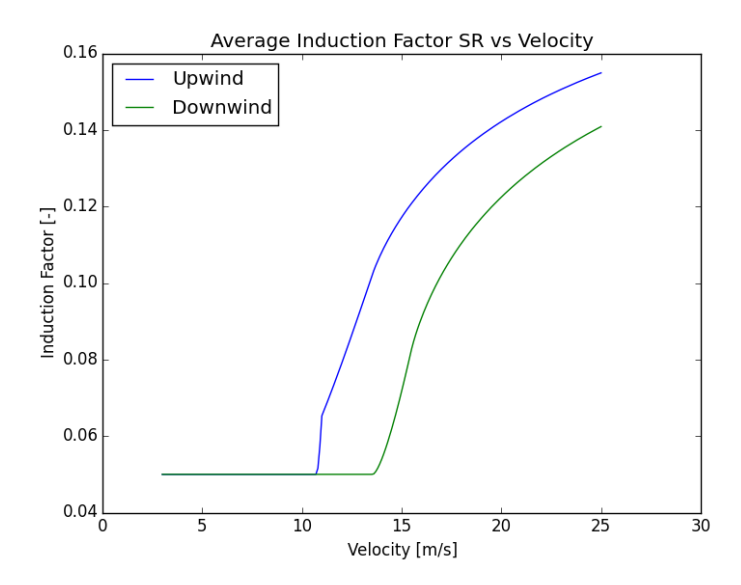


Figure 7.6: Change of Induction factor secondary rotor over velocity range

At a certain point, the increase in secondary rotor induction factor will not be enough to counteract the torque of the primary rotor because the maximum induction factor is reached. Figure 7.7 shows both upwind and downwind secondary rotor reach the maximum induction factor for a large part of the primary rotor rotation at a wind speed of 17.5m/s. The secondary rotor thrust force cannot be increased further. This indicates the torque of the primary rotor has to be decreased. The primary rotor is now allowed to accelerate over part of the rotation. Figure 7.8a shows the rotational velocity of the primary rotor is already increased from a velocity of 16m/s onward. Figure 7.8b shows the variation of rotational velocity of the primary rotor at the cut-out velocity of 25m/s.

The increasing rotational velocity has a beneficial effect to the power production of the wind turbine. This can be seen in Figure 7.3. When the rotational velocity of the primary rotor is allowed to increase over the rotation from 16m/s onward, the slope of the power curve becomes less negative. This suggests that more power is produced because of the fact that the secondary rotors experience a larger velocity. Limits for the acceleration of the primary rotor will have to be specified later in a more detailed structural analysis. However this should be enough to keep counteracting the primary torque until cut-out conditions. If the maximum acceleration were to be reached, and the torque of the primary rotor is not counteracted anymore, the emergency system is engaged and the primary rotor blades are pitched to reduce power of the primary rotor, reducing the torque.

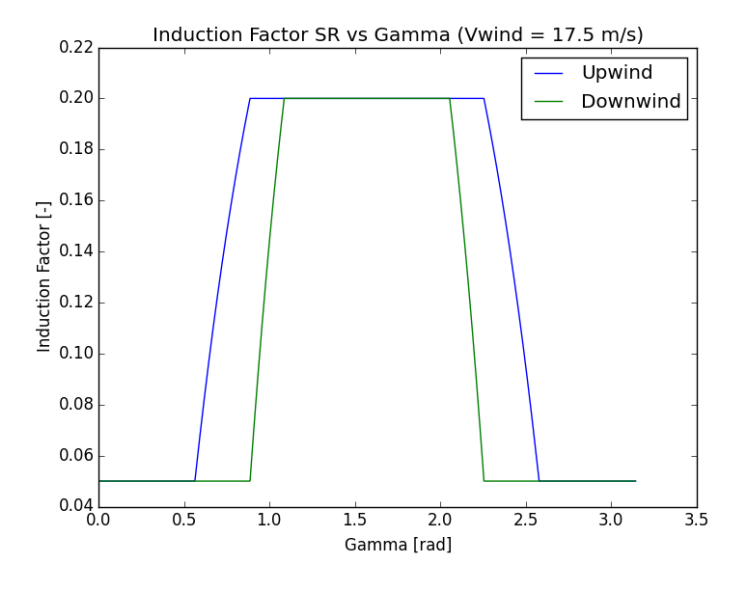
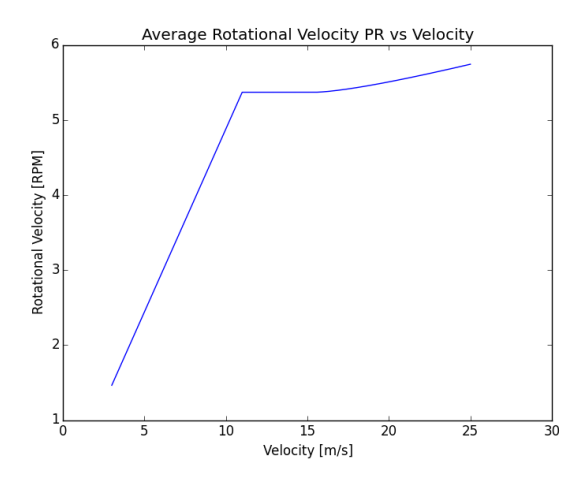
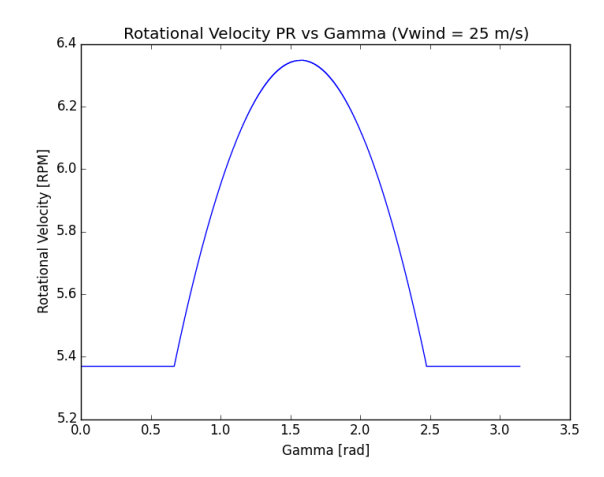


Figure 7.7: Induction factor variation secondary rotor at 17.5m/s





(a) Variation of rotational velocity primary rotor with wind (b) Variation of rotational velocity primary rotor over rovelocity tation at 25m/s

Figure 7.8: Rotational velocity of primary rotor

7.4 Limiting values

In order to calculate all the values for the control strategy, some limiting values had to be used as input in the python program. Table 7.2 gives an overview of these values. The values for the primary rotor were taken from a reference [8]. The maximum induction factor of the secondary rotor is chosen to be 0.2. In the aerodynamic analysis it was found that an induction factor of 0.24 can be achieved with a pitch angle of 0 deg. However, the tip speed ratio would be too large in this case. That is why a maximum induction factor of 0.2 is chosen. This can be achieved at a lower tip speed ratio and a pitch angle of 5 deg.

Table 7.2: Limiting input values python code

Parameter	Value
$a_{s_{max}}$	0.20
$Cp_{s_{max}} \ (a_s = 0.05)$	0.13
$\lambda_{s_{opt}} \ (a_s = 0.05)$	2.10
$Cp_{p_{max}}$	0.39
$\lambda_{p_{opt}}$	4.65

After running the code, some limiting values were obtained as output. Table 7.3 gives an overview of these at a wind velocity of $25 \ m/s$. The table contains values for maximum Mach number the blade tips of the secondary rotors will see. This maximum will happen at cut-out, since the tip speed ratio has to be increased in order to obtain higher induction factors, and the rotational velocity of the primary rotor reaches its highest value at cut-out conditions. The highest value regarding rotational velocity of the secondary rotor will be reached at this velocity for the same reason. The maximum value for generator torque at rated power output is shown as well. This will be used as input for the generator sizing in chapter 8. Finally, a value for capacity factor could be determined as well. This is based on the power curve shown in Figure 7.3 and a reference Weibull distribution of wind speed data at the OWEZ wind farm [34]. The Weibull distribution parameters are A = 10.6 and k = 2.2, these values yield a capacity factor of 0.5711.

Table 7.3: Limiting output values python code at a wind velocity of 25 m/s

Parameter	Value
$V_{tip_p}[\frac{m}{s}]$	85.5
Mach secondary	0.75
$\Omega_p[rpm]$	6.35
$\Omega_s[rpm]$	200
Generator torque [kNm]	770

7.5 Sensitivity analysis

For the control strategy, the blade design plays a large role in the values that are obtained. If, for example, the induction factor of the secondary rotor is able to reach values of $a_s = 0.4$, the rotational velocity of the primary rotor would not have to be increased anymore to make the braking torque of the secondary rotors equal the primary rotor torque. However, the range of tip speed ratios that the blade design can operate in also plays an important role. To achieve the maximum induction factor, the tip speed ratio has to be increased. A consequence of this is that higher Mach numbers are reached at the secondary rotor blade tips. Higher tip speed ratios thus mean a lower margin to operate in due to Mach number restrictions.

Furthermore, it is assumed the accelerations of the primary rotor which have been calculated can be supported by the structure. If this were not the case, another solution would have to be found to control the system. A possibility is that the primary rotor has to pitch over the rotation. However, this would increase the use of primary pitch systems a lot which would also increase failure rates and maintenance cost.

Another thing that was not considered in this analysis is the pitching of the secondary blades. In the future, an optimum pitch regime will have to be found. The expectation is however that the blades of the secondary rotors will have to be pitched almost continuously during operation because of the variations in wind speed that it encounters during a rotation of the primary rotor. This could introduce a challenge for the failure rates and maintenance of the pitch systems. If the pitch rates that are required for the secondary rotors are unacceptable, another control strategy has to be found as well.

A quantitative sensitivity analysis can be done by increasing the limiting input values by 10% and analyzing the effect on the limiting output values. The results of this can be found in 7.4. From this table it becomes clear the induction factor does not have a particularly large effect to any of the output values with the largest change being the Mach number with 1.33%. The $Cp_{s_{max}}$ and the $\lambda_{s_{opt}}$ both have a relatively large effect on the rotational velocity of the secondary rotor, and therefore also on the generator torque. Accordingly this sensitivity should be considered in the structural and power analysis. The $Cp_{p_{max}}$ is only sensitive to the rotational velocity of the primary rotor, for which does not pose a problem. Finally, the $\lambda_{p_{opt}}$ has the largest effect on the rotational velocity of the secondary rotor and therefore also on the generator torque. As with the $\lambda_{s_{opt}}$, this sensitivity should be taken into account in choosing the generator and performing the structural analysis.

Table 7.4: Changes in limiting output parameters due to a 10 % change in limiting input parameter at a wind velocity of 25 m/s

Parameters	New value	V_{tip_p}	Mach	Ω_s	Ω_p	Generator torque
Original value		85,5 [m/s]	0,748 [-]	200 [RPM]	6,35 [RPM]	768 [kNm]
Increasing values						
$a_{s_{max}}$	0,220 [-]	-1,05%	-1,07%	-1,00%	-1,57%	0,00%
$Cp_{s_{max}}$	0,143 [-]	1,05%	0,94%	5,00%	1,42%	-5,86%
$\lambda_{s_{opt}}$	2,310 [-]	0,00%	10,29%	10,50%	0,00%	-9,11%
$Cp_{p_{max}}$	0,429 [-]	0,00%	0,00%	0,00%	4,88%	0,00%
$\lambda_{p_{opt}}$	5,115 [-]	4,33%	4,28%	20,50%	5,98%	-21,22%
Decreasing values						
$a_{s_{max}}$	0,182 [-]	0,94%	0,94%	1,00%	1,26%	0,00%
$Cp_{s_{max}}$	0,118 [-]	-1,17%	-1,20%	-5,00%	-1,73%	6,90%
$\lambda_{s_{opt}}$	1,909 [-]	0,00%	-9,09%	-9,00%	0,00%	10,03%
$Cp_{p_{max}}$	0,355 [-]	0,00%	0,00%	0,00%	-4,57%	0,00%
$\lambda_{p_{opt}}$	4,227 [-]	-4,09%	-4,01%	-16,50%	-5,67%	27,08%

7.6 Verification and validation

In order to verify the numerical model written in python, an analytical model in excel was used. This analytical model was already constructed in the midterm phase where it was used to size the system. The model has been adapted slightly in order to check values for rotational velocity, tip speed and torque for both primary and secondary rotors. This was done by entering several operational points, and checking if the calculated values match with an acceptable accuracy. If the values did not match, the code was checked for bugs by doing unit tests. Parts of the code were isolated and checked separately in order to find the part where a bug was present.

This bug could then be corrected and the code was tested against the analytical model again, this procedure was then iterated until the values of analytical and numerical model matched.

Once the code was finished, graphs were produced which depict, among other things, the rotational velocity of the primary rotor over a full rotation, the power curves, and the induction factors of the secondary rotors. These graphs were then checked for logic, and it was checked if the values do not exceed their specified limits. An example of a simple logic check is producing a graph with the torque of the primary rotor and the braking torques of the secondary rotors, and to then check if the sum of the braking torques is equal to the torque of the primary rotor. Another example is producing a graph for the generator torque of a secondary rotor, another graph with the power of that secondary rotor, and another graph with the rotational velocity of the secondary rotor. It can then be checked if the values make sense when the relation between torque, power, and rotational velocity is considered.

7.7 Limitations and recommendations

The control optimization strategy uses a python code written that assumes infinite pitch rate. This implies that the graphs and trends presented in this chapter are theoretical optimal values. Implementing a realistic pitch rate will produce smooth curves and trends that present the reality of the control system better. It is therefore recommended to implement the pitch rate to achieve practical results. Afterwards a pitch optimization code should be added to the strategy to constrain the pitch angle to not change drastically over the rotation and the range of velocities.

Chapter 8: Power and electronics

In this chapter, it will become clear if the goal of the design is at least partially reached as the aim of the project was to reduce drivetrain mass. Using the value for maximum torque that was calculated in the previous chapter, the mass of the generator can be obtained. In section 8.1 the cost, mass and size of the drivetrain is estimated. In section 8.2, an electrical block diagram is constructed showing a general overview of the electrical components in the system assuming a wind farm layout. After that, a sensitivity analysis on the results found in this chapter is done in section 8.3 while some limitations and recommendations are given in section 8.4. The mass of the drivetrain is an important outcome of this chapter. Not only does it give an idea of the probability of achieving the goal of the project, it is also a required input for the structural analysis. Furthermore, the generator cost will be used in the cost analysis of the design as well.

8.1 Drivetrain

Figure 8.1 shows the typical energy conversion process for a wind turbine. The energy in the wind is converted to mechanical energy by the rotor. This mechanical energy is then transported by a gearbox, note that a gearbox is not required when a direct drive generator is used. The mechanical energy is converted into electrical energy by a generator. Depending on the power output of the generator and the required transportation of the electricity, power converters are required. After transportation of electricity, it is supplied to the grid.

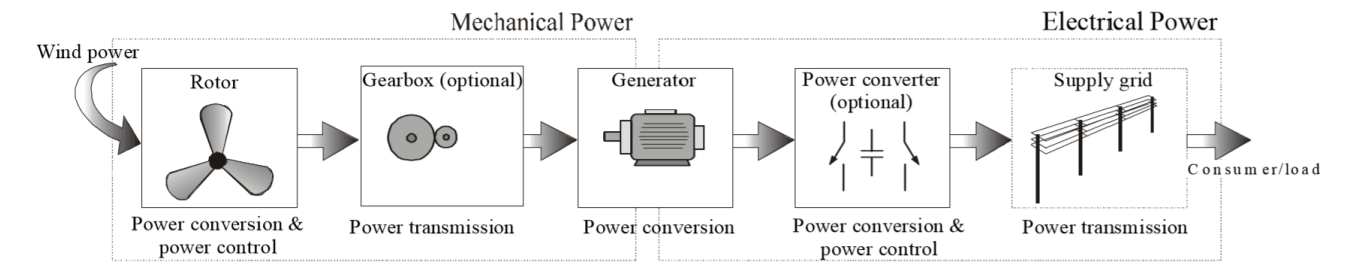


Figure 8.1: Energy conversion in a wind turbine [35]

8.1.1 Direct drive vs gearbox

A simplified representation of the drivetrain consists of an optional gearbox, a generator and a mechanical brake. A choice has to be made between a direct drive and a geared generator design. Geared systems are usually lighter, smaller and cheaper than direct drive systems. However, they have a lower reliability implying additional maintenance costs and are less efficient [36]. This means that even though the material cost of a geared generator is lower, due to the maintenance required it will likely turn out to be more expensive. This is because maintenance is a real issue for offshore wind turbines and this design will have two generators as opposed to the single generator and gearbox in conventional turbines, increasing the maintenance cost even more. Furthermore, the mass of a direct drive generator is heavier than a geared generator. The mass requirement however states that a mass reduction compared to a conventional turbine should be achieved. This means that because of the low torques in this design, a direct drive generator in this design can be lighter than a geared generator in a conventional turbine. The reliability issue and the consequential maintenance costs that a geared generator has is the most important reason that a direct drive generator is chosen for this design. This direct drive generator will be a permanent magnet synchronous generator.

8.1.2 Mass and cost

A mass estimation for a direct drive generator is done based on the torque of the secondary rotor found in chapter 7 and a generator mass-torque relation based on a statistical relation for offshore direct drive generators [36]. Using a torque of 770kNm and considering $25\frac{kg}{kNm}$, a generator mass of 19.25tonnes is found. In this reference, it can also be seen that a lower torque implies a larger mass fraction of active material compared to

inactive material. However, this relation is slightly arbitrary, it is therefore assumed that the active material accounts for all of the generator mass. Considering that there are two generators in this turbine, a total generator mass of 38.5tonnes is used for comparison with conventional turbines. Using the same statistical relation, a conventional 10MW direct drive wind turbine will have a generator mass of 239tonnes. This means that a generator weight reduction of almost 84% is achieved compared to a conventional direct drive wind turbine. Comparison with a 10MW geared generator is difficult since a lot of the large offshore wind turbines are using a direct drive generator, so it is hard to find mass data for a 10MW geared generator.

For the cost estimation of this generator, a rough estimation is made since data is again hard to find. Table 8.1 shows the mass and specific cost of each material in the generator. All values are for a single generator, the total mass and cost of both generators is shown in the table as well. The specific cost of the material is used to estimate the cost of the generator [37]. The mass of lamination is assumed to account for 73% of the total mass, while copper accounts for 19% of the generator mass. The mass fraction of permanent magnet material is then 8% [38][39]. It is found that the total generator cost of the system will be $378,840 \in$.

Material	Weight	Cost
Lamination	14.1 tonnes	$3 \in \frac{\epsilon}{kg}$
Copper	3.7 tonnes	$15 \frac{\epsilon}{kg}$
Permanent magnet	1.5 tonnes	$60 \frac{\epsilon}{kg}$
Total single generator	19.25 tonnes	189.4 k€
Total	38.5 tonnes	378.8 k€

Table 8.1: Generator mass and cost breakdown

In order to get to the total drivetrain cost, the power electronics have to be considered and added to the generator cost. The cost of power electronics in the drivetrain is assumed to be $40 \frac{\epsilon}{kW}$ [39]. Considering 7500kW per generator and the fact that there are two generators in this design, this gives a total power electronics cost of $600,000\epsilon$. This brings the total drivetrain cost to $978,840\epsilon$. The power electronics of this system mainly consist of the power converters but also the wiring and other electrical components. The task of the power electronic converter is to convert the AC power output of the generator to a DC power output that can be connected to an offshore substation. This power converter can perform speed and power control. A cost comparison can also be done with a conventional wind turbine.

8.1.3 Sizing

The size of the generator is also important for the analysis of the design. This can be determined using Equation 8.1 [40]:

$$\pi r_g^2 l_g = \frac{P_g}{2\omega_g F_d} \tag{8.1}$$

Here, F_d is usually between $25 - 50 \frac{kN}{m^2}$. Considering that $\frac{P_g}{\omega_g} = T_g$ and that the torque of the generator is equal to the torque of the secondary rotor in case of a direct drive generator, the torque of the secondary rotor can be substituted in the equation. Instead of the radius, it is easier to define the diameter of the generator in the equation, since this is mostly used in literature for comparison. An expression can then be found for a combination of generator length and diameter given by Equation 8.2:

$$l_g D_g^2 = \frac{2T_g}{\pi F_d} \tag{8.2}$$

For the torque of 770kNm, the expression $l_gD_g^2$ is calculated to be between $9.8-19.6m^3$. An optimal ratio of axial length over air gap diameter of $\frac{l_g}{D_g}=0.3$ is used to minimise mass [36]. Combining these values and using the worst case force density gives a maximum generator length of $l_g=1.21m$ and a maximum diameter of $D_g=4.03m$.

8.1.4 Summary table

Table 8.2 gives an overview of the most important values that were found for the drivetrain. The length and diameter are given for each generator. The total generator mass and cost are given as well, each generator contributes to half of this value. Finally, the total cost for the power electronics is given.

Generator length [m]	1.2
Generator diameter [m]	4.0
Mass of single generator [ton]	19.25
Cost of single generator [k€]	189.4
Total power electronics cost [k€]	600

987.8

Total drivetrain cost [k€

Table 8.2: Summary table drivetrain

8.2 Electrical block diagram

Figure 8.2 shows the electrical block diagram for the power transmission from the generator to the grid. The permanent magnet synchronous generator in the secondary rotor has an AC power output. This is then converted to a DC power output, after which the voltage is stepped up to medium voltage within the secondary rotor. The benefit of having a power conversion system for each secondary rotor is the fact that speed and power control can then be applied separately to every secondary rotor. The DC power of all the secondary rotors is then collected in an offshore substation. The internal grid that connects different wind turbines can either be AC or DC. Here, a DC internal grid is chosen because of the relatively high power of the wind turbines, DC cabling can support higher powers at a lower cable mass and cost [41]. Since this turbine is relatively large and current wind farms are being built increasingly far offshore, it is assumed that the wind turbine designed in this project will be part of a wind farm relatively far offshore. This means that a HVDC transmission link is assumed to connect the offshore substation to the onshore substation as this reduces losses compared to a HVAC link. Furthermore, AC step-up converters are heavier than DC converters, meaning that it is more difficult to construct an offshore HVAC substation. This makes a HVDC offshore substation more attractive for the wind farm design [42]. In the offshore HVDC substation, the medium voltage from the secondary rotors is stepped up to a high voltage, this reduces cable losses significantly when the power is transported over a large distance. The power from the offshore substation is collected by an onshore substation, where the HVDC power is converted to HVAC power. After that, the voltage of the AC power is stepped down in a transformer in order to be supplied to the grid.

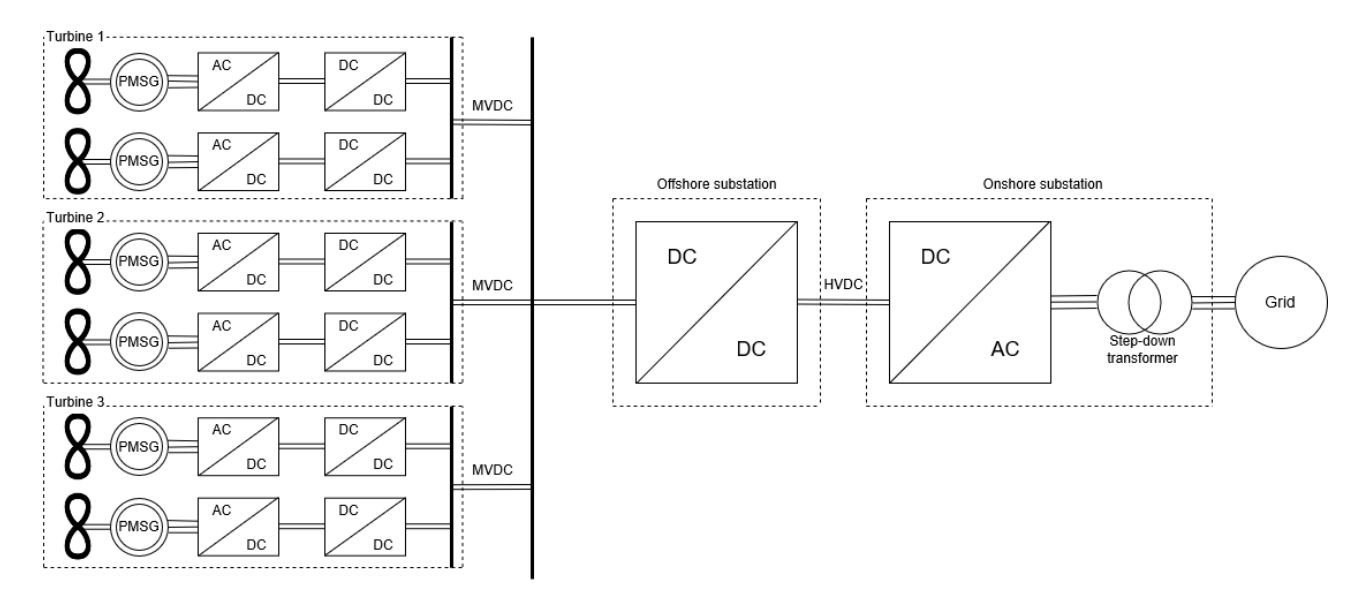


Figure 8.2: Electrical block diagram wind farm configuration

8.3 Sensitivity analysis

A downside of using a direct drive generator is that it uses permanent magnets. These permanent magnets are made of rare-earth materials and the price of these materials tends to fluctuate. Different reports give different values for permanent magnet cost, where a value of $120\frac{\epsilon}{kg}$ was reported in 2012 [43]. This is double the value that was used to calculate the cost in this report so it means that a sudden change in price has to be taken into account in the generator choice. Using the value of $120\frac{\epsilon}{kg}$ as the cost of permanent magnet material, the cost of a single generator would increase to $281,820\epsilon$. This is a 49% increase in cost. If the material cost of permanent magnet generators becomes too high in the future, a geared generator can be considered.

Besides material prices, also inaccuracies in previous calculations have to be considered. The most important input parameter for the drivetrain calculations is the generator torque that was calculated in the control chapter. This torque is 770kNm, however this value will not be perfectly accurate. If it were 10% off, it would mean the generator has to be sized for 847kNm instead. This will change the values for the generator as shown in Table 8.3.

Table 8.3: Change in generator parameters with 10% torque increase

Parameter	Value	Change
Mass [ton]	21.2	+10%
Cost [k€]	208.4	+10%
Diameter [m]	4.16	+3%
Length [m]	1.25	+3%

For the electrical block diagram, the distance to the shore has a big impact on the topology of the wind farm. If the distance to the shore is relatively small, the big investment cost of a HVDC substation is not compensated by the reduction in cable losses anymore. This means that the distance to the shore can change the offshore substation from HVDC to HVAC or, if the distance to shore is very small, there might not even be an offshore substation. In case of an offshore HVAC substation, the DC/DC step up converters in the secondary rotor can also be replaced by a DC/AC converter. The internal grid connecting the turbines is then also an AC grid, while it is now DC.

8.4 Limitations and recommendations

It is important to note that the generator sizing only uses preliminary sizing equations. Moreover, the mass and cost estimations are based on statistical values, meaning that they will likely not be very accurate. The values given in this chapter are meant to provide an initial estimation but a detailed design of the generator still has to be done in the future. Once a more detailed design of the generator is done, the electrical components of the system can also be sized. The cost and mass of the drivetrain can then be estimated more accurately. Now, only the mass of the generator is estimated to be able to compare with conventional turbines and to get an idea of the weight savings of this design.

Chapter 9: Structural Analysis

In this chapter, the aerodynamic analysis, the drivetrain analysis and the system performance values from the control chapter will be combined to do a structural analysis. This will start on the outside with the secondary rotor structural analysis in section 9.1. Then, the analysis moves toward the centre of the wind turbine with an analysis of the primary rotor in section 9.2. The way the structures are attached is covered in section 9.3. The structural analysis is then moved further to the centre with the analysis of the tower and the strut in section 9.4 and section 9.5, respectively. A sensitivity analysis is done in section 9.7 and verification and validation is done in section 9.8.

9.1 Structural analysis of the secondary rotor blades

This section starts with defining the aim of the structural analysis in optimizing the blade design to satisfy driving requirements. To do this, an initial study on the wind turbine blade structure is performed. Next, additional requirements are derived for the structures department, these will need to be fulfilled during the design process. The loads acting on the structure are presented in subsection 9.1.3, fatigue and its effects are analysed in subsection 9.1.4. The Co-Blade software is used for the structural analysis of the SR and furthermore the results of the study are presented in subsection 9.1.6.

9.1.1 Blade design

The secondary rotor is comprised of 5 blades rotating in the horizontal axis, attached to the tips of the bottom primary rotor blades. The wind turbine has two primary rotor blades consisting of an upper and lower blade element. The secondary rotor blades require an optimum cross section for aerodynamic efficiency in order to generate power by braking the primary rotor. In addition, the structure of the rotor must be able to resist the design loads acting on the blades and be optimized for minimum weight. The mass optimization of the secondary rotor blades will also ensure a reduction in weight of the primary blade, horizontal strut and tower since the magnitude of the loads also decreases.

Along the blade length, weight optimization is performed with the rotor blades having a taper and twist angle. The taper is implemented throughout the overall length of the blade and throughout the thickness of the cross section. This is done since the highest loads are experienced at the root and decrease towards the tip. The taper and the twist angles are optimized in previous aerodynamic analysis however the cross sectional thickness of the blade elements is evaluated in Table 9.1.5.

The materials and manufacturing processes are also going to induce limitations on the design. The internal structure and shape of the cross section will define the stiffness and strength of the loaded blade. However, the material chosen for the design should have a high stiffness to weight ratio to minimize flapwise (in the wind direction) and edgewise (perpendicular to the wind) deflections and fatigue loads caused by the weight of the blade itself.

The most common used materials for blade designs are glass fiber reinforced polymers (GFRP) and carbon fiber reinforced polymers (CFRP). This is primarily because both these materials have a high stiffness to weight ratio as seen in Figure 9.1 and a high resistance to fatigue. CFRP has better material properties than GFRP but it is less often used because of its high cost.

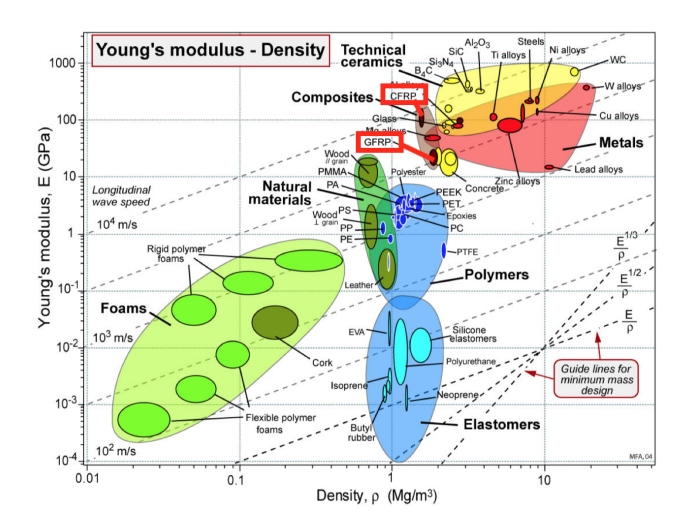


Figure 9.1: Graph showing stiffness to weight ratios for different materials, the CFRP and GFRP are highlighted

The structure of the wind turbine blade can therefore be assumed to be primarily made out of composite materials and more specifically GFRP. The use of composites is advantageous because it allows the manipulation of the material such that different parts of the blade have different material properties. This is necessary for blade mass optimization as indicated by the different loading cases in Figure 9.2.

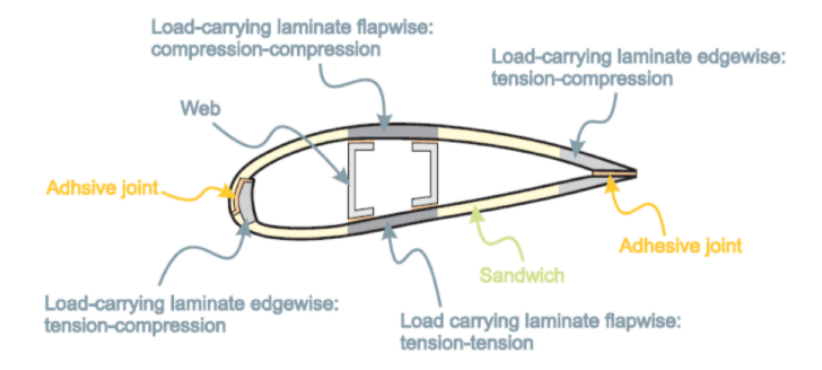


Figure 9.2: The structure of a wind turbine blade [44]

As shown in Figure 9.2 a wind turbine blade is made up of three main elements summarized below with their respective functions.

- Outer shell providing aerodynamic shape made of sandwich structure to provide buckling resistance
- Load carrying beam-like structure with two thick spar caps providing flapwise bending stiffness (caused by wind pressure) and shear webs carrying shear loads
- Leading edge and trailing edge reinforcements providing edgewise bending stiffness (caused by gravitational loads and torque)

The main elements are typically manufactured separately and combined using adhesive bonding.

Different factors causing performance degradation and consequently failure in wind turbine blades are listed below.

- During operation: Delamination, Bond lines failure, Erosion/wear, Laminate failure due to fatigue induced loads or ultimate loads
- Material factors: Plasticity, Ductile/brittle failure
- Geometry of structure: Buckling, Excessive deflections, Folding
- Due to manufacturing process: Initial distortion, Residual stresses, Production defects
- Environmental conditions: UV rays, Rain, Temperature, Lightning strikes, Humidity, Corrosion [45]

It is crucial to identify these factors and take them into account in the design of the structure. This will ensure that the operations and maintenance costs are minimised, that the annual energy production is maximised and that the cost of energy is minimized. The high rotational velocity of the secondary rotor makes it more sensitive to the performance degrading factors and it is therefore important to analyse the structure using accurate loads.

9.1.2 Requirements for the secondary blade design

Requirements for the secondary blade design regarding the output parameters of the structural analysis.

- **DES-1** The number of the cross sections analysed in the region between the largest chord length and the tip shall be more than 10.
- **DES-2** The distance between two cross sections (in the region between the root and the largest chord length) shall be smaller than the shortest chord length in the same region.
- **DES-3** The distance between two cross sections (in the region between the largest chord length and the tip) shall not be larger than 1.5 times the length of the smaller chord length of the two.
- **DES-4** All the critical stations (where a web starts or ends, spar caps location) shall be distinguishable.
- **DES-5** The analysis along the chord shall be performed in such a way that all important structural members (such as sandwich panels, spar caps) are distinguishable and evaluation of the highest stresses and strains is possible.
- DES-6 The aerodynamic shape shall be specified at each cross section that is analysed, including:
 - the chosen airfoil
 - chord length
 - twist angle
 - pitch axis location
- **DES-7** Structural analysis for maximum allowable stress, tip deflection of the blade and buckling stress shall be performed for the extreme loading case.
- **DES-8** All blade parts (skin, spar caps, shear webs) shall be analysed at each cross section everywhere along the length of the blade. The analysis shall be performed for the extreme loading case.
- **DES-9** The failure modes shall be analysed separately.
- DES-10 For the buckling analysis the boundary conditions and equations used shall be specified
- **DES-11** For each failure mode the design criterion shall be satisfied.
- MAT-1 For all materials used the designations shall be provided.
- MAT-2 Mechanical properties of materials used for the secondary blade structure shall be specified.
 - Engineering constants E_{11} (Young's modulus in longitudinal direction), E_{22} (Young's modulus in transverse direction), G_{12} (shear modulus), v_{12} (Poison ratio)
 - Ultimate longitudinal tensile strength s_{11T}
 - Ultimate longitudinal compressive strength s_{11C}
 - Ultimate shear stress s_{12}
 - Density ρ
 - Fibre volume fraction V_F
- SAND-1 The effective properties of the sandwich panels shall be specified:
 - Effective Young's modulus E_{eff}
 - Effective shear modulus G_{eff}
- SAND-2 For the sandwich panels, it shall be specified which core material is used in combination with which face sheet material and which technology for processing is chosen.
- ADH-1 For adhesive joints the compatibility between part material and adhesive shall be ensured.

- ADH-2 For adhesive joints the type of processing (co-bonding, co-curing, adhesive boning) shall be specified
- ER-1 The surface of the blade shall be well protected against environmental influences. The leading edge and tip erosion shall be prevented by applying proper coatings/protective films. If the surface protection life time is shorter than the blade life time, inspection or maintenance periods shall be documented.
- MAN-1 For fibre reinforced polymer, composites the type of processing (pultrusion, hand lay-up, prepreg, infusion) shall be specified
- RATT-1 The blade root attachment shall be described.
- CLEA-1 The secondary rotor blades shall not collide with the primary blades or the tower.
- RES-1 Maximum allowable stresses shall be specified.
- **RES-2** Maximum tip deflection shall be specified.

9.1.3 Loads acting on the secondary rotor blade

During its operational lifetime the secondary rotor blade experiences different types of load cases that it has to withstand to prevent damage. The loads acting on the structure are shown in Figure 9.3. In this figure, the blade reference frame is used, with the axis defined along the pitch axis of the airfoil.

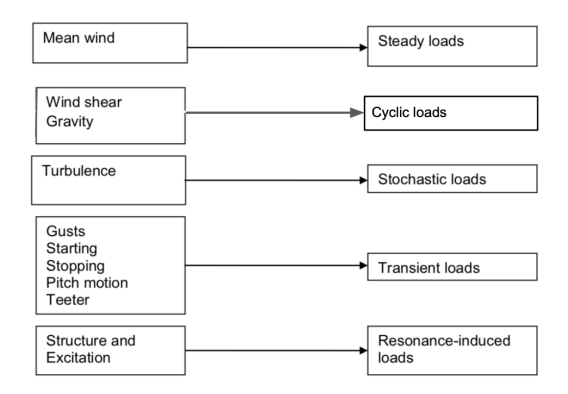


Figure 9.3: Loads the structure will experience during wind turbine operation

The mean wind is contributing to the steady loads acting on the structure, it induces the aerodynamic forces of lift and drag. These forces are plotted as the normal p_{xa} and tangential forces p_{ya} acting on the structure at the aerodynamic center. The weight of the blades generates cyclic loads on the structure, acting in the x direction p_{wx} Due to the rotation of the blades, the centrifugal force is also acting on the blade, in the axial direction. Stochastic, transient and resonance-induced loads cannot be estimated for since more elaborate and complex models should be used to accurately simulate such loads. However the effect of the load uncertainties can be accounted for using partial safety factors.

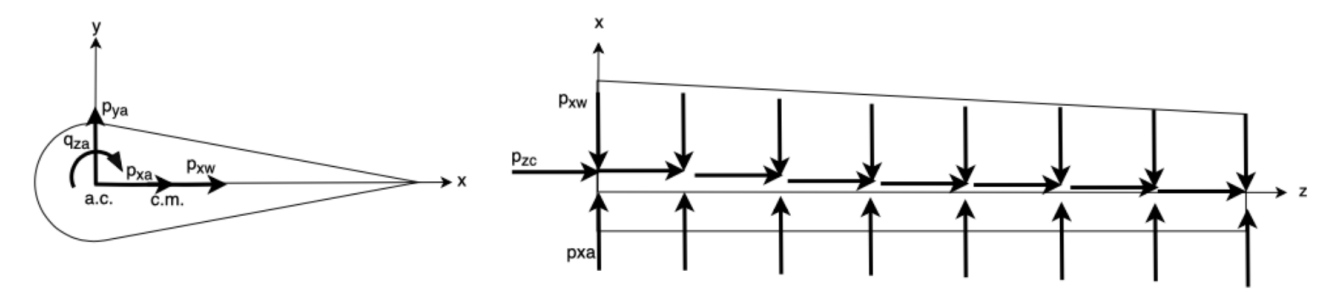


Figure 9.4: Free body diagrams of the loads acting on the cross section of the secondary rotor blade (in the x-y axis frame) and along the length of the blade (in the x-z axis frame)

Using the graphs displayed in Figure 9.5 the centrifugal force is the most critical force for the design of the secondary rotor blade since its rotational velocity is very high. The centrifugal force is approximately 20 times larger than the aerodynamic tangential and normal forces. To evaluate the structure at its critical loading case, the aerodynamic forces have been computed for each pitch angle and the maximum forces have been plotted for each cross section along the length of the blade.

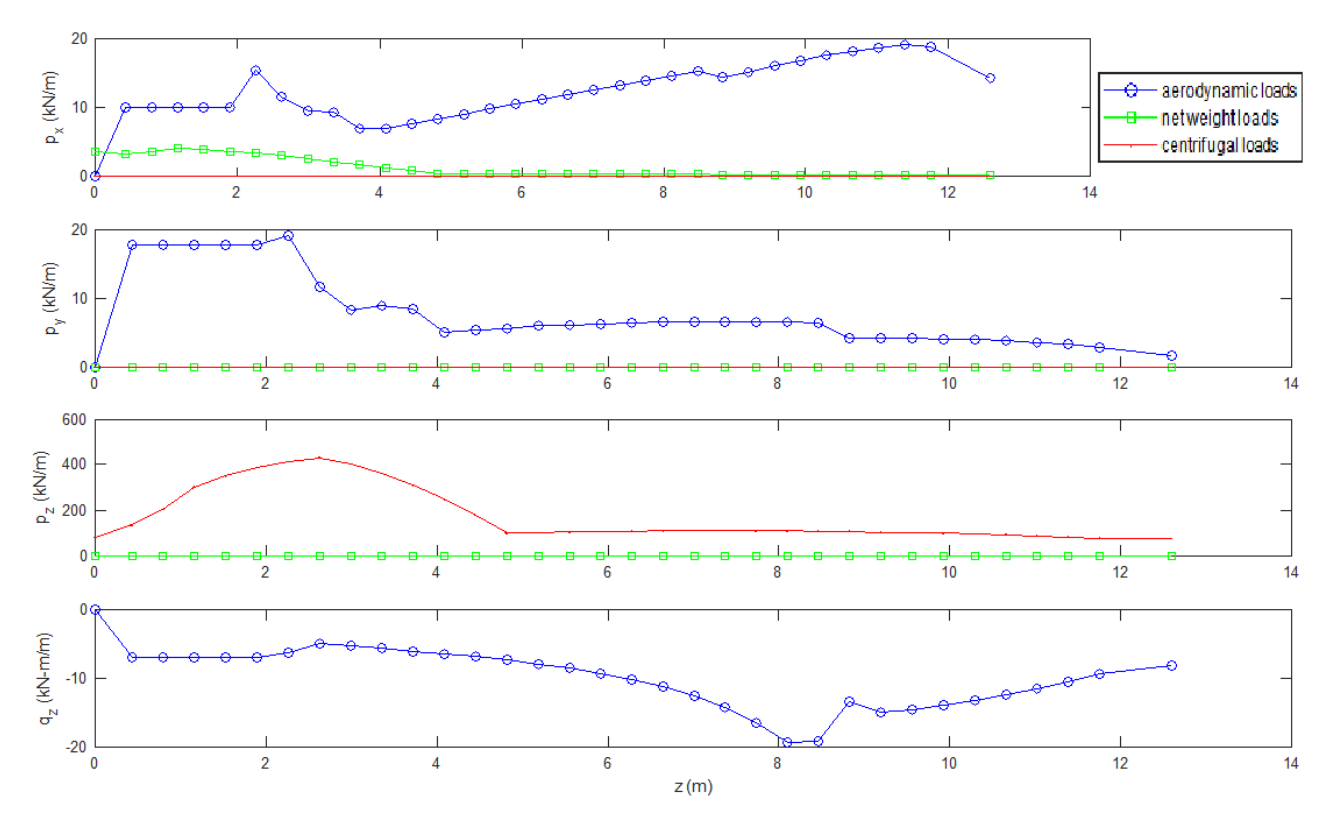


Figure 9.5: Applied Loads

9.1.4 Fatigue considerations

The wind turbine blade is subjected to different types of loads including cyclic loads that cause fatigue in the structure. Within one rotation of the primary rotor, both the upwind and downwind secondary rotors will see variable wind flow velocities that will induce cyclic loading cases. Additionally the gravity loads induce fatigue loads because they reverse twice every blade rotation. It is therefore important to take resistance to fatigue into account when designing the wind turbine blade structure. The most common used materials for blades are composites primarily due to their superior fatigue performance.

For a composite material the fatigue strength is dependent on the following aspects:

- The fiber material
- The fiber material to resin volume ratio
- The fiber orientation
- The resin type
- The material sensitivity to moisture
- The materials' thermal treatment
- The presence of any imperfections (e.g. misalignments)

When fibres are oriented and run in the direction of the applied loads, fatigue life is mostly dependent on the fibres. This is because laminates with highest amount of fibres in the load direction show the highest fatigue strength.

During operation, the maximum rotational velocity of the secondary rotor is approximately 200rpm. The number of load cycles is computed with the rotational speed of the rotor at the rated velocity in Equation 9.1.

$$n = \text{RPM}$$
 at rated windspeed * design lifetime (in minutes) = $140 * (25 * 365 * 60)$ (9.1)

The number of load cycles that the structure has to withstand is approximately 76.7 million cycles therefore fatigue is a very important issue for future analyses. Performing an accurate fatigue analysis of the blade structure gives an estimation of the component lifetime. For now, the lifetime has not been estimated with respect to the secondary rotor blade structure but has been qualitatively analysed. For future studies it would

be recommended to do a more detailed analysis of the fatigue lifetime of the structure. As well as this specimens of the same structure as the secondary rotor can be tested with emphasis on the most severe fatigue loading, the reverse loading case (tension-compression).

9.1.5 Co-Blade software

In order to design a composite structure for the secondary blade, a FEM analysis can be used to account for the complex geometry and to allow for some optimization process. However due to the many degrees of freedom at that stage of the design, it is not efficient to use such an accurate detailed tool. For that reason a simplified numerical model is chosen to analyze the structure. An open source code (named Co-Blade) is available for that which is written in Matlab [46]. This tool is specifically designed for structural optimization of composite blades for wind turbines. It is based on classical lamination theory (CLT), Euler-Bernoulli and shear flow theory.

Co-Blade method

The secondary blade length is divided into sections (number of which is an input in the code that can be changed) and the airfoil at each section is called a station. As described in subsection 9.1.1 and visualized in Figure 9.2 a station cannot be treated as a homogeneous structure since it consists of discrete portions with different material properties. Each portion is considered to be a sandwich panel that consists of a core and face sheets symmetrically positioned with respect to it. The number of the plies in the sandwich structure and their material properties are inputs for the code and with the help of the CLT (described in Table 9.1.5), which is also implemented in the code, the effective material properties of the sandwich panels are computed at each section along the length of the blade.

For the analysis the length of the secondary blade (12.22m) is divided into 34 cross-sections (stations). The blade root includes the first three stations (the length up to the fourth station - 1.12m), starting with a circle with a radius of 0.5m and followed by two transitions. Some data from the aerodynamic analysis is then used for the main input file - twist, chord length, aerodynamic forces and moment and airfoil at each station. The LS-0417 MOD airfoil is used for 70% of the blade length, starting from station 4 to station 25, and NASA SC-0410 airfoil for the rest of the length (from station 26 to station 34). The program enables the implementation of spar caps and shear webs in the cross section, for which different sandwich panels can be used. In order to avoid imbalance and cross-coupled stiffnesses, the structures of the top and bottom surface of the blade are symmetric with respect to the chord line.

The materials used for the different sandwich panels in the start design and their properties are presented in Table 9.1. The matrix of the laminate composites is Epoxy resin (EP-3). The glass fabrics used are E-LT-5500 for unidirectional and Saertex for biaxial. The properties of the triaxial composite (SNL Triax) are derived by averaging those of the unidirectional and biaxial [47].

For the structure of the blade root (up to the fourth station) no spar caps are assumed and the same sandwich panel is used everywhere along the cross sections. Its structure consists of a foam core and two symmetrically placed (with respect to it) plies of triaxial composite material. Considering the surface of the blade (between stations 4 and 31) from leading to trailing edge, three different sandwich panels can be distinguished - leading edge panel, spar cap panel and trailing edge panel. The core material for all panels is foam. The materials used for the symmetrically placed plies w.r.t the core of the leading and trailing edge panels are biaxial and/or triaxial composite materials depending on the station they are placed on. For the spar cap sandwich panel a combination of uni-directional and biaxial or tiraxial composite material is used. For the end three stations (32-34) instead of a sandwich panel, the structure consists of just a ply of triaxial composite material everywhere along the cross-section. Furthermore no shear webs are used for the start design.

Control points (the number of which is an input) are implemented in the code such that the thickness of each ply varies linearly between them along the length of the blade. Higher degree-of-freedom is desired (more control points) but for efficient computation the number of the control points is set to two.

All data used as input for the design of the secondary rotor blade is for the maximum loading case, therefore the rpm of the secondary rotor is set to 200 in the input file. A maximum tip deflection of 1.5m is also set.

The Euler Bernoulli and shear flow theory is then used to calculate the normal and shear stresses. Detailed explanation of the formulas and calculations can be found in the following reference [48]. For the buckling criteria calculation it is important to specify the assumptions made. The surfaces of the blade are idealized as curved

plates, which experience both compression and shear. For the boundary conditions it is assumed that the plates are simply - supported on four sides.

Table 9.1: Properties of the materials used for the sandwich panels of the start design of the secondary rotor blade

Material	V_F [%]	$\begin{bmatrix} E_{11} \\ [GPa] \end{bmatrix}$	$\begin{bmatrix} E_{22} \\ [GPa] \end{bmatrix}$	$\begin{bmatrix} G_{12} \\ [GPa] \end{bmatrix}$	v_{12} [-]	$\rho \ [kg/m^3]$	$\begin{bmatrix} s_{11T} \\ [MPa] \end{bmatrix}$	$\begin{bmatrix} s_{11C} \\ [MPa] \end{bmatrix}$	$\begin{bmatrix} s_{12} \\ [MPa] \end{bmatrix}$
Foam	-	0.26	0.26	0.02	0.3	200	-	-	-
E-LT-5500/EP-3	54	42	14	3	0.28	1920	972	-702	30
Saertex/EP-3	44	14	14	12	0.5	1780	144	-213	90
SNL Triax	-	28	14	7	0.4	1850	144	-213	60

CLT

Since for the design of the secondary blade a fully composite structure is considered, it is important to properly design for strength in all directions. Since a fiber reinforced composite shows good performance only in the direction of the fiber orientation, it is necessary to design a lamination that consists of plies oriented in different angles, in order to withstand loading applied in multiple directions. This implies that the composite laminate will have plies with different material properties, which cannot be treated as an isotropic material anymore and more complicated stress-strain relationships are expected. For that reason the Classical Lamination Theory (CLT) is used - to help the calculations of the effective material properties, so that an iterative design process for the structure of the secondary blade is possible in order to perform an optimization in terms of mass. The CLT is based on the following assumptions [49]:

- 10 x $t_l < a_l$ and 10 x $t_l < b_l$, where a_l and b_l are the width and length of the sandwich structure
- Small displacement in transverse direction $(w_l < < t_l)$

Plate theory assumptions (also valid for CLT):

- Normals remain straight (no bending)
- Normals remain unstretched (same length)
- Normals remain normal (right angle to the neutral plane)

Assumptions regarding bonding:

- The volume occupied by the bonding is negligible (t_l does not account for thickness of the bonding).
- Shear is not present within the bonding (the plies cannot slip relative to each other).
- The strength of the bonding is not considered (the different plies together act as an isotropic material with special effective properties).

The CLT is using the material properties of each ply that the lamination panel includes and the applied forces, to compute the effective material properties of the whole sandwich panel [50]. Such panels are then used to construct the secondary airfoil and the design of each vary with respect to the loading of the different parts of the airfoil at different locations along the blade length.

Mass optimization method

Within the Co-Blade program there is an optimization module that can utilize one of three different types of algorithms to find the most suited blade cross section parameters to minimize blade mass. The optimization is performed on design variables such as the width of the spar, the thicknesses of the material at the blade root and within the LEP, TEP, spar cap and shear webs. The program is therefore able to find the minimum mass required in order to satisfy the design loads for the given external blade shape as defined by the aerodynamic analysis of the secondary blade. The program uses the fitness function as defined by Equation 9.2 with \vec{x} being the vector of all the previously specified design parameters undergoing the optimization and described in subsection 9.1.5.

$$f(\vec{x}) = Blademass * \Pi_{n=1}^{7} max\{1, p_n\}^2$$

$$(9.2)$$

In Equation 9.2 the p_n parameter defines the penalty factors that set the constraints regarding certain design parameters. The penalty factor for maximum allowable normal stresses are given by p_1 to p_4 , for the shear stresses the penalty factor is p_5 , the blade tip deflection is set in p_6 and buckling criteria. The equations for the penalty factors are given in Table 9.2.

Table 9.2: Penalty factors used for computing the fitness function for the optimization process

$p_1 = \frac{\sigma_{11,max}}{\sigma_{11,fT}}$	$p_5 = \left(\frac{ \tau_{12,max} }{\tau_{12,y}}\right)$
$p_2 = \frac{\sigma_{11,min}}{\sigma_{11,fC}}$	$p_6 = \left(\frac{\sigma}{\sigma_{buckle}}\right)^{\alpha} + \left(\frac{\tau}{\tau_{buckle}}\right)^{\beta}$
$p_3 = \frac{\sigma_{22,max}}{\sigma_{22,yT}}$	$p_7 = \frac{tipdeflection}{tipdeflection_{max}}$
$p_4 = \frac{\sigma_{22,min}}{\sigma_{22,yC}}$	

The optimization aims to reduce the blade mass which is satisfied when all the penalty factors are less than 1. Analyzing the penalty factors, if the penalty factor is higher than 1 this means that the failure criteria are surpassed for example the stresses in the structure exceed the maximum stresses, or the maximum tip deflection is exceeded with these design parameters. However, the further the penalty factors are from 1, the more overdesigned the design parameters are leading to a higher blade mass.

The optimization method used is the stochastic particle swarm method. It is based on iteratively sampling each of the points from within the feasible domain based on the results of other points, finding in this way the global optimum for each iteration.

The particle swarm optimization method is less sensitive to the initial guess and satisfies all of the design criteria in the form of penalty factors [46].

Limitations of Co-Blade

Co-Blade is an efficient numerical model for developing a preliminary design, but it cannot replace the FEM analysis and have it has its own limitations. For example, cross-coupled terms of the stiffnesses, calculated with the help of CLT are not implemented in the beam equations and therefore this analysis tool can only work with symmetrically positioned and balanced laminates.

The numerical model is in a good agreement with results obtained from analytical analysis, but it is also limited in terms of validation studies. Future work is recommended on validation procedures regarding the buckling failure mode, anisotropic layups and the stress-strain relationships of the laminas.

Another feature of the analysis tool, which imposes some limitations is the control points input. Setting this to higher values allows for more degrees-of-freedom, but this also means that the computational time of the optimization is increased as well. During the iteration processes it was established that no more than two control points shall be used considering time issues. For the design this means that two regions of linear variation of the laminate thicknesses along the blade length will be present. This combined with the fact that the structure of the airfoil is symmetric with respect to the chord may result in an over-designed secondary rotor blade.

9.1.6 Results for the secondary rotor design

The particle swarm optimization module is run with the Co-Blade code to define the geometrical and material parameters of each of the cross sections along the length of the blade, optimized for minimum blade mass. The following graphs present the results of this optimization.

The resultant shear forces and bending moments applied along the length of the blade are shown in Figure 9.6. It is clear that the centrifugal force V_z , acting in the axial direction, is the most critical force due to the high rotational speed of the secondary rotor blades. The V_x is the resultant of the weight and the tangential force acting on the blade cross section. The resultant shear force V_y represents the normal forces acting on the blade cross section. The normal and tangential forces are due to the lift and drag distributions obtained from the aerodynamics results.

The bending moment M_z is evaluated at the shear center and is a combination of the aerodynamic moment and the forces p_{xa} and p_{xw} . It has the lowest magnitude and therefore is the least critical in the analysis. The

bending moment in y direction comes from the centrifugal force. It has the largest moment at the root since the centrifugal force is the largest at the blade and decreases towards the blade tip.

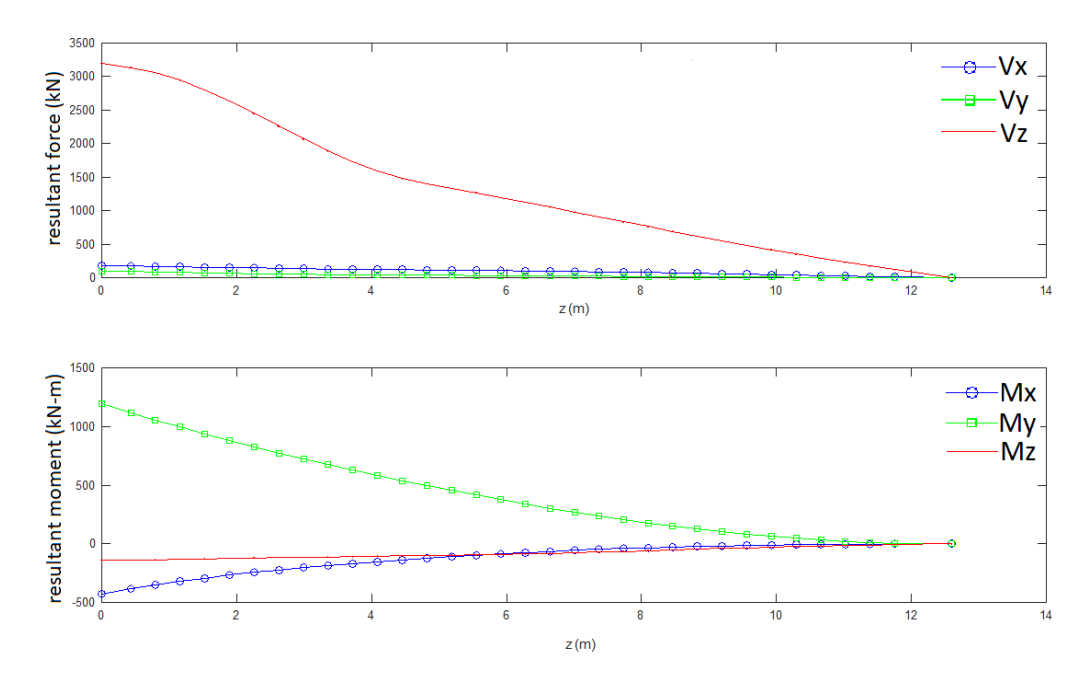


Figure 9.6: Resultant forces and moments on the secondary rotor blade structure

The graph in Figure 9.7 shows the panel thickness throughout the length of the airfoil. The graph shows the thickness being equal within each cross section but varying along the length of the blade. At the blade root, where the blade experiences the largest bending moment, the thickness is maximal at approximately 52mm. Towards the blade tip the thickness of the panel decreases to approximately 10mm.

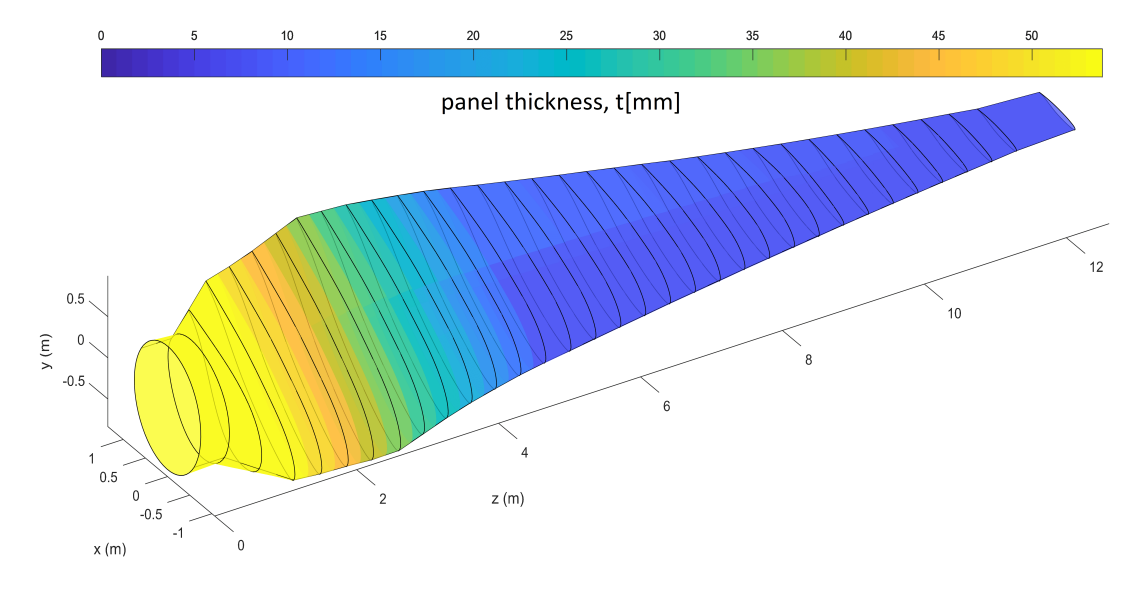


Figure 9.7: Thickness variation

Effective Properties

The effective mechanical properties computed using the CLT method are presented below. The Figure 9.8 shows the effective Young's modulus which is a measure of stiffness along the length of the blade. As is seen from the graph the effective Young's modulus is approximately 27GPa and at the trailing edge it decreases to 18GPa within the middle of the LS-0417 MOD airfoil.

The effective shear modulus is shown in Figure 9.9 with a value of 7GPa along the cross section of the blade decreasing to 4.8GPa along the trailing edge similar to the situation in Figure 9.8. This is because

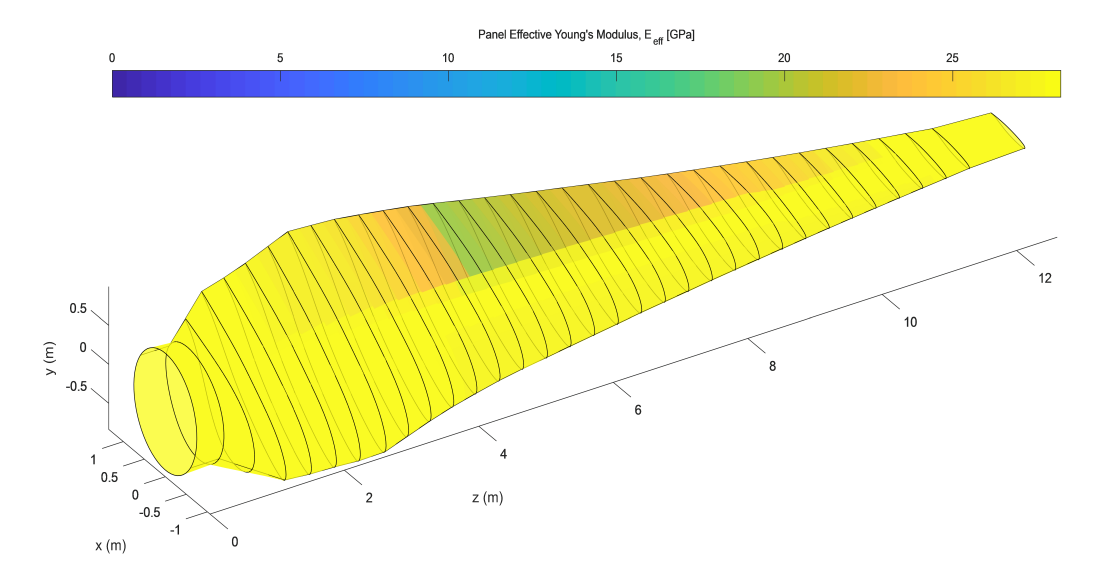


Figure 9.8: Effective Young's modulus

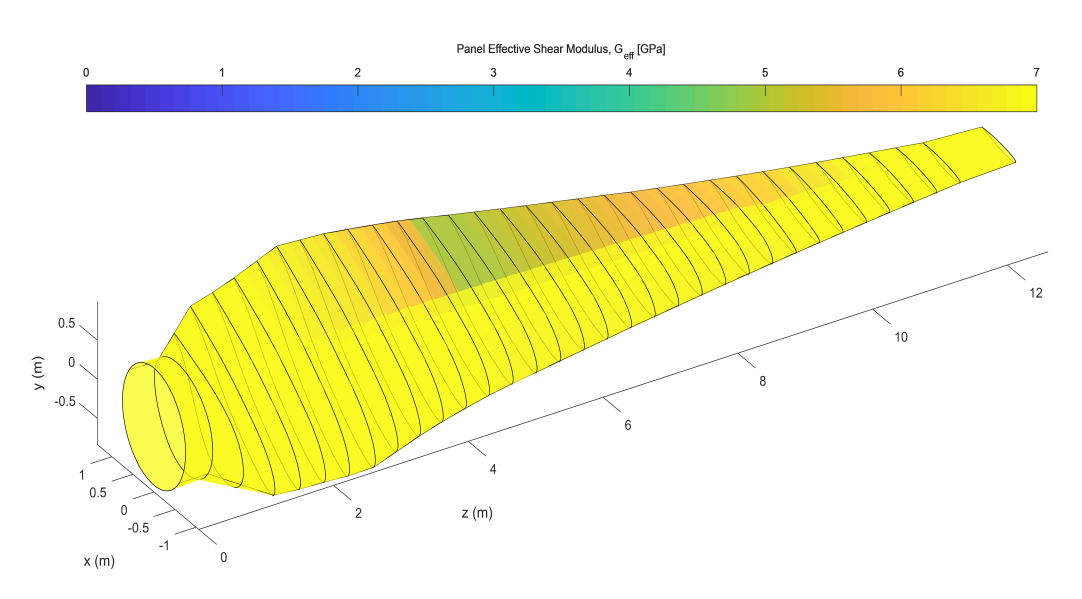


Figure 9.9: Effective shear modulus of the secondary rotor blade

Maximum stresses in the structure

The failure modes for which the structure of the secondary rotor blade is analysed are maximum stress (tension and compression) in both longitudinal and transverse direction, shear, buckling and a maximum tip deflection is also set. The most critical of them for the design appears to be the buckling failure mode. Regardless that the failure criteria for it is satisfied, the results shows that the trailing edge of the bottom surface of the blade between sections 14 and 32, experiences stress corresponding to values of the buckling penalty factor between 0.98 and 0.7. This is considered to be quite high and due to the lack of validation (specifically for buckling analysis) of the numerical model used for creating this design, future work is recommended to further explore and validate the safe performance of the blade.

For all failure modes except for buckling, it can be concluded that the blade design is on the safe side of the margin. The highest experienced stress is normal tension stress in longitudinal direction on the top surface of the blade, for which the penalty factor is shown in Figure 9.10. It is clear from the graph that the highest value is not more than 0.6 and the maximum normal stress experienced is around 82MPa in the leading edge area in the middle of the top surface.

The maximum shear stress is experienced in the bottom surface of the blade and is about 30MPa - shown in Figure 9.11. Again, a safe penalty factor of maximum of 0.5 is observed.

The deflection of the blade along its centroidal axes $(u_0, v_0 \text{ and } w_O, \text{ the centroidal reference frame is rotating})$

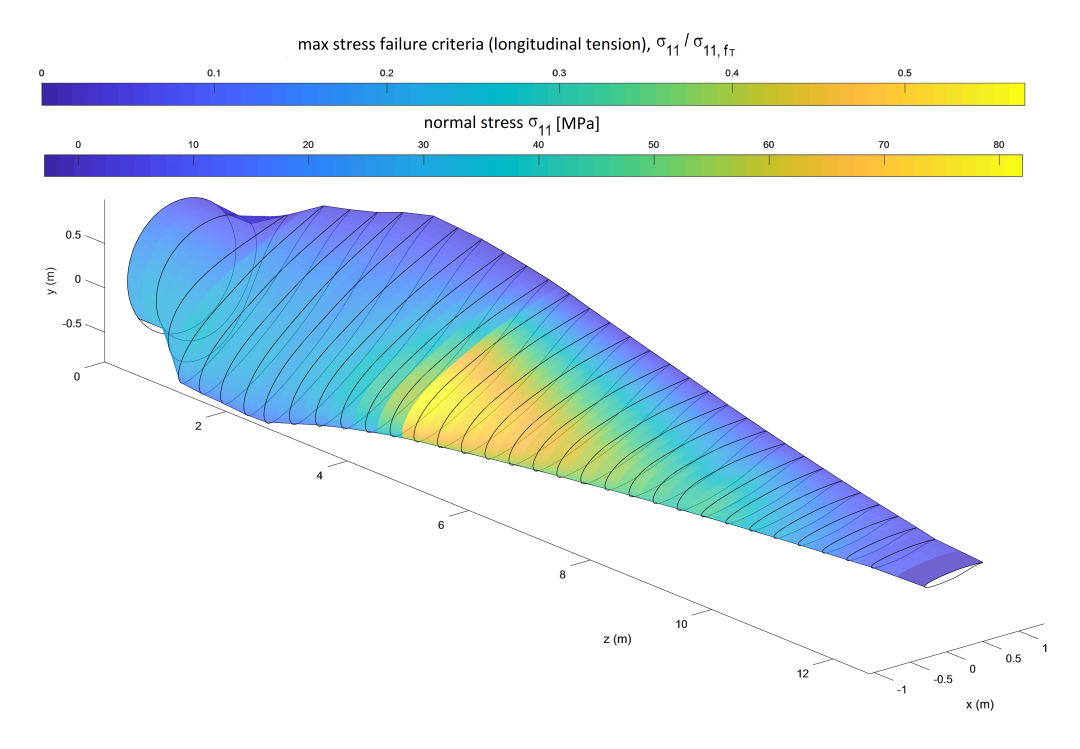


Figure 9.10: Maximum normal stress experienced by the secondary rotor structure and the corresponding penalty factor

with the length of the blade due to the twist) is represented in Figure 9.12. The maximum deflection found at the tip of the blade along the centroidal axes is then projected on the axis parallel to the secondary rotor shaft and calculated to be 0.0124m in the direction of the primary rotor blade. The torsional deflection of the rigid blade is also shown in Figure 9.12.

Other design considerations

Different performance degrading factors were described in subsection 9.1.1. The secondary rotor blade design incorporates solutions for keeping the efficiency of the system at its highest.

Leading edge erosion is considered one of the most critical factors for the secondary rotor blade design. This type of erosion occurs at the leading edge, due to the impact of particles in the air such as rain or salt spray. This type of erosion typically limits the wind turbine blade tip speed to 100m/s however the secondary rotor blades experience much higher velocities, making the choice of a suitable coating critical. The current market proposes different coatings such as metal, polymer and ceramic coatings.

For helicopter blades, the leading edge is protected by aluminum sheets that have to be regularly replaced. This option does not sound very efficient for the SR application since replacing metal sheets on each blade of both rotors can be very time consuming. However, a combination of both metal and polymer paint is found to be a better option. The metal coating (applied by hot dip galvanising or thermal spraying) is first placed on the blade with a polymer coating over it. This duplex system is considered to be maintenance free for the design lifetime of the wind turbine [51]. This is an important aspect in the choice of coating since the blades need to perform efficiently and the cost of blade maintenance for offshore turbines is significant especially for two rotors of five blades.

Another option is to use polymer coatings such as epoxy, polyurethane or acrylic. The polymer coatings are typically applied in layers and have high performance properties such as resistance to corrosion, high durability, high toughness and ensure a smooth finish of the blade. These coatings can either be applied in the form of tapes (during repair) or they can be implemented in the factory (in-mould).

There are two types of methods for applying coatings. In-mould coatings influence the performance of the whole blade and they use resins such as epoxy or polyurethane. The coating process becomes part of the blade manufacturing process therefore costs are cut with respect to the time required for manufacturing. Post-mould coatings 1

¹https://www.coating.co.uk/wind-turbine-coatings/

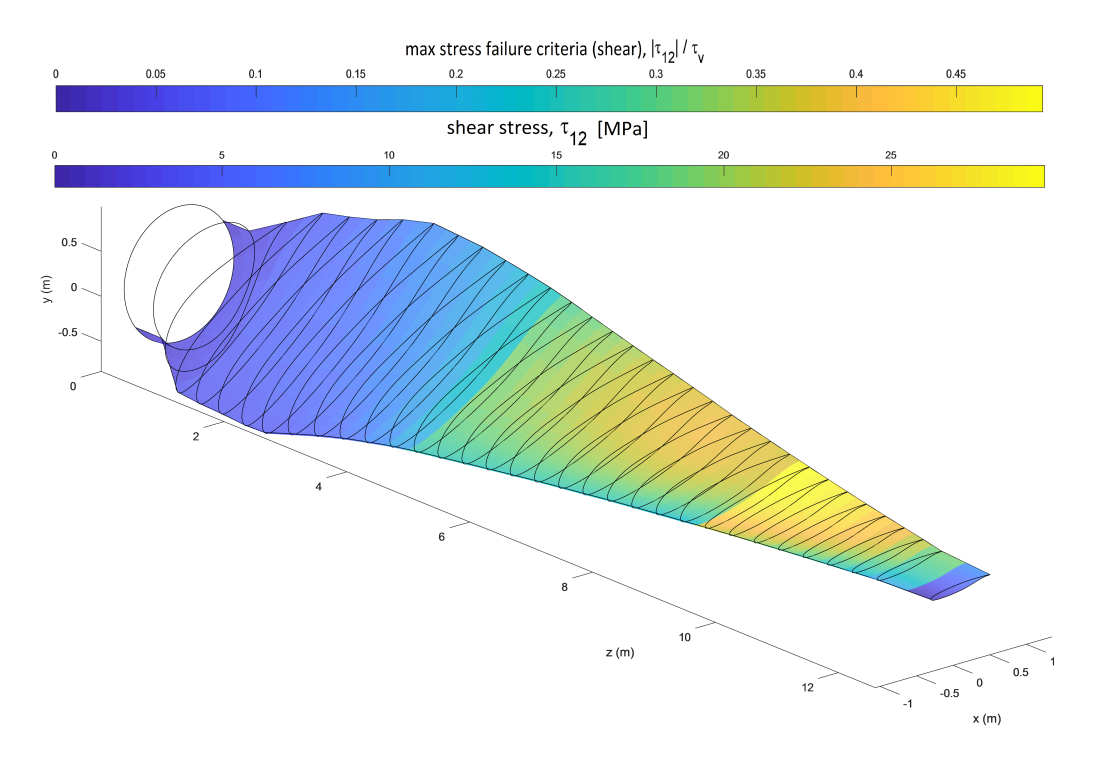


Figure 9.11: Maximum shear stress experienced by the secondary rotor structure and the corresponding penalty factor

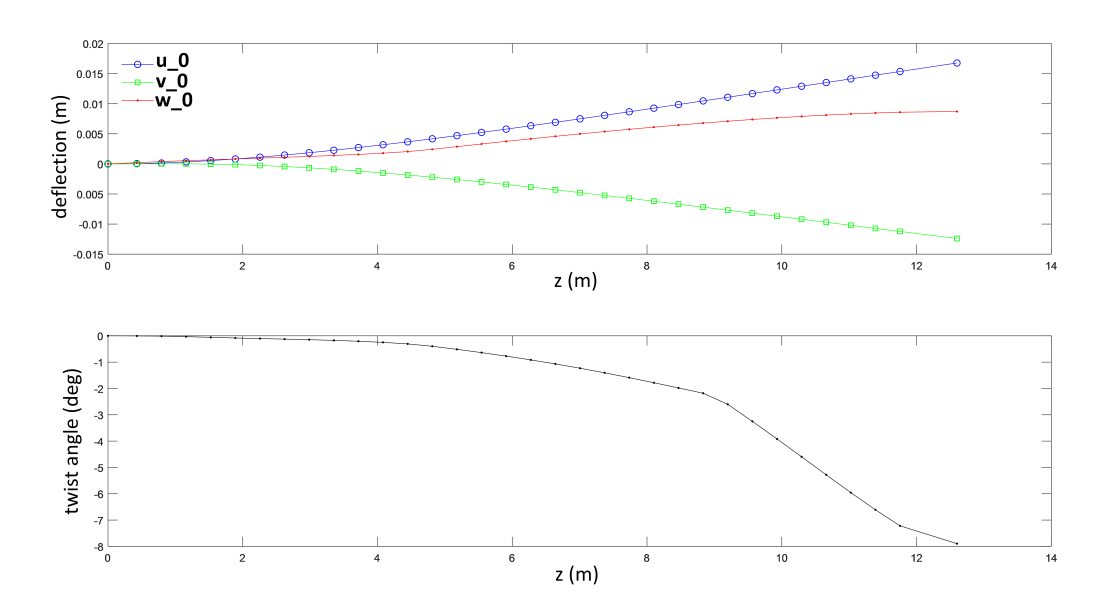


Figure 9.12: Displacements of the secondary rotor blade along its centroidal axes

Lightning strikes are another important factor to consider. Protection against lightning strikes can be given in the form of a copper mesh (due to coppers' good electrical conductivity) laminated close to the outer surface. [52]

9.2 Structural design of the primary blade

The primary blade consist of 4 blades rotating in the vertical axis. Two blades are attached at the each end of the horizontal strut. Two different blade structure design were made for the analysis.

9.2.1 Choice of chord length

Before any analysis of the loading of the wind turbine blade can begin, several design parameters have to be set. In the control section, several values were chosen for the main wind turbine, such as RPM ranges and C_p values among others. Considering all of these, the chord of the primary blade remains a free value that can be set to any combination of values that is able to output 10MW at the given TSR and rated velocity.

To keep the blades as light as possible, the chord would ideally be larger to achieve a higher moment of inertia for the same weight, as the moment arms increase while thickness decreases. The increase of chord is limited by the possibility of buckling, which much more prominently as the walls of the structure get thinner. Increasing the chord, however, also has implications on the TSR and C_p , as a larger chord means a reduction in the TSR and thus a lower achievable C_p .

As the main purpose of the design of the primary rotor is to get a mass estimation, the chord value was chosen experimentally using QBlade. A representation of the primary rotor lower blade was created with several differing chords and a simulation was ran. Starting with the scaled up values from an initial x-rotor design of a 28m to 14m tapered chord, the design was iterated to eventually end up with a root chord of 20m and a tip chord 10m.

9.2.2 Loading analysis

It is essential to identify all possible loads which act on the structure before the design process can start. The free body diagrams were created to help visualize all possible loads.

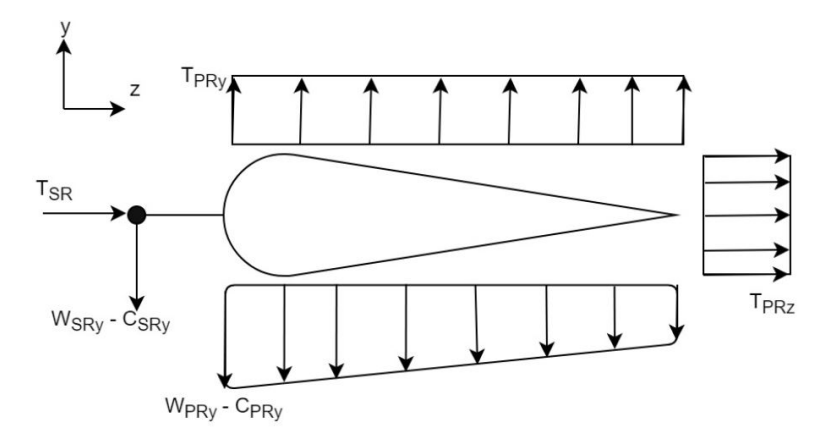


Figure 9.13: Primary blade free body diagram Y-Z coordinate

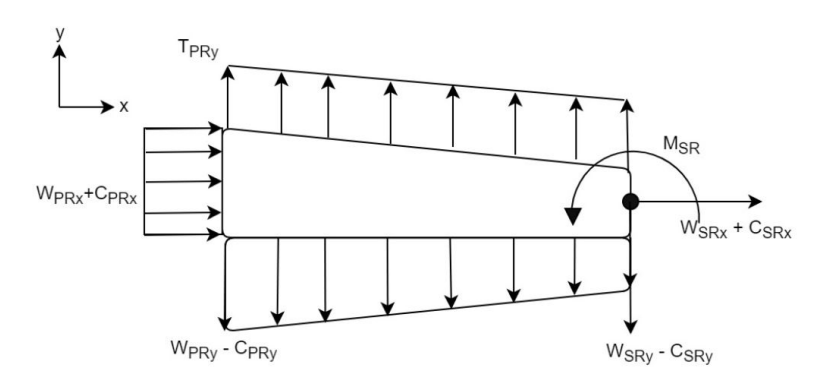


Figure 9.14: Primary blade free body diagram X-Y coordinate

To design a structure, the cross section on the Y-Z plane as shown in Figure 9.13 must be able to resist the internal loading resulting from the external loads acting on the primary blade. The thrust acting on the airfoil will follow a C_p curve and will distributed along the blade. For the purposes of simplification, however, this force will be assumed to be acting on the aerodynamic center. As the density of the blade is uniform, the weight force is also simplified to a point force acting on the center of gravity, which is the centroid of the area. These assumptions potentially overlook the possibilities for stress concentrations present in the structure, but as the primary blade is not the focus of this design project, it will be presumed to be negligible. These forces are still

taken to be distributed along the span of the blade in the x-axis. As the generator and secondary rotor are slightly offset from the main blade, the shear forces and moments due to the their masses and the drag of the secondary rotor are applied at the tip.

The program for the loading and structural analysis will be written in MATLAB and will take a text file as an input and will produce a text file as an output. This output text file will contain the x-locations with the corresponding internal forces and moments, as well as the chord, blade length, and section length.

The design of the blade must be able to withstand all forces present during nominal operation. It was observed in the preliminary calculations that the operating mode will result in higher loading on the blade than the standstill mode, and as such the chosen loading case is taken to be when the angular velocity of the wind turbine is at its highest at the wind speed of $25 \ ms^{-1}$. As the wind turbine spins one blade will be downwind and the other, upwind. This results in higher loading for one of the blades, and the blades will alternate between upwind and downwind every half rotation. As such the design loading case will be for the highest angular velocity resulting in highest centrifugal forces as well as the position along its rotation when the blade sees the highest velocity, and as such creates the highest lift.

9.2.3 Metal wing box

The loading case of the lower primary blade of the wind turbine appears to be similar to one of an airplane wing. While wind turbine blades are usually made out of a glass fiber composite, it was considered worthwhile to investigate the required dimensions for wingbox made out of metal. This is due to the presence of higher shear forces, with the main contributions being the centrifugal acceleration created by the rotation of the main rotor as well as the thrust of the secondary rotor. For the structure to remain lightweight, the metal used should have a high specific strength, and at first aluminium alloys are considered.

As the rest of the blade would nonetheless be made out of glass fiber composite, which has a lower E-modulus than most metals, it can be assumed the designed wingbox would be taking all of the loads. The main loading occurring in the wingbox will be normal stress due to bending moment and shear stresses, which is what the wingbox will primarily be designed for. The wingbox will contain the basic elements of a skin at the top and the bottom, connected by two spars at each end. In a metal wing box, the compressive and shear stresses can cause buckling, therefore stiffeners and stringers will be added to prevent this.

Failure criteria - von Mises stress

The von Mises stress is a combination of the bending and shear stresses derived from the following equation:

$$\sigma_{\text{von mises}} = \sqrt{\frac{(\sigma_{xx} - \sigma_{yy})^2 + (\sigma_{yy} - \sigma_{zz})^2 + (\sigma_{zz} - \sigma_{xx})^2 + 6(\tau_{xy}^2 + \tau_{yz}^2 + \tau_{zx}^2)}{2}}$$
(9.3)

The von Mises stresses are calculated for each section, and when the section length is chosen to be sufficiently small, the axial stresses created by thrust and weight forces will be several magnitudes smaller when compared to the internal shear forces resulting from the sections before it. Considering also that there is no shear along the x-axis, Equation 9.3 can be simplified to:

$$\sigma_{\text{von mises}} = \sqrt{\frac{(\sigma_{xx})^2 + (-\sigma_{xx})^2 + 6(\tau_{yz}^2)}{2}}$$
 (9.4)

While designing for the yield stress of a metal would be an ideal case, the cyclical loading of the wind turbine means that the effects of fatigue have to be investigated. Most metals do not perform well in terms of fatigue, and aluminium is particularly weak in this criteria. An investigation was then done into the fatigue endurance life of metals, and based on Figure 9.15, 4340 Steel was chosen as it had the highest fatigue endurance limit to weight ratio, able to handle stresses up to 480 MPa for any number of times. It is important to note, though, that the von Mises stress is not an entirely accurate representation of stress for fatigue life calculations. For the purpose of these calculations this effect is considered to be negligible.

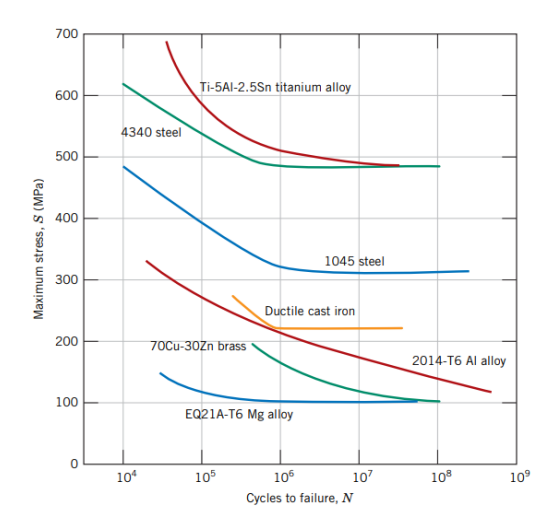


Figure 9.15: Maximum stress (S) versus the logarithm of the number of cycles to fatigue failure (N) for seven metal alloys [53].

Failure criteria - shear and compression buckling

There are two types of buckling failure mode which are present in the wingbox structure made out of the metal. First buckling failure mode is the compression buckling in which allowable skin stress can be calculated using Equation 9.5 [54].

$$\sigma_{cr} = K_c E \left(\frac{t}{b_s}\right)^2 \tag{9.5}$$

The appropriate value of K_c can be obtained from Figure 9.16a, where a indicates the distance between two ribs and b represents the stringer pitch.

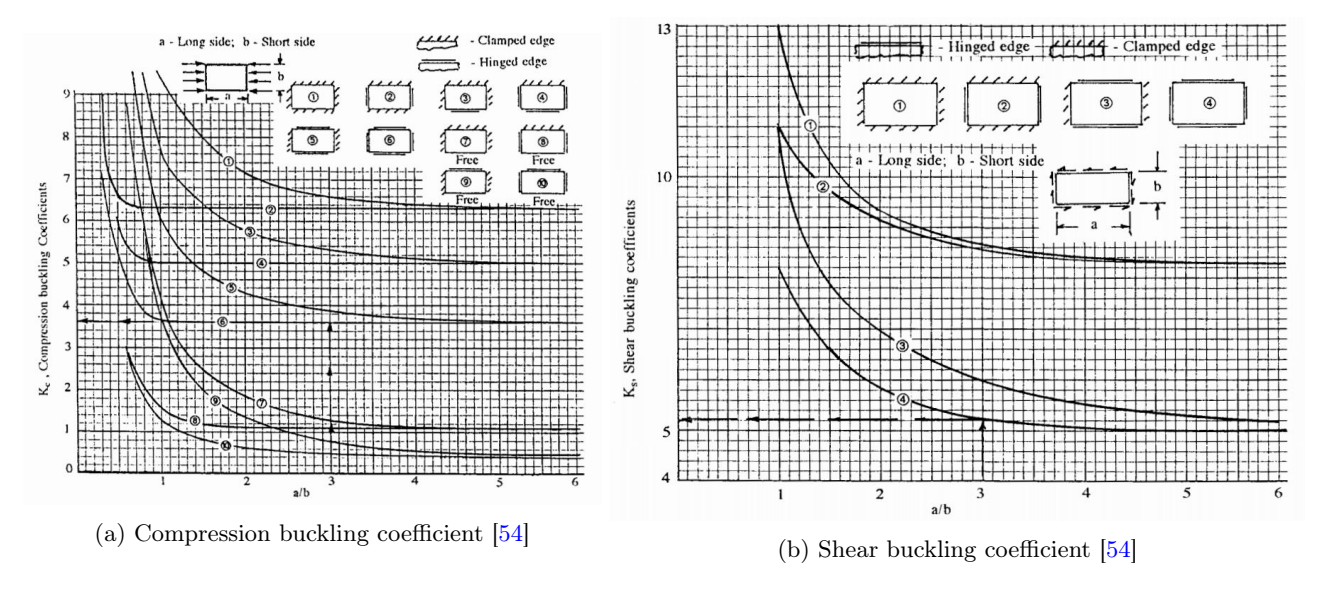


Figure 9.16: Different buckling coefficient

The other buckling failure mode is the shear buckling in which allowable skin stress can be calculated using Equation 9.6 [54]. The appropriate value of K_s can be obtained from Figure 9.16b.

$$\tau_{cr} = K_s E \left(\frac{t}{b}\right)^2 \tag{9.6}$$

9.2.4 Composite wing box

As mentioned in subsection 9.1.1, composite materials are often the material of choice for the wind turbine blades [55]. The wing box made out of composites is constructed very similarly to a metal wingbox, with the exception of the stiffening elements. The structure is defined in Figure 9.2, and it can be noted that the wingbox is nonetheless the main load-carrying structure of the blade. Thus, to ensure that the blade is able to withstand the loads, it only needs to be ensured that the wingbox alone could as well.

For these blades, the most commonly used composite material is GFRP, and while glass fiber is normally a unidirectional material, the composite will have to be laid up to be able to resist loading on a plane. This is due to the presence of high shear forces from the thrust of the primary blade and the secondary rotor. As composite does not describe a single material, it is important to define them as a function of orientation and fiber content. In Materials Science and Engineering by W.D. Callister, it is stated that when fibers are orientated in a plane, the reinforcement factor can be taken as $\frac{3}{8}$, meaning it has a fraction of its longitudinal strength when laid up in such a way [53]. Furthermore, Callister states that for a composite involving glass fibers, the common volume fractions are between 0.1 and 0.6. As high strength and stiffness is desirable in this design, the highest volume fraction of 0.6 is chosen.

The primary blade is designed for failure in the same way that the secondary rotor is, taking into account the axial strength, shear strength, and buckling criteria, which are described in the previous section. The method of calculation does not differ too much between the composite and metal wingbox, as most of the stresses are obtained using moment of inertia calculations and shear flow over the section.

9.2.5 Comparison of designs

	Composite	Steel
Stringer area (mm ²)	N/A	200
Mass (tons)	N/A	2.71
Spar thickness (mm)	16	10
Mass (tons)	13.13	34.42
Skin thickness (mm)	26	10
Mass (tons)	37.77	95.32
Total Mass	50.90	135.35

Comparison	

	Composite	Steel
Thickness as		
% of chord	25%/12%	25%/25%
[root/tip]		
Location of spars		
as % of chord	20%/50%	25%/75%
[front/rear]	,	,
Design Axial	259	480
Strength (MPa)	259	460
E-Modulus (GPa)	44.5	207
Density (kg/m^{-3})	2004	7850
Cost (\$/kg)	3.66	2.55

Table 9.4: Comparison of wingbox design and material properties

The purpose of the design is to create a wingbox that can withstand the loads acting on the blade and make the wingbox as light and cheap as possible. Table 9.3 provides a rundown of the minimum masses of the wingbox components that is required to support the loads. For the steel wingbox, the thickness of the elements is lower than the composite wingbox, yet due to the higher density the entire wingbox turns out to be over 2.5 times heavier than its composite counterpart. The main reason for this disparity, is that composite materials are capable of sustaining cyclic loads much better than metals. While the steel chosen has a yielding stress of over 1400MPa, the fatigue endurance stress has to be chosen to ensure that the blade will not fail prematurely. This reduces the strength to weight ratio, and thus the performance, of the steel greatly. While the steel wingbox is mainly designed for compressive yielding at the root, buckling criteria dictate the minimum thickness past the midway point. This means that to ensure sufficient performance of the wingbox, stringers have to be added or the skin has to be made thicker. This effect does not manifest itself as prominently in the composite design and as such the cross-section can be reduced, reducing the overall weight of the blade.

One thing to note however, is that while a steel wingbox has a much higher E-modulus than the rest of the blade, the composite wingbox does not. GFRP will be used to construct the skin in front and behind the wingbox, this means that the skin in the case of the composite wingbox will take some loads. This would mean that the composite wingbox is overdesigned, and the design could potentially be scaled down and weight further reduced.

Overall, the total mass of the blade using a composite wingbox compared to steel is lighter. While being more

expensive per unit mass, the total cost of the blade will nonetheless be lower. The lower weight also means that the supporting structure for the blade can be lighter, further reducing the cost of the wind turbine. As such the composite design is chosen for the primary lower blade.

As the comparison between the two materials was done on the lower blade, it can be reasonably assumed that this will also hold true for the upper blade. Using the same program for the design of the upper blade composite wingbox, the results obtained are documented in Table 9.5.

Table 9.5: Design parameters of wingbox of upper blade

Spar thickness [root/tip] (mm)	Mass (tons)	Skin thickness [root/tip] (mm)	Mass (tons)	Total Mass (tons)	Thickness as % of chord [root/tip]	Spar locations as % of chord [front/rear]
16/12	17.73	28/13	50.73	68.46	25%/8%	20%/50%

9.3 Connection points

There are several connection locations that are crucial to the design of the SRVAWT. The design is made up of many extra components compared to conventional wind turbine designs therefore attachment points play a large role in the SRVAWT design.

The connection points in wind turbine blades have the following characteristics. [56]

- Ability to withstand very high fatigue loading
- Their failure could cause blade damage
- Designed for minimal maintenance
- Provide locations for crack initiation, propagation and moisture ingress
- Add mass to blades when using steel inserts for example

The critical connection points in the SRVAWT design are between the following components.

- nacelle and primary blade
- secondary rotor blades and rotor hub

The secondary rotor blade and hub attachment is very important because of high bending moments at the root of the blade as well as the large number of connections that will be needed for the SRVAWT. The 10 connections need to be designed for maximum strength and reliability. The T-bolt and the root inserts are discussed below.

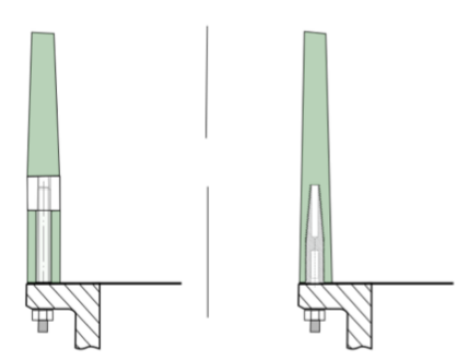


Figure 9.17: The T-bolt (left) and the insert connection concepts for the secondary rotor blade attachment to the rotor hub

The most common blade to hub attachment is the T-bolt, it is primarily used because of relatively simple installation. However, the blade root thickness needs to be slightly larger to account for the local damage in the laminate structure due to the stress concentrations around the nut.

For the secondary rotor connection however the insert connection will be used at the blade root. This is because with this method of attachment 35% more bolts can be implemented thereby increasing the strength of the connection. Moreover, compared to the T-bolt, no damage due to drilling is present in the connection. [56]

Both attachments will have to be subjected to extensive testing to directly compare the two concepts with the applied loads experienced on the blade root.

The nacelle and primary blade connection is a new element of the SRVAWT design compared to conventional HAWT. The primary blade attachment has to be designed for maximum strength, good resistance to high fatigue loads and maximum reliability. The primary rotor blade tip has to also withstand high tip loads due to the weight of the secondary rotor and the nacelle assembly including the generator.

To come up with a concept for the connection points, the engineering design of the attachment of the fuselage and wing spars of the aircraft can be looked at in more detail. This is an engineering example where a cylindrical shape is attached to a long wing. The fuselage can represent the cylindrical nacelle and the wing - the primary blade. The attachment of a wing to the fuselage is done by the use of lugs, tension bolts and spliced plates. It is difficult to however attach a connection from the nacelle because the structure is manufactured with GFRP and the use of cutouts in the structure is to be avoided because they introduce stress concentrations making the attachment more prone to failure.

Both the structure of the nacelle and the primary blade are manufactured using GFRP therefore the attachments listed above need to be modified. The Figure 9.18b shows the attachment of a tube to a lug. The tube represents the nacelle which will house the generator assembly and the attachment will join it to the tip of the primary blade. The attachment is made of CFRP because this material has better material properties than the GFRP (higher stiffness to weight ratio, lower density). The attachment can be manufactured using filament winding or resin transfer moulding (RTM). [57] In order to reduce the stress concentrations on the attachment, more lugs can be manufactured along the length of the tube. In this configuration the generator assembly will be accessed from the front and back of the nacelle.

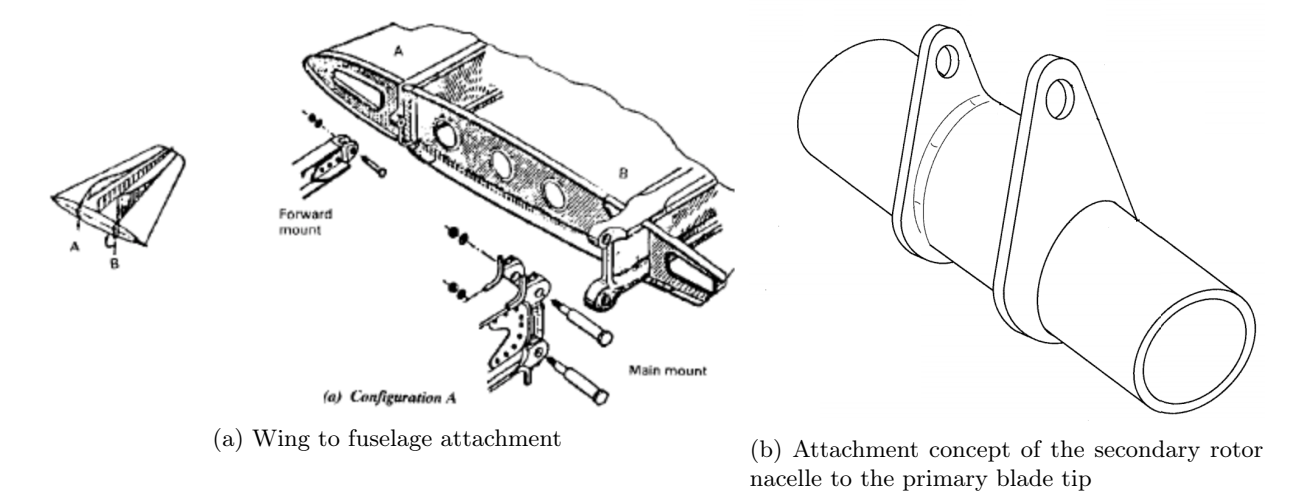


Figure 9.18: Attachment concepts

9.4 Structural analysis of the tower

The tower of the wind turbine is commonly made out of steel [58], hence steel tubular tower will be used. The free body diagram of the tower was made to visualize the loads acting on the tower Figure 9.19. The loading which acts on the tower are shear stress and bending moment which are transferred from the strut, weight of the tower itself and the drag. Shear acts at the top of the tower as a point load. Weight and drag acts as distributed load on the tower.

9.4.1 Vibrations and natural frequency

A wind turbine is cyclical in nature, resulting in a risk of superimposition of the loads resulting in larger stresses than expected. This happens when the natural frequency of the tower, or its multiple, is the same frequency as the loading of the wind turbine. To calculate the natural frequency of the tower, a cylindrical beam with a tip mass is assumed, giving a reasonable approximation to the real value. This is calculated using Equation 9.7:

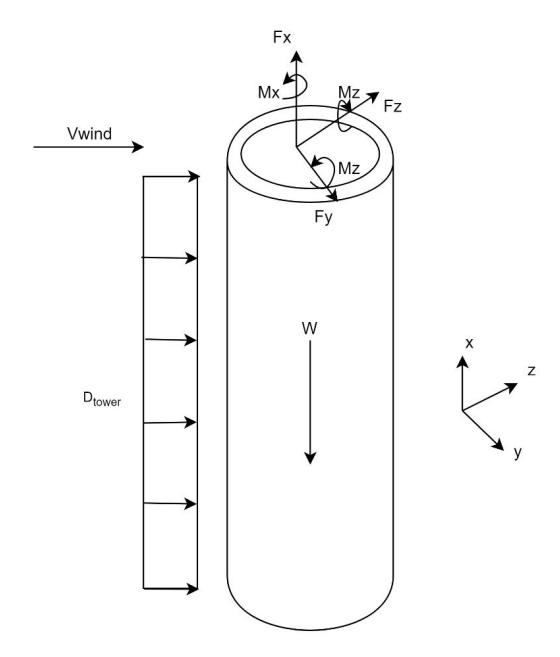


Figure 9.19: Tower free body diagram

$$f = \frac{1}{2\pi} \sqrt{\frac{3EI}{\left(m + \frac{m_{tower}}{4}\right)H^3}} \tag{9.7}$$

The wind turbine has an RPM range between 1 and 6 during operation, resulting in a maximum frequency of 0.1Hz. To design a structure that meets the requirements a higher natural frequency should be achieved. This can be achieved by choosing materials with a high stiffness and by increasing the moment of inertia while lowering the mass of the tower. The initial sizing of the tower resulted in a tower natural frequency of 0.442Hz, thereby meeting the requirement.

9.4.2 Failure criteria - von Mises

The concept of von Mises stresses is already explained in subsection 9.2.3, and it is applicable to this structure as well. The tower is mainly loaded in compressive stress due to bending, while the shear has a considerably lower contribution. This essentially means that to resist the von Mises stress, the structure should just have a high moment of inertia. This guides the design towards a wider and thinner structure.

9.4.3 Failure criteria - Cylindrical buckling

The tower is in the shape of the cylinder, hence buckling of cylindrical shell is looked at. For hollow cylinders, there are several different equations that govern when the structure will buckle and fail. For this analysis, three formulas were considered such as general buckling, buckling for long cylinders, and buckling for short cylinders. In the case of this design, the critical load of the compression buckling is governed by the long cylinder buckling equation, and can be calculated using Equation 9.8 [59], where Z is the Batdorf parameter commonly used in buckling analysis.

$$\sigma_{cl} = \frac{\pi^2 E}{12(1 - v^2)} \left(\frac{t}{l}\right)^2 \cdot \frac{4\sqrt{3}}{\pi^2} Z = 0.605 \frac{Et}{r} Z \qquad \qquad = \frac{l^2}{rt} \sqrt{(1 - \nu)^2}$$
(9.8)

9.5 Structural analysis of the horizontal strut

The horizontal strut which supports the primary blades onto the tower will be made out of the steel wing box. Composite structure which was used for the blade will not be used due to its low resistance against normal loads. The strut will experience high normal load which originates from the primary blade. The free body

diagram was made to visualize the types of loading on the strut. The coordinate system is defined in such a way that the X-axis is along the span, the Y-axis is perpendicular to the ground and the Z-axis is in the same direction as the rotation. The different types of loading which are experienced by the strut includes Shear loads $(F_x, F_y \text{ and } F_z)$ and bending moment $(M_x, M_y \text{ and } M_z)$ which originates from the primary blades (upper and lower). The drag (D) and the weight (W) of strut itself are also considered in the loading analysis. Only half of the strut is shown in the free body diagram Figure 9.20a and Figure 9.20b for the simplicity.

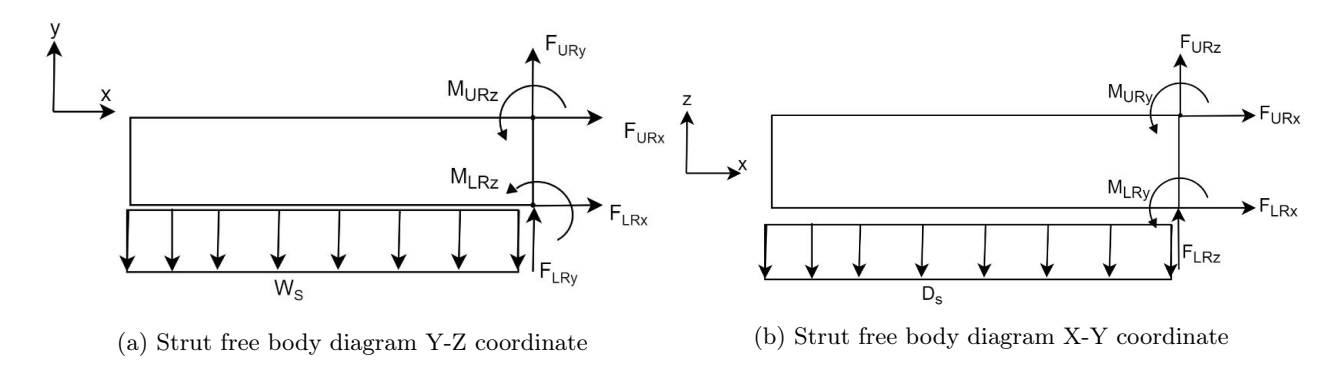


Figure 9.20: Free body diagram strut

Failure criteria

Since the metal wing box structure is implemented, the same failure criteria as described in the metal wingbox for the primary rotor subsection 9.2.3 and Figure 9.2.3 applies. Analysis on those failure modes are done to make sure the structure will not fail during the operation and the standstill.

9.6 Mass breakdown

One of the driver requirements of the design of the SRVAWT is the mass reduction compared to conventional HAWT. Due to the aerodynamic analysis, control strategy, generator sizing and structural calculations performed on the wind turbine components, the final mass of the structure is evaluated. The mass breakdown of the SRVAWT components is presented in Table 9.6. The values for the mass are for one single component and the number of components is given in brackets.

Components	Mass Value
Secondary rotors [t]	2.048 (x10)
Upper blade PR [t]	92 (x2)
Lower blade PR [t]	65 (x2)
Tower and strut [t]	484
Generator [t]	19.25 (x2)
Hub [t]	7.634 (x2)
Nacelle cover [t]	16.27 (x2)
Total Pitch System [t]	0.472 (x10)
Shaft [t]	1.753 (x2)
Bearing [t]	0.462 (x2)
Total [t]	913.9

Table 9.6: Mass breakdown of the SRVAWT

The components such as rotor hub, control systems (pitch systems, sensors, main computer), brake, nacelle structure, foundation, bearings were not analysed as part of structural analysis therefore mass estimations were used from literature [60].

The rotor hub mass is calculated in Equation 9.9 and gives the value for conventional three bladed blades however the estimation can be used for the secondary rotor as a first value.

$$Hub Mass[kg] = 0.954 * Single Blade Mass[kg] + 5680.3$$

$$(9.9)$$

The mass of the nacelle is calculated in Equation 9.10 and the mass of the pitch systems is found using Equation 9.12. The mass of the shaft and the bearing mass were estimated by scaling the component mass from the 3MW example turbine used in [60] with respect to the rotor diameter.

Nacelle Cover Mass
$$[kg] = \frac{\text{Nacelle cost}[\$]}{10}$$
 (9.10)

Total Pitch Bearing
$$Mass[kg] = 0.1295 * Total Blade Mass[kg] + 491.31$$
 (9.11)

Total Pitch System
$$Mass[kg] = Total Pitch Bearing Mass[kg] * 1.328) + 555$$
 (9.12)

A summation is made of all the component masses to find a final value of 913.9t for the SRVAWT. The mass of the system is expected to vary as the design process further matures.

9.7 Sensitivity analysis

Since the focus of this project is the design of the secondary rotor, the sensitivity analysis on a structural subsystem level is carried out in order to investigate the effect of certain design parameters on the design for the secondary rotor. Therefore analysis regarding the primary rotor structure is not executed. The main requirement regarding the structure of the wind turbine is to reduce the weight in comparison to conventional HAWT, therefore the mass of the secondary rotor blade is examined in the cases of different design parameter and offsets, while keeping all the failure criteria satisfied. The materials used for the structure, together with the rpm of the secondary rotor are design parameters, the change of which may significantly influence the resulting design.

An alternative combination of materials for the sandwich panels is presented in figure Table 9.8[48]. These materials have lower densities and competitive strength properties, but also higher prices. Carbon fibre shows superior properties and since its price is high it is proposed for an unidirectional laminate that will only be used in the spar caps. For the rest of the sandwich panels another set of biaxial and triaxial glass fabrics is suggested and for the core the same foam is assumed. With this new combination of materials the aim is to reduce the weight without significantly increasing the cost. The mass reduction is represented in Table 9.7.

In order to perform a maximum reduction of weight, a fully carbon epoxy solution is also presented. The secondary rotors are designed for maximum 200 rpm, but in order to investigate the effect of inaccurate calculation of the maximum rpm, the sensitivity analysis shows how a 25 % increase of the rotational speed affects the mass of the rotor such that the forces can still be handled. Moreover a reduction of weight is also expected in the case of higher estimated rpm.

Design Par	Mass	
3.5	Material set	-8%
Materials	from Table 9.8	- , ,
	Full Carbon	-26%
	Epoxy Solution	
RPM	$25\% \ (+50 \mathrm{rpm})$	2.8%
	-25% (-50rpm)	-2.2%

Table 9.7: Sensitivity analysis of the secondary rotor structure

9.8 Verification and validation

The verification procedure of the secondary rotor blade structural analysis consists of firstly checking the numerical model that was used. The Co-Blade package source codes were checked to verify the equations used in the analysis. This procedure was actually carried out when this model was first downloaded. This is because the model had to be examined to make sure it is applicable to the analysis

Moreover the magnitude of the mass and the cross sectional parameters of the secondary blade are verified by making a comparison. The design of the secondary rotor blade is unprecedented since the rotational velocity

Table 9.8: Properties of materials used for an optimized design of the secondary rotor blade

Material	V_F [%]	$\begin{bmatrix} E_{11} \\ [GPa] \end{bmatrix}$	$\begin{bmatrix} E_{22} \\ [GPa] \end{bmatrix}$	$\begin{bmatrix} G_{12} \\ [GPa] \end{bmatrix}$	v_{12} [-]	$rho \ [kg/m^3]$	$s_{11T} \ [MPa]$	$s_{11C} \ [MPa]$	$\begin{bmatrix} s_{12} \\ [MPa] \end{bmatrix}$
Foam	-	0.26	0.26	0.02	0.3	200	-	-	-
NCT307-D1-E300 E-Glass (triax)	47	35.5	8.33	4.12	0.33	1780	1005	-788	112
NB307-D1-7781-497A E-Glass (biax)	39	19.2	19.2	3.95	0.13	1670	337	-497	115
NCT307-D1-34-600 Carbon (uni)	53	123	8.2	4.71	0.31	1470	1979	-1000	103

experienced by the blade is so high. The results obtained for the SRVAWT design are compared to both wind turbine [61] and helicopter propeller blades [62].

Table 9.9: Overview of data used for the verification of the SRVAWT blade mass

Model	NREL 5MW WT	LEANWIND 8MW WT	SA 349/2 Helicopter	SRVAWT
Blade radius [m]	63	82	5.25	12.22
RPM range/Design RPM	6.9-12.1	6.3-10.5	387	25-200
Blade Mass [kg]	17740	35000	39.64	2048

The helicopter blades have constant chord of 0.35m and a thickness of the airfoil of 0.0315m making the airfoil extremely slender. This can explain the extremely low weight of the structure for such high loads induced by the centrifugal force. Scaling the wind turbine blade designs for the same blade length dimensions as the SRVAWT design, the blade mass becomes 3.44t for the NREL 5MW turbine and 5.22t for the LEANWIND 8MW turbine. The SRVAWT design at the preliminary design refinement stage has a blade mass that is between both the conventional wind turbine sizing and the helicopter blade sizing. It was previously noted that the SR blade is slightly overdesigned and a further decrease in the mass is expected at further design stages.

To validate the results from the Co-Blade numerical model, a model of the secondary blade is also created in QBlade using the same data from the aerodynamic analysis, with the purpose of generating results that can be compared with the output of the code model. Using the same loading conditions applied to the structure, the values for maximum resultant stresses and deflection are then compared for both models. Unfortunately this procedure cannot validate the calculations of the effective properties, which is quite important to ensure the accuracy of the numerical model.

The maximum experienced stress in the validation model shown in Figure 9.21 appears in the region of stations 14 and 15 near the leading edge, which is a good indication, as it can also be seen in Figure 9.10 that the maximum stress region start also from station 14. However comparing the maximum values of the two models, no agreement is present. In the QBlade model two highly stressed regions can be distinguished also on the trailing edge - one being close to the root and one around station 14. The highly stressed root region can be explained with the fact that in QBlade, the transition between the first circular cross-section and the airfoil shape can not be implemented as gradually as in the CoBlade code. This rapid transition then can result in a highly stressed structure there. The highly stressed trailing edge area however is a result that is in strong contradiction with the CoBlade results, according to which that area is experiencing considerably low values of stress. The flapwise and edgewise deflections according to the Qblade model are 0.0974097m and 0.020459m, which are also not in an agreement with the values from CoBlade - 0.013m and 0.012m flapwise and edgewise respectively.

It is concluded that due to the great simplification of the recreated model in QBlade the suggested validation process is not applicable.

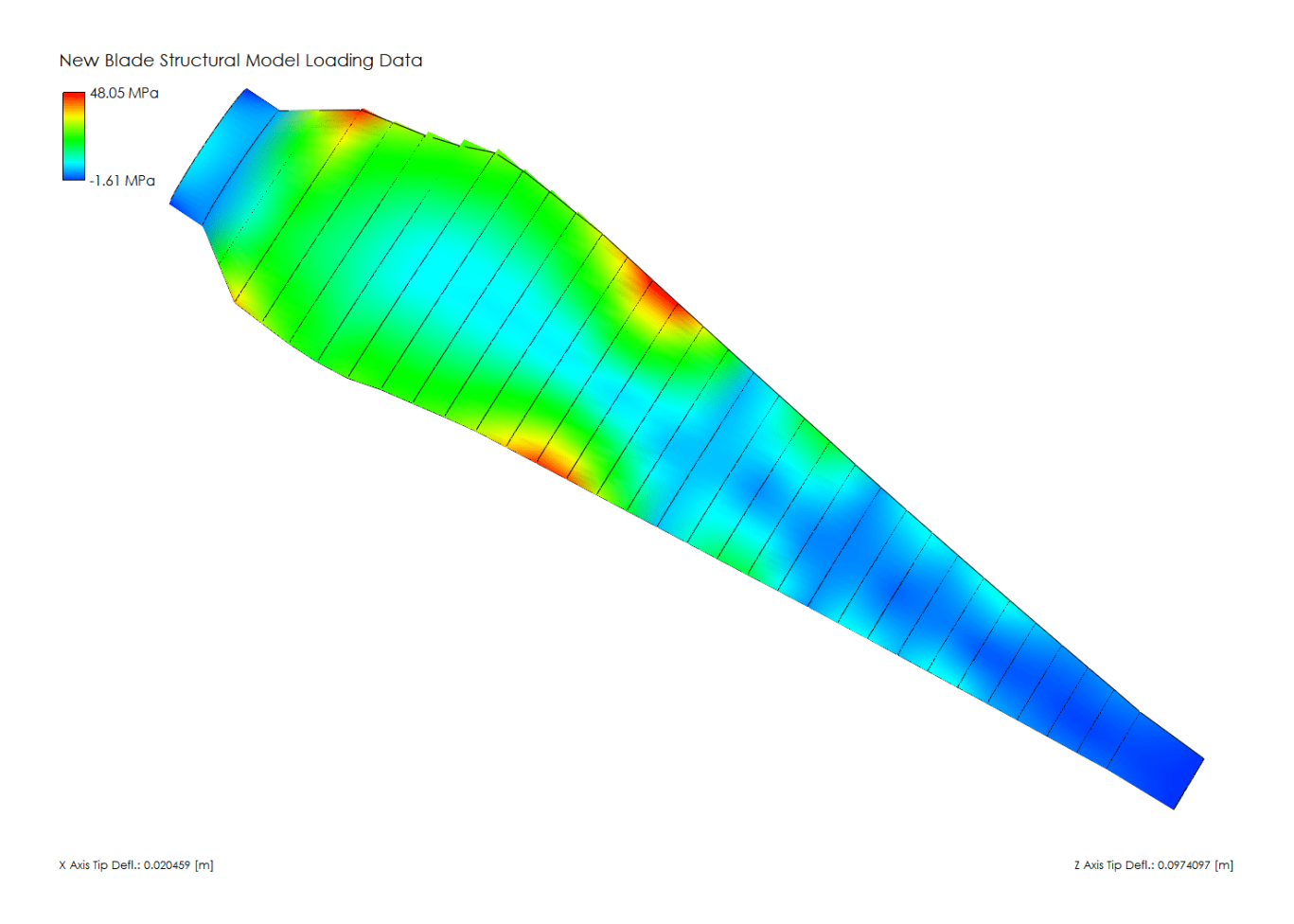


Figure 9.21: Maximum stress on the secondary blade structure model made with QBlade

The Co-Blade code is validated by its authors using it to model a cylindrical beam of complex composite layups and comparing the results for stiffness and beam deflection with those of the same model created by a different finite element code - ABAQUS. The resulting values are found to be quite similar, which is a sign of an accurate tool for modeling. [46].

Chapter 10: Production plan

In this chapter the manufacturing, assembly and integration plan is presented for the secondary rotor wind turbine design based on the material choices from the previous chapter. The plan gives an overview of the components of a wind turbine in section 10.1 and the manufacturing process of those components in section 10.2. The installation of the turbine is then discussed in section 10.3. The other processes that happen during the lifetime of the wind turbine will be discussed in the next chapter.

10.1 Wind turbine components

For the production planning, the manufacturing methods for the key components of the secondary rotor VAWT are presented. Since the design is innovative and very different from other VAWT or HAWT most of the components will have to be manufactured with new equipment in the form of moulds for example. Moreover for an offshore wind turbine, the manufacturers of the largest and most critical components are chosen such that their factories are located near the harbours. This will enable easy transport to the assembly site onshore since the components can be directly shipped from the factories. When transporting the parts by sea, there are less constraints on the design dimensions compared to transport by roads or rail. On the other hand, transportation by sea will induce higher costs. The assembly site is chosen to be onshore, as close as possible to the wind farm site.

10.2 Manufacturing

In this section, the manufacturing methods of the main components are discussed. It is important to note that sensors used for the control of the wind turbine are implemented within the manufacturing phase. For example the load and damage monitoring sensors placed on the secondary rotor blades are placed within the structure of the blade, within the lay-up of laminates.

10.2.1 Blades

The blade manufacturing process is analysed in Figure 10.1 since the material choice, manufacturing technique and geometrical properties of the structure is closely related. For the secondary blade, the chosen material is fibreglass and the optimal manufacturing process chosen is vacuum-assisted resin transfer molding (VARTM). Within the blade manufacturing factory, once the mould for the blade shape has been created, both the top skin and the bottom shells are manufactured separately. The webs running the length of the blade are also manufactured separately and the blade components are bonded together using adhesive bonding. In a typical blade manufacturing factory, the blades are typically produced in a 24 hour cycle, having a high throughput. During the manufacturing process, additional blades are made that are sent to testing sites to verify the design models and predictions.

The blade structure consists of sandwich panels that include a foam core and symmetrically placed GFRP face sheets (unidirectional, biax and triax). The blade manufacturing process is presented in Figure 10.1 and is generalized for the primary rotor and secondary rotor blades that are all manufactured from GFRP using the VARTM manufacturing method.

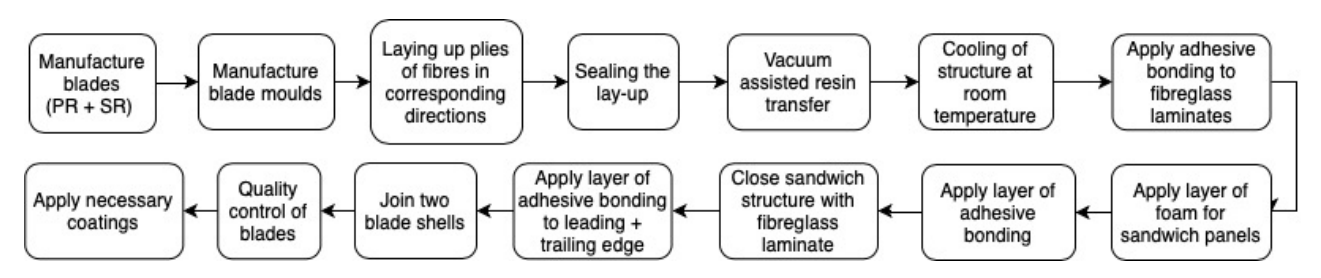


Figure 10.1: Blade manufacturing flowchart

10.2.2 Tower

The tower design is a conical steel tube. The manufacture process includes dividing it into smaller sections of 20m to 30m (This is limitation imposed by the road/rail transportation. For larger markets and bigger projects larger sections are allowed, since it is not efficient to transport for more than 1000km and the towers are manufactured close to the shore [58]), that are steel plates rolled into a conical subsection, for which different tension in the rollers is applied at the ends to bend the plates properly. A flange is then welded to both sides of a section. Before welding two sections, they are bolted together so that a controlled process of the welded flanges deformation is possible [63]. Once the tower is assembled, it undergoes ultra sound testing. After that an anti corrosive coating is applied, due to the aggressive offshore environment. Corrosion is an important aspect that needs to be considered, since it reduces the lifetime significantly. Influence on fatigue lifetime is also expected, in case corrosion is not prevented. That is why a careful use of several layers of coating is applied. In order to ensure the proper adhesion of the coating, the wind turbine is cleaned from rust and oil stains by sand blasting with a high speed jet stream. The process is presented in Figure 10.2.

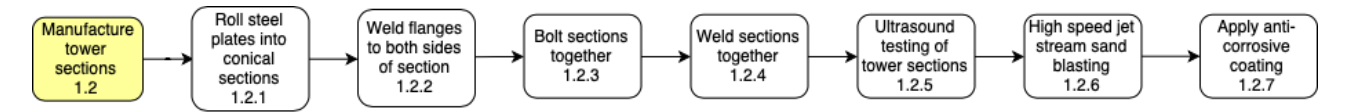


Figure 10.2: Tower manufacturing flowchart

10.2.3 Generator

The permanent magnet direct drive 7.5MW generators used for the secondary rotor wind turbine are specific to this product design. This means that no previous designs exist with the dimensions, power output and rpm and additional operating conditions of the generator. There exist a number of companies producing direct drive generators that can be contacted to produce this type of generator one of which is The Switch.

10.2.4 Rotor hub

The rotor hub consists of both the load carrying element and the nose cone to provide an aerodynamic outer shape [64]. The load carrying element is typically made of cast iron that has to be able to withstand aerodynamic loads induced by the blades but also rotation and dynamically induced loads. The aerodynamic cover of the hub is often made out of composite materials for weight optimization.

10.3 Offshore turbine installation

Once the wind turbine components have been manufactured, the components are transported to the assembly site. The assembly site is chosen to be onshore as close as possible to the harbour area and to the offshore wind farm to decrease time and cost of transportation of components. It is important to reduce the necessary complexity of the installation and the time taken to complete it at the wind farm site. This is because the locations for installing offshore wind farms are areas with generally high wind speeds, therefore also wave heights and expected harsher sea conditions. The installation of the wind turbine has to be carefully planned in accordance with the weather conditions. The available weather window is therefore limited for safe installation. To decrease costs and uncertainties regarding the installation process on the wind farm site, the assembly onshore of wind turbine components is a crucial process. The assembly onshore should be optimized such that the maximum number of components can be assembled together to decrease the installation time. On the other hand there are limitations on this process with respect to the operational conditions of the marine vessels used for installation. Some of these limitations include the operational conditions of the ship: dimensions of the ship, the free deck surface area, the maximum payload and the crane limitations: available crane capacity in terms of weight and maximum crane length. The largest wind turbine installation vessel on the market is the Seajacks Scylla which has a useable deck space of $5000m^2$, 1500t crane and can hold up to 8000t of variable load. This installation vessel will set the limit for the number of components that can be transported at one time by one

Figure 10.3 and Figure 10.4 presents a flow diagram, showing the order of steps which must be taken during the manufacturing, assembly and installation processes. Within the installation process there are three phases

that can be distinguished the first of these being on-shore activities such as production of parts, their transport to the port and the assembly of the sub-assemblies. The second being the preparation of the off-shore site, the equipment and the necessary crew and the final being the actual installation of the turbine at the off-shore wind farm site.

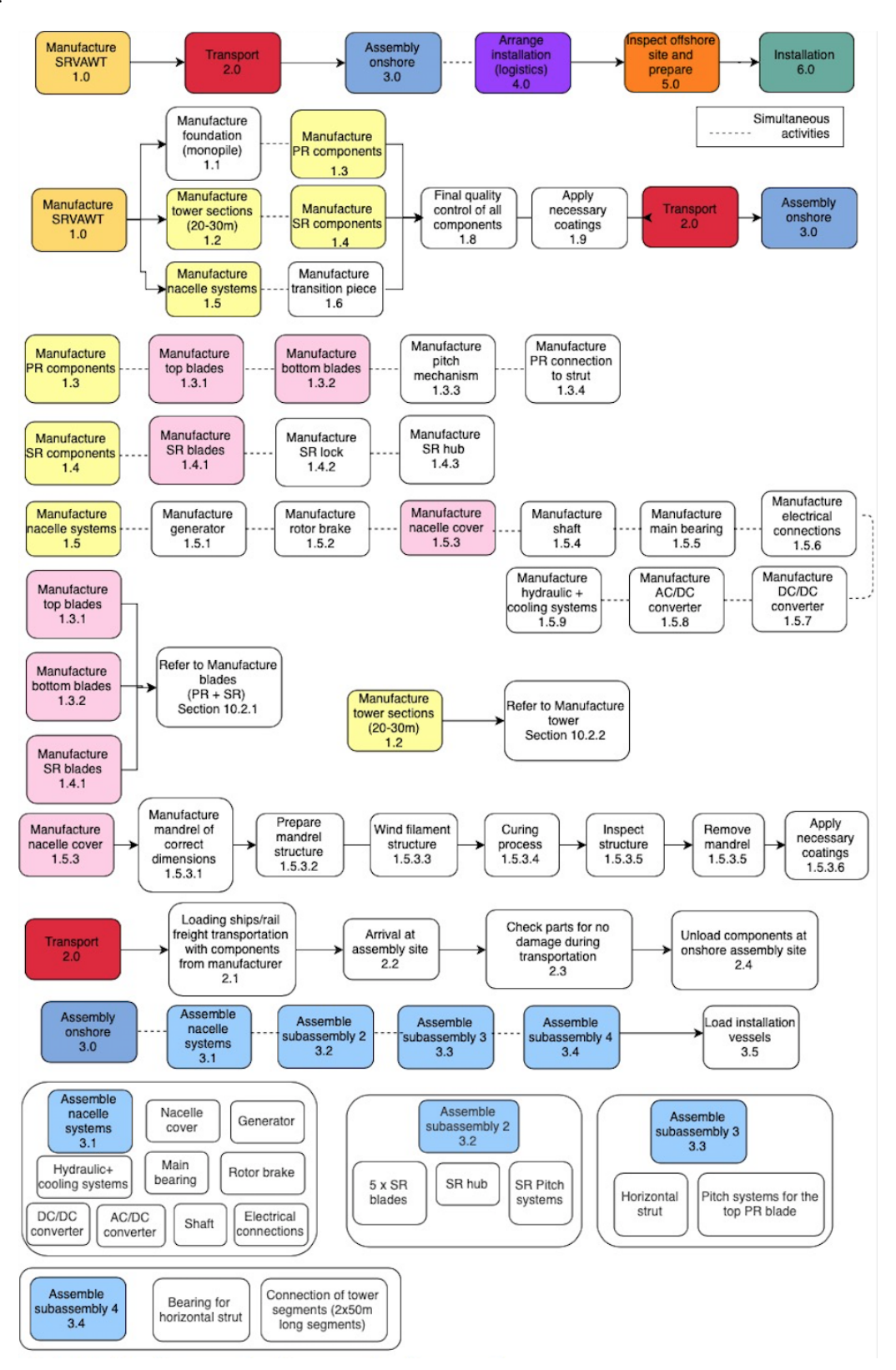


Figure 10.3: Installation plan

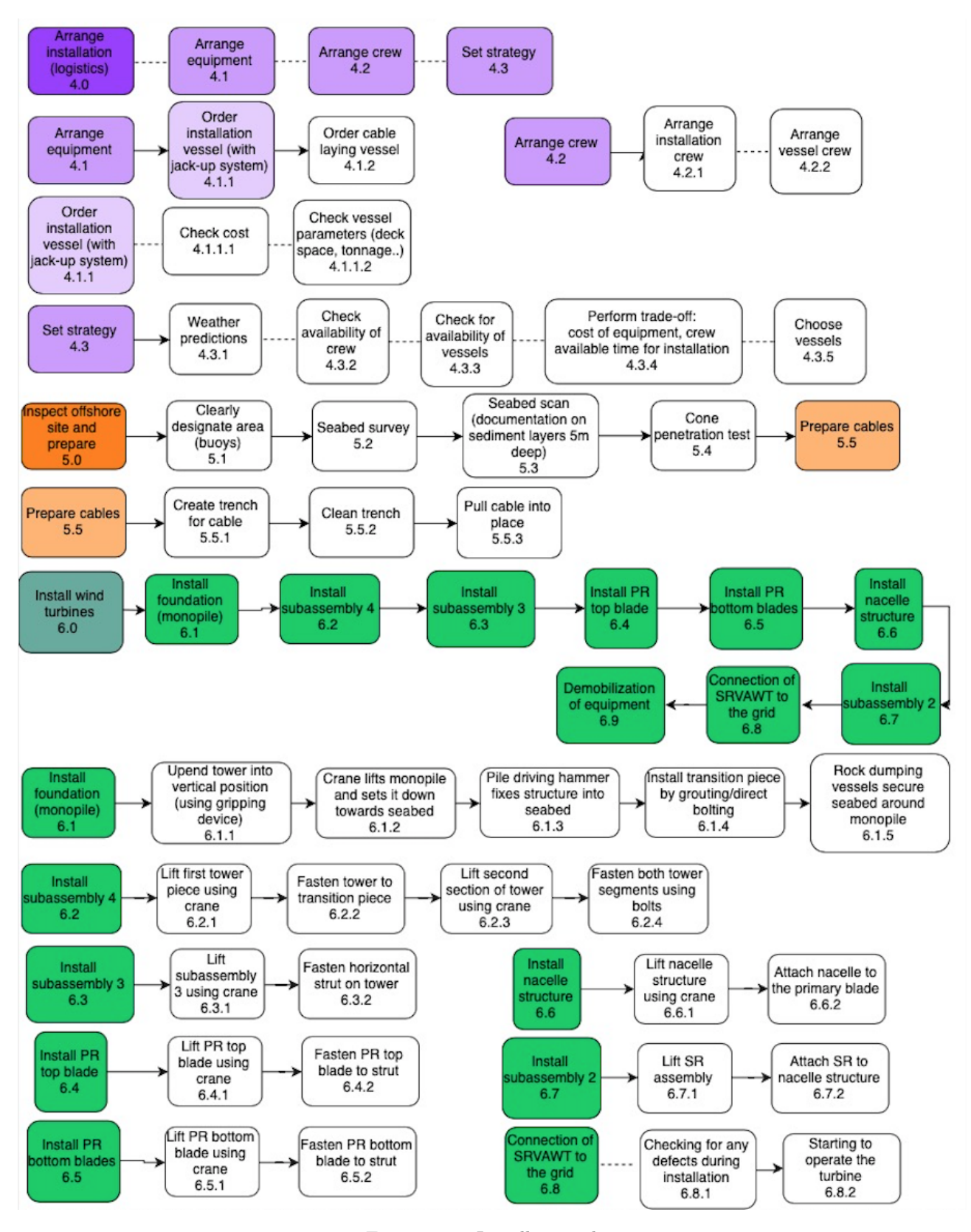


Figure 10.4: Installation plan

Chapter 11: Operations and logistics

Now that the production and installation phases of the wind turbine have been discussed, this chapter will focus on the commissioning, operational and decommissioning phases. A first version of the operations and logistics plan concerning the SRVAWT was provided in the midterm report [9]. This chapter provides an elaboration on that first version.

The initial commissioning is discussed in section 11.1, this is when the operational life of the turbine starts. During the operational life, a good maintenance strategy is of primary importance. This will be discussed in section 11.2 after which the turbine health monitoring is described in section 11.3, this was also described in the control chapter. This health monitoring is done continuously in order to properly plan maintenance trips, this planning is described in section 11.4. Finally, the decommissioning phase will be discussed in section 11.5.

11.1 Commissioning

The commissioning phase is the phase after installation, during which the wind farm is tested and inspected intensively before operation can begin. Within conventional turbines, commissioning can take just over two days per turbine with an experienced crew [65]. Commissioning of the SRVAWT, especially upon the installation of a first wind farm, is expected to take a bit longer than that. This is due to the fact that this is a new turbine, so the procedure will be different and there is no precedent for it.

A more detailed commissioning procedure is recommended for later design stages, however a preliminary procedure is given in this section, featuring those steps which shall be taken as a minimum. The procedure complies with what is described in the wind turbine certification guidelines described by Germanischer Lloyd [21].

The following tests are used to check the functioning of the safety and braking system:

- Function of all emergency stop buttons
- \bullet Function of all sensors and switches that act on the safety system
- Measurement of the essential parameters of the braking systems
- Response of all necessary plant functions after activation of the safety system
- Verification of independence of the safety system from the supervisory control system
- Response to a grid loss
- Testing of all limiting values and parameters that have been set for the safety system

The functioning of the supervisory control system shall be checked by use of the following tests:

- Functioning of the automatic start-up
- Shut-down with all braking procedures
- Plausibility check of the measurement values
- Comparison of the limiting values and parameters which were set with the prescribed values as documented

Other working steps which shall be performed, include:

- Registration of the data on the rating plates of the primary components
- Possible settings to be made in the control system on the basis of the measurement results
- Familiarization of the turbine personnel
- Visual inspection (to conclude commissioning)
- Checking of the required notices and warning plates (to conclude commissioning)

In addition to these commissioning activities, any hazardous situations which may occur during commissioning shall be described and countermeasures shall be specified beforehand. After commissioning, a commissioning report shall be made, documenting the execution of all steps of the procedure and their results.

11.2 Maintenance strategy

It is important to define a maintenance strategy and all the processes which maintenance entails during the operational lifetime of the wind turbine. This will make sure that the maintenance activities are carried out with minimal expenditure and downtime, while keeping maximum performance at a low environmental impact. The Scroby Sands wind farm has 30 wind turbines and there are 1500 wind turbine visits per year which accounts to 8 visits each working day. Approximately 4000 crew members are transferred per year in order to keep the wind farms in operation. This example outlines the importance of evaluating the maintenance strategy and the accessibility of the wind turbines in the design phase of the project.

Four main maintenance strategies exist¹. They include:

- Reactive maintenance (RM)
 Only fix something when it is broken
- Preventive maintenance (PvM) Regular inspection and repair
- Predictive maintenance (PdM)
 Predict when failures will occur and repair accordingly
- Reliability-centred maintenance (RCM)

 Per component a criticality analysis is performed, on which its maintenance plan is based

Ideally, RCM would be applied to the secondary rotor wind turbine. However, this strategy requires a lot of time, skill and financial resources to be developed properly and effectively and is therefore discarded. Reactive maintenance is very sensitive to increased downtime if big failures occur, which causes a loss in energy production and thus reduces profit. This strategy is thereby deemed unviable, leaving PvM and PdM as the two options. PdM has the potential of saving costs on the man-hours spent, although the installation of measurement systems will be more expensive. It also allows better insights in the turbines performance with respect to PvM. With this knowledge one can see that PdM is the more effective solution and will be chosen as the main maintenance strategy. Nonetheless, some components of the turbine are quite cheap, making PvM the optimal maintenance strategy, as replacing the components is more optimal than installing PdM sensors on them. In conclusion, a combination of PvM, for simple and cheap components, and PdM, for more expensive and critical components, is followed for the maintenance strategy.

Concerning the monitoring systems and sensor techniques, it is decided to select them based on reliability and accuracy, where reliability is deemed more important. Monitoring systems and sensor techniques are discussed in the next section.

11.3 Turbine health monitoring

As the wind turbine is commissioned, one immediately wants to know how it performs and develops further. This includes its physical and operational states. Moreover, one examines these states and predicts its future states in order to plan the necessary maintenance activities.

Conventionally, regular inspection of a wind turbine is required to observe the current state. This is especially important in the offshore environment since corrosion degrades materials and erosion degrades blade geometry, reducing the efficiency of the blade. Composite delamination, lightning damage, and cracks can also reduce efficiency and therefore require regular inspections. The faster an issue is detected, the faster measures can be taken, reducing the resulting costs. Inspection can be performed either remotely or by sending people to the site. Remote inspection techniques include the installation of cameras and microphones along with novel methods, such as having drones collect images of the wind turbine.

Despite its effectiveness, inspection is not without drawbacks. First of all, it is costly to send people to all wind turbines regularly. Secondly, it requires assessment of videos, pictures, or sounds by humans, which is inherent to subjectivity. As a result, more sophisticated methods have been suggested to monitor a wind turbine's physical state. These are often designed to monitor key parameters of the entire turbine, or one of its subsystems, with the ability to 'zoom-in' on certain specific parameters. The ones proposed for the secondary rotor vertical axis wind turbine are listed below. In addition to these monitoring methods, conventional inspection activities are still necessary to verify the outcome of these monitoring methods, but on a less regular basis.

 $^{^{1} \}texttt{https://www.fiixsoftware.com/blog/evaluating-maintenance-strategies-select-model-asset-management/selection}$

11.3.1 Supervisory Control and Data Acquisition

One of the most commonly used systems is the Supervisory Control and Data Acquisition (SCADA) system, which acquires, manipulates and stores data regarding the turbine's subsystems, but also the ambient and grid conditions [66]. Examples of the measured parameters are wind speed, blade pitch angles, power, and component temperatures.

11.3.2 Conditions monitoring systems

Condition monitoring systems collect data at a higher frequency (up to 50 Hz) than SCADA systems and are applied to individual components such as the gearbox, generator and the bearings. The sensing items include accelerometers, oil particle counters, acoustic microphones, and thermographic sensors [66].

11.3.3 Structural health monitoring

Structural health monitoring (SHM) systems sense the onset and progress of structural damage, such as fatigue cracks and corrosion, and are typically applied to the turbine blades and tower. They collect data at frequencies of 50 Hz and more and determine the remaining lifetime of individual components.

Decisions have to be made on where to place sensors, as well as how many sensors to place there. It is suggested to place sensors only at the structural damage hot spots within the turbine. The following places are identified as such [67]:

- At 30%-35% and 70% along the blades measured from their roots, which also corresponds to the transition of airfoil sections along the blade for the secondary rotors, which is therefore deemed a very important place to be monitored
- Blade roots considering fatigue stresses and buckling
- Upper spar cap at 35% 40% and 70% 75% of the blade length
- The connection between the foundation and the tower
- The tower's splash zone, considering corrosion

Techniques that can be used to quantify structural health should be able to perform well under the limitations of a small number of measurement location without a prior knowledge on damage locations. The possible techniques, including some advantage and disadvantages, include:

- Acoustic emission events detection method Accurate up to microscale, but less capable in damage characterization
- Thermal imaging method Full field measurement in image form which allows fast evaluation, but a problem is the thermal excitation method which may increase damage
- Ultrasonic method

 Not so accurate in laminates
- Not so accurate in laminate
- Modal-based approach
 Good option if high bandwidth piezoceramic sensors and actuators are available, but difficult so experts
 are needed
- Fibre optics method Good for blades, but costly
- Laser Doppler vibrometer method

 Few sensors for high spatial resolutions and can employ modal based techniques, can be used for in-service
 wind turbines, but not economic yet for WT application
- Electrical resistance-based damage detection method
 For CFRP and in-serivce rotating WT, but sensitive to delamination and a priori knowledge of hot spots needed
- Strain memory alloy method Not known effect on load bearing capability, so more study needed, but it is cost ineffective

- X-radioscopy method
 Fast technique, but a priori knowledge of hot spots and novel strategy for image acquisition are needed, also hard to interpret images
- Eddy current method CFRP only, no promising strategy in scanning an in-service wind turbine blade
- Algorithms

An elaboration on each method was found in an article about structural health monitoring and a choice on the methods was made based on the recommendations given there [67]. A more detailed study is nonetheless required on the current state of these methods to determine which techniques could be employed best. The following are selected at this point:

- Fibre optics method

 This strain monitoring technique is able to to obtain global load conditions. It is quite costly though.
- Acoustic emission damage detection
 The onset of damage and impact events are registered by these sensors. They are sensitive to a wide range of damage types and can locate damages accurately.
- Non-contact ultrasound-induced thermography
 Used in the non-composite parts of the wind turbine
- Also the Laser Doppler vibrometer is suggested as a very plausible option. However, this technique must be adjusted for wind turbine applications first

11.4 Planning

In the case of both planned physical inspections as well as service activities, all necessary resources (transportation, equipment, personnel) can be arranged beforehand. Due to this, weather conditions are the main factor which play a role in the time it takes to perform the maintenance activities. The actual maintenance activities, namely service, repair and overhaul are presented in chapter 12. In contrast, the planning of these is presented here in Figure 11.1, as it concerns logistical aspects. It contains the steps taken during the operational and maintenance phases in the wind turbines lifetime.

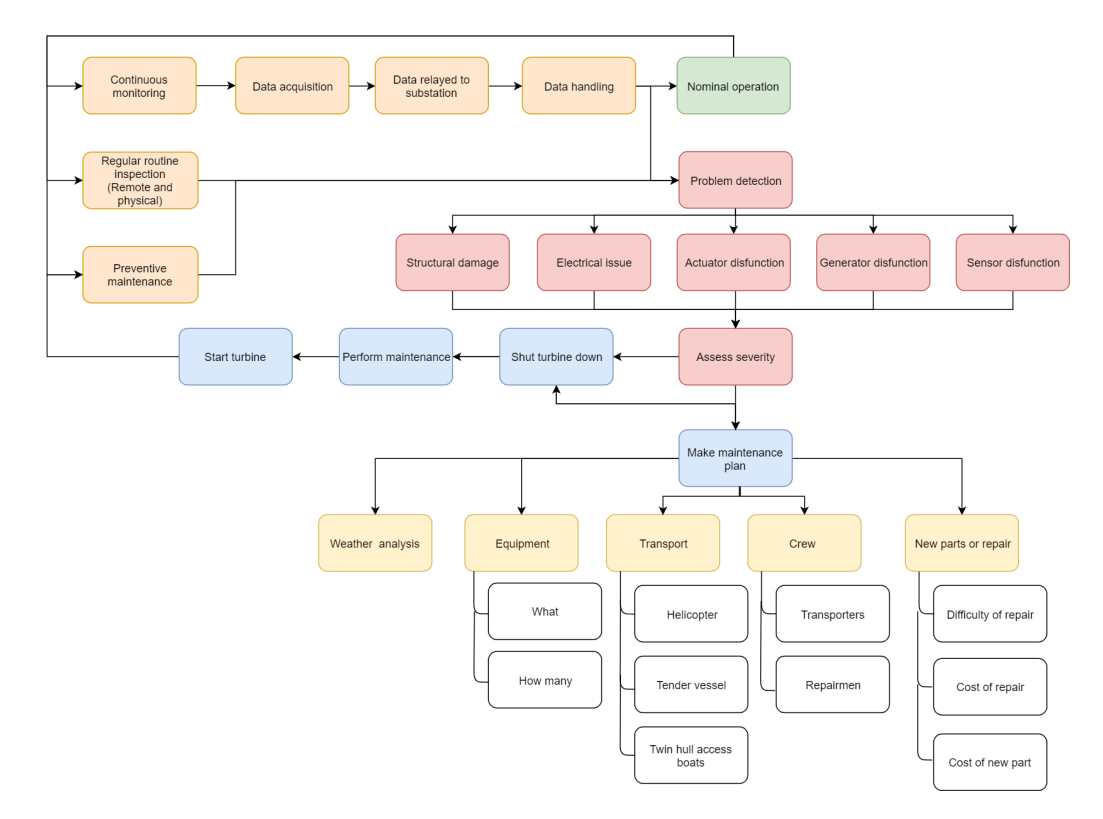


Figure 11.1: Maintenance logistics plan

A more concrete planning of routine maintenance operations is presented in Table 11.1. Here it is adhered to that one modern turbine needs approximately 40 hours of routine maintenance per year ², but is conservatively brought up 50 hours for the SRVAWT in its initial operational phases. After an amount of time, these may be brought down as maintenance needs can be predicted more accurately. The planning is based on half-yearly visits to the wind turbine. Some activities are only needed every full year ³ and therefore some visits will take less time than expected. The visits in which all activities are included, will take about 19 hours for a person. It is therefore advised to send three people to the wind turbine to do perform maintenance on a single day. The visits in which only part of the activities have to be performed will take about 6 hours, which be done by one person in one day.

Type of maintenance	WT component	Duration [hours]	Interval [months]
General inspection	Blades	6	6
General inspection	Generators	2	6
General inspection	Attachments	4	6
General inspection	Hydraulics	8	12
PvM	Change oil	6	12
PvM	Lubricate bearings	6	12
PvM	Torqueing bolts	6	12
		Total hours per year	50

Table 11.1: Maintenance planning

11.5 Decommissioning Phase

At the end of the turbines operational life, it must be removed from its location. The procedure in which this is done and the method of component disposal or reuse is provided in Figure 11.2. It is assumed that the possibility of only replacing the secondary rotor has already been evaluated and that at this point the entire turbine is to be decommissioned. The whole system is at the end of its life.

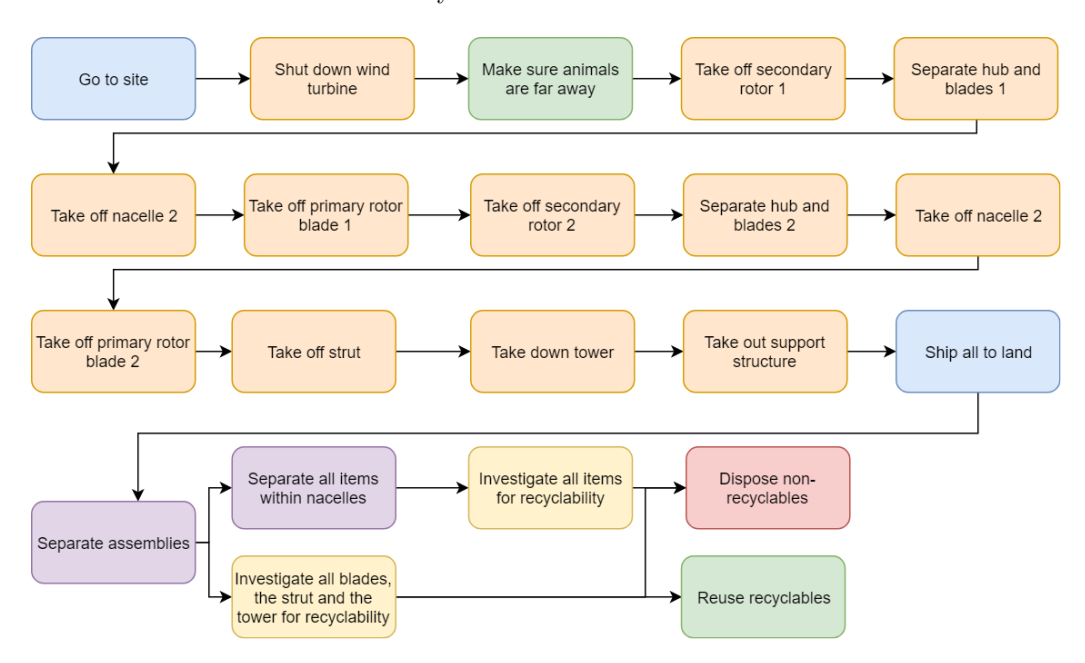


Figure 11.2: Flow diagram showing the different steps within the decommissioning phase

²https://www.renewableenergyworld.com/articles/print/volume-12/issue-2/wind-power/wind-farm-design-planning-research-and-com/articles/print/volume-12/issue-2/wind-power/wind-farm-design-planning-research-and-com/articles/print/volume-12/issue-2/wind-power/wind-farm-design-planning-research-and-com/articles/print/volume-12/issue-2/wind-power/wind-farm-design-planning-research-and-com/articles/print/volume-12/issue-2/wind-power/wind-farm-design-planning-research-and-com/articles/print/volume-12/issue-2/wind-power/wind-farm-design-planning-research-and-com/articles/print/volume-12/issue-2/wind-power/wind-farm-design-planning-research-and-com/articles/print/volume-12/issue-2/wind-power/wind-farm-design-planning-research-and-com/articles/print/volume-12/issue-2/wind-power/wind-farm-design-planning-research-and-com/articles/print/volume-12/issue-2/wind-power/wind-farm-design-planning-research-and-com/articles/print/volume-12/issue-2/wind-power/wind-farm-design-planning-research-and-com/articles/print/volume-12/issue-2/wind-power/wind-farm-design-planning-research-and-com/articles/print/volume-12/issue-2/wind-power/wind-farm-design-planning-research-and-com/articles/print/volume-12/issue-2/wind-power/wind-farm-design-planning-research-and-com/articles/print/volume-12/issue-2/wind-power/wind-po

³https://www.ecmweb.com/content/wind-service cited 20-06-2019

Chapter 12: RAMS characteristics

This chapter describes the reliability, availability, maintainability and safety (RAMS) aspects of the designed wind turbine. These aspects are especially important in the case of offshore wind turbines, considering that operations are significantly more complicated and expensive when dealing with a wind farm located (far) offshore. The goal of this chapter is to come up with a numerical estimate for the turbine reliability and availability, as well as to describe its maintainability and safety characteristics. This includes an outline of the proposed maintenance activities, a list of safety critical functions and the way in which the redundancy philosophy has been applied.

For the sake of consistent and accurate results, only one study is used throughout this chapter for the numbers on failure rates and downtimes. This is important, due to the fact that wind turbine reliability studies can vary significantly in their approaches, definitions, and subsequent findings. The study that is used in this chapter, is a study performed in 2015 by the University of Strathclyde [68]. It was deemed the most relevant for this project because it is a recent, comprehensive study focusing on modern, multi-MW turbines which operate offshore.

In section 12.1, the reliability aspect of the wind turbine is presented, which flows into the availability in section 12.2. The maintainability is described in section 12.3, a basis for this was already constructed in the previous chapter. The final aspect of the RAMS analysis is safety, which can be found in section 12.4.

12.1 Reliability

The term reliability is generally defined as: "the probability that a product or a system will perform its intended functions satisfactorily (i.e., without failure and within specified performance limits) for a specified length of time, when operating under specified environmental and usage conditions" [69]. Within the context of a complex system like a wind turbine, overall reliability is determined by the reliability of its subsystems, including hardware and software, and the connections between them. Over the years, numerous studies have been performed on the reliability of wind turbines, both on- and offshore. This section describes the reliability of conventional offshore turbines, after which an estimate is made for the reliability of the SRVAWT.

12.1.1 Conventional turbine reliability

The Strathclyde reliability study investigated the reliability of individual subsystems within conventional, multi-MW offshore turbines. This resulted in annual failure rates and average repair times, subdivided into 19 subsystem types and four types of failures. Reliability is estimated by calculating the mean time between failures (MTBF), which in turn can be obtained from the annual failure rate, λ [70], by Equation 12.1.

$$MTBF = \frac{1}{\lambda} \tag{12.1}$$

In this, it is assumed that failures are roughly equally spread out over time. In the case of a complex system like a wind turbine, this is generally an acceptable assumption to make [70]. An annual failure rate of 8.27 failures over the whole turbine is found, of which the majority of failures (6.18 failures) are those which require a minor repair. This failure rate results in a mean time between failures of about 1059 hours, or 44.1 days. The subsystem which contributes most to the overall failure rate is the pitch and hydraulics system (13%), followed by the generator (12.1%), gearbox (7.6%) and the blades (6.2%). 'Other components', which consists of components which are auxiliary to the subsystems' functioning, makes up about 12.2% of the overall failure rate.

12.1.2 SRVAWT reliability

The wind turbine designed in this project differs significantly from the conventional turbines investigated in the Strathclyde study. Therefore, the appropriate modifications are made in order to estimate the SRVAWT reliability. Those differences in configuration which are considered significant and for which modifications are made, are described in the following text. The remaining subsystems in the SRVAWT are considered similar

enough to conventional turbines to have similar failure and downtime characteristics, thus no modifications are made.

Absence of gearbox and yaw system

Firstly, a few of the subsystems described in the study are absent in the turbine designed in this project. The SRVAWT has a vertical axis primary rotor and therefore does not require a yaw system. Additionally, due to the choice for a direct-drive configuration in the secondary rotors, gearboxes are also absent. The reliability is modified by taking out the failure occurrences of these subsystems.

Increase in subsystem numbers

Second, the SRVAWT has a different number of some of the subsystems than conventional wind turbines. For one, it has 12 pitch systems instead of three. The number of blades increases from 3 to 14. The turbine has two generators and two hubs instead of one of each, due to the double secondary rotors. In each subsystem case, the reliability is adjusted by multiplying the expected failure rate for each failure type according to the increase in subsystem quantity.

Different subsystem types

Finally, the SRVAWT uses some subsystems which are of a different type than the ones on the turbines investigated by Strathclyde. The most significant of these are the type of generator and the type of pitch system. The SRVAWT uses two permanent magnet generators (PMG), instead of one doubly-fed induction generator (DFIG), which is the most common type and also what the turbines in the Strathclyde study use. Also, electric pitch systems are used instead of hydraulic systems, which are also used on the turbines investigated by Strathclyde.

Modifications regarding the generator are made based on a different study performed by Strathclyde[71], which investigated the differences in reliability between PMG and DFIG drive trains. It was found that the failure rate of a PMG itself is lower than that of a DFIG, mainly due to the fact that the PMG does not require a slip ring, which is the component which causes most failures within a DFIG. This increased reliability is however completely mitigated by the fully rated converters (FRC) used in PMG drive trains, which have a failure rate five times as high as partial load converters (PRC), used with DFIG drive trains. The PMG configuration numbers which were found in this study were used to substitute the DFIG configuration numbers, in order to better estimate the SRVAWT reliability.

Finally, the SRVAWT will make use of an electric pitch system, instead of a hydraulic system. A 2016 study by manufacturer Moog and DNV GL, which aimed to benchmark pitch system reliability, found that within conventional turbines, the failure rates of electric and hydraulic pitch systems are roughly the same[30]. The difference between the types of systems is the types of failure they encounter: hydraulic systems fail mainly due to hydraulic fluid leaks, fluid contamination and fluid rotary joint failures. To the contrary, motors, drive train electronics and power back-up batteries are the main sources of failure within electric pitch systems[30]. It is possible that the SRVAWT pitch systems will have a lower failure rate than conventional electric pitch systems, thanks to the use of ultracapacitors instead of conventional batteries[25]. However, no hard numbers can be found on this at this moment. For this reason, the hydraulic pitch system failure rates found by Strathclyde will be kept in the reliability estimate, possibly resulting in a slightly higher failure rate than what would occur in reality.

12.1.3 Results and comparison

Incorporating all previously discussed modifications, the following results are found: the SRVAWT has an expected failure rate of 13.36 failures per year, equivalent to a MTBF of 27.3 days. This decrease in reliability is largely due to the increase in pitch systems and blades used. The vast majority (78.5%) of failures are those which require a minor repair, also mostly stemming from the pitch systems and the blades. A comparison of failure rate contributions from the different subsystems is shown graphically in Figure 12.1.

Annual failure rate

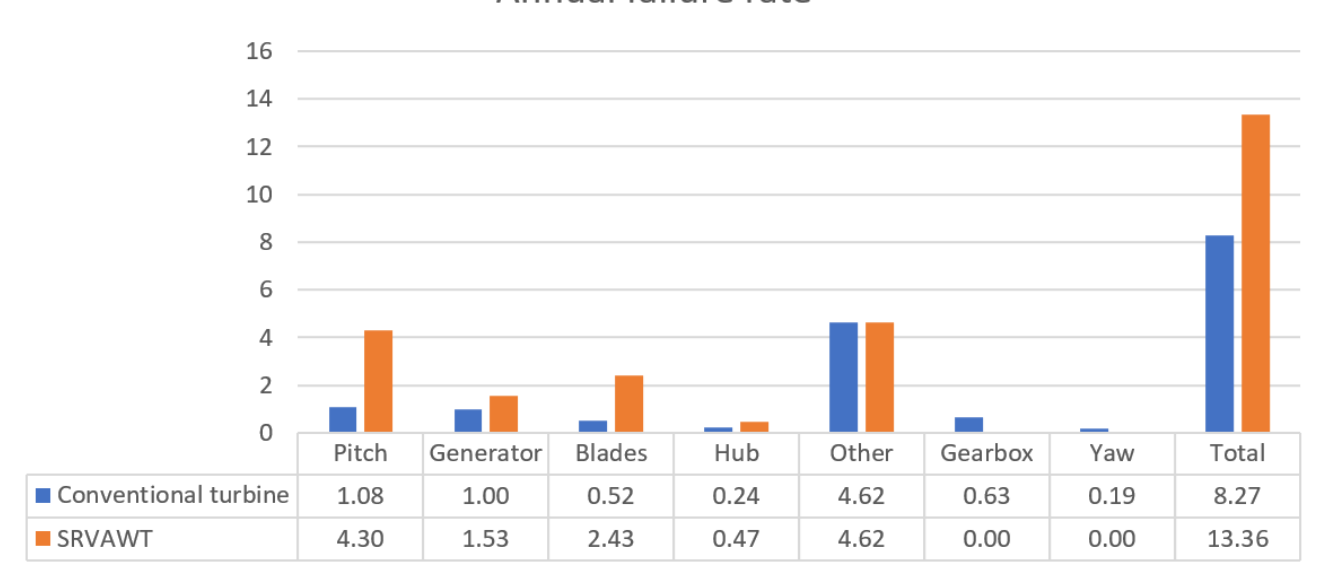


Figure 12.1: Subsystem contributions to the annual failure rate, for both conventional turbines and the SRVAWT

12.2 Availability

Availability is defined as the operable percentage of time, i.e. the percentage of time during which the turbine is in operation or can operate. It is an aspect which is crucial to the success and competitiveness of a wind turbine, as it plays a significant role in the annual energy production, which in turn goes into the cost of energy. Even the most efficient turbines, placed in locations with high winds, do not stand a chance of generating power at a low cost of energy if their availability is poor. An availability estimate shall therefore always be made in the design process.

The general definition of availability is presented in Equation 12.2 and is the ratio between the mean time to failure (MTTF), i.e. how much time passes on average between the end of a repair and a new failure, and the sum of the MTTF and the mean time to repair (MTTR), i.e. the amount of time needed for the corrective maintenance of failures: [70]

$$Availability = \frac{MTTF}{MTTF + MTTR} \tag{12.2}$$

Within offshore wind energy, there are a few more factors which go into 'downtime': not only the average time it takes to repair the turbine matters, but also the mean logistic delay time (MLDT) and the mean waiting time (MWT) go into the availability equation. These additional terms stem from causes like the unavailability of spare parts, a vessel or crew, as well as bad weather prohibiting the work boat from leaving the harbour. Availability then becomes: [70].

$$Availability = \frac{MTTF}{MTTR + MLDT + MWT + MTTF}$$
 (12.3)

As said before, a 2015 study performed by the University of Strathclyde is used and modified to come up with a reliability and availability estimate for the SRVAWT design. When it comes to availability, one issue that was encountered with this study is the fact that it describes only the average repair time per failed component, i.e. the MTTR per subsystem per failure type. For this reason, an estimate for the annual cumulative repair time of the SRVAWT is made and compared with that of conventional turbines. Based on this, an estimate for the actual availability is made for the SRVAWT.

The general approach is to take the annual failure rate per subsystem per turbine, and multiply it with the average repair time that is associated with it. The sum of all these products is an estimate of the annual cumulative repair time. This is done for conventional turbines using the failure rates and repair times as found by Strathclyde. For the SRVAWT, it is done by taking the modified failure rates which have been found as described in section 12.1, and again the repair times from Strathclyde. In this, it is thus assumed that the repair times per subsystem per failure type of the SRVAWT is the same as that on conventional turbines. The repair

times per subsystem found with this approach are shown for both conventional turbines and the SRVAWT in Figure 12.2.

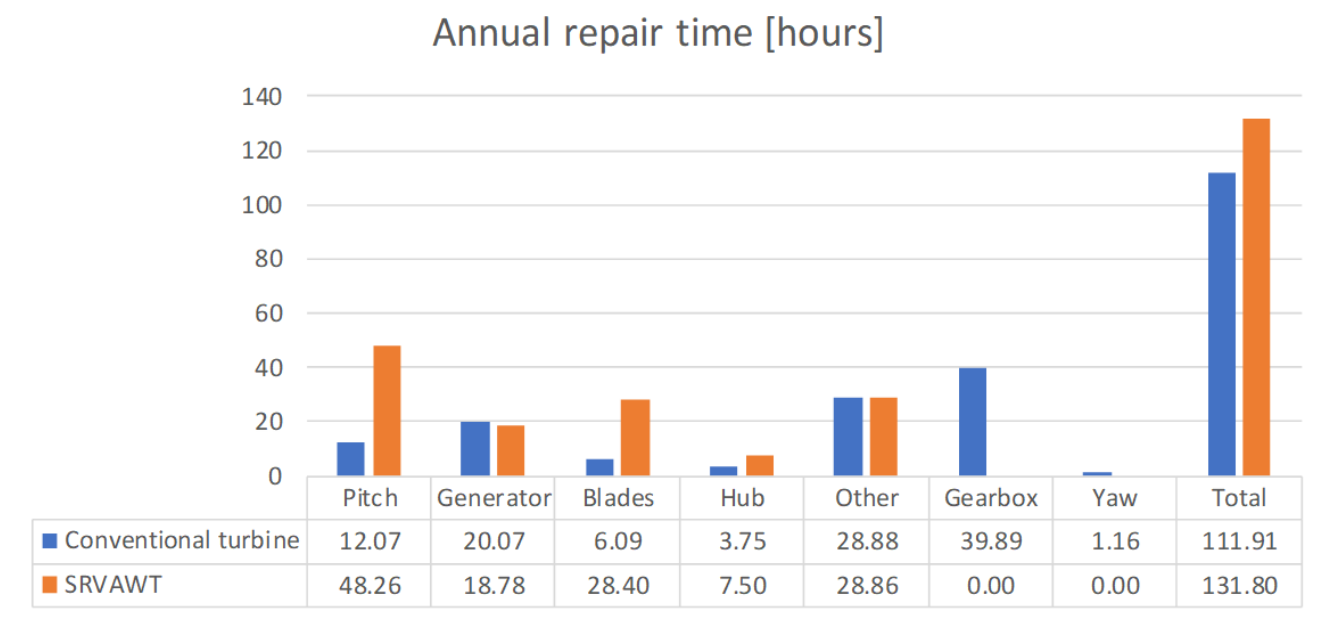


Figure 12.2: Subsystems contributions to the annual repair time, for both conventional turbines and the SR-VAWT

The calculations resulted in the following results: the SRVAWT is expected to have an annual cumulative repair time of 131.8 hours, versus 111.9 hours on a conventional turbine. This increase is largely due to the larger number of pitch systems and blades, which account for 37% and 22% of the annual SRVAWT repair time, respectively. For this reason, it is proposed to introduce a form of failure-tolerance in the turbine operations: when the pitch system of one of the secondary rotors fails, the failure is detected and communicated as normal, but operation continues. This could potentially be done multiple times per turbine, however more research is recommended to look into the possibilities and limitations of this option. The proposal does not apply to a failure of the primary rotor pitch system, as there are only two of these systems and it must still be ensured that the turbine can come to a halt safely. The proposed idea does not increase reliability per se (the pitch systems still contribute to the failure rate when they do fail), however still continuing operation after a secondary rotor pitch system failure means less downtime and thus higher availability.

When this mode of operation is taken to be used on the SRVAWT, availability is expected to be similar to or higher than that of conventional turbines. Therefore, a possibly somewhat conservative estimate of 92.5% real availability is taken for now, i.e. the availability as described by Equation 12.3. This is a typical value for modern offshore turbines, as found in 2016 by The SPARTA (System Performance, Availability and Reliability Trend Analysis) initiative in the UK [72]. This is thus a first estimate for the SRVAWT availability, which will also be used in its cost of energy analysis.

12.3 Maintainability

Maintainability is a measure of the speed and ease with which maintenance activities can be carried out. It includes aspects such as system and component accessibility, the ease with which a repair can be carried out, and the way in which the procedure has been designed [73]. This section describes an outline of the maintenance activities which will take place on the SRVAWT, as prescribed in the project guide [1]. The (remote) monitoring of the turbine is considered a different form of maintenance, and is described in more detail in section 11.3.

12.3.1 Service and inspections

Service, also known as routine maintenance, is a form of planned maintenance which consists of routine, elementary activities which do not require special equipment, parts or personnel. The reason for the servicing of turbines is the fact that although wind turbines have a life expectancy of 20 to 25 years, most of their components do not. Service activities include cleaning of the turbine, visually inspecting the structure, blades

and electronics, tightening connections, checking liquid levels, refilling lubrication, adjusting sensors, etc. A planning of these activities was already given chapter 11.

12.3.2 Repair

If any defects are discovered during the health monitoring of the turbine, section 11.3, which limits its operations, a repair must be performed. Since the wind turbine is located offshore, a number of logistical activities must be carried out when a repair is necessary. The number and types of activities which must be planned depend on the type of repair to be performed. For repairs distinction is made between external and internal repairs. Internal repairs include, but are not limited to, repairs of the electronic systems or generator and external repairs most often are repairs of the blade structure.

As stated earlier several activities must be planned when repairs need to be done. Depending on the type of damage, a specialized crew must be arranged capable of performing the mission. In case of replacement of parts they must be ordered. Transport to the wind turbine must be arranged, for which there are several options, namely by helicopter or by boat. In case of large repairs, such as for example generator replacements or rotor replacement, machinery capable of performing heavy lifting tasks must also be arranged.

In case of the wind park where the turbine is located far off-shore, it is important to plan maintenance repair activities efficiently. Travelling all the way to the wind park for only a single repair could be very cost ineffective. Therefore, when repair is needed, a trade-off must be performed to determine if it is worthwhile performing the single repair, or if it is more efficient to wait until other repair jobs arise near the wind turbine, for example in the same wind park. In case of it being more expensive to keep the turbine inoperative instead of repairing it, and if crew and machinery are available, preference shall always go towards performing the repair. If this is not the case one shall have to consider postponing the repair.

12.3.3 Overhaul and modernization

Overhaul is a form of maintenance where an extensive inspection of the system is conducted. This includes disassembly of large parts of the system to be able to do the inspections. Often also large components are replaced such as turbine rotors, generators or other major components. Overhaul could be combined with modernization, during which the turbine is retrofitted with the newest technology available for the specific type of turbine. Modernizing a turbine is a big investment in the existing turbine. It extends the lifespan of the machine and as a result operational performance is often improved. [74]

When an overhaul or modernization is performed, the turbine needs to be completely shut-down. Due to the size and weight of the different major components, chances are high lifting equipment and a specialized crew is needed to perform the operations. Also parts need to be present in case components need to be replaced. To make sure the operation runs as smooth as possible a lot of logistical activities come into play and a thorough planning must be present. Furthermore, in case of the turbine being located far off-shore it would be efficient to plan such an operation for multiple turbines located at the wind park. [74]

12.4 Safety

Safety is a turbine characteristic which is highly important but hard to quantify. Within this section, it is split up into safety of the personnel working on the turbine and the safety of the turbine itself. The latter of these has been discussed in more detail during the design process of the supervisory control and safety system in chapter 6.

12.4.1 Personnel safety

The safety of the maintenance crew working on the turbine is an important aspect which must already be considered during the turbine's design phase. Increasing the safety of personnel can be increased not only by increasing safety during maintenance activities, but also by simply designing in such a way that fewer maintenance activities are required.

The latter of these measures can be achieved by designing a turbine using fewer components (a lean design), components with higher reliability, and components which have a longer operational lifetime. An example of how this has been integrated in the SRVAWT design is the use of ultracapacitors instead of conventional lead-acid batteries for energy storage within the turbine. These devices have an operational lifetime of up

to 12 years, versus about two to four years for lead-acid batteries [25]. This results in a reduced number of replacements which is needed throughout the turbine's lifetime, increasing safety and decreasing O&M costs. In addition to component choices, making use of turbine health monitoring systems, such as the ones described in section 11.3, has the potential to reduce the number of physical maintenance activities needed. This not only increases worker safety, but it also decreases O&M costs.

To ensure workers' safety during maintenance activities, some measures should also be taken during the design phase of the turbine. These measures may include, among others, guardrails, safety nets and personal fall arrest systems to prevent workers from falling from large heights. Workers should also always wear non-slip shoes to prevent them from slipping in rainy and wet conditions, as well as noise protection on their ears to prevent hearing damage from harsh weather conditions. Proper training and communication are especially crucial: workers should always be up-to-date on emergency procedures, and they should preferably also receive first-aid training [75].

12.4.2 Turbine safety

The safety of the turbine is the responsibility of its supervisory control and safety system, which is described in detail in chapter 6. Therefore, this section consists of some concluding remarks of this chapter.

Safety critical functions

The safety critical functions within this turbine are those functions which are performed by the safety system. This is due to the fact that this system serves as a safety back-up for all other functionalities, therefore failure of any of the safety system functionalities is the only scenario which could truly have catastrophic consequences. Safety critical functions are therefore the following functions:

- Activation of the safety system
- Drawing power from back-up storage
- Disengaging the generator
- Pitching of the primary rotor blades to feather
- Pitching of the secondary rotor blades to feather
- Apply mechanical brake on primary rotor for complete standstill
- Apply mechanical brake on secondary rotor for complete standstill
- Apply locks on all rotors to ensure no further rotation

In addition, the back-up energy storage which powers the safety system shall be monitored to ensure that there is enough energy to perform at least one emergency stop.

The redundancy philosophy

Applying redundancy is an important measure which can be taken to ensure turbine safety. On a system level, redundancy is applied within the SRVAWT by having a safety system on top of a supervisory control system. This system works independently from the supervisory control system, and is powered by a back-up energy supply. This ensures turbine safety even in the case of a grid loss.

In addition to that, there is redundancy applied on a subsystem level. This includes making use of individual pitch control instead of collective control, such that all rotors can still be safely brought to a halt in the case of a pitch control system failure. Furthermore, there is redundancy in sensors: there are two sensors for each application, of which the outputs are constantly compared and checked with each other. In case the outputs differ too much from each other, this is likely caused by a failure of one of the sensors and this is communicated through the control system. The application of redundancy is explained in more detail in chapter 6.

Chapter 13: Technical risk management

In the systems engineering world, risk connects the technical performance, cost resources and the schedule time in a project. This chapter will focus on the technical risks during the operational lifetime of the final design. There are several steps that have to be taken for successful risk management: identifying risks, assessing the risks based on likelihood of occurring and the impact that they will have, developing a plan to mitigate the risks and at last monitoring the risks. The identified and assessed risks can be found in a risk register together with an initial risk map in section 13.1. The proposed risk mitigation plan and an updated risk map can be found in section 13.2.

13.1 Risk identification and assessment

The first step is to identify all technical risks and put them into a risk register. In order to keep a clear overview, all risks are divided into categories. The risks that are associated with this specific design are placed in the Design category. The general risks that are related to offshore wind energy in general are divided into the following categories: environmental, power and electronics, structures and mechanical. All risks are assigned an ID, such that identifying and controlling them can be done quickly, easily and clearly. All risks are then assessed on their probability and severity of occurrence, using scales ranging from remote (1) to almost certain (5) on probability, and from negligible (1) to catastrophic (5) on severity. The risk register before mitigation can be found in Table 13.1, most of which was already identified in the project midterm report [9]. Small changes and updates have been made, based on the findings of this design phase.

Table 13.1: Technical Risk Register

ID	Category	Cause	Risk event	Consequence	Probability	Seve- rity
D1	Design	Secondary rotor too large and heavy	Primary rotor has a too low rpm at low wind speeds	Lower power production than expected, shift of power curve	2	4
D2	Design	Wrong calculations of natural frequencies and Campbell diagram	Resonance	Failure of the turbine	2	5
D3	Design	Failure of both supervisory control and safety system	Run-away rotor	Failure of turbine	2	5
D4	Design	High rpm of rotors	Excessive noise levels	Negative impact on ecology, bad publicity	4	3
D5	Design	Not considered flow variation due to rotation	Dynamic stall	Reduced power conversion, stall-induced flutter	2	3
D6	Design	No vibration measure during design phase	Excessive vibration	Shorter operational life cycle. More frequent maintenance	3	4
D7	Design	Actuator or brake power insufficient, controller to slow	Lack of control over turbine	Turbine failure, danger to safety and environment	2	4
D8	Design	Insufficient thrust from secondary rotors	Unable to start primary rotor at low wind speeds	No power conversion	2	4
D9	Design	Primary rotor blades large compared to secondary	More interference with flow to secondary rotor than expected	Secondary rotors face more wake effects and smaller velocity, less power produced	2	3
D10	Design	No maintenance consideration during design phase	Poor maintainability and accessibility	More frequent and longer maintenance visits, higher costs	3	3

D11	Design	Much higher rotational velocities of secondary rotors than conventional turbines	Excessive erosion of secondary rotor blades	Reduced structural and aerodynamic performance, decreased power output	3	4
D12	Design	More intensive pitching compared to conventional turbines, cyclic loading	Pitch bearing fatigue failure	Detachment of blades, damage to environment	2	4
E1	Environment	Weather events (storms)	Turbine struck by lightning	Structural damage, fire	4	3
E2	Environment	Birds flying near wind farm	Bird strike to blades	Impact damage to structure	3	3
Е3	Environment	Weather	Regular extreme wind gusts	Fatigue, vibrations	4	3
E4	Environment	Weather, tides	Extreme waves	Vibrations, fatigue, corrosion	4	2
E5	Environment	Oil, insects, birds and other dirt	Dirty blades	Increase of mass, reduced lift performance	5	2
P1	Power and electronics	Damage to stator windings, un-even air gaps, mechanical problems, overheating	Generator failure	Loss of power and income	2	4
P2	Power and electronics	Hardware/software issues	Supervisory control computer failure	Loss of control and communication	2	4
P3	Power and electronics	Overheating, de-attachment	Sensor failure	Loss of measurements, inaccurate measurements	3	3
P4	Power and electronics	Power converter failure	Loss of voltage control	Overloading of generator/grid	3	3
P5	Power and electronics	Rectifier/inverter failure	Loss of frequency control	Overloading of generator/grid	3	3
P6	Power and electronics	Human activities, erosion	Cable damage	Short circuit, loss of output	2	3
P7	Power and electronics	Wear, fatigue in shaft	Shaft failure	Loss of output, damage to generator	2	4
P8	Power and electronics	Short circuit	Power storage failure	No power storage, decreased competitiveness	3	3
S1	Structures	Fatigue, vibrations	Permanent deformation of blades	Decreased turbine output	2	4
S2	Structures	Fatigue, vibrations in main rotor bearing	Detachment of primary or secondary rotor	Complete turbine failure, damage to environment	1	5
S3	Structures	Fatigue, vibrations of pitch bearing	Detachment of primary or secondary blade	Turbine failure, damage to environment	1	5
S4	Structures	UV, chemicals, water, fatigue	Blade delamination	Structural weakening	2	3
S5	Structures	Fatigue in blades	Cracks in blades near stress concentrations	Structural weakening	2	3
S6	Structures	Cracks, fatigue, resonance, clearance	Topple, collapse of tower	Complete turbine failure	1	5
S7	Structures	Rain, salty sea water, oxidation	Erosion of primary and secondary rotor blades	Reduced structural and aerodynamic performance, decreased power output	4	4

M1	Mechanical	Brake pads wearing thin	Brake failure	Loss of control over rotor	3	4
M2	Mechanical	Fatigue, oil leakage	Generator bearing failure	Increased friction and heat, less power generated	2	4
М3	Mechanical	Hydraulic leakage	Actuator failure	Rotors cannot be controlled	3	3
M4	Mechanical	Motors failing	Pitch control failure	Power output cannot be controlled	4	3

To show the risk level of each risk, they can be put in a risk map, using their previously assigned IDs. This shows which risks are deemed to pose a low (green), moderate (yellow) or high (red) risk to the turbine. The risk map after risk identification and assessment is shown in Table 13.2.

Almost Certain E_5 D4, E1, E3, $\mathbf{E4}$ Likely **S7** M4D10, E2, P3, Possible P4, P5, P8, D6, M1, D11M3D1, D7, D8, D5, D9, P6, Unlikely P7, S1, M2, D2, D3 S4, S5 D12, P1, P2 S2, S3, S6 Remote Neglible Marginal Moderate Critical Catastrophic

Table 13.2: Risk Map after risk identification and assessment

13.2 Risk mitigation

The next step in the process of risk management is to respond to the identified and assessed risks shown in section 13.1. A mitigation plan is made for the risks that form the highest threats. The risks that are in the red part of Table 13.2 have to be mitigated. On top of that the events that pose a moderate risk, will also be mitigated if this can be done within reasonable resources. The mitigation plan for the risks together with their new scores can be found in Table 13.3.

New New IDRisk event Mitigation **Effect** probability severity Excessive noise Assess noise levels, D4Reduced probability 2 3 levels put tip speed limits Construct vibration assessment, make D6Excessive vibration changes where necessary, Reduced probability 2 4 re-evaluate supervisory control system Construct maintenance Poor maintainability D10 2 3 assessment, make Reduced probability and accessibility changes where necessary Extensive testing to model Excessive erosion of Reduced probability D11 how erosion behaves 2 4 secondary rotor blades under high rpm Pitch bearing fatigue Maintenance, D12Reduced probability 1 4 failure regular inspections Turbine struck Use an attractor $\mathbf{E1}$ Reduced severity 2 by lightning plate on the surface Choose location with low Bird strike $\mathbf{E2}$ bird population, out Reduced probability 3 to blades of migration pathways

Table 13.3: Risk mitigation plan

E3	Regular extreme	Choose location with a	Reduced probability	3	3
	wind gusts	low turbulence intensity	recured probability		
E5	Dirty blades	Choose airfoil that is insensitive to roughness, regular cleaning of blades	Reduced probability and severity	3	1
P1	Generator failure	Regular maintenance and inspections	Reduced probability	1	4
P2	Supervisory control computer failure	Validation & verification, use fail-safe safety system	Reduced probability	1	4
P3	Sensor failure	Validation & verification, if cost effective use redundant sensors	Reduced probability	2	3
P4	Loss of voltage control	Regular maintenance	Reduced probability	2	3
P5	Loss of frequency control	Regular maintenance	Reduced probability	2	3
P6	Cable damage	Burial and protection of cables, have redundancy in inter-connections	Reduced probability and severity	1	2
P7	Shaft failure	Maintenance, regular inspections	Reduced probability	1	4
P8	Power storage failure	Maintenance, parallel system	Reduced probability	2	3
S1	Permanent deformation of blades	Stricter requirement	Reduced probability	1	4
S4	Blade delamination	Use of coatings	Reduced probability	1	3
S5	Cracks in blades near stress concentrations	Maintenance, stricter requirement	Reduced probability	1	3
S7	Erosion of primary and secondary rotor blades	Use of a protective coating, structural health monitoring and/or regular inspections	Reduced probability	2	4
M1	Brake failure	Maintenance, redundant system	Reduced probability and severity	2	3
M2	Generator bearing failure	Maintenance	Reduced probability	1	4
M3	Actuator failure	Maintenance, back up actuator	Reduced probability	2	3
M4	Pitch control failure	Maintenance	Reduced probability	2	3

After the mitigation plan is executed, their scores for probability and severity can be changed in the risk register. These are the final risks (for now) that have to be monitored. The risk map after mitigation is shown in Table 13.4.

Table 13.4: Risk map after mitigation

Almost Certain					
Likely		E1, E4			
Possible	E 5				
Unlikely			D5, D9, D4, D10, E2, P3, P4, P5, P8, M1, M3, M4	D1, D7, D8, D6, D11, S7	D2, D3
Remote		P6	S4, S5	D12, P1, P2, P7, S1, M2	S2, S3, S6
	Neglible	Marginal	Moderate	Critical	Catastrophic

Chapter 14: Sustainable development strategy

In all fields of engineering, sustainability is becoming more important. It has to be taken into account for every new design. Even though a wind turbine is sustainable already, there are still things to consider in the sustainability aspect, those things will be discussed in this chapter.

In section 14.1 the design, production and installation phase of the wind turbine are covered. After that, the operational phase is discussed in section 14.2. The decommissioning phase is also an important aspect in wind turbine design, this part can be found in section 14.3. In section 14.4, an overview of the sustainability goals is given. Finally, the impact of noise is assessed in section 14.5. The values for noise were already calculated in the aerodynamic analysis, which is why in this chapter, the impact of noise will only be described qualitatively.

In this chapter, section 14.1, section 14.2, section 14.3 and section 14.4 are taken from [10].

14.1 Design, production and installation phase

During the conceptual design phase, sustainability will be used as one of the trade-off criteria. The design, production and installation phases will have to consider the following aspects:

- The material choices and the use of protective coatings will have to induce minimal impact on the environment. The importance of making sustainable material choices is given by the following example. It is estimated that by 2050 the demand for minerals will grow by 250% [76], increasing the need mining.
- The energy required for the manufacturing process of each wind turbine component is a good indicator of how sustainable the wind turbine concept will be.
- The assembly phase onshore should be maximised such that the turbine structures are easier and quicker to assemble offshore. This would decrease both the time, complexity and costs of the final assembly on-site [77].
- All parts of the wind turbine have to be transported to the site of installation, the effect of which has to be accounted for in the study on sustainability.
- Installation at sea requires vessels and the effect of anchoring the turbine into the seabed on marine life and environment has to be studied.
- The impact of trenching cables under the seabed will have to be minimised. Trenching cables will impact the marine environment, ornithology, shipping and navigation. [78]

14.2 Operational phase

During the operational phase sustainability needs to be taken into account in the following aspects.

- The effect of noise created by the wind turbine during operation needs to be investigated. In the case of this particular wind turbine, the secondary rotors will have high angular velocities therefore they will induce high dynamic loads and vibrations within the structure. A further elaboration on the noise levels the turbine produces and the possible effects of this is given in section 14.5.
- Vibrations from the wind turbine could be transmitted into the sea via the tower and disrupt surrounding marine animals, similar to noise.
- Counting the bird strike is also a good indicator of sustainability. Tracking the flight path of the birds can be used to evaluate the impact of the wind turbine.
- Harmful materials and coatings being used for the construction of the wind turbines can change the local pH level and increase heavy metal levels in the ocean which can lead to an unsuitable environment for fish and other marine animals in the area.
- Another indicator of sustainability is the number of species of marine animals in the surrounding area. By measuring how many species migrate from the wind farm area, the disruption of the wind turbine to the

surrounding area can be evaluated for both marine and land animals. Denmark has funded a monitoring programme to investigate effects of offshore wind farms on marine environment [79].

- The wind turbine is attached to a support structure namely a monopile. The drilling penetrates approximately 30-40m, disrupting the marine habitat [80]. A solution for this would be to contact a start-up called GBM Works that is working on a silent method for installing offshore wind turbine foundations. The company claims to install foundations more efficiently in terms of speed, environmental impact (reduction in noise levels that could influence marine life) and creating less fatigue damage to the foundation structure extending its fatigue lifetime.
- Operational life cycle is a good indicator of sustainability as well. The longer the wind turbine is able to function, the more energy can be extracted from the wind during its longer life cycle, thus contributing to the sustainability of the design. However, the longer the wind turbine is able to operate, the higher the probability that maintenance trips would be needed to ensure correct functioning of all systems.
- During maintenance, the method of the maintenance will have an impact on sustainability. If a helicopter is being used for transportation, huge noise levels are created that will disrupt the surrounding area. If a ship is being used, less noise is induced in the sky, but more vibrations will be induced in the ocean. The effects of material being used for maintenance also have to be investigated.

14.3 Decommissioning phase

Finally, the decommissioning phase of the wind turbine life cycle should be considered. Leaving the wind turbine as it is, is very unsustainable, of course. The team must think of ways to handle decommissioning in a sustainable manner. This is done through considering the following aspects.

- Re-powering the wind turbines can be considered as a means of decommissioning to decrease the costs. The foundations and transmission cables can be reused for future projects and the primary rotor can be designed for a higher lifetime such that the secondary rotors can be replaced, reusing the primary rotor.
- Environmental impact of the on-shore transportation of the turbine parts should be considered.

14.4 Key sustainability goals

In addition to the previously mentioned considerations, the design team has defined a number of key sustainability goals. These goals will define how sustainable the design shall be.

- The cost of energy plays an important role in sustainability since it is directly correlated with the efficiency of the system. The more efficient the design, the lower the cost of energy will be. The aim is that the cost of energy is competitive within the existing market with it equalling between $60-80 \in /MWh$.
- The focus of the decommissioning phase will be to try and recycle and reuse as much of the wind turbine materials and components. It is reported that approximately 83-89% of a Vestas wind turbine is recyclable [81]. Because sustainability is an important requirement, the secondary rotor wind turbine design will aim to recycle more materials than the competitors. The aim is to recycle above 90% of the wind turbine components. The tower, foundations and horizontal strut can be recycled fairly easily at their end-of-life since they are made from steel. The composite blades need to be treated onshore. The composites can either be disposed of at landfills, incinerated or recycled (mechanically, chemically or using pyrolysis). [82]. Since it is more sustainable to recycle fiberglass wind turbine blades the company Fiberglass solutions was found on the market. Both the primary and the secondary rotor blades will be recycled and reused by that company. The recycling process consists of transporting the blades onshore, cutting the blades into smaller pieces, crushing the blades, adding additives (rocks and fillers) and reusing the fiberglass blades in the form of, for example, manholes ¹.

¹http://compositesmanufacturingmagazine.com/2017/11/global-fiberglass-solutions-finds-success-recycling-turbine-blades/cited 27-6-2019

14.5 Turbine Noise

For onshore wind turbines the noise levels a turbine produces is of large importance, mainly because people do not want to live close to noisy machines. In the case of off-shore turbines noise often is of a far less concern. Still noise levels must be assessed to get an idea of the noise the machine will produce.

14.5.1 Sources of Noise

Wind turbine noise consists out of two types of noise sources, namely mechanical noise due to vibrations and aerodynamic noise because of rotating blades. For modern wind turbines, which are getting larger and larger, aerodynamic noise is the dominant source of the two. Both sources will be elaborated on in the following sections.

Mechanical noise

Most of the mechanical noise of a wind turbine gets developed inside the nacelle due to the relative movement of several components of the machinery installed. Two categories of mechanical noise exist, which are air-borne noise and structure-borne noise. Air-borne noise gets directly emitted into the atmosphere. An example for this is noise due to the vibrations of the gearbox, which reaches the atmosphere via holes which are present in the nacelle. When noise is transmitted via vibrations within the structure it is called structure-borne. The noise which comes from the gearbox is seen as the main source of mechanical noise. [83]

Aerodynamic noise

In the process of aerodynamic noise generation, several different flow phenomena play a role. Three main aerodynamic noise mechanisms can be distinguished:[83]

- Turbine blade loading noise
- Self-induced noise (Noise due to interaction between incoming air and the airfoil)
- Turbulent inflow noise

The first of this summation contains noise due to the uneven loading of the turbine blades. Its noise is related to the low-frequency spectrum and is generated because of wakes generated by other turbine blades, velocity gradients of the inflow or flow deficiencies because of obstruction by stationary turbine components.

Continuing to the second entry, which actually summarizes a group of noise sources and covers noise generated by the airfoil itself. This noise will always be present when a flow goes around the airfoil, even for perfectly homogeneous flows. This type of noise is associated to laminar or turbulent boundary layers and their interaction with the airfoil. It generates either noise of a broadband spectrum or noise with a tonal nature.

The final entry of the list, turbulent inflow noise, is noise due to atmospheric turbulence. It causes local pressure to fluctuate or fluctuations in the global net force around the section. This causes both high- and low-frequency noise. Due to the unpredictable nature of turbulence, this type of noise is difficult to predict [19][83].

14.5.2 Effects of noise

Now that larger and larger wind turbines are being build, more studies are done on the effects of wind turbine noise on humans. The main effects of turbine noise are annoyance and sleep deprivation. The main reason for this is the rhythmic character of the sound and the low frequency components of it [84]. However, since the turbine will be located at sea, influence on humans will not be too much of an issue for this turbine. When it comes down to sustainability for off-shore turbines, the effect of noise on the animals living in the sea is much more of an interest. Unfortunately very little is known about the effects of wind turbine noise on the health of the animals [85].

In section 5.14 the noise the turbine produces is estimated both at 0 and 100 meters distance from the tower and set to be 62.2dB(A) and 79.2dB(A)) respectively. These values would be experienced by humans as annoying, therefore it is possible this is also the case for animals. As an important side note however, these sound pressure levels are corrected for the sensitivity of the human ear, thus the A-weighted SPL correction is applied, and as an consequence the effects of lower frequency are damped out drastically. Therefore, noise levels can be experienced differently by animals with a different hearing range from that of the human ear.

14.5.3 Recommendations

The detailed analysis of an effects of the estimated noise levels for maintenance or repairs on animals, but also on people must be assessed in the future. If the noise levels have a negative influence on a wildlife, measures must be taken to limit either the noise or the noise effects on wildlife. Limiting the noise generated by the turbine could be reached by altering the geometry of the rotor, such as sweep or choosing a different airfoil. Limiting the effects of the noise on wildlife could be done by locating the turbine somewhere with very little animals. If such a location is chosen, negative effects on the animals because of turbine installation can be minimized. The effects of these measures however must be studied and considered if they are worth the extra cost.

Another aspect which must be investigated is the noise transmitted underwater due to vibrations of the wind turbine. For this, an extensive analysis on the vibrations of the several subsystems must be done. Once the mechanical noise levels are determined, their effects on the creatures living underwater must be assessed.

Chapter 15: Cost analysis

This chapter will combine all the previously analyzed subsystems in order to obtain a cost estimation. In section 15.1, a breakdown of all the costs is shown. With the values calculated in this section, a return on investment and operational profit can be obtained in section 15.2. Since the cost is one of the most important requirements of the design, it is important to do a sensitivity analysis, which can be found in section 15.3. The calculations done in this chapter will also be verified and validated in section 15.4. Finally, some recommendations regarding the cost are made in section 15.5.

15.1 Cost breakdown structure

In this section the cost of each component and aspect of the turbine over its life cycle is calculated and presented in an overview called the cost breakdown structure. The equations used to obtain the cost of the turbine components are taken mostly from the National Renewable Energy Laboratory (NREL) cost estimation model [60]. This cost model serves as a crude approximation, as the equations are based on offshore HAWT. As such, modifications are made to account for the primary rotor (which is a VAWT) and for the secondary rotor which has a higher rpm than conventional HAWT. The modifications from the cost model are summarized below and the main equations can be found in Table 15.1.

- Equation 15.7: Material cost of the blade is calculated based on the blade mass and material cost per kilogram. Primary blade are made out of glass fiber composite with 60% glass fiber and 40% epoxy, hence \$3.29 per kg assuming \$6 per kg for epoxy and \$2.5 per kg for glass fiber [53]. Secondary blade are assumed to be made out of 50% glass fiber and 50% epoxy for this cost estimation.
- Cost of the generator was derived based on the sized generator in chapter 8 .
- Transportation cost is calculated based on the machine rating. The value of \$250/kW was derived by scaling the logistic cost diagram found in [86].
- Offshore maintenance cost is assumed to be 30% with respect to the life cycle cost [87]. The same assumption can be found in the wind turbine with similar configuration [8].
- Eq.15.23: Cost of steel for the cost estimation of the tower is changed to \$2.55 per kg due to different steel being used for the tower.
- The unit of the cost in NREL is in \$, which was at the end converted to €using the conversion rate of \$1 per 0.9 €[88].
- From chapter 12 it is calculated that the availability is 92.5 % which decreases the annual energy production (AEP) by 7.5 %.
- Nose cone mass, bearings cost and yaw drive cost are derived by scaling linearly with diameter from 3MW offshore wind turbine available in [60].
- The Fixed charge rate (FCR) in Equation 15.1 is estimated to range between 7% and 8.8 %. In this range the upper limit refers to the nominal FCR and the lower limit refers to the real FCR. Both extremes are used in the calculation to find a Cost of Energy range [89]

The Cost of Energy (COE) is the unit cost to produce energy in (\in/MWh) [13]. This can also be formulated as the total cost divided by the energy produced. The total cost includes: Manufacturing, commissioning, operations and maintenance over the entire design life and providing the necessary infrastructure at the site [90]. A more detailed equation of the COE is given by Equation 15.1.

$$COE \left[\text{€/kWh} \right] = \left(\frac{(FCR[1/yr] \cdot ICC[\$])}{AEP_{net}[kWh/yr]} + AOE \left[\$/kWh \right] \right) \cdot 0.9 \left[\text{€/\$} \right]$$

$$(15.1)$$

To calculate the COE using this equation, the annual operating expenses (AOE), the fixed charge rate (FCR) and the initial capital cost (ICC) are needed. The AOE can be calculated using Equation 15.2 and the FCR was estimated to be between 0.07 to 0.088 per year by the NREL [89]. This FCR includes the return on debt and equity, financing fees, depreciation, property tax and insurance and income tax. The ICC is calculated using the costs of the primary rotor, the secondary rotor, the drive train, the tower, the control and safety systems and

Table 15.1: Component cost equations

Identification	Equation
Eq. 15.7	Blade Cost [\$] = $\frac{\text{(Blade Mass} \cdot 3,66 \cdot BCE + 2.7445 \cdot r[m]^{2.5025} \cdot GDPE)}{(1-0.28)}$
Eq. 15.8	$Hub Cost [\$] = Hub Mass [kg] \cdot 4.25 [\$/kg]$
Eq. 15.9	Total Pitch System Cost $[\$] = 2.28 \cdot (0.2106 \cdot (2r [m])^{2.6578})$
Eq. 15.10	Nose Cone Cost [\$] = Nose Cone Mass [kg] · 5.57 [\$/kg]
Eq. 15.11	Shaft Cost $[\$] = 0.01 \cdot D[m]^{2.887}$
Eq. 15.12	Total Bearing System Cost [\$] = $2 \cdot \text{Bearing Mass [kg]} \cdot 17.6$
Eq. 15.13	Brake Cost [\$] = 1.9894[\$/ kW] · Machine Rating [kW] - 0.1141[\$]
Eq. 15.14	Generator Cost $[\$] = \420.89
Eq. 15.15	Total Cost VSE [\$] = Machine Rating [kW] \cdot 79 [\$/kW]
Eq. 15.16	Mainframe Cost $[\$] = 303.96 \cdot (2r[m])^{1.067}$
Eq. 15.17	Electrical Connection Cost [\$] = Machine Rating [kW] \cdot 40 [\$/kW]
Eq. 15.18	Hydraulic, Cooling System Cost $[\$] = \text{Machine Rating } [kW] \cdot 12 \; [\$/kW]$
Eq. 15.19	Nacelle Cost [\$] = 11.537 [\$/kW] · Machine Rating [kW] + 3849.7 [\$]
Eq. 15.20	Total Cost Tower [\$] = Mass [kg] $\cdot 2.55$ [\$/kg]
Eq. 15.21	Total Cost Control $[\$] = \$55,000$
Eq. 15.22	Offshore BLC [\$/yr] = 0.00108 [\$/kWh] \cdot AEP _{net} [kWh/yr]
Eq. 15.23	Offshore LRC [$\$/yr$] = 17 [$\$/kWyr$] · Machine Rating [kW]

the additional costs for offshore adjustment. The costs for the offshore adjustment are taken from the NREL model and therefore not explicitly stated here [60].

AOE
$$[\$/kWh] = LLC [\$/kWh] + \frac{(O\&M[\$/yr] + LRC[\$/yr])}{AEP_{net}[kWh/yr]}$$
 (15.2)

The last piece unknown for the cost of energy calculation is the operation and maintenance cost (O&M). This is needed to estimate the AOE and it is estimated to be approximately 30 % of the life cycle cost [87]. This assumption is a rough approximation and the O&M cost will probably be reduced due to the higher availability compared to conventional HAWT [8]. This has been explained in more detail in chapter 12. Apart from this it is also known that the cost for O&M is heavily dependent on the location of the wind turbines [91]. From [91] it becomes clear for example that the difference in O&M cost between IJmuiden Ver and Hollandse Kust (Zuid) already equals 35 %. Therefore choosing a location with good site characteristics will reduce the O&M cost even further, this includes distance to the nearest harbour, water depth and soil conditions.

The results from the cost model lead to the cost breakdown structure as shown in Table 15.2. This structure contains the ICC and the levelized cost of the wind turbine and how they relate to the total cost of energy. The total cost of energy is calculated using Equation 15.1 and the result is shown below. As explained in the beginning of the section, the FCR is taken as a range from 0.07 to 0.088 which results in a range for the COE as shown below.

$$COE = \left(\frac{0.088[1/yr] \cdot 2.20 \cdot 10^7[\$]}{4.65 \cdot 10^7[kWh/yr]} + 0.0302[\$/kWh]\right) \cdot 0.9[\$/\$] = 0.0585[\$/kWh]$$
(15.3)

$$COE = \left(\frac{0.07[1/yr] \cdot 2.20 \cdot 10^{7}[\$]}{4.65 \cdot 10^{7}[kWh/yr]} + 0.0302[\$/kWh]\right) \cdot 0.9[\$/\$] = 0.0478[\$/kWh]$$
(15.4)

The COE of the design can be compared with ones from conventional HAWTs and wind parks as reported by the PBL [91]. The PBL estimates five wind parks in the Netherlands where the COE ranges from 61 to 78 $[\in]$ /MWh]. The O&M cost in this document does not include the decommissioning cost which is included in Table 15.1. This means that the current design which has a COE between 47.8 to $58.5 \in]$ /MWh is already competitive with existing wind turbines and with the possibility of reducing the O&M cost it will become even more competitive as will be proven in the sensitivity analysis at the end of this chapter.

Table 15.2: Cost breakdown structure

Components			Components	COE [%]	Cost [k€]
		Duine any not an	Pitch mechanism, rotor lock	0.95	292
		Primary rotor	Blades	11.60	3,564
			Pitch mechanism, rotor lock	0.02	7.673
		Secondary rotor	Blades	0.37	115
			Hub + nose cone	0.19	68.91
			Generator	1.23	378.8
			Rotor brake	0.09	26.86
	Turbine		Nacelle cover	0.53	162.7
		Nacelle system	Nacelle structure	0.06	17.56
			Shaft and bearing	0.19	59.1
			Electrical connections	1.76	540
Initial capital			Hydraulic and cooling	0.53	162
costs (Non-		Electrics and control Variable speed system		3.47	1,067
recurring cost)		Tower		3.59	1,102
		Control, safety system	and condition monitor	0.16	49.5
			Support structure	8.79	2,700
			Transportation	7.33	2,250
	Balance of	of station	Port and staging	0.59	180
			Personnel access equipment	0.18	54
			Scour protection	1.61	495
			Installation	2.93	900
			Electrical interface	7.62	2,340
	Offshore	component	Offshore warranty	4.23	1,299
			Marinazation	3.35	1,030
			Surety bond and permit	2.96	909
	<u> </u>	<u> </u>	O&M	30.00	1,067
Levelised cost (1	Recurring of	cost)	BLC	1.27	45.22
			LRC	4.30	153

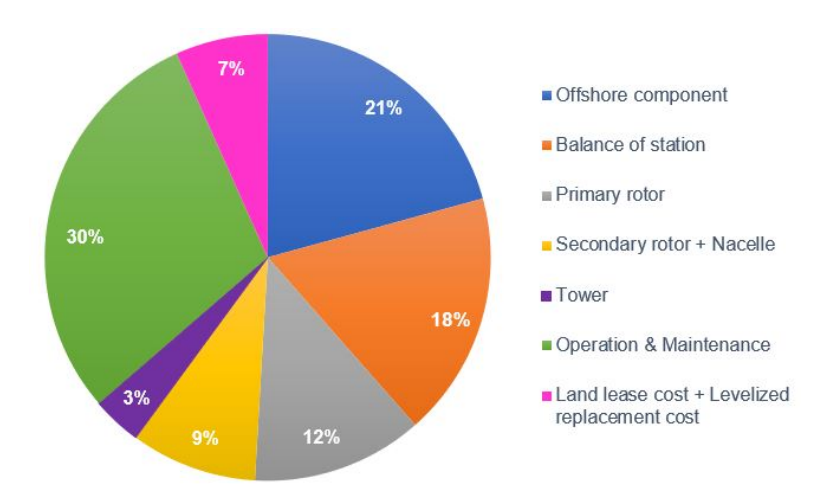


Figure 15.1: Cost breakdown

15.2 Return on investment and operational profit

The return on investment and operational profit can be estimated using the cost breakdown structure calculated in the previous section. The total cost of the turbine was divided in the previous section as initial capital cost (ICC) and levelised cost. These two values and cost of substation are the expenses of the system. The profit of the system is determined by the whole sale price of the electricity which is estimated to be equal to 0.0714 [\in /kWh], or 71.4 [\in /MWh]. This is based on the electricity price which equals to 204 [\in /MWh] in Europe and whole sale equals to 35% of electricity price [92]. This price will change in the coming years and currently there is a downward trend but in this section the price for energy is assumed to be constant.

The average interest rate is assumed to be equal to be constant and equal to $1.00\%/yr^{-1}$. The operational profit (OP) for a given year can then be calculated using Equation 15.5, where OP_0 is the ICC. OP and ROI are calculated assuming the design of 1GW wind farm [93] in which currency was converted from 1£to $1.12 \in {}^{2}$.

$$OP_{i+1} = (OP_i \cdot \frac{100 + interest[\%]}{100} - AOE \ [\$/kWh] + POE \ [\$/kWh] \cdot AEP_{net} \ [kWh/yr]) \cdot \frac{100 + inflation \ [\%]}{100}$$
(15.5)

Operational profit over 25 years is shown in Figure 15.2. This graph shows that payback period is 11 years and that the total operational profit is 3.4 Billion euros after 25 years.



Figure 15.2: Operational Profit vs Time

The return of investment (ROI) can be calculated using Equation 15.6 and the annualized ROI can be calculated using Equation 15.7³ with the input from Table 15.3. The calculated value of ROI is 67.8%, and annualized ROI is 2.09% over 25 years operational period.

$$ROI = \frac{\text{Net return on investment } [\mathbf{\epsilon}]}{\text{Cost of investment } [\mathbf{\epsilon}]} \times 100\% = \frac{3,356,211,919}{4,947,291,779} \times 100\% = 67.8\%$$
 (15.6)

Annualized ROI =
$$[(1 + ROI)^{1/n} - 1] \times 100\% = [(1 + 0.678)^{1/n} - 1] \times 100\% = 2.09\%$$
 (15.7)

15.3 Sensitivity analysis

In this section, the influence of change in design parameter on the outcome is analyzed both quantitatively and quantitatively for each parameter. For each design parameter, analysis of its influence on the ICC, AOE, AEP, COE of the wind turbine and payback period and OP of the wind farm is discussed. For the quantitative analysis, Table 15.4 shows the change in outcome in percentage when each design parameter is increased and decreased by 10%.

¹https://tradingeconomics.com/netherlands/bank-lending-rate, cited 21-6-2019

²https://www.xe.com/currencyconverter/convert/?Amount=1&From=GBP&To=EUR cited 23-6-2019

 $^{^3}$ https://www.investopedia.com/articles/basics/10/guide-to-calculating-roi.asp, cited 21-7-2019

Table 15.3: Input variable for ROI with 25 years operational period

Value
1000
1979
2573
39.2
28
5.6
246.4
56
8.96
11.2
4947
8304
1
67.8
2.09

Table 15.4: Cost sensitivity analysis

Parameters	New value	ICC	AOE	AEP	COE	Payback period	OP in 25 years
Original value		19.8 [M€]	1.03 [M€/yr]	$\frac{46.5}{[\mathrm{MWh/yr}]}$	58.5 [€/MWh]	11 [yr]	3,356 [M€]
Increasing valu	ies						
Machine rating	11[MW]	6.1%	7.2%	10%	-3.2%	0%	16%
Capacity factor	0.6281	0%	0.63%	10%	-8.9%	-9.1%	26%
O&M	1.185 [M€/yr]	0%	8.1%	0%	3.1%	9.1%	-6.6%
Rotor mass	369.3 [tonnes]	0.95%	0.69%	0%	0.85%	9.1%	-1.2%
Downtime	0.077	0%	-0.047%	-0.75%	0.74%	9.1%	-1.9%
Whole sale	78.5 [€/MWh]	0%	0%	0%	0%	-9.1%	24%
Decreasing val	ues						
Machine rating	9.0 [MW]	-6.1%	-7.2%	-11%	4.7%	9.1%	-18%
Capacity factor	0.5139	0%	-0.67%	-11%	12%	27%	-28%
O&M	0.9695 [M€/yr]	0%	-8.1%	0%	-2.3%	0%	4.8%
Rotor mass	302.1 [tonnes]	-0.95%	-0.74%	0%	-0.12%	0%	-0.74%
Downtime	0.063	0%	0.047%	0.75%	-0.73%	0%	2.1%
Whole sale	64.3 [€/MWh]	0%	0%	0%	0%	27%	-28%

Increasing machine rating will increase the ICC, AOE, AEP, OP but reduced the COE. The ICC and AOE are increased due to an increase in the cost of the generator, electronics, permit and many more which require bigger components to withstand higher power. The AEP is increased simply due to more power production. The COE was reduced even when the ICC and AOE increase due to an increase in AEP which out scaled influence of the ICC and AOE on the COE. The OP increased due to a reduction in COE as well as increase in AEP.

There is no change in the ICC when the capacity factor is increased because changing the capacity factor will not change the cost of each component, however, an increase in the capacity factor increases the AEP which results in a reduction of the COE. An increase in the capacity factor also increases the AOE because bottom lease cost scales (part of AOE) with AEP. As the COE is reduced, the OP is increased.

A change in O&M affects only the AOE, COE and OP. The AOE simply increases when O&M is increased, which leads to an increase in the COE. As the COE is increased, the OP is reduced.

An increase in rotor mass increases rotor cost, hub cost and many more due to the fact that more material will be required and that has to be supported. This results in an ICC increase, which increases the AOE and the COE. The OP is reduced because of increase in the COE.

An increase in the downtime reduces the AOE because the bottom lease cost is reduced. The AEP is reduced as the downtime increases. A reduction in the AOE and AEP contributes to an increase in the COE, which reduces the OP.

Changes in the whole sale price have the biggest effect on the payback period and the operational profit where decreasing the whole sale price to $64.3 \in /MWh$ has the biggest effect.

From the quantitative analysis in Table 15.4 it becomes clear that the capacity factor has the biggest influence on the cost of energy. However even when the the capacity factor would be decreased by 10 % the cost of energy requirement would still be met. The machine rating and 0&M also have a large influence on the COE and the whole sale price has the biggest influence on the return of investment.

15.4 Verification and validation

The cost model was made in Microsoft Excel. For verification, all equations which have been used for the cost analysis were checked to avoid typos. Output of each equation was also checked using different input parameters to see if the value changes as expected. The output of cost model was compared with the components cost of 3MW offshore wind turbine available in [60]. These cost are then scaled up to fit 10MW accordingly with their scaling factor used in [60]. Difference between these two values are checked to see if the output of cost model is valid.

The cost model was validated by comparing a representative cost split from [94] with the cost split from the model. This is already presented in a table in [11] on page 300 where also the differences in percentages are shown. From this comparison it becomes clear that the models deviate on same parts to a large extent. Both models use the mass of the components to estimate the cost and these differences can thus be explained by the different trends and data that are used. Since the NREL model is newer it has more data available for these trends and could therefore be considered to be more accurate. However these differences should still be considered and taken into account for further detailed development of the cost breakdown of the wind turbine.

15.5 Limitations and recommendations

The cost estimation method used in this analysis has some limitations. To improve the accuracy of the cost model, several recommendations are given below.

First of all the labour cost for making the blades for the VAWT has to be researched to get to a better value than the one used now. It is hypothesized that the labour cost for the VAWT will be reasonably lower than the labour cost for a HAWT but this has to be researched.

The O&M cost should also be researched further because the current analysis is lacking accuracy on this part. The O&M cost is particularly important because it is 30% of the total COE at his moment. A better defined O&M would bring down the margin of error and, possibly, the total COE. The location of the wind park is also of importance as it has a large influence on the cost of O&M. Some locations are significantly harder to install turbines on and also the distance from the harbor plays a role. The recommendation is that more research should be done for the location of the wind turbine to lower the COE.

The cost estimation method used is an old method from 2003 while the wind energy sector is constantly evolving and each year new data and trends become available. It is recommended that for further cost research newer cost models should be used as these will not only provide more accurate results, they will also have a lower COE due to a lower overestimation.

Overall the COE of energy is below the required $80 \in /MWh$ but it is thought that this is an overestimation due to the reason mentioned above. It is unclear to what degree this is an overestimation and this should therefore also be researched in the future.

Chapter 16: Market analysis

An extensive market analysis of the wind energy market, in which the SRVAWT has to operate, has been performed in the first phase of the design project, as presented in the baseline report [10], and will be shortly discussed in this chapter. The SRVAWT design has been developed with the characteristics and developments of the current market in mind. At this point, the market analysis comes into play again. The SRVAWT concept has been translated into a refined preliminary design and now its performance is to be compared with the current market, to predict its competitiveness.

This chapter will start off with a general description of the current wind energy market in section 16.1. It will continue with the observed developments within this market in section 16.2. An overview of current wind turbines that are seen as the main competitors of this design is shown in section 16.3. This concludes the initial market analysis and the chapter finishes with a discussion of the performance and competitiveness of the SRVAWT within the wind energy market in section 16.4.

16.1 The current wind energy market

This section describes the current state of the wind energy market. In subsection 16.1.1, a general overview of the global market is given, both for onshore and offshore wind energy. The European offshore market is then discussed in subsection 16.1.2, as this is the market that this turbine is intended for.

16.1.1 The global market

2018 saw the installation of 51.3 GW of wind power worldwide, of which 75% was installed by the following countries: Germany, USA, India, Brazil and China. Among these, China has been the global leader in wind power since 2008, with a current total capacity of over 200 GW. The Global Wind Energy Council estimates an annual wind power capacity increase of 2.7% for the coming years [95].

Danish turbine manufacturer Vestas is the global market leader, their turbines accounting for 17% of all installed wind power capacity [96]. Siemens-Gamesa, formed through a merge between Siemens Wind Power and Gamesa, and in 2018, commissioned over 4GW of power across Europe, the Americas, and Asia. Goldwind is the largest Chinese manufacturer and accounted for a third of the 19.3GW of wind power installed in China over 2018 [96]. General Electric (GE) Renewable Energy installed a total of 5GW last year, mostly in the USA, where the manufacturer is based. GE is currently working on the development of the world's largest and most powerful wind turbine, the 12MW Haliade-X [97].

16.1.2 The European offshore market

Within Europe, the offshore wind energy market has been steadily growing since 2008. 2.6GW of offshore capacity was installed in 2018, resulting in a total of 18.5GW, most of which located in the North Sea. The largest contributors to this newly installed capacity were Germany and the UK, together accounting for 85% of it [98].

Siemens Gamesa is the largest manufacturer in Europe by far, responsible for 69% of the installed offshore capacity, or 12.8GW. MHI Vestas comes second, with 24%, or 3.8GW installed capacity in total. Servion, Bard Engineering and GE are smaller players within the European offshore market, accounting less than 5% each [99].

When it comes to the turbines used within European offshore wind farms, their average rated power is steadily increasing. The current average rated power lies at 6.8MW, however the MHI Vestas Offshore V164, with a rated power of 8.8MW, was first installed in the UK last year [99]. Current developments indicate a further increase in the average turbine rated power: both MHI Vestas and Siemens-Gamesa are developing wind turbines with rated powers in excess of 9MW, estimated to be ready for installation within a few years [99].

16.2 Developments

Not only the current wind energy market is of importance to this specific project. The development of a wind turbine from conceptual design up to being build and ready for operation takes many years. Therefore, designers must think about developments going on in the market to predict the future market in which they will end up. Several developments going on in the current wind energy market will be discussed next.

The most prominent development in the wind energy market is the increase in offshore wind farms. It took a long time since the operation of the first wind turbines before the first offshore turbines were built. However, at this moment there is a great increase going on in the number of wind farms to be built offshore [7]. Also the trend of going further offshore than before is more than noticeable [98]. This is largely due to the larger area which is available offshore, higher wind velocities, as well as a decrease in noise and visual impact.

The capacity of wind turbines is increasing. This is partially due to increased sizes, but also due to increased efficiency. In addition, wind farms are increasing in capacity [98], which is partially due to the increase in size of the wind turbines themselves, but also due to more turbines being placed in a single wind farm. A decrease in the capital cost per unit of installed power comes with this upscaling of wind farms. The reasons include learning effects, technology improvements and economies of scale.

Capacity factors are expected to increase gradually in the future. In Denmark, they have been increasing over the past decades, from about 25% around 1992 to as much as 45% in 2012 [100]. Globally, the International Renewable Energy Agency (IRENA) predicts capacity factors to increase up to 50% by 2022 [101]. IRENA also mentions one project having achieved a capacity factor of 65% in Scotland. This definitely shows the potential within the wind energy market. One reason for increasing capacity factors is the increasing number of wind turbines installed globally.

16.3 Competitive designs

The biggest wind turbine currently in operation has a rated power of 8.8 MW, installed in Scotland [102]. However, wind turbines of 10 MW rated power and higher have been designed and are planned to be built. These designs are most probably competitors for the proposed design. A study was performed on a few of these designs, as well as on the 8.8 MW turbine currently in operation. The data found on these designs is presented in Table 16.1 1 .

Wind turbine	Manu- facturer	Rated power [MW]	Blade mass [t]	Nacelle mass [t]	Rotor Diameter [m]	Blade length [m]	Hub height [m]	Angular velocity at rated [rpm]	Operational liftetime [yrs]
Haliade-X	General Electric	12	55	600	220	107	135	7.8	-
SG 10.00- 193 DD	Siemens Gamesa	10	-	-	193	94	-	-	-
V164-10.0 MW	MHI Vestas	10	35	390	164	80	105-140	9.95	25
SeaTitan 10 MW	AMSC's Windtech Solutions	10	-	-	190	-	125	10	-
V164-8.8 MW	MHI Vestas	8.8	35	390	164	80	105-140	-	-

Table 16.1: Key data of competitive turbines [102] [103] [104] [105] [106]

16.4 The SRVAWT on the market

This section describes the expected chances of the SRVAWT on the wind energy market. It includes a SWOT analysis, a qualitative and a quantitative market performance assessment.

¹https://en.wind-turbine-models.com/

16.4.1 SWOT analysis

An analysis of the strengths, weaknesses, opportunities and threats (SWOT) of a new concept is a useful tool to evaluate its chances on the market. Both internal (strengths, weaknesses) and external (opportunities, threats) aspects of the developed product are evaluated. It forces the developer to think critically about what sets their concept apart from its competition, and what opportunities and challenges it might face when brought on the market. A preliminary SWOT analysis for the SRVAWT was performed in the baseline report [10]. The SWOT analysis for the final design is summarized below.

Strengths

• The higher rpm of the secondary rotors eliminate the need for gearboxes or large diameter multipole generators and allow to design for a smaller and lighter drive train. This results in a lower total mass and an easier installation process. Corresponding cost reductions are expected.

Weaknesses

- A shorter lifetime of the secondary blade coatings is expected due to the higher rpm, which also results in more frequent secondary blade maintenance.
- The high rpm of the secondary rotors will cause high noise levels. However, this is not necessarily a problem, as the turbine is intended for offshore operation.
- Structural implications are expected due to the secondary rotors attachments to the primary blades. This
 will likely cause the primary rotor blades to be heavier and more expensive than conventional turbine
 blades.

Opportunities

- The concept developed is quite innovative and innovation is needed to keep the growing rate of the offshore wind energy sector.
- Thanks to fewer components and a higher overall reliability, this turbine is expected to require less maintenance than conventional turbines. This means that the turbine will be suitable to be placed further offshore than conventional turbines, resulting in a higher capacity factor and even higher competitiveness due to increased wind speeds.

Threats

- The concept is completely new and has not been tried before. Based on one or more of several characteristics it may turn out that the proposed new concept is not feasible or competitive in the modern world.
- Tried and true solutions, which have been proven to work, may be preferred among investors over a new, innovative design as they carry less risk than radical new designs.

16.4.2 Qualitative market performance prediction

Now that calculations have been made regarding the SRVAWT cost of energy, return on investment, and operational profit, an initial prediction can be made of how the turbine will perform on the market. This is mainly done by considering what sets this turbine apart from its competition, and what the turbine can contribute to the developments in the wind energy sector.

A cost of energy range of 47.8 to $58.5 \in /MWh$ was found during the cost analysis in chapter 15. This complies with the top-level requirement given and is in the range of the average cost of energy of offshore wind power, which lies between 60 and $80 \in /MWh[1]$. The SRVAWT will thus provide power at a lower cost to other current offshore wind turbines.

The difference with respect to conventional turbines comes into play when the focus is shifted towards the future of the wind energy sector. Some recent developments which are expected to continue in the coming years, have been described in section 16.2. In case this turbine is able to jump in on the trends taking place and answer to the future demands from the industry, a large degree of competitiveness is expected.

The first development which the SRVAWT could show a significant benefit in, is the trend of building wind farms further offshore. The SRVAWT is expected to be especially suitable for (far) offshore operations, due to its lower maintenance needs, compared to conventional turbines. Sites which are further offshore generally have higher wind speeds, resulting in a higher capacity factor and energy yield. This has the potential to bring the cost of energy down further.

Upscaling of turbine capacity is another trend which the turbine may be able to jump into. Within conventional turbines, upscaling of rated power requires larger blades and imposes significant additional (dynamic) loading, most notably on the drivetrain. A 2012 study at the University of Leuven wrote that drivetrain reliability may decrease under upscaling due to these increased loads. In addition, larger issues are encountered concerning noise and vibrations, especially those coming from the gearbox[107]. The SRVAWT is expected to encounter fewer issues in upscaling than conventional turbines, due to its vastly different configuration. The most obvious way to upscale the turbine is to add more primary rotor blades with secondary rotors attached to them, which could increase the turbine capacity significantly. More research is recommended into the possibilities of this. Alternatively, the relatively small secondary rotors could be upscaled to a higher capacity. This would not introduce as many drivetrain issues as it does in conventional turbines, due to the absence of gearboxes. However, noise coming from the secondary rotors might increase if this option is chosen.

16.4.3 Quantitative market performance prediction

Building further on the developments described in section 16.2, the potential for the need for the proposed SRVAWT can be shown. As predicted by [7], added offshore wind capacity in Europe ranges between 2 and 4 GW per year until 2022. In addition, [108] expects the cumulative offshore installations in Europe to have reached at least 49.5 and at most 100 GW by 2030, meaning the annual installations will increase as well. Showing the market potential, the question arises how long the development of the SRVAWT will take and when it thus will be ready for installation.

Completion of a wind farm project for a specific turbine may take a decade². Such a project can only start when the considered turbine has been developed to a far extent, but it does not necessarily have to finished completely. It is estimated that the development of the SRVAWT will take at least five to ten more years before it can be manufactured, installed and tested. Therefore, it is expected that the SRVAWT will not be operated within an offshore wind farm before 2035.

Comparing the market shares of different wind turbine manufacturers within Europe's offshore market, as presented subsection 16.1.2, quite some differences are noted. Three main market leaders are identified, namely Siemens Gamesa, MHI Vestas and Envion, with market shares ranging between 5% and 70%. Also General Electric Renewable Energy should be added to this list, as it is a fast growing contributor to offshore wind energy in Europe [98]. From these numbers it is concluded that a 5% market share should be reasonable to be attained within the European offshore wind energy market by the year 2040. Here it is assumed that the SRVAWT will be able to compete with the largest and best wind turbines designed today. This 5% market share is expected to correspond to an installation of 2 to 5 GW of wind capacity, or 200 to 500 SRVAWTs, depending on the difference between the current predictions and the real developments in the future. Depending on the developments of wind farm size this would correspond to 1 to 5 wind farms.

²http://www.futuren-group.com/en/lenergie-eolienne/realisation-dun-projet-eolien

Chapter 17: Technical Resource Budgeting

In this chapter a look will be taken at how the values for mass and cost of the turbine evolved over the maturity of the design. At the start of the project budgets have been set regarding these mass and costs, together with their contingency allowances for several design maturities. These budgets were initially presented in the baseline report[10]. First a look is taken at the mass, section 17.1, and thereafter at the cost of the turbine section 17.2. The latter will start with a few additions to what has been stated in the baseline report[10].

17.1 Turbine mass

The mass of the turbine has been one of the characteristics on which a budget has been set at the beginning of the project. The reason for this was the fact that one of the top-level requirements was given to be that the design 'Shall have a reduction in overall structure weight compared to conventional wind turbines'.[1] The mass of a conventional 10MW wind turbine was at the time found to be 1300 tonnes[109]. Also for different components the mass fractions where given of total mass regarding a conventional wind turbine. An overview of the estimated values, together with the values for the different design maturities is given in Table 17.1. It was expected the fraction for the drive train would go down, because of the larger angular velocities of the secondary rotors. The mass of the blades however was expected to go up, mainly because of the fact that the primary rotors must carry the generators and structure, but also because there simply are more blades compared to a conventional turbine.

Taking a look at how the mass evolved when the design matured, it can be seen that the mass estimated for the preliminary design, Table 17.1, is much higher than what had been set to a limit, namely 2487 tonnes compared to limiting 1300 tonnes. Even with the allowed contingency of 20%, the mass remains way above the budgeted value. The expected trend however of a decrease in drive train mass, one of the main objectives of this design, indeed was identified. The expected trends regarding the increase in blade mass and fixed fraction in tower mass were not identified.

Moving on the the refined preliminary design, this has a total mass of 914 tonnes. This is below the limiting budget of 1300 tonnes set at the beginning of the project. For the refined preliminary design a contingency of 10% was expected for the blades, and 5% for the tower and generator. Applying those contingencies to the obtained values it gives an upper limit for the turbine mass of 945.2 tonnes. Therefore, it can be stated that the mass is within its set budget. Taking a look at the mass fractions and their trends compared to those of a conventional turbine, indeed the expected increase in blade mass and decrease in drive train mass can be observed. As predicted, the mass fraction related to the tower is approximately the same as that for conventional wind turbines.

Although the mass of the machine is within bounds for the current design stage, it must be noted that, as for most engineering projects the mass tends to increase when the design matures. Therefore the mass must be strictly monitored during future design to avoid it increasing and exceeding the limit.

Component	Total	Secondary rotor	Primary rotor	Drivetrain	Tower
Budget	1300	227	.5	418.6	653.9
	100%	17.5	32.2%	50.3%	
Preliminary design	2487.4	2.2 (x2)	212.5 (x2)	62 (x2)	1934
	100%	0.18%	17.1%	4.99%	77.8%
Refined preliminary design	914	16.4 (x2)	154 (x2)	29.6 (x2)	484
	100%	3.71%	34.8%	6.70%	54.8%

Table 17.1: Evolution of mass for different design maturities. Masses are in tonnes.

17.2 Cost

The second characteristic on which for which a budget has been determined, is the cost of the turbine. By one of the requirements it was determined that the ICC for the turbine to be designed had to be equivalent to

that of conventional turbine, for which $1000 \in /kW$ is taken as a rule of thumb. Therefore, since the design will produce 10MW, the upper limit regarding the budget is 10 million euros for the manufacturing costs. At the start of the project only the manufacturing costs were set as a budget, however as the project moved one it was realized that cost of energy also a driving design parameter, hence therefore this also has been added to the budget. The budget as set for the COE is deducted from the top-level requirements, where is was stated that the COE shall be between 60 and $80 \in /MWh$. The initial set budgets, together with their obtained values for different design maturities, are presented in Table 17.2.

During the preliminary design, the manufacturing cost were not determined. The reason for this was the fact that too little information was known about the nature of the turbine. However an estimate on the COE was performed and determined to be $90.25 \in /MWh$. The contingency allowance for this design phase was determined to be 20%. Applying this to the COE in such a manner that the actual COE is lower than what has been determined, this will equal $72.2 \in /MWh$. This would be within bounds of the set budget.

For the refined preliminary design a manufacturing cost of 7.5 million euros was found, which resulted in a COE range of 47.8 to $58.5 \in /MWh$. For this point in the design, a contingency of 10% was allowed. Looking at the manufacturing cost, in case of a 10% contingency, this will equal 8.25 million euros, which will still be within bounds of the set budget. The value for COE is within the set budget. Since still a contingency of 10% is allowed it could be that the actual value for COE is larger than the upper bound of $80 \in /MWh$.

Although both the manufacturing cost and the COE are within the set budget for the current design maturity, still special care should be taken regarding the cost of the turbine during future design. Since the COE already is close to the upper boundary of the budget, it must be assured it does not exceed this boundary.

Table 17.2: Evolution of cost for different design maturities

	Manufacturing [€]	COE [€/MWh]
Budget	10 million	60-80
Preliminary design	unknown	90.25
Refined preliminary design	7.5 million	47.8 to 58.5

Chapter 18: Sensitivity analysis

A sensitivity analysis for several aspects of the wind turbine design has already been performed in the chapters before. An overview of these sections is shown in Table 18.1. A sensitivity analysis performed on the system as a whole shows how the different subsystems relate to each other and how a change in certain design parameters affects the entire design. It is possible that a design parameter from one subsystem has an effect on another subsystem which would affect the entire system, however this would not be detected in case the sensitivity analyses stayed limited to the individual design parts.

Table 18.1:	Overview	of the	sensitivity	analyses	already	presented

Design element	Sensitivity analysis section
Initial sizing	section 4.3
Aerodynamic design	section 5.10
Control optimisation strategy	section 7.5
Power and electronics	section 8.3
Structural analysis	section 9.7
Cost analysis	section 15.3

The turbine design procedure starts with an aerodynamic analysis where, for a certain initial sizing, the aerodynamic characteristics are determined (lift curves, planform design, aerofoil selection, etc.). These characteristics are an input for the control optimisation strategy which outputs tip velocities, rotational velocities and torques. The torque is an input for the generator sizing and the rotational velocities and aerodynamic forces are an input for the structural analysis. Finally the cost is determined using mass estimations from the structural analysis, capacity factor estimation from the control optimisation strategy and a mass estimation from the generator sizing. It is therefore possible to change the outcome of the aerodynamic analysis which will flow down the design and show which variables will change due to which design parameters. In this sensitivity analysis, the aerodynamic values of the secondary rotor will be adjusted by 10 percent since only the secondary rotor is designed aerodynamically. The design parameters that are changed for this analysis are the C_{p_s} and the TSR of the secondary rotor. The quantitative overview of the sensitivity analysis is shown in Table 18.2. It should be noted that these are not all the variables that change with C_{p_s} and λ_s , but these are considered to be the most important variables for the design. The overview of how these parameter relate to each other is shown in Table 18.3 in the form of an N2 chart. In this N2 chart the initial sizing is at the top since the entire design is dependent on the values that are set up there and the rest of the chart is illustrated as explained in the beginning of this paragraph. Again this chart does not include all the parameters, only the ones that change and that are considered important for the design.

Table 18.2: The sensitivity analysis on system level

		Change in percentage		
Parameters	Original values	Increasing λ_s	Decreasing λ_s	Decreasing $C_{p_{s_{max}}}$
		to 2.31	to 1.89	to 0.117
Generator Torque	777 [kNm]	-10.1%	8.8%	5.7%
Rotational velocity SR	200 [RPM]	10.5%	-9.0%	-5.0%
Capacity factor	0.5711 [-]	0.0%	0.0%	1.4%
Generator mass	19.25 [ton]	-9.3%	9.8%	6.7%
Generator cost	189.4 [k€]	-9.3%	9.8%	6.7%
Mass SR per blade	2.05 [ton]	0.7%	-1.0%	-0.8%
Mass PR upper blade	91.3 [ton]	0.0%	0.0%	2.4%
Mass PR lower blade	65.9 [ton]	-1.6%	3.0%	-2.9%
COE	47.8 - 58.5 [€/MWh]	-0.3%	0.3%	-1.2%
ROI	315 [%]	0.4%	-0.3%	1.6%

From the sensitivity table it becomes clear that the control variables are very sensitive to the λ_s increase and decrease with an 8.8 to 10 percent change. Also the $C_{p_{s_{max}}}$ decrease has a substantial effect with a 5 % change. The blade masses do not vary a lot with the biggest change being 2.93 % for the PR lower blade. From this it can be concluded that the mass of the blades are not that sensitive to $C_{p_{s_{max}}}$ and λ_s but they are also not

Table 18.3: Simplified N2 for the sensitivity analysis

Initial sizing	a_s, R_s	a_s, R_s	P_{gen}				
	Aerodynamics	c_{p_s}, λ_s					
a_s, R_s	Control	Generator	Ω_s, R_s	Capacity			
	a_s, n_s	Torque		factor			
			Down	Power	Mass of	Cost of	
			1 Ower	generator	generator		
				Structures	Mass of		
					Structures	blades	
					Cost	COE, ROI	

sensitive to a the rotational velocity change of 10 %. The generator mass and cost are increased to almost 10 % with a 10 % change in ω_s which is quite significant. This change is completely due to the new generator torque and definitely requires a new generator selection. The capacitor factor only changes with $C_{p_{s_{max}}}$ for which it becomes a better value so there is not a problem with this variable. The COE is only increased with a decrease in λ_s but only with 0.34 % which is not significant even with an operational life time of 25 years. The ROI is increased whenever COE is reduced. All in all, the 10 % changes in the design parameters of the system do not change the values of the subsystems to unacceptable values.

Chapter 19: Compliance matrix

Now that the end of this design phase has been reached, it is time to check the validity of the design with the user requirements. The user requirements were presented in chapter 2. The first requirements were set by the client and these are evaluated now. Table 19.1 contains a list of the client requirements and gives a briefs assessment of the current design's compliance with them.

Table 19.1: Compliance matrix of the user requirements

Requirement	Description	Compliance	Comment
SRVAWT-CLI-01	Reduced or equivalent cost		The cost of energy ranges between 47.8 to 58.5 €/WWh, which is below the required range. However, there is a significant reduction in cost energy yet. This could be extended in the future by analysing the O&M in more detail.
SRVAWT-CLI-01.1	Reduce manufacturing cost		The manufacturing costs, including material costs, are €7.6 million, which equals €760 per kW of rated power. This is significantly lower than the requirement of €1000 per kW.
SRVAWT-CLI-01.2	Reduce material cost		See SRVAWT-CLI-01.1
SRVAWT-CLI-02	Reduce weight		The overall mass of the system has been reduced compared to conventional wind turbines to 914 tonnes, compared to 1300 tonnes for conventional turbines.
SRVAWT-CLI-03	Similar system reliability		The reliability of the system is reduced. This is mainly due to the amount of blades and pitch systems. It can be increased by using collective pitch per rotor.
SRVAWT-CLI-04	Risk of rotor detaching		The current group of designers were not able to assess the risk of detaching rotors. In addition, no reliable information was found on the risk of detaching blades in conventional turbines, so if the group was able to compare, it was unclear what to compare it to. Concepts have been proposed as to the nacelles and attachments of the secondary rotor, which should be assessed by experts to determine the risk of this event.
SRVAWT-CLI-05	More appealing in market		The SRVAWT shows a lot of potential for upscaling and for far offshore wind farms.

Chapter 20: Conclusion

As explained in chapter 1, the main purpose of this project is to design a wind turbine that produces 10MW of power with a lower drive train mass and size compared to conventional turbines of similar rated power. In doing so, the overall mass of the turbine can be reduced. In addition, it is crucial to achieve competitive cost levels and reliability to conventional turbines, in order to establish competitiveness.

The design solution to meet the requirements was found in a secondary rotor vertical axis wind turbine. In order to produce 10MW of rated power, a two-bladed primary vertical axis rotor with a radius of 91m is required. It has two secondary rotors with a radius of 12.2m attached to the tips of its bottom blades, which each have a direct-drive generator.

In terms of drivetrain mass, the goal of the project is achieved. The generator mass in this design is only 19.25 tonnes. Considering two secondary rotors, this brings the total generator mass to 38.5 tonnes. This means that a generator weight reduction of 84% is achieved compared to a conventional direct drive wind turbine generator of the same capacity as this weighs 239tonnes. The reason that this drivetrain mass is significantly lower than for a conventional wind turbine is the fact that the torque is lower. This is caused by the very high rotational velocities that the secondary rotor operates at with a maximum of 200rpm. This means that the tips of the blades will reach Mach numbers of 0.75. This reduction in drivetrain mass also caused an overall mass decrease.

Another aspect that determines competitiveness on the wind energy market is reliability and risk. In this wind turbine, there is no gearbox and no need for yaw systems. Due to the many pitch systems however, the overall reliability of the system is not improved compared to conventional turbines. However, the severity of a pitch system failing is lower as there are five blades on each secondary rotor that can pitch individually, allowing for redundancy. This reduces the severity of secondary rotor pitch system failure and allows better maintenance planning, which may be more cost effective.

In today's world, every engineering project needs to consider sustainability aspects. For the SRVAWT, the most important ones include the turbine's lifetime, the noise it produces and the emissions caused by all required transportation. Concerning noise, at a distance of 100 m from the turbine, noise levels reach 79.2 dB. This sound pressure level is corrected for the human ear and therefore can be experienced differently by the animals living in the sea. What the overall effects of noise on animals are is still uncertain. The turbine is assumed to have an operational life time similar to conventional turbines. However, for the SRVAWT limitations in lifetime are mainly expected to be due to degradation of the secondary rotors. By replacing only the secondary rotors when they reach their end of life, the primary rotor, tower and foundation can be used for a longer amount of time, which makes it more sustainable. Concerning transportation, it was found that this turbine would need less maintenance than conventional ones. Therefore, less transportation actions are required. Also because the severity of failures is lower, more maintenance activities can be combined, so less transportation is needed.

Chapter 21: Limitations and recommendations

In several of the previous chapters a limitations and recommendations section was present. These sections were used to show limitations and recommendations for those particular subsystems or analyses. In this chapter the limitations and recommendations of the overall project and system are provided. In section 21.1, an overview is given of the limitations that made the design process more difficult. The recommendations to overcome this for the future design process are given in section 21.2.

21.1 Limitations

The biggest limitation that was encountered during this project is the lack of theoretical background on wind energy. Throughout the Aerospace Engineering BSc programme, the focus has been mostly on aircraft. This means that composite wind turbine blade design was completely new. Furthermore, the control of a wind turbine was a completely new concept. This meant that the team had to do an extensive literature study to get a better understanding of wind turbine design. The limitations stated above were only amplified by the fact that this design is not a conventional wind turbine, meaning that a lot of the literature study on wind turbines was not applicable. Especially in the aerodynamics department, where a secondary rotor blade had to be designed for a low induction factor, which is anything but conventional. For the control department, the strategy is a lot more complicated than one would normally find in wind turbines, as more systems are involved.

Due to the mentioned lack of theoretical background and the additional required literature study that this implies, time constraints started playing a large role as well. This time issue limited the aerodynamic analysis to just the secondary rotor. Incorporating an optimal pitch strategy in the control simulation could also not be accomplished withing the given time frame. For the same reason the generator sizing is very preliminary. Moreover, the risk of secondary rotors detaching could not be assessed. This is a problem because it is a user requirement, given in the project guide.

Another limitation is the accuracy of the models used for the design. An online code was used for the structural analysis, which was not written by the team, making it difficult to estimate its accuracy. For the aerodynamic analysis of the secondary rotor, a code was used for the blade design. This code was also not written by the team, which made it difficult to design for the parameters that were required. Usually, a blade is designed for optimal induction factor. Since this design does not operate at that induction factor, the code had to be changed as well.

21.2 Recommendations

Based on the limitations mentioned before, some recommendations can be made for future design activities. A first recommendation is to make more accurate models for the structural and aerodynamic designs. For the aerodynamic blade design, it can be attempted to design the primary blade as well, since the parameters for this rotor were based on assumptions in this report. Secondly, a more detailed control simulation should be made in order to find the required pitch rates and limiting pitch angle values. The cost estimation model can also be improved in accuracy by using a newer model that has more data and trends available.

There are also some possibilities for this design to be looked into in the future. It is seen that the generator mass is almost negligible for the structure, this means that this design can be easily upscaled. It is expected that upscaling to 15MW or more is possible, this can be done by increasing the secondary rotor and generator size. In order to do this, the primary rotor would have to be redesigned as well in this case. Extension of turbine lifetime can be investigated as well. This means that after a lifetime of 20 to 25 years, the secondary rotors are replaced but the primary rotor and foundation is reused. This could potentially reduce the cost of energy by reducing the operation and maintenance cost. Finally, some effort has to be put into the research of floating offshore structures. Vertical axis rotors are more symmetric and therefore suited for floating structures, this could also potentially reduce cost of energy as the turbine could be put further offshore, increasing the capacity factor.

Chapter 22: Future planning

At this point a preliminary design has been presented and it is time to look ahead. In Figure 22.1 and Figure 22.2 a logical flow diagram is presented which covers the basic steps to be taken in the wind turbine's development process, its manufacturing and installation, its operation and its decommissioning. This flow diagram was initially presented in [10], but it has been updated since. It forms the bases of what should be done after the DSE and how this wind turbine would continue through the last design phases and the post design phases.

Using the logical flow diagram it is possible to make a Gantt chart for the post DSE activities. The Gantt chart is shown in Figure 22.3 and provides an overview of the steps to be taken after the end of this DSE exercise. During the past ten weeks, the wind turbine was fully designed and plans for its maintenance and manufacture were written up. To put these tasks into perspective, a timeline is created with an estimated amount of time that each task should take. One advantage of using a Gantt chart to do this is the possibility of visualizing chokepoints in the plan, where all available resources are not being used or are being wasted. This allows for optimization of the timeline, allowing the project to cut costs and shorten deadlines. One example of this, is the particularly long manufacture and installation period that can only start after the contracts are signed.

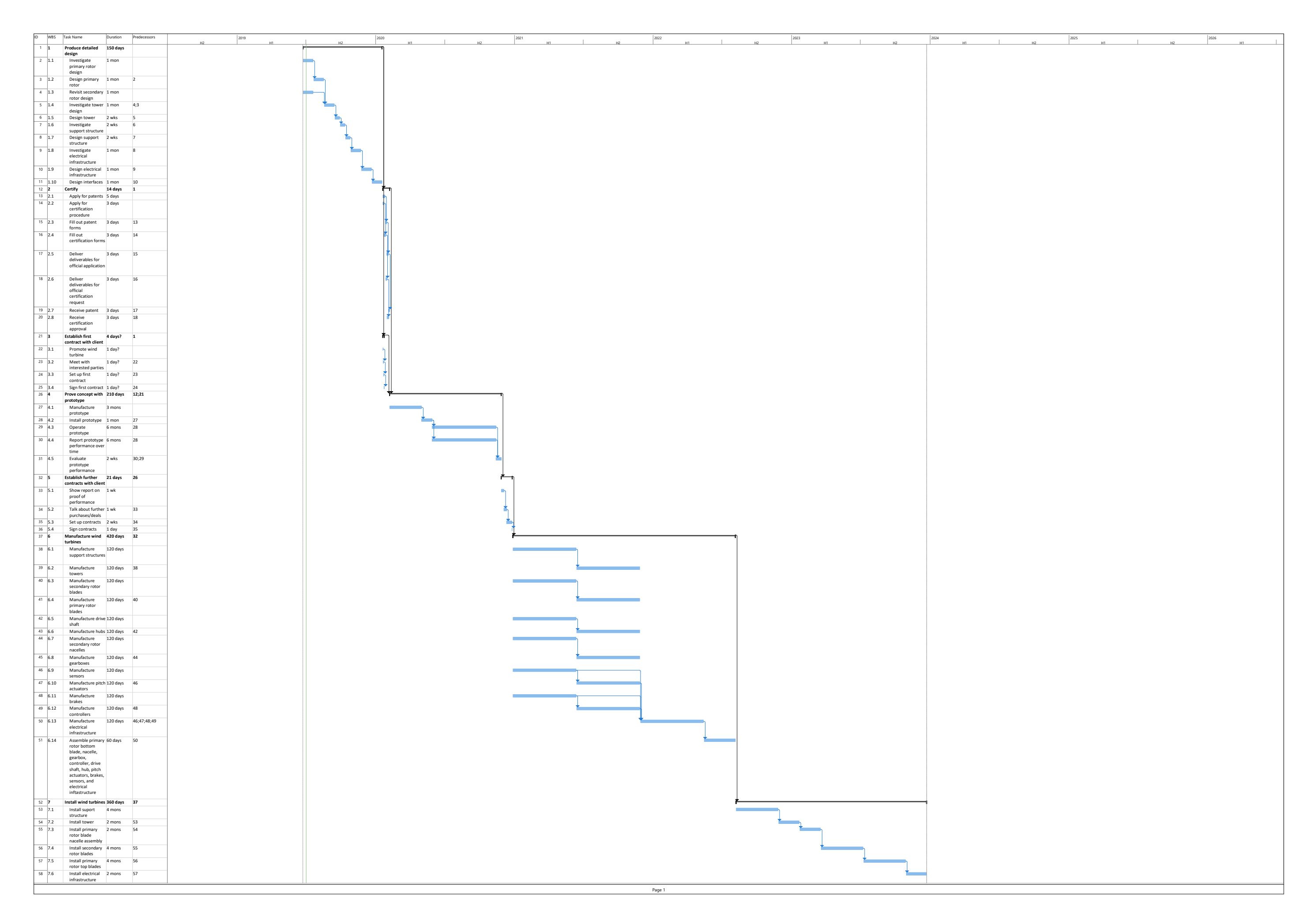


Figure 22.3: Post DSE Gantt Chart

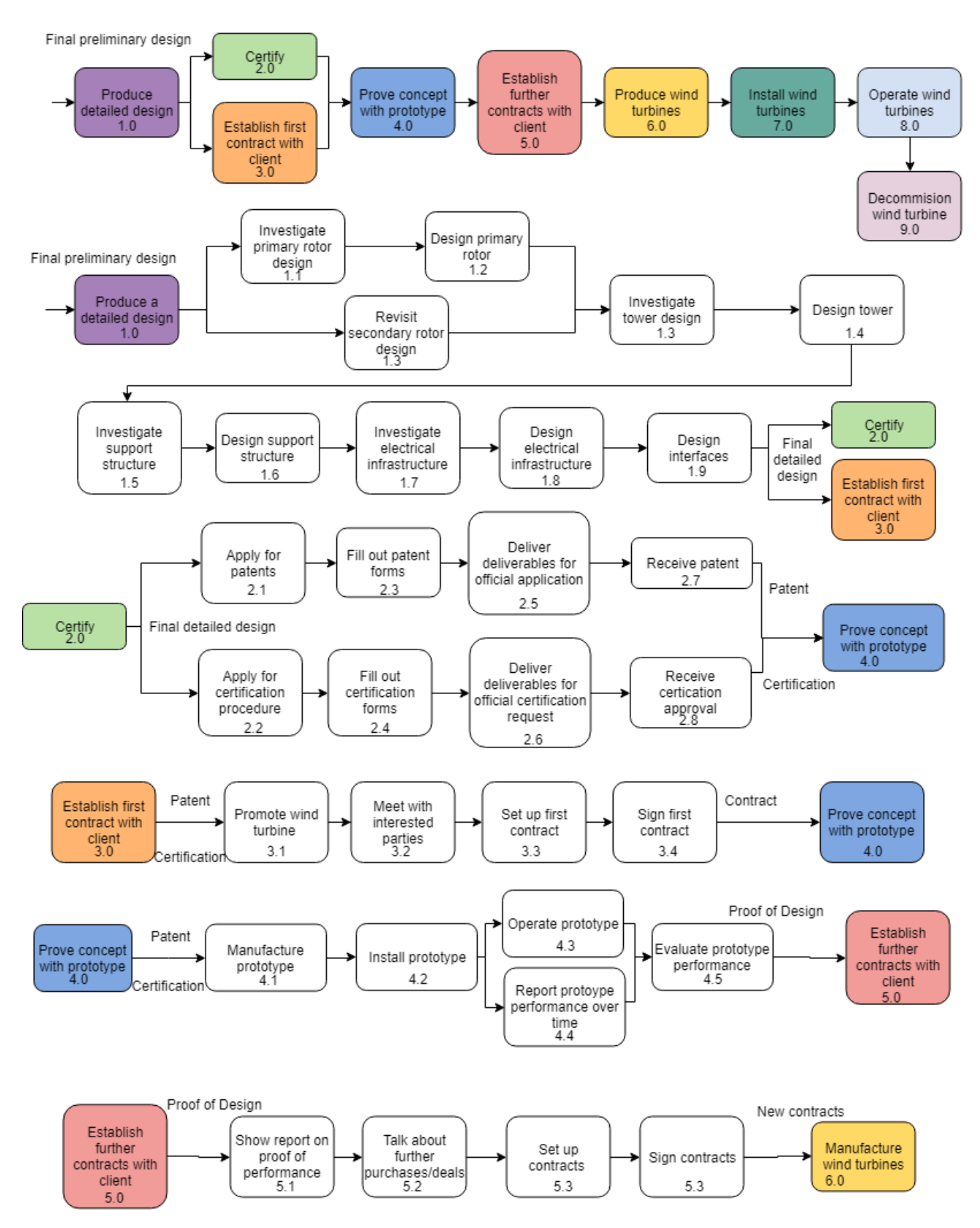


Figure 22.1: Future Project Design & Development Logic Flow Diagram part 1

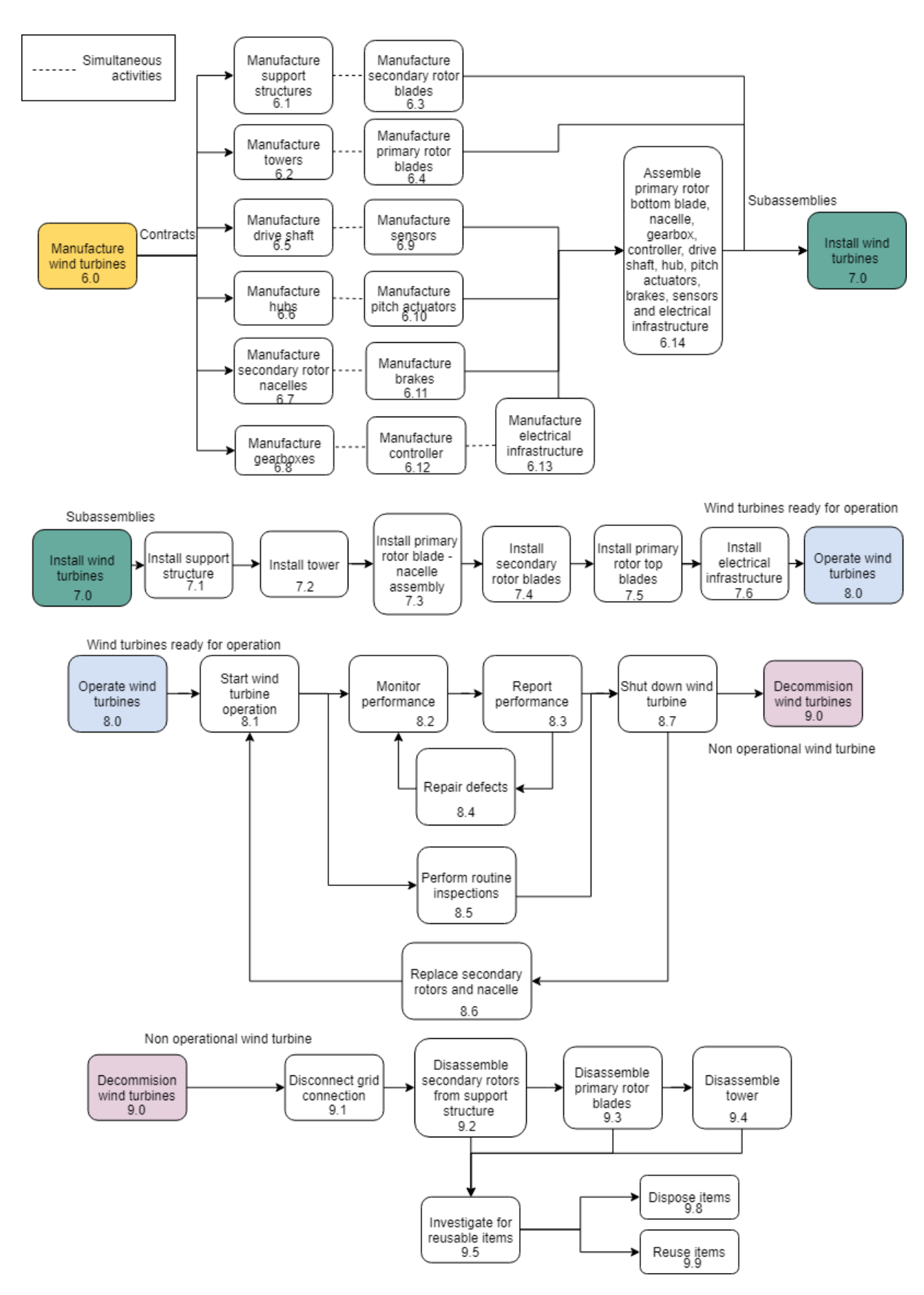


Figure 22.2: Future Project Design & Development Logic Flow Diagram part 2

Bibliography

- [1] C. Ferreira and S. Watson, Project Guide Design Synthesis Exercise, Development of a secondary rotor wind turbine. 2019.
- [2] B. Sorensen, "A history of renewable energy technology", *Energy Policy*, vol. 19, no. 1, pp. 8–12, Feb. 1991
- [3] J. David L. Morton, "Reviewing the history of electric power and electrification", *Endeavour*, vol. 26, no. 2, pp. 60–63, Jun. 2002.
- [4] P. D. Fleming and S. D. Proben, "The evolution of wind-turbines: An historical review", *Applied Energy*, vol. 18, no. 3, pp. 163–177, 1984.
- [5] M. Islam, D. S.-K.Ting, and A. Fartaj, "Aerodynamic models for darrieus-type straight-bladed vertical axis wind turbines", *Renewable and Sustainable Energy Reviews*, vol. 12, no. 4, pp. 1087–1109, May 2008.
- [6] J. K. Kaldellis and D. Z. rakis, "The wind energy (r) evolution: A short review of a long history", Renewable Energy, vol. 36, no. 7, pp. 1887–1901, Jul. 2011.
- [7] Wind energy in europe: Outlook to 2022, http://greenagenda.gr/wp-content/uploads/2018/09/Wind-energy-in-Europe-Outlook-to-2022.pdf, 2018.
- [8] B. Leithead, A. Camciuc, A. K. Amiri, and J. Carroll, *The x-rotor offshore wind turbine concept*, Retrieved 01-05-2019 from https://www.sintef.no/globalassets/project/eera-deepwind-2019/presentations/al_carrol_leithead_strathclyde.pdf, 2019.
- [9] Group 21, Secondary rotor vertical axis wind turbine midterm report, Delivarable for the course AE3200, May 2019.
- [10] —, Secondary rotor vertical axis wind turbine baseline report, Delivarable for the course AE3200, May 2019.
- [11] T. Burton, D. Sharpe, N. Jenkins, and E. Bossanyi, Wind Energy Handbook. John Wiley & Sons, Ltd, 2001, ISBN: 0-471-48997-2.
- [12] C. S. Ferreira, *Programming a bem model*, Delft University of Technology, Course AE4135 Rotor/Wake Aerodynamics Module 2.2.3, Retrieved 05/05/2019 from https://github.com/csimaoferreira/RotorWakeAerodynamicsBEM/blob/master/BEMmodel.ipynb, 2019.
- [13] J. F. Manwell, J. G. McGowan, and A. L. Rogers, Wind Energy Explained: Theory, Design and Application. John Wiley & Sons, Ltd, 2009, ISBN: 978-0-470-01500-1.
- [14] W. A. Timmer and R. P. J. O. M. van Rooij, "Summary of the delft university wind turbine dedication airfoils", 2003, Retrieved on 3rd of June 2019. [Online]. Available: http://lr.home.tudelft.nl/fileadmin/Faculteit/LR/Organisatie/Afdelingen_en_Leerstoelen/Afdeling_AEWE/Wind_Energy/Research/Publications/Publications_2003/doc/Timmer_PaperAIAA20030352.pdf.
- [15] C. D. Harris, Nasa supercritical airfoils a matrix of familiy-related airfoils, Retrieved 06-06-2019 from https://ntrs.nasa.gov/archive/nasa/casi.ntrs.nasa.gov/19900007394.pdf, Mar. 1990.
- [16] D. Marten and J. Wendler, *Qblade guidelines* v0.6, http://q-blade.org/project_images/files/guidelines_v06.pdf, 2013.
- [17] H. A. Madsen, The actuator cylinder a flow model for vertical axis wind turbines, Aalborg University Center, Jan. 1982.
- [18] H. H. Hubbard, "Aeroacoustics of flight vehicles: Theory and practice", Hampton, Virginia, Tech. Rep., 1991.
- [19] S. Wagner and R. Bareiß, Wind Turbine Noise. Springer-Verlag GmbH, 1996, ISBN: 9783642887123.
- [20] DNV GL AS, "Control and protection systems for wind turbines", Apr. 2016, DNVGL-ST-0438. [Online]. Available: https://rules.dnvgl.com/docs/pdf/DNVGL/ST/2016-04/DNVGL-ST-0438.pdf.
- [21] Germanischer Lloyd, Guideline for the Certification of wind Turbines. Hamburg, DE: Germanischer Lloyd Industrial Services GmbH, Jun. 2010.
- [22] International Electrotechnical Commission, Wind turbines Part 1: Design requirements. Geneva, CH, 2014, IEC61400-1:2014, ISBN: 978-2-8322-2262-1.
- [23] R. J. M. Fernando D. Bianchi Hernán De Battista, Wind Turbine Control Systems. Springer, 2007, ISBN: 1-84628-492-9.
- [24] Jha, A. R., Wind Turbine Technology. Boca Raton (FL), USA: CRC Press, 2010.
- [25] J. Venegas, The key to reliable emergency backup power for wind pitch control, Retrieved 16/06/2019 from http://cdn.pes.eu.com/v/20160826/wp-content/uploads/2017/09/PES-W-3-Maxwell-talking-point-4-1.pdf, 2018.

- [26] M. Froese, The key role of energy storage backup power for wind-turbine pitch control, Retrieved 16/06/2019 from https://www.windpowerengineering.com/electrical/power-storage/key-role-energy-storage-backup-power-wind-turbine-pitch-control/, Feb. 2018.
- [27] K. E. Johnson, "Adaptive torque control of variable speed wind turbines", National Renewable Energy Laboratory, Tech. Rep., 2004.
- [28] Dr.ir. M.B. Zaaijer, *Wind turbine components*, Introduction to wind turbines: physics and technology (AE4W02TU), Nov. 2018.
- [29] M. Wilkinson, B. Hendriks, F. Spinato, and K. Harman, "Methodology and results of the reliawind reliability field study", European Wind Energy Conference, Tech. Rep., 2010.
- [30] P. Padman, J. Xu, F. Vanni, E. Echavarria, and M. Wilkinson, The effect of pitch system reliability on wind power generation's levelized cost of energy, Retrieved 22/06/2019 from http://www.moogwind.com/Global/FileLib/wind/Moog_Whitepaper_Pitch_System_Reliability-en.pdf, 2016.
- [31] C. Ganesh, S. Anupama, and B. Mekalathur, "Maximum power extraction of wind energy conversion system in the sub rated region using extremum seeking", *International Journal of Applied Engineering Research*, vol. 10, pp. 3350–3355, Jan. 2015.
- [32] M. Jelavic, V. Petrovic, M. Barisic, and I. Ivanovic, Wind turbine control beyond the cut-out wind speed, Retrieved 17/06/2019 from https://bib.irb.hr/datoteka/619383.EWEA13_clanak.pdf, 2015.
- [33] C. L. Bottasso, A. Croce, and C. E. D. Riboldi, "Optimal shutdown management", *Journal of Physics: Conference Series*, vol. 524, p. 012050, Jun. 2014. DOI: 10.1088/1742-6596/524/1/012050.
- [34] J. Wagenaar and P. Eecen, Measurements of wind, wave and currents at the offshore wind farm egmond aan zee, Retrieved 09/05/2019 from http://www.noordzeewind.nl/wp-content/uploads/2012/02/OWEZ_R_122_Wave_20050701_20081231-20100107.pdf, 2009.
- [35] F. Blaabjerg, Z. Chen, R. Teodorescu, and F. Iov, Power electronics in wind turbine systems, 2006.
- [36] D. Bang, H. Polinder, G. Shrestha, and J. Ferreira, Review of generator systems for direct-drive wind turbines, 2008.
- [37] N. A. Bhuiyan and A. Mcdonald, Optimization of offshore direct drive wind turbine generators with consideration of permanent magnet grade and temperature, 2018.
- [38] H. Polinder, F. F. A. van der Pijl, G.-J. de Vilder, and P. J. Tavner, "Comparison of direct-drive and geared generator concepts for wind turbine", *IEEE Transactions on Energy Conversion*, vol. 21, no. 3, Sep. 2018.
- [39] H. Polinder, D. Bang, R. van Rooij, A. McDonald, and M. Mueller, "10 mw wind turbine direct-drive generator design with pitch or active speed stall control", *IEEE International Electric Machines & Drives*, 2007.
- [40] "Design of 2.25 mw, permanent magnet direct drive generator for wind energy applications with concentrated windings and reduction of eddy current losses in the rotor back iron", TECHNICAL UNIVERSITY DELFT, 2008.
- [41] H. Ahmad, Offshore wind park connection to an hvdc platform, without using an ac collector platform, Retrieved 14/06/2019 from http://www.computationalrenewables.com/bahriuzunoglu/publications/Haseeb_Ahmad.pdf, 2012.
- [42] F. Deng and Z. Chen, "Operation and control of a dc-grid offshore wind farmunderdctransmissionsystemfaults", *IEEE Transactions on power delivery*, vol. 28, no. 3, Jul. 2013.
- [43] Z. Zhang, A. Matveev, R. Nilssen, and A. Nysveen, Large-diameter ironless permanent magnet generator for offshore wind power application, 2012.
- [44] L. M. Jr., K. Branner, H. N. Petersen, J. Beauson, M. McGugan, and B. F. Sørensen, "Materials for wind turbine blades: An overview", Nov. 2017, Retrieved on 14th of May 2019. [Online]. Available: https://www.ncbi.nlm.nih.gov/pmc/articles/PMC5706232/.
- [45] P. J. Teuwen, Manufacturing and quality of wind turbine blades, TU Delft, Asset management of Offshore Wind Farms (AE3512), Sep. 2018.
- [46] D. Sale, Co-blade: Software for analysis and design of composite blades, Retrieved 14/06/2019 from https://nl.mathworks.com/matlabcentral/fileexchange/38224-co-blade-software-for-analysis-and-design-of-composite-blades, 2019.
- [47] D. T. Griffith and T. D. Ashwill, The sandia 100-meter all-glass baseline wind turbine blade: Snl100-00, Retrieved 11/06/2019 from https://energy.sandia.gov/wp-content/gallery/uploads/113779.pdf, 2011.
- [48] M. M. Danny Sale Alberto Aliseda, Structural optimization of composite blades for wind and hydrokinetic turbines, Retrieved 11/06/2019 from https://pdfs.semanticscholar.org/dd5b/77bc.pdf, 2013.
- [49] eFunda, Classical lamination theory, Retrieved 11/06/2019 from https://www.efunda.com/formulae/solid_mechanics/composites/comp_laminate.cfm, 2019.
- [50] —, A summary of classical lamination theory, Retrieved 11/06/2019 from https://wstein.org/edu/2010/480b/projects/05-lamination_theory/A%20summary%20of%20Classical%20Lamination%20Theory.pdf, 2019.

- [51] A. Bjørgu, Coatings for wind turbines, Retrieved 11/06/2019 from https://www.sintef.no/globalassets/project/nowitech_new/final-seminar-august2017/presentations/astrid-bjorgum_sintef.pdf,
- [52] P. Brøndsted and R. P. Nijssen, Advances in Wind Turbine Blade Design and Materials. Woodhead Publishing Series in Energy, 2013, ISBN: 978-0-85709-426-1.
- [53] Callister, W. D., Materials science and engineering: An introduction, 9th ed. New York (NY), USA: John Wiley & Sons, 2014.
- [54] M. C. Y. Niu, Airframe Stress Analysis and Sizing. Hong Kong Conmilit Press LTD, 1999.
- [55] A. A. Bulent Eker and A. Vardar, "Using of composite material in wind turbine blades", 2006.
- [56] N. R.P.L., de Ruiter M.J., L. F., and K. E., "Connection methods in wind turbine rotor blades", 2018.
- [57] W. E. Luce, Attachment of composite lug to composite structural tube, 2016.
- [58] "Steel solutions in the green economy", 2012. [Online]. Available: https://www.worldsteel.org/en/dam/jcr:41f65ea2-7447-4489-8ba7-9c87e3975aab/Steel+solutions+in+the+green+economy: +Wind+turbines.pdf.
- [59] J. Amdahl, "Chapter 5: Buckling of cylindrical shells", 2005. [Online]. Available: http://www.ivt.ntnu.no/imt/courses/tmr4205/literature/chpt5_Buckling_of_cylindrical_shells.pdf.
- [60] L. Fingersh, M. Hand, and A. Laxson, Wind turbine design cost and scaling model, Retrieved 16-05-2019 from https://www.nrel.gov/docs/fy07osti/40566.pdf, 2006.
- [61] C. Desmond, J. Murphy, L. Blonk, and W. Haans, Description of an 8 mw reference wind turbine, IOP Publishing, Sep. 2016.
- [62] G. K. Yamauchi, R. M. Heffernan, and M. Gaubert, Hub and blade structural loads measurements of an sa349/2 helicopter, NASA Technical Memorandum 101040, Dec. 1988.
- [63] C. International, Wind turbine tower manufacturing process, Retrieved 19/06/2019 from http://www.steelwindtower.com/services/, 2019.
- [64] H. Snel and G. van Bussel, Wind energy (ae3w02), 2018.
- [65] E. W. E. Association, Commissioning, operation and maintenance, Retrieved 22/06/2019 from https://www.wind-energy-the-facts.org/commissioning-operation-and-maintenance.html.
- [66] E. Arzaghi, Scada, pm modelling & logistic delays, Asset Management (AE3513), 2016.
- [67] C. C. Ciang, J.-R. Lee, and H.-J. Bang, "Structural health monitoring for a wind turbine system: A review of damage detection methods", 2008, Retrieved on. [Online]. Available: https://www.researchgate.net/publication/311664061_Structural_optimisation_of_wind_turbine_towers_based_on_finite_element_analysis_and_genetic_algorithm.
- [68] J. Carroll, A. McDonald, and D. McMillan, Failure rate, repair time and unscheduled o\mathbb{G}m cost analysis of offshore wind turbines, University of Strathclyde, Aug. 2015.
- [69] T. Letcher, Wind Energy Engineering. Academic Press, 2017, ISBN: 9780128094297.
- [70] E. Arzaghi, Ae3512 asset management, slides lecture 7, 2019.
- [71] J. Carroll, A. McDonald, and D. McMillan, Reliability comparison of wind turbines with dfig and pmg drive trains, University of Strathclyde, Jun. 2014.
- [72] S. Pfaffel, S. Faulstich, and K. Rohrig, "Performance and reliability of wind turbines: A review", Fraunhofer Institute for Wind Energy and Energy System Technology, Tech. Rep., 2017.
- [73] P. Tavner, Offshore Wind Turbines Reliability Availability and Maintenance. Published by The Institution of Engineering and Technology London United Kingdom, 2019, ISBN: 978-1-84919-230-9.
- [74] Greenbyte, Power performance upgrades to wind turbines, https://www.greenbyte.com/fileadmin/documents/Evaluation_of_Power_Performance_Upgrades_to_Wind_Turbines.pdf.
- [75] J. Snook, Wind farm safety, Retrieved 21/06/2019 from https://www.initiafy.com/blog/wind-turbine-safety/, 2018.
- [76] A. Aid, Human rights in wind turbine supply chains, Retrieved https://www.somo.nl/wp-content/uploads/2018/01/Final-ActionAid_Report-Human-Rights-in-Wind-Turbine-Supply-Chains.pdf, 2018.
- [77] M. Kaiser and B. Snyder, Offshore Wind Energy Cost Installation and Decommissioning. Springer, 2012.
- [78] D. for Business Entreprise and R. Reform, Review of cabling techniques and environmental effects applicable to the offshore wind farm industry, Retrieved 07-05-2019 from https://tethys.pnnl.gov/sites/default/files/publications/Cabling_Techniques_and_Environmental_Effects.pdf, 2008.
- [79] E. Roth, L. Verhoef, and M. Dingenouts, Overview of environmental impacts of offshore wind energy, Concerted action for offshore wind energy deployment (COD), Sep. 2004.
- [80] G. Wolfgang and M. B. Brunner, New bauer flydrill system drilling monopiles at barrow offshore wind farm, uk, Retrieved 07-05-2019 from https://scholarsmine.mst.edu/cgi/viewcontent.cgi?article=2929&context=icchge, 2008.
- [81] Vestas, Vestas annual report 2018, Retrieved 07-05-2019 from https://www.vestas.com/~/media/vestas/investor/investor20pdf/financial20reports/2018/q4/2018_sustainability.pdf, 2019.

- [82] S. Pickering, Recycling technologies for thermoset composite materials current status, ScienceDirect, May 2005.
- [83] W. Tong, Wind Power Generation and Wind Turbine Design. WIT Press, 2010, ISBN: 9781845642051.
- [84] F. van den Berg and I. van Kamp, "Shealth effects related to wind turbine sound", Acoustics Australia / Australian Acoustical Society, 2017.
- [85] L. Bergstrom, L. Kautsky, R. Rosenberg, and M. Wahlberg, "Effects of offshore wind farms on marine wildlife a generalized impact assessment", *Environmental Reserrach Letters*, Feb. 2014.
- [86] K. Smith, Windpact turbine design schaling studies technical area 2: Turbine, rotor, and blade logistics, Retrieved 01-05-2019 from https://www.nrel.gov/docs/fy01osti/29439.pdf, 2000.
- [87] "Research: Offshore wind energy operations & maintenance analysis", 2012.
- [88] Currency calculator, Retrieved 20/05/2019 from https://www.x-rates.com/calculator/?from=USD&to=EUR&amount=1,
- [89] D. H. Tyler Stehly Philipp Beiter and G. Scott, "2017 cost of wind energy review", 2017.
- [90] P. Jamieson, Innovation in wind turbine design. John Wiley & Sons, Ltd, 2018, ISBN: 9781119137900.
- [91] S. Lensink and I. Pisca, "Costs of offshore wind energy 2018", 2019.
- [92] D. Merino and A. Ebrill, "Acer/ceer annual report on the results of monitoring the internal electricity and natural gas markets in 2017 electricity wholesale markets volume", 2018.
- [93] "Guide to an offshore wind farm", 2019.
- [94] P. Fuglsang and K. Thomsen, "Cost optimization of wind turbines for large-scale offshore wind farms", 1998
- [95] GWEC, Global Wind Report 2018. Global Wind Energy Counsil, 2019.
- [96] M. Froese, Vestas gains impressive lead as top wind-turbine manufacturer, Retrieved 12/06/2019 from https://www.windpowerengineering.com/business-news-projects/vestas-gains-impressive-lead-as-top-wind-turbine-manufacturer/, 2019.
- [97] G. R. Energy, World's largest offshore wind turbine, Retrieved 11/06/2019 from https://www.ge.com/renewableenergy/wind-energy/offshore-wind/haliade-x-offshore-turbine, 2017.
- [98] W. Europe, Offshore wind in europe: Key trends and statistics 2018, Retrieved 12/06/2019 from https://windeurope.org/about-wind/statistics/offshore/european-offshore-wind-industry-key-trends-statistics-2018/#explore, 2019.
- [99] D. A. Jarquin-Laguna, Oe44120 offshore wind farm design, slides lecture 3b, 2019.
- [100] P.-F. Bach, Capacity factor degradation for danish wind turbines, Retrieved 07-05-2019 from http://www.pfbach.dk/firma_pfb/pfb_capacity_factor_degradation_2012.pdf, 2012.
- [101] IRENA, Offshore innovation widens renewable energy options, Retrieved 07-05-2019 from https://www.irena.org/-/media/Files/IRENA/Agency/Publication/2018/Sep/IRENA_offshore_wind_brief_G7_2018.pdf, 2018.
- [102] E. F. Merchant, World's most powerful wind turbine, Retrieved 01-05-2019 from https://www.greentechmedia.com/articles/read/vattenfall-installs-worlds-most-powerful-wind-turbine#gs.98zlvp, 2018.
- [103] general electric, *Haliade-x offshore wind turbine platform*, Retrieved 01-05-2019 from https://www.ge.com/renewableenergy/wind-energy/offshore-wind/haliade-x-offshore-turbine, 2019.
- [104] S. Siemens Gamesa Renewable Energy, Sg 10.0-193 dd offshore wind turbine, Retrieved 01-05-2019 from https://www.siemensgamesa.com/en-int/products-and-services/offshore/wind-turbine-sg-10-0-193-dd, 2019.
- [105] M. V. O. W. A/S, Mhi vestas launches the first 10 mw wind turbine in history, Retrieved 01-05-2019 from http://www.mhivestasoffshore.com/mhi-vestas-launches-the-first-10-mw-wind-turbine-in-history/, 2018.
- [106] AMSC, Seatitan[™]10 mw wind turbine, Retrieved 01-05-2019 from https://www.amsc.com/wp-content/uploads/wt10000_DS_A4_0212.pdf, 2012.
- [107] J. Helsen, F. Vanhollebeke, D. Vandepitte, and W. Desmet, Some trends and challenges in wind turbine upscaling, Retrieved 20/06/2019 from https://pdfs.semanticscholar.org/adb4/5ab7.pdf, 2012.
- [108] Wind energy in europe: Scenarios for 2030, https://windeurope.org/wp-content/uploads/files/about-wind/reports/Wind-energy-in-Europe-Scenarios-for-2030.pdf, 2017.
- [109] C. D. et al, "Description of an 8 mw reference wind turbine", Journal of Physics: Conference Series, Tech. Rep., 2016.